Surgery-stimulated tumor growth

preclinical and clinical studies on colorectal liver metastases

Maarten W. Nijkamp

Surgery-stimulated tumor growth
preclinical and clinical studies on colorectal liver metastases
Thesis, Utrecht University, The Netherlands

The work described in this thesis was supported by the Dutch Cancer Society (grant number 2006-3711), The Netherlands Organisation for Scientific Research (ZonMw, AGIKO grant number 920-03-534) and de Catharijne Stichting (grant number 07.019).

Publication of this thesis was financially supported by:
Dit proefschrift werd mede mogelijk gemaakt met financiële steun van:

Amgen BV, Baxter, Chipsoft, Chirurgisch Fonds UMC Utrecht, ConvaTec Nederland BV, Covidien Nederland BV, GlaxoSmithKline, J.E. Jurriaanse Stichting, KWF Kankerbestrijding, Millipore BV, Novartis Oncology, Olympus Nederland BV, PQR BV, Roche Nederland BV, Sanofi-Aventis, Sigma Medical, Solvay Pharma BV, Tebu-bio

ISBN: 978-94-6108-071-4
Lay out: Wendy Schoneveld-Tijsterman
Cover: M.W. Nijkamp, Gildeprint Drukkerijen
Printer by: Gildeprint Drukkerijen BV, Enschede

Surgery-stimulated tumor growth

preclinical and clinical studies on colorectal liver metastases

Chirurgie-gestimuleerde tumor groei
preklinische en klinische studies betreffende colorectale levermetastasen
(met een samenvatting in het Nederlands)

Proefschrift

ter verkrijging van de graad van doctor aan de Universiteit Utrecht
op gezag van de rector magnificus, prof. dr. J.C. Stoof,
ingevolge het besluit van het college voor promoties
in het openbaar te verdedigen op

donderdag 30 september 2010 des middags te 12.45 uur

door

Maarten Willem Nijkamp

geboren 24 december 1979 te Eelde

Promotor Prof. dr. I.H.M. Borel Rinkes

Co-promotor dr. O. Kranenburg

voor papa

Contents

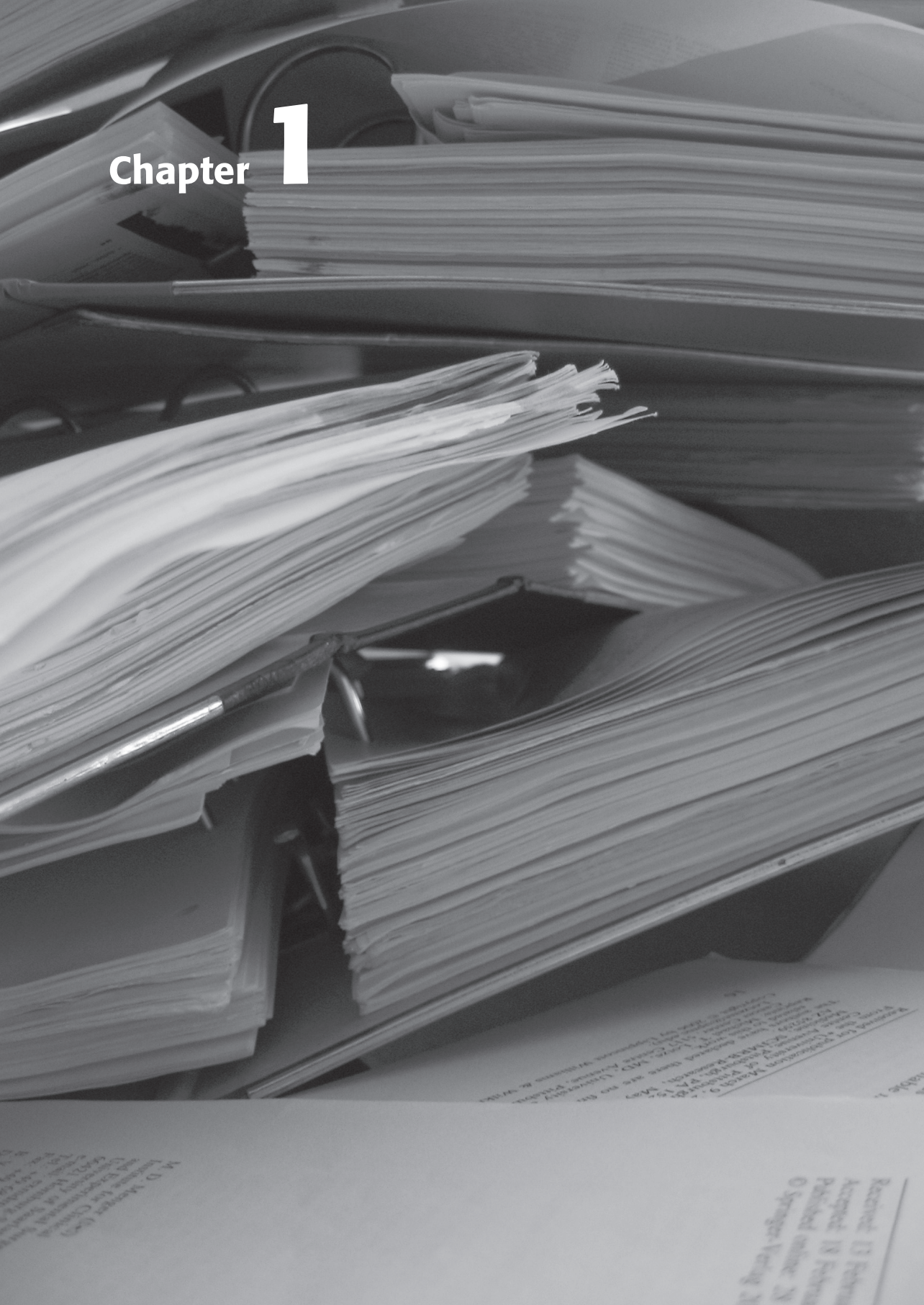

Chapter 1

General introduction and outline of the thesis

K-Ras mutation in the development of colorectal cancer and its metastases

The formation of colorectal carcinoma from normal colonic tissue is driven by the accumulation of genetic changes over time, collectively known as the adenoma-carcinoma sequence.[1] Activating mutations in the proto-oncogene K-Ras are found at the early pre-malignant stages of colorectal cancer development and are thought to drive tumor progression. Like other members of the Ras family, the K-Ras protein is a membrane-bound GTPase which is regulated by a GDP/GTP cycle. K-Ras acts as a molecular on/off switch that transduces extracellular signals to intracellular effector pathways. K-Ras is inactive when bound to GDP and active when bound to GTP. Activating mutations in the *K-Ras* gene interfere with its intrinsic GTPase activity, resulting in constitutive activation of K-Ras. As a consequence, growth-factor independent signaling will occur. Approximately 30% of all human malignancies contain an oncogenic point mutation in one of the RAS genes (*H-Ras, N-Ras, K-Ras*). K-Ras is by far the most frequently mutated isoform and is mutated in 35-45% of colorectal cancer patients.[2,3]

Colorectal cancer is diagnosed in more than one million new patients each year. Although localized primary tumor growth may cause significant organ failure, it rarely causes death. Metastasis formation of colorectal cancer is the main reason why colorectal cancer is among the most common causes of cancer-related deaths worldwide, particularly in the western world.[4] The liver is the main site of metastasis formation in colorectal cancer patients due to hematogeneous spread of tumor cells through the portal system.[5] Approximately 50% of patients diagnosed with colorectal carcinoma will eventually develop liver metastases.[6]

Tumor cells located in primary colorectal tumor have to complete a sequence of events before a liver metastasis can be formed (metastatic cascade).[7,8] First, the interaction between tumor cells in the solid primary tumor and the interaction between the tumor cells and the supporting matrix need to be disrupted. The detached tumor cells encounter a tumor-surrounding basement membrane which must be degraded before they can migrate to a blood vessel (or a lymphatic vessel in case of lymphogenous metastasis).[9] After invading through the endothelial cell layer, tumor cells enter the circulation (intravasation).[10,11] In case of colorectal cancer, circulating colorectal tumor cells enter the gut-draining mesenteric veins and reach the liver through the portal system. Circulating tumor cells are trapped in the liver sinusoidal system where they are exposed to cells of the immune system, including constitutively active hepatic NK cells ('pit cells'), NK-T cells, T cells and Kupffer cells.[12,13] In order to form metastases, tumor cells need to be resistant to this immune response. Next, tumor cells need to migrate through the sinusoidal endothelial layer and degrade the basement membrane before reaching the liver parenchyma.[14] Further outgrowth of the tumor cells requires the formation of new blood vessels, providing nutrients and oxygen.[15]

K-Ras is well known for its role in the early stages of colorectal cancer progression. Considerably less is known about its contribution to the multistage process of metastasis formation. Nonetheless, K-Ras activation might influence several aspects of this process. Studies addressing this have mostly focused on the first phase of the metastatic cascade including regulation of cell adhesions[16], local tumor cell invasion[17,18], migration[19] and anoikis-resistance.[20] However, a role for K-Ras in survival of tumor cells in the hepatic microenvironment has not been thoroughly addressed.

Treatment of colorectal liver metastases

Once metastases have formed, the survival rate of colorectal cancer patients decreases significantly. If left untreated, patients with colorectal liver metastases have a poor prognosis with a median survival

between 3 and 12 months.[21-23] Tumor response rates of 40-50% are reported when using systemic therapy based on a combination of chemotherapy and biological agents. Nonetheless, the median survival in patients treated with systemic therapy alone is approximately 20 months and survival beyond 5 years is uncommon in these patients.[24,25]

Until now, partial liver resection is the only curative treatment option for patients with colorectal liver metastases. Large case series show overall 5-year and 10-year survival rates of 36-58% and 22-26%, respectively.[26-30] Unfortunately, not all patients are amenable for partial liver resection, despite expansion of the criteria for resectability over the last decades.[31-33] For patients with non-resectable colorectal liver metastases, radiofrequency ablation (RFA) offers an alternative treatment option. RFA involves induction of heat coagulation to destroy tumor tissue. Electrodes placed within the tumor tissue induce a high frequency alternating current resulting in friction heat due to ion movement. Cell death is eventually the result of coagulation necrosis, the irreversible thermal damage of tissue proteins at temperatures over 55-60˚C.[34,35] Using RFA, the initial achievable lesion size is approximately 2-3 cm. Inflow occlusion during RFA[36,37], usage of multiple probes[38] and internally cooled probes[39] are widely used techniques to increase the lesion size. However, despite these advances, the total tumor volume that can be ablated using RFA remains limited.

Nowadays, RFA is used in approximately one-third of all surgical procedures for metastatic colorectal cancer confined to the liver, either alone or in combination with resection.[40-42] Most studies on outcome following RFA for colorectal liver metastases involve patients with non-resectable disease. The EORTC-CLOCC trial was the first randomized study involving RFA for colorectal liver metastases, comparing chemotherapy alone with chemotherapy combined with RFA. Toxicity profiles were similar between the groups, but the primary endpoint (overall survival) was never reached due to poor recruitment.[43] In non-randomized studies, 5-year survival rates range from 15-30%[44-46], including 25-50% for patients with solitary liver metastases.[44,47-49] Nonetheless, since patients selected for partial liver resection are different from patients undergoing RFA, comparison of survival data following resection or RFA is not appropriate.[41] Although RFA is currently being used for small resectable liver metastases in approximately 10% of cases[50], randomized controlled trials are needed before RFA should be used as a replacement for resection of colorectal liver metastases in selected cases.

Recurrence following surgery for colorectal liver metastases

In approximately 60% of the patients undergoing surgery for colorectal liver metastases the disease will recur. Intrahepatic recurrences most often occur during the first two years following surgery.[50,51] Repeat hepatectomy for recurrent liver disease is only applicable in 10% of these patients.[50,52,53] As a consequence, RFA is increasingly used for recurrent liver metastases.[54-56]

RFA is accompanied by intrahepatic recurrence rates similar to surgical resection.[57] In addition to intrahepatic recurrence, local perinecrotic recurrence following RFA is encountered in approximately 9-18%.[40,58,59] Several factors have been reported to be related to higher local recurrence rates (up to 60%), such as the size of the tumor[58,60,61], location of the tumor adjacent to large vessels[60] and a percutaneous RFA approach.[58,62] Interestingly, the risk of developing local recurrence following RFA is higher in colorectal liver metastases, compared to hepatocellular carcinoma or non-colorectal metastases.[60]

Tumor recurrence following surgery for colorectal liver metastases may develop from two distinct sources. First, circulating tumor cells occurring peri- and postoperatively in 20-50% of cases may lead to recurrence.[63-65] Second, residual metastatic tumor cells or small micrometastases in the liver

may be present after surgery. Indeed, large patient series demonstrate that microscopic residual tumor deposits in the resection plane (R1 resection) occur in 5-10% of patients.[26-30] In addition, when using RFA, incomplete heat destruction of the tumor periphery will result in residual tumor tissue in the rim of the generated lesion. Moreover, studies on biopsies from remnant liver tissue show that occult hepatic micrometastases can be detected in 26-70% of patients with colorectal liver metastases.[66-69] These micrometastases can reside within the liver tissue in a state of dormancy for years.[70,71] Balanced apoptosis and proliferation in combination with angiogenesis suppression may result in non-growing micrometastases.[70,72] In addition, the adaptive immune system can hold micrometastases in a dormant state as well.[73] Events such as surgery may disturb this equilibrium, resulting in tumor outgrowth. Data on this possible disturbance due to surgery is lacking. Nonetheless, development of recurrent disease is strongly associated with the presence of residual micrometastases. In this thesis, the effects of liver surgery on the outgrowth of colorectal micrometastases are investigated.

Surgery-stimulated tumor growth

The role of wound healing and inflammation as a promoter of tumor development was mentioned for the first time by Virchow in the 1860s. Since that time, many studies have been published on the effects of wound healing on tumor growth. Taken together, these studies show that wounds create a pro-tumorigenic micro-environment caused by the presence of inflammatory cells producing growth factors, metalloproteases and cytokines.[74-77] Surgery, by definition, generates tissue injury and thereby induces wound healing. This may promote the outgrowth of local pre-existing micrometastases. Surgery may also stimulate the formation and growth of liver metastasis in several additional ways. Handling of the tumor during resection can result in dissemination of tumor cells into the circulation and into the peritoneal cavity.[63,78] Interestingly, preclinical studies show that surgical trauma promotes the implantation of tumor cells in the abdomen, due to increased tumor cell adhesion.[79-81] Furthermore, removal of the primary tumor may result in a growth induction of metastases in the liver, due to loss of anti-angiogenic factors that are produced by the primary tumor[72,82,83] and a possible shift in balance between apoptosis and proliferation of metastatic cells.[84] Finally, transient post-surgical immunosuppression may result in reduced function of anti-tumor immunity, which may facilitate the formation and outgrowth of micrometastases.[85,86]

Liver surgery and hypoxia

The effect of liver surgery on residual micrometastases has been the subject of many studies. Since liver resection is associated with regeneration of the remnant liver, many of these studies focused on the influence of liver regeneration on residual tumor tissue.[87-89] Local paracrine stimulation by factors related to liver regeneration, including cytokines and angiogenic factors, play an important role in the observed tumor growth stimulation.[90] Furthermore, in patients undergoing portal vein embolization to increase the future remnant liver volume following major liver resection, tumor progression has been observed.[91] In addition to liver regeneration and portal vein embolization, ischemia-reperfusion injury following vascular clamping during liver surgery stimulates the outgrowth of micrometastases.[92,93] Moreover, accelerated outgrowth of micrometastases following ischemia/reperfusion injury is associated with chronic tissue hypoxia.[94] To what extent ischemia/reperfusion-induced hypoxia drives accelerated tumor outgrowth remains to be elucidated. Nonetheless, hypoxia can induce adaptive changes in tumor cells resulting in tumor cell survival, including apoptosis

resistance[95] and shift to anaerobic metabolism.[96] In addition, hypoxia can stimulate invasion and migration of tumor cells.[97,98]
Hypoxia is a hallmark of wound healing[77,99] and is instrumental in recruiting endothelial progenitor cells from the bone marrow towards injured tissue.[100] Endothelial progenitor cells can promote tumor recurrence by induction of (neo)angiogenesis.[101] Indeed, challenging the tumor by treatment with vascular disrupting agents or chemotherapy results in tumor necrosis (injured tissue) but the tumor re-grows from the viable tumor rim aided by the recruitment of endothelial progenitor cells.[102,103] Moreover, liver surgery for colorectal liver metastases can induce a rise of endothelial progenitor cells as well.[104] The mechanisms causing this rise following liver surgery need to be elucidated.

Outline and research questions addressed in this thesis

This thesis studies factors that influence the development and outgrowth of colorectal liver metastases. As almost half of the primary colon carcinoma cells harbour mutations in the K-Ras oncogene, but relatively little is known about K-Ras in metastases, we first address the role of oncogenic K-Ras in metastasis formation by colorectal tumor cells in the liver (**chapter 2**). In this chapter, we concentrate on the survival of colon carcinoma cells in the hepatic micro-environment. The following chapters of this thesis describe how surgery affects residual tumor tissue. In the preclinical studies, the effects of liver surgery on the outgrowth of micrometastases are explored. Hypoxia is known to play an important role in ischemia/repefusion-induced outgrowth of colorectal liver metastases. Since hypoxia can induce rapid adaptations in tumor cells, we study the early effects of liver surgery on tumor cells. Additionally, we provide mechanistic insight into the underlying principles of surgery-induced hypoxia on micrometastasis behavior. For this purpose, a highly standardized murine model of colorectal micrometastases in the liver is used. Two different surgical techniques are used to assess the effects of surgery on micrometastatic outgrowth: radiofrequency ablation (RFA, **chapters 3-5**) and ischemia-reperfusion injury due to vascular clamping of the hepatic inflow (**chapter 6**).
In the clinical studies, we focus on the role of surgery in tumor recurrence. In **chapter 7** we investigate the effects of prolonged vascular clamping on tumor recurrence. Finally, since (endothelial) progenitor cells can play a role in tumor (recurrence) outgrowth, we study the influence of liver surgery on the release of (endothelial) progenitor cells (**chapter 8**).

The studies presented in this thesis were guided by the following research questions:

1. How does oncogenic K-Ras contribute to the metastatic potential of colorectal tumor cells? (**chapter 2**)
2. Does RFA promote the outgrowth of residual micrometastases and, if so, what drives this phenomenon? (**chapters 3-5**)
3. Does the same mechanism apply to ischemia/reperfusion-stimulated tumor outgrowth? (**chapter 6**)
4. Do the adverse effects of liver surgery as demonstrated in the murine models also apply to patients? (**chapters 7 and 8**).

References

1. Cho KR and Vogelstein B. Genetic alterations in the adenoma--carcinoma sequence. Cancer 1992; 70: 1727-1731.
2. Loupakis F, Pollina L, Stasi I, Ruzzo A, Scartozzi M, Santini D, Masi G, Graziano F, Cremolini C, Rulli E, Canestrari E, Funel N, Schiavon G, Petrini I, Magnani M, Tonini G, Campani D, Floriani I, Cascinu S, Falcone A. PTEN expression and K-RAS mutations on primary tumors and metastases in the prediction of benefit from cetuximab plus irinotecan for patients with metastatic colorectal cancer. J Clin Oncol 2009; 27: 2622-2629.
3. Roth AD, Tejpar S, Delorenzi M, Yan P, Fiocca R, Klingbiel D, Dietrich D, Biesmans B, Bodoky G, Barone C, Aranda E, Nordlinger B, Cisar L, Labianca R, Cunningham D, Van CE, Bosman F. Prognostic role of K-Ras and BRAF in stage II and III resected colon cancer: results of the translational study on the PETACC-3, EORTC 40993, SAKK 60-00 trial. J Clin Oncol 2010; 28: 466-474.
4. American Cancer Society. Cancer Facts & Figures 2008. Atlanta: American Cancer Society 2008.
5. Welch JP and Donaldson GA. The clinical correlation of an autopsy study of recurrent colorectal cancer. Ann Surg 1979; 189: 496-502.
6. Steele G, Jr. and Ravikumar TS. Resection of hepatic metastases from colorectal cancer. Biologic perspective. Ann Surg 1989; 210: 127-138.
7. Fidler IJ. The pathogenesis of cancer metastasis: the 'seed and soil' hypothesis revisited. Nat Rev Cancer 2003; 3: 453-458.
8. Smakman N, Borel Rinkes IH, Voest EE, Kranenburg O. Control of colorectal metastasis formation by K-Ras. Biochim Biophys Acta 2005; 1756: 103-114.
9. Liotta LA. Tumor invasion and metastases--role of the extracellular matrix: Rhoads Memorial Award lecture. Cancer Res 1986; 46: 1-7.
10. Fisher ER and Fisher B. Recent observations on concepts of metastasis. Arch Pathol 1967; 83: 321-324.
11. Fisher B and Fisher ER. The interrelationship of hematogenous and lymphatic tumor cell dissemination. Surg Gynecol Obstet 1966; 122: 791-798.
12. Seki S, Habu Y, Kawamura T, Takeda K, Dobashi H, Ohkawa T, Hiraide H. The liver as a crucial organ in the first line of host defense: the roles of Kupffer cells, natural killer (NK) cells and NK1.1 Ag+ T cells in T helper 1 immune responses. Immunol Rev 2000; 174: 35-46.
13. Kenna T, Golden-Mason L, Norris S, Hegarty JE, O'Farrelly C, Doherty DG. Distinct subpopulations of gamma delta T cells are present in normal and tumor-bearing human liver. Clin Immunol 2004; 113: 56-63.
14. Nicolson GL. Cancer metastasis: tumor cell and host organ properties important in metastasis to specific secondary sites. Biochim Biophys Acta 1988; 948: 175-224.
15. Folkman J. How is blood vessel growth regulated in normal and neoplastic tissue? G.H.A. Clowes memorial Award lecture. Cancer Res 1986; 46: 467-473.
16. Voulgari A, Voskou S, Tora L, Davidson I, Sasazuki T, Shirasawa S, Pintzas A. TATA box-binding protein-associated factor 12 is important for RAS-induced transformation properties of colorectal cancer cells. Mol Cancer Res 2008; 6: 1071-1083.
17. Cavallo-Medved D, Dosescu J, Linebaugh BE, Sameni M, Rudy D, Sloane BF. Mutant K-ras regulates cathepsin B localization on the surface of human colorectal carcinoma cells. Neoplasia 2003; 5: 507-519.
18. Cavallo-Medved D, Mai J, Dosescu J, Sameni M, Sloane BF. Caveolin-1 mediates the expression and localization of cathepsin B, pro-urokinase plasminogen activator and their cell-surface receptors in human colorectal carcinoma cells. J Cell Sci 2005; 118: 1493-1503.
19. Pollock CB, Shirasawa S, Sasazuki T, Kolch W, Dhillon AS. Oncogenic K-Ras is required to maintain changes in cytoskeletal organization, adhesion, and motility in colon cancer cells. Cancer Res 2005; 65: 1244-1250.
20. Derouet M, Wu X, May L, Hoon YB, Sasazuki T, Shirasawa S, Rak J, Rosen KV. Acquisition of anoikis resistance

promotes the emergence of oncogenic K-ras mutations in colorectal cancer cells and stimulates their tumorigenicity in vivo. Neoplasia 2007; 9: 536-545.
21. Bengmark S and Hafstrom L. The natural history of primary and secondary malignant tumors of the liver. I. The prognosis for patients with hepatic metastases from colonic and rectal carcinoma by laparotomy. Cancer 1969; 23: 198-202.
22. Bengtsson G, Carlsson G, Hafstrom L, Jonsson PE. Natural history of patients with untreated liver metastases from colorectal cancer. Am J Surg 1981; 141: 586-589.
23. de Brauw LM, van de Velde CJ, Bouwhuis-Hoogerwerf ML, Zwaveling A. Diagnostic evaluation and survival analysis of colorectal cancer patients with liver metastases. J Surg Oncol 1987; 34: 81-86.
24. Hurwitz H, Fehrenbacher L, Novotny W, Cartwright T, Hainsworth J, Heim W, Berlin J, Baron A, Griffing S, Holmgren E, Ferrara N, Fyfe G, Rogers B, Ross R, Kabbinavar F. Bevacizumab plus irinotecan, fluorouracil, and leucovorin for metastatic colorectal cancer. N Engl J Med 2004; 350: 2335-2342.
25. Tol J, Koopman M, Cats A, Rodenburg CJ, Creemers GJ, Schrama JG, Erdkamp FL, Vos AH, van Groeningen CJ, Sinnige HA, Richel DJ, Voest EE, Dijkstra JR, Vink-Borger ME, Antonini NF, Mol L, van Krieken JH, Dalesio O, Punt CJ. Chemotherapy, bevacizumab, and cetuximab in metastatic colorectal cancer. N Engl J Med 2009; 360: 563-572.
26. Fong Y, Fortner J, Sun RL, Brennan MF, Blumgart LH. Clinical score for predicting recurrence after hepatic resection for metastatic colorectal cancer: analysis of 1001 consecutive cases. Ann Surg 1999; 230: 309-318.
27. Choti MA, Sitzmann JV, Tiburi MF, Sumetchotimetha W, Rangsin R, Schulick RD, Lillemoe KD, Yeo CJ, Cameron JL. Trends in long-term survival following liver resection for hepatic colorectal metastases. Ann Surg 2002; 235: 759-766.
28. Rees M, Tekkis PP, Welsh FK, O'Rourke T, John TG. Evaluation of long-term survival after hepatic resection for metastatic colorectal cancer: a multifactorial model of 929 patients. Ann Surg 2008; 247: 125-135.
29. Wei AC, Greig PD, Grant D, Taylor B, Langer B, Gallinger S. Survival after hepatic resection for colorectal metastases: a 10-year experience. Ann Surg Oncol 2006; 13: 668-676.
30. Nuzzo G, Giuliante F, Ardito F, Vellone M, Giovannini I, Federico B, Vecchio FM. Influence of surgical margin on type of recurrence after liver resection for colorectal metastases: a single-center experience. Surgery 2008; 143: 384-393.
31. Mayo SC and Pawlik TM. Current management of colorectal hepatic metastasis. Expert Rev Gastroenterol Hepatol 2009; 3: 131-144.
32. Pawlik TM, Schulick RD, Choti MA. Expanding criteria for resectability of colorectal liver metastases. Oncologist 2008; 13: 51-64.
33. Poston GJ, Adam R, Alberts S, Curley S, Figueras J, Haller D, Kunstlinger F, Mentha G, Nordlinger B, Patt Y, Primrose J, Roh M, Rougier P, Ruers T, Schmoll HJ, Valls C, Vauthey NJ, Cornelis M, Kahan JP. OncoSurge: a strategy for improving resectability with curative intent in metastatic colorectal cancer. J Clin Oncol 2005; 23: 7125-7134.
34. Heisterkamp J, van Hillegersberg R, Ijzermans JN. Interstitial laser coagulation for hepatic tumours. Br J Surg 1999; 86: 293-304.
35. Nikfarjam M, Muralidharan V, Christophi C. Mechanisms of focal heat destruction of liver tumors. J Surg Res 2005; 127: 208-223.
36. Wiersinga WJ, Jansen MC, Straatsburg IH, Davids PH, Klaase JM, Gouma DJ, van Gulik TM. Lesion progression with time and the effect of vascular occlusion following radiofrequency ablation of the liver. Br J Surg 2003; 90: 306-312.
37. Ritz JP, Lehmann KS, Isbert C, Reissfelder C, Albrecht T, Stein T, Buhr HJ. In-vivo evaluation of a novel bipolar radiofrequency device for interstitial thermotherapy of liver tumors during normal and interrupted hepatic perfusion. J Surg Res 2006; 133: 176-184.
38. Goldberg SN, Gazelle GS, Dawson SL, Rittman WJ, Mueller PR, Rosenthal DI. Tissue ablation with radiofrequency using multiprobe arrays. Acad Radiol 1995; 2: 670-674.

39. Goldberg SN, Gazelle GS, Solbiati L, Rittman WJ, Mueller PR. Radiofrequency tissue ablation: increased lesion diameter with a perfusion electrode. Acad Radiol 1996; 3: 636-644.
40. Abdalla EK, Vauthey JN, Ellis LM, Ellis V, Pollock R, Broglio KR, Hess K, Curley SA. Recurrence and outcomes following hepatic resection, radiofrequency ablation, and combined resection/ablation for colorectal liver metastases. Ann Surg 2004; 239: 818-825.
41. Gleisner AL, Choti MA, Assumpcao L, Nathan H, Schulick RD, Pawlik TM. Colorectal liver metastases: recurrence and survival following hepatic resection, radiofrequency ablation, and combined resection-radiofrequency ablation. Arch Surg 2008; 143: 1204-1212.
42. Stang A, Fischbach R, Teichmann W, Bokemeyer C, Braumann D. A systematic review on the clinical benefit and role of radiofrequency ablation as treatment of colorectal liver metastases. Eur J Cancer 2009;
43. Ruers T, van Coevorden F, Pierie J, Borel Rinkes IH, Punt CJ, Lederman J, Poston GJ, Bechstein WO, Lentz M, Collette L, Nordlinger B. Radiofrequency ablation (RFA) combined with chemotherapy for unresectable colorectal liver metastases (CRC LM): Interim results of a randomised phase II study of the EORTC-NCRI CCSG-ALM Intergroup 40004 (CLOCC). Journal of Clinical Oncology, 2008 ASCO Annual Meeting Proceedings Vol 26 (May 20 suppl): abstract #4012.
44. Aloia TA, Vauthey JN, Loyer EM, Ribero D, Pawlik TM, Wei SH, Curley SA, Zorzi D, Abdalla EK. Solitary colorectal liver metastasis: resection determines outcome. Arch Surg 2006; 141: 460-466.
45. Gillams AR and Lees WR. Radio-frequency ablation of colorectal liver metastases in 167 patients. Eur Radiol 2004; 14: 2261-2267.
46. Machi J, Oishi AJ, Sumida K, Sakamoto K, Furumoto NL, Oishi RH, Kylstra JW. Long-term outcome of radiofrequency ablation for unresectable liver metastases from colorectal cancer: evaluation of prognostic factors and effectiveness in first- and second-line management. Cancer J 2006; 12: 318-326.
47. Berber E, Tsinberg M, Tellioglu G, Simpfendorfer CH, Siperstein AE. Resection Versus Laparoscopic Radiofrequency Thermal Ablation Of Solitary Colorectal Liver Metastasis. J Gastrointest Surg 2008; 12: 1967-1972.
48. Hur H, Ko YT, Min BS, Kim KS, Choi JS, Sohn SK, Cho CH, Ko HK, Lee JT, Kim NK. Comparative study of resection and radiofrequency ablation in the treatment of solitary colorectal liver metastases. Am J Surg 2009; 197: 728-736.
49. Abitabile P, Hartl U, Lange J, Maurer CA. Radiofrequency ablation permits an effective treatment for colorectal liver metastasis. Eur J Surg Oncol 2007; 33: 67-71.
50. de Jong MC, Pulitano C, Ribero D, Strub J, Mentha G, Schulick RD, Choti MA, Aldrighetti L, Capussotti L, Pawlik TM. Rates and patterns of recurrence following curative intent surgery for colorectal liver metastasis: an international multi-institutional analysis of 1669 patients. Ann Surg 2009; 250: 440-448.
51. Simmonds PC, Primrose JN, Colquitt JL, Garden OJ, Poston GJ, Rees M. Surgical resection of hepatic metastases from colorectal cancer: a systematic review of published studies. Br J Cancer 2006; 94: 982-999.
52. Adam R, Pascal G, Azoulay D, Tanaka K, Castaing D, Bismuth H. Liver resection for colorectal metastases: the third hepatectomy. Ann Surg 2003; 238: 871-883.
53. Petrowsky H, Gonen M, Jarnagin W, Lorenz M, DeMatteo R, Heinrich S, Encke A, Blumgart L, Fong Y. Second liver resections are safe and effective treatment for recurrent hepatic metastases from colorectal cancer: a bi-institutional analysis. Ann Surg 2002; 235: 863-871.
54. van der Pool AE, Lalmahomed ZS, de Wilt JH, Eggermont AM, Ijzermans JM, Verhoef C. Local treatment for recurrent colorectal hepatic metastases after partial hepatectomy. J Gastrointest Surg 2009; 13: 890-895.
55. Schindera ST, Nelson RC, Delong DM, Clary B. Intrahepatic tumor recurrence after partial hepatectomy: value of percutaneous radiofrequency ablation. J Vasc Interv Radiol 2006; 17: 1631-1637.
56. Elias D, de Baere T., Smayra T, Ouellet JF, Roche A, Lasser P. Percutaneous radiofrequency thermoablation as an alternative to surgery for treatment of liver tumour recurrence after hepatectomy. Br J Surg 2002; 89: 752-756.

57. Kosari K, Gomes M, Hunter D, Hess DJ, Greeno E, Sielaff TD. Local, intrahepatic, and systemic recurrence patterns after radiofrequency ablation of hepatic malignancies. J Gastrointest Surg 2002; 6: 255-263.
58. Mulier S, Ni Y, Jamart J, Ruers T, Marchal G, Michel L. Local recurrence after hepatic radiofrequency coagulation: multivariate meta-analysis and review of contributing factors. Ann Surg 2005; 242: 158-171.
59. Siperstein AE, Berber E, Ballem N, Parikh RT. Survival after radiofrequency ablation of colorectal liver metastases: 10-year experience. Ann Surg 2007; 246: 559-567.
60. Berber E and Siperstein A. Local Recurrence After Laparoscopic Radiofrequency Ablation of Liver Tumors: An Analysis of 1032 Tumors. Ann Surg Oncol 2008; 15: 2757-2764.
61. van Duijnhoven FH, Jansen MC, Junggeburt JM, van Hillegersberg R, Rijken AM, van Coevorden F, van der Sijp JR, van Gulik TM, Slooter GD, Klaase JM, Putter H, Tollenaar RA. Factors influencing the local failure rate of radiofrequency ablation of colorectal liver metastases. Ann Surg Oncol 2006; 13: 651-658.
62. Eisele RM, Neumann U, Neuhaus P, Schumacher G. Open Surgical is Superior to Percutaneous Access for Radiofrequency Ablation of Hepatic Metastases. World J Surg 2009; 33: 804-811.
63. Koch M, Kienle P, Hinz U, Antolovic D, Schmidt J, Herfarth C, von Knebel DM, Weitz J. Detection of hematogenous tumor cell dissemination predicts tumor relapse in patients undergoing surgical resection of colorectal liver metastases. Ann Surg 2005; 241: 199-205.
64. Topal B, Aerts JL, Roskams T, Fieuws S, Van PJ, Vandekerckhove P, Penninckx F. Cancer cell dissemination during curative surgery for colorectal liver metastases. Eur J Surg Oncol 2005; 31: 506-511.
65. Fruhauf NR, Kasimir-Bauer S, Gorlinger K, Lang H, Kaudel CP, Kaiser GM, Oldhafer KJ, Broelsch CE. Peri-operative filtration of disseminated cytokeratin positive cells in patients with colorectal liver metastasis. Langenbecks Arch Surg 2005; 390: 15-20.
66. Wakai T, Shirai Y, Sakata J, Valera VA, Korita PV, Akazawa K, Ajioka Y, Hatakeyama K. Appraisal of 1 cm hepatectomy margins for intrahepatic micrometastases in patients with colorectal carcinoma liver metastasis. Ann Surg Oncol 2008; 15: 2472-2481.
67. Linnemann U, Schimanski CC, Gebhardt C, Berger MR. Prognostic value of disseminated colorectal tumor cells in the liver: results of follow-up examinations. Int J Colorectal Dis 2004; 19: 380-386.
68. Nanko M, Shimada H, Yamaoka H, Tanaka K, Masui H, Matsuo K, Ike H, Oki S, Hara M. Micrometastatic colorectal cancer lesions in the liver. Surg Today 1998; 28: 707-713.
69. Yokoyama N, Shirai Y, Ajioka Y, Nagakura S, Suda T, Hatakeyama K. Immunohistochemically detected hepatic micrometastases predict a high risk of intrahepatic recurrence after resection of colorectal carcinoma liver metastases. Cancer 2002; 94: 1642-1647.
70. Holmgren L, O'Reilly MS, Folkman J. Dormancy of micrometastases: balanced proliferation and apoptosis in the presence of angiogenesis suppression. Nat Med 1995; 1: 149-153.
71. Luzzi KJ, MacDonald IC, Schmidt EE, Kerkvliet N, Morris VL, Chambers AF, Groom AC. Multistep nature of metastatic inefficiency: dormancy of solitary cells after successful extravasation and limited survival of early micrometastases. Am J Pathol 1998; 153: 865-873.
72. O'Reilly MS, Holmgren L, Shing Y, Chen C, Rosenthal RA, Moses M, Lane WS, Cao Y, Sage EH, Folkman J. Angiostatin: a novel angiogenesis inhibitor that mediates the suppression of metastases by a Lewis lung carcinoma. Cell 1994; 79: 315-328.
73. Koebel CM, Vermi W, Swann JB, Zerafa N, Rodig SJ, Old LJ, Smyth MJ, Schreiber RD. Adaptive immunity maintains occult cancer in an equilibrium state. Nature 2007; 450: 903-907.
74. Abramovitch R, Marikovsky M, Meir G, Neeman M. Stimulation of tumour growth by wound-derived growth factors. Br J Cancer 1999; 79: 1392-1398.
75. Baker DG, Masterson TM, Pace R, Constable WC, Wanebo H. The influence of the surgical wound on local tumor recurrence. Surgery 1989; 106: 525-532.
76. Hockel M and Dornhofer N. The hydra phenomenon of cancer: why tumors recur locally after microscopically complete resection. Cancer Res 2005; 65: 2997-3002.
77. Hofer SO, Molema G, Hermens RA, Wanebo HJ, Reichner JS, Hoekstra HJ. The effect of surgical wounding on tumour development. Eur J Surg Oncol 1999; 25: 231-243.

78. Schott A, Vogel I, Krueger U, Kalthoff H, Schreiber HW, Schmiegel W, Henne-Bruns D, Kremer B, Juhl H. Isolated tumor cells are frequently detectable in the peritoneal cavity of gastric and colorectal cancer patients and serve as a new prognostic marker. Ann Surg 1998; 227: 372-379.
79. ten Raa S, Oosterling SJ, van der Kaaij NP, van den Tol MP, Beelen RH, Meijer S, van Eijck CH, van der Sijp JR, van Egmond M, Jeekel J. Surgery promotes implantation of disseminated tumor cells, but does not increase growth of tumor cell clusters. J Surg Oncol 2005; 92: 124-129.
80. van den Tol MP, Ten RS, van Grevenstein WM, van Rossen ME, Jeekel J, van Eijck CH. The post-surgical inflammatory response provokes enhanced tumour recurrence: a crucial role for neutrophils. Dig Surg 2007; 24: 388-394.
81. van der Bij GJ, Oosterling SJ, Bogels M, Bhoelan F, Fluitsma DM, Beelen RH, Meijer S, van EM. Blocking alpha2 integrins on rat CC531s colon carcinoma cells prevents operation-induced augmentation of liver metastases outgrowth. Hepatology 2008; 47: 532-543.
82. O'Reilly MS, Boehm T, Shing Y, Fukai N, Vasios G, Lane WS, Flynn E, Birkhead JR, Olsen BR, Folkman J. Endostatin: an endogenous inhibitor of angiogenesis and tumor growth. Cell 1997; 88: 277-285.
83. Peeters CF, de Waal RM, Wobbes T, Ruers TJ. Metastatic Dormancy Imposed by the Primary Tumor: Does it Exist in Humans? Ann Surg Oncol 2008; 15: 3308-3315.
84. Peeters CF, de Waal RM, Wobbes T, Westphal JR, Ruers TJ. Outgrowth of human liver metastases after resection of the primary colorectal tumor: a shift in the balance between apoptosis and proliferation. Int J Cancer 2006; 119: 1249-1253.
85. Benish M, Bartal I, Goldfarb Y, Levi B, Avraham R, Raz A, Ben-Eliyahu S. Perioperative use of beta-blockers and COX-2 inhibitors may improve immune competence and reduce the risk of tumor metastasis. Ann Surg Oncol 2008; 15: 2042-2052.
86. Shakhar G and Ben-Eliyahu S. Potential prophylactic measures against postoperative immunosuppression: could they reduce recurrence rates in oncological patients? Ann Surg Oncol 2003; 10: 972-992.
87. de Jong KP, Lont HE, Bijma AM, Brouwers MA, de Vries EG, van Veen ML, Marquet RL, Slooff MJ, Terpstra OT. The effect of partial hepatectomy on tumor growth in rats: in vivo and in vitro studies. Hepatology 1995; 22: 1263-1272.
88. Drixler TA, Borel Rinkes IH, Ritchie ED, van Vroonhoven TJ, Gebbink MF, Voest EE. Continuous administration of angiostatin inhibits accelerated growth of colorectal liver metastases after partial hepatectomy. Cancer Res 2000; 60: 1761-1765.
89. Picardo A, Karpoff HM, Ng B, Lee J, Brennan MF, Fong Y. Partial hepatectomy accelerates local tumor growth: potential roles of local cytokine activation. Surgery 1998; 124: 57-64.
90. Christophi C, Harun N, Fifis T. Liver Regeneration and Tumor Stimulation-A Review of Cytokine and Angiogenic Factors. J Gastrointest Surg 2008; 12: 966-980.
91. de Graaf W, van den Esschert JW, van Lienden KP, van Gulik TM. Induction of tumor growth after preoperative portal vein embolization: is it a real problem? Ann Surg Oncol 2009; 16: 423-430.
92. Man K, Ng KT, Lo CM, Ho JW, Sun BS, Sun CK, Lee TK, Poon RT, Fan ST. Ischemia-reperfusion of small liver remnant promotes liver tumor growth and metastases--activation of cell invasion and migration pathways. Liver Transpl 2007; 13: 1669-1677.
93. van der Bilt JD, Kranenburg O, Nijkamp MW, Smakman N, Veenendaal LM, Te Velde EA, Voest EE, van Diest PJ, Borel Rinkes IH. Ischemia/reperfusion accelerates the outgrowth of hepatic micrometastases in a highly standardized murine model. Hepatology 2005; 42: 165-175.
94. van der Bilt JD, Soeters ME, Duyverman AM, Nijkamp MW, Witteveen PO, van Diest PJ, Kranenburg O, Borel Rinkes IH. Perinecrotic hypoxia contributes to ischemia/reperfusion-accelerated outgrowth of colorectal micrometastases. Am J Pathol 2007; 170: 1379-1388.
95. Dong Z, Nishiyama J, Yi X, Venkatachalam MA, Denton M, Gu S, Li S, Qiang M. Gene promoter of apoptosis inhibitory protein IAP2: identification of enhancer elements and activation by severe hypoxia. Biochem J 2002; 364: 413-421.
96. Dang CV and Semenza GL. Oncogenic alterations of metabolism. Trends Biochem Sci 1999; 24: 68-72.

97. Semenza GL. Targeting HIF-1 for cancer therapy. Nat Rev Cancer 2003; 3: 721-732.
98. Harris AL. Hypoxia--a key regulatory factor in tumour growth. Nat Rev Cancer 2002; 2: 38-47.
99. van der Bilt JD and Borel Rinkes IH. Surgery and angiogenesis. Biochim Biophys Acta 2004; 1654: 95-104.
100. Ceradini DJ and Gurtner GC. Homing to hypoxia: HIF-1 as a mediator of progenitor cell recruitment to injured tissue. Trends Cardiovasc Med 2005; 15: 57-63.
101. Carmeliet P. Angiogenesis in life, disease and medicine. Nature 2005; 438: 932-936.
102. Shaked Y, Ciarrocchi A, Franco M, Lee CR, Man S, Cheung AM, Hicklin DJ, Chaplin D, Foster FS, Benezra R, Kerbel RS. Therapy-induced acute recruitment of circulating endothelial progenitor cells to tumors. Science 2006; 313: 1785-1787.
103. Shaked Y, Henke E, Roodhart JM, Mancuso P, Langenberg MH, Colleoni M, Daenen LG, Man S, Xu P, Emmenegger U, Tang T, Zhu Z, Witte L, Strieter RM, Bertolini F, Voest EE, Benezra R, Kerbel RS. Rapid chemotherapy-induced acute endothelial progenitor cell mobilization: implications for antiangiogenic drugs as chemosensitizing agents. Cancer Cell 2008; 14: 263-273.
104. Lemoli RM, Catani L, Talarico S, Loggi E, Gramenzi A, Baccarani U, Fogli M, Grazi GL, Aluigi M, Marzocchi G, Bernardi M, Pinna A, Bresadola F, Baccarani M, Andreone P. Mobilization of bone marrow-derived hematopoietic and endothelial stem cells after orthotopic liver transplantation and liver resection. Stem Cells 2006; 24: 2817-2825.

Chapter 2

Oncogenic K-Ras turns death receptors into metastasis-promoting receptors in human and mouse colorectal cancer cells

Gastroenterology 2010; 137: 2357-2367

Frederik J.H. Hoogwater[1]
Maarten W. Nijkamp[1*]
Niels Smakman[1*]
Ernst J.A. Steller[1]
Benjamin L. Emmink[1]
B. Florien Westendorp[1]
Danielle A.E. Raats[1]
Martin R. Sprick[2]
Uta Schaefer[3]
Winan J. van Houdt[1]
Menno T. de Bruijn[1]
Ron C.J. Schackmann[1]
Patrick W.B. Derksen[1]
Jan-Paul Medema[3]
Henning Walczak[4]
Inne H.M. Borel Rinkes[1]
Onno Kranenburg[1]

[*] these authors contributed equally

Departments of [1]Surgery and [2]Medical Oncology, University Medical Center Utrecht, Utrecht, The Netherlands
[3]Laboratory of Experimental Oncology and Radiobiology, Academic Medical Center, Amsterdam, The Netherlands
[4]Department of Immunology, Division of Medicine, Imperial College London, London, UK

Abstract

Background
Death receptors expressed on tumor cells can prevent metastasis formation by inducing apoptosis, but they can also promote migration and invasion. The determinants of death receptor signaling output are poorly defined. Here we investigated the role of oncogenic K-Ras in determining death receptor function and metastatic potential.

Methods
Isogenic human and mouse colorectal cancer cell lines differing only in the presence or absence of the K-Ras oncogene were tested in apoptosis and invasion assays using CD95 ligand and TRAIL as stimuli. Metastatic potential was assessed by intrasplenic injections of GFP- or luciferase-expressing tumor cells, followed by intravital fluorescence microscopy or bioluminescence imaging, and confocal microscopy and immunohistochemistry. Ras-effector pathway control of CD95 output was assessed by an RNA-interference and inhibitor-based approach.

Results
CD95 ligand and TRAIL stimulated invasion of colorectal tumor cells and liver metastases in a K-Ras-dependent fashion. Loss of mutant K-Ras switched CD95 and TRAIL receptors back into apoptosis mode and abrogated metastatic potential. Raf1 was essential for the switch in CD95 function, for tumor cell survival in the liver and for K-Ras-driven formation of liver metastases. K-Ras and Raf1 suppressed ROCK/LIM kinase-mediated phosphorylation of the actin-severing protein cofilin. Overexpression of ROCK or LIM kinase allowed CD95L to induce apoptosis in K-Ras-proficient cells and prevented metastasis formation, while their suppression protected K-Ras-deficient cells against apoptosis.

Conclusions
Oncogenic K-Ras and its effector Raf1 convert death receptors into invasion-inducing receptors by suppressing the ROCK/LIM kinase pathway and this is essential for K-Ras/Raf1-driven metastasis formation.

Introduction

Metastasis formation by colorectal tumors occurs primarily in the liver and is the major determinant of patient survival. The mutations that drive initiation and progression of primary colorectal carcinomas have been well documented.[1] Mutational inactivation of the *APC* and *TP53* tumor suppressor genes and activating mutations in the *K-Ras* proto-oncogene are by far the most frequently occurring mutations driving human colorectal tumorigenesis.[1,2] Large-scale sequence analysis of paired primary and metastatic tumors has shown that invasive carcinomas and metastases share the vast majority of their mutations and that once an invasive carcinoma has formed, metastasis formation ensues relatively rapidly, possibly without the requirement for additional mutations.[3] This implies that (part of) the genetic changes that cause the formation of invasive primary carcinomas may also drive metastasis formation, at least in colorectal cancer.[3]

One of the first genes to be mutated during the course of colorectal cancer development in humans is the proto-oncogene *K-Ras*. Activated *Ras* genes promote tumor cell motility, invasion and survival in a number of distinct cell types.[4] However, it remains unclear how endogenous oncogenic *K-Ras* alleles, in the presence of a multitude of other genetic alterations, contribute to the metastatic potential of colorectal tumor cells.

Metastasis formation can be suppressed by the activation of death receptors on tumor cells.[5-8] Among the best studied death receptors are CD95 and TNF-related apoptosis-inducing ligand (TRAIL) receptors.[9] Apoptosis has long been thought to be the primary outcome of death receptor activation and this has lead to the development of death receptor-stimulating agents as anti-tumor therapeutics.[9] However, more recent data suggest that CD95 and TRAIL receptors can also act in a pro-tumorigenic fashion by stimulating tumor cell proliferation, survival and invasion.[10-15]

The determinants of death receptor signalling output are poorly defined. Here we provide evidence that endogenous oncogenic K-Ras transforms anti-metastatic death receptors into invasion-stimulating pro-metastatic ones. We further show that Raf1-mediated suppression of the Rho kinase (ROCK)/LIM kinase pathway is responsible for death receptor transformation downstream of K-Ras and for K-Ras-driven metastasis formation.

Materials and Methods

Cell lines and cell cultures

C26 cells were obtained from the American Type Tissue Culture Collection (ATCC, Rockville, MD). C26 cell lines in which the endogenous K-Ras^{D12} allele is stably suppressed by RNA interference (C26-K-RASKD) and control cells (C26-pLL) were described before.[16] HCT116 and DLD1 cells and their isogenic derivatives lacking K-Ras^{D13} (Hkh2 and DKO4 respectively) were kindly provided by Dr Shirasawa and were described before.[17] HCT116 cells lacking β-catenin$^{\Delta S45}$ and p53 were kindly provided by Dr B Vogelstein. C26 cells expressing the firefly luciferase gene (C26-luc) were described previously.[18] All cells were cultured in Dulbecco's Modified Eagle's Medium (DMEM; Dulbecco, ICN Pharmaceuticals, Costa Mesa, CA) supplemented with 5% (v/v) fetal calf serum, 2 mM glutamine, 0.1 mg/ml streptomycin, and 100 U/ml penicillin. All cells were kept at 37°C in a humidified atmosphere containing 5% CO_2. A manuscript describing the isolation and characterization of the patient-derived colorectal spheroid cultures is currently in preparation.

Lentiviral transduction
Lentiviral transductions were performed as described.[18] All lentiviral constructs are specified below.

Animals and surgery
Colorectal liver metastases were induced as described, using male BALB/c or BALB/c-AnNCrl-*Nu*BR mice aged 8-10 weeks (Charles River Laboratories, Maastricht, The Netherlands).[18] In separate experiments C26-luc, C26-KrasKD-luc, DLD1-luc, or DKO4-luc cells, suspended in 50 µl PBS, were injected just under the capsule of the left liver lobe aftera midline abdominal incision.

Intravital microscopy
Liver metastases were induced by intrasplenic injection as described above. On post-operative days (POD) 0, 3, and 7 (n=3/day/group) the liver was exposed through a midline abdominal incision. Intravital fluorescence microscopy was performed using a Nikon TE-300 inverted microscope (Uvikon, The Netherlands). 10 random fields (magnification 100X) per animal were recorded digitally with a charge coupled device camera (Exwave HAD, Sony, The Netherlands) and stored for off-line data analysis. Data are average counts performed by two independent observers blinded to treatment.

Confocal microscopy
Cells were fixed in 3.7% formaldehyde for 10 minutes and were subsequently permeabilized (PBS 0.05% TritonX100; 1% BSA; 2 min) and blocked (PBS 3% BSA; 1h). Anti-CD95 primary antibody and FITC-coupled secondary antibody with Alexa-568-conjugated phalloidin were incubated for 1 hour. Coverslips were mounted in Vectashield with DAPI (H-1200, Vectorlabs). Image acquisition and analysis was performed using a Zeiss Axiovert 200M and Zeiss LSM 510 Software.

Viability assays
Cells (5000 cells/96-well) were stimulated with CD95L (2 ng/ml to 10 ng/ml) or TRAIL (25 ng/ml to 100 ng/ml) and viability was analyzed 24h later by 3-(4,5dimethylthiazolyl-2)-2,5-diphenyltetrazoleumbromide (MTT) assays (Roche Diagnostics) according to the manufacturer's instructions. For anoikis assays the cells were cultured under non-adherent conditions at 37°C in a humidified atmosphere under constant low speed rotation. Cells were collected by centrifugation (1500 rpm, 3 min) at the indicated time points and cell viability was subsequently assessed by MTT assays.

CD95 ligand, TRAIL and anti-CD95
The following reagents were used in this study: CD95 Ligand (FasL), membrane bound (#01-210) from Upstate Cell Signaling Solutions, Lake Placid, NY. HisTRAIL: The bacterial expression plasmid pETdwHisTRAIL(114-281) for human TRAIL was kindly provided by Dr. D.W. Seol. His-TRAIL was purified by using the His-bind Resins beads and buffer systems from Novagen. Recombinant isoleucine zipper-tagged murine TRAIL (izmuTRAIL) was generated and purified as described.[19] To remove endotoxins, an additional washing step with 0.1% Triton-X-114 was used during the purification procedure. The protocol for endotoxin removal was adapted from.[20] Anti-CD95 CH11 was used at a concentration of 10 ng/ml.

FACS analysis

For cell surface CD95 expression, the cells were plated onto six-well plates at a density of $4x10^5$ cells/well. 24 Hours after plating the cells were trypsinized, washed in PBS/BSA 1% and incubated for 1 hour on ice with anti-CD95 (CH11). Secondary antibodies were fluorescein isothiocyanate-conjugated anti-mouse IgM. For sub-G1 DNA content analysis, cells were stimulated with either CD95L or TRAIL and were harvested by centrifugation, washed with PBS and then fixed in chilled 80% ethanol on ice. The cells were washed and suspended in PBS and treated with RNase A (200 µg/ml) at room temperature for 30 min. The cells were then stained with Propidium Iodide (50 µg/ml) for 30 min. All samples were analyzed using a FACSCalibur flow cytometer (Becton Dickinson, San Jose, CA, USA).

C26-KrasKD cells were transfected with the dominant-negative GFP-LIMK-kinase dead mutant and cells were either left untreated or were stimulated with CD95L (10 ng/ml) overnight. Cells were trypsinized and stained with propidium iodide to determine the amount of apoptotic (PI-positive) cells by FACS.

Live cell imaging and motility assays

Cells were seeded in a Lab-Tek® Chambered #1.0 Borosilicate Coverglass System (Nalgene Nunc International, Rochester, NY14625, USA) and were mounted on a Zeiss Axiovert 200M microscope for live cell imaging (5% CO2; 37°C) overnight. Phase contrast images were captured every 5 min using a Photometrics Coolsnap CCD camera (Scientific, Tucson, AZ). Images were processed using Metamorph software (Universal Imaging, Downington, PA). The number of cells displaying membrane ruffling was scored by off-line analysis of the generated videos and plotted as means ± SEM from all cells in 20 videos from 3 independent dishes. For motility assays cells were filmed for 48h (20 videos; 3 dishes). The average speed of tumor cells in each dish was then quantified in pixels per hour. For studying directed cell migration either CD95L or isoleucine-zipper-tagged murine TRAIL (iz-muTRAIL) were mixed with soluble Matrigel which was then allowed to solidify in a small droplet in the middle of a culture dish in 24 well format. Cells were seeded into the dish and allowed to migrate towards, or away from, the Matrigel during 24h incubation. Cells were then fixed and stained with crystal violet.

Invasion assay

Invasion was measured using 24-well BioCoat Matrigel invasion chambers (BD Biosciences, Alphen aan den Rijn, The Netherlands) according to the manufacturer's instructions using CD95L (20 ng/ml) or iz-muTRAIL (200 ng/ml) as stimuli.

Immunohistochemistry

Mouse livers were harvested and fixed in 4% buffered formaldehyde and embedded in paraffin for further immunohistochemical processing. Anti-active caspase 3 was used for assessment of apoptotic tumor cells. As secondary antibody PowerVision+ (Immunologic, Duiven, The Netherlands) with 2% mouse serum was used. Reactions were developed using diaminobenzidine/H_2O_2 as a chromogen substrate. Primary antibody-omitted negative controls were treated with the antibody diluent alone and were all free of non-specific background staining. Quantification was performed by counting the number of active capase-3-positive cells in 20 randomly chosen high-power fields in 3 non-consecutive tissue sections in 4 mice. The bar diagrams represent the average numbers of caspase-3-positive cells per field in 20x3x4 fields.

TRAIL treatment *in vivo*

Mice carrying 2-day micrometastases received isoleucine zipper-tagged murine TRAIL (iz-muTRAIL; 6 mg/kg bodyweight/day) (n=4) or vehicle (n=4) for 2 days via tail vein injections. Livers were then harvested and analyzed by confocal microscopy. The length of the longest distance between tumor cells in each metastasis was measured in 10 randomly chosen metastases per mouse using Zeiss LSM image examiner software. These values were used to calculate the average longest trail-length within metastases in control- and TRAIL-treated animals.

Cell fractionation

Cells were lysed in 0.1% Triton buffer (20 mM Hepes pH7.4, 0.1% TrirtonX100, 150 mM NaCl, 5 mM MgCl2, 10% glycerol). Lysates were then cleared by sequential low speed (13.000 rpm Eppendorff tablecentrifuge) and high speed (Beckmann airfuge, 100.000g) centrifugation at 4°C.

Antibodies and reagents

The following antibodies were obtained from Cell Signaling Technology Inc., Danvers, MA: mouse anti-caspase-8 (1C12, #9746), rabbit anti-FADD (human specific, #2782), anti-Raf1 (#9422), anti-A-Raf (#4432) anti-B-Raf (L12G7, #9434), phospho-ERK1/2 T202/T204 (#9101), phospho-Akt Ser473 (193H12, #4058), anti-Akt (#9272), phospho-cofilin S3 (#3311), cofilin (#3312), phospho-ezrin Thr567 (#3141), ezrin (#3145), and anti-RalB (#35235). Mouse anti-Fas (human, activating), clone CH11 (#05-201) was obtained from Upstate Cell Signaling Solutions, Lake Placid, NY. Anti-human TRAILR1/DR4 was obtained from R&D Systems Europe Ltd., Abingdon, UK (#AF347). Anti-DR5 (#160770) was obtained from Cayman Chemical, Ann Arbor, MI. Anti-FLIP (F9800) was obtained from Sigma-Aldrich, Saint Louis, Missouri. Mouse anti-Bcl2 (#M0887, clone 124) was obtained from DAKO, DK-2600 Glostrup, Denmark. Anti-active caspase 3 for immunohistochemistry (BD559565), anti-RalA (BD610221) and anti-ROCK (BD611136) were obtained from BD Biosciences, San Jose, USA. Mouse anti-β-actin was purchased from Novus Biological, Littleton, CO (NB 600-501).

Expression vectors

The cDNA encoding dominant-negative FADD (DN-FADD) was cut from pRVQ7- FADD-DN (kindly provided by Dr. J. Borst) by using BamH1/Xho1, and ligated into BamH1/Sal1-cut pWPT-GFP to generate pWPT-dnFADD. pWPT-GFP and the lentiviral packaging system were kindly provided by Prof D. Trono. All lentiviral knockdown vectors were in the pLKO1 background and were purchased from Open Biosystems (Huntsville Al, USA). A panel of 5 constructs was tested for each set. The following vectors were used for stable knockdown of Raf1 (TRCN0000055140 (#1), TRCN0000055138 (#2),TRCN0000055142 (#3)), B-Raf (TRCN0000054345), RalA (TRCN0000004867, TRCN0000004868), RalB (TRCN0000072954, TRCN0000072955). The ROCK targeting sequences were: TGTCGAAGATGCCATGTTA (#1) and GACCTTCAAGCACGAATTA (#2) were cloned into the lentiviral shRNA vector pLV-THM (AddGene). The lentiviral constructs targeting Erk1 and Erk2 were kindly provided by Dr Riccardo Brambilla and were described before.[21] pREP4-Bcl2 was kindly provided by Dr. A Shvarts. The caspase-8a and –b open reading frames were excised from pIRES2-GFP-caspase-8 together with parts of the GFP and the CMV-promoter sequence. Subsequently, they were ligated into a modified pWPTS (Addgene). The final constructs were verified by sequencing. pRRL-CMV-luciferase was kindly provided by Dr. RC Hoeben. Expression constructs for GFP-LIMK

and GFP-LIMKkinase-dead[22] were kindly provided by Prof John Condeelis. The expression construct for constitutively active ROCK (ROCKΔ3)[23] was kindly provided by Prof Christopher Chen.

Statistical Analysis

Differences between groups were evaluated using the Mann-Whitney test. Results are presented as means ± standard error of the mean. All P values were two-tailed. $P < 0.05$ was considered statistically significant.

Results

An essential role for oncogenic K-Ras in liver metastasis formation

To assess the contribution of endogenous oncogenic K-Ras to liver metastasis formation we analyzed how deletion or suppression of endogenous oncogenic *K-Ras* alleles from colorectal tumor cells affected tumor growth in the liver when compared to subcutaneous tumor growth.

DLD1 cells and isogenic cells lacking *K-Ras*^{D13} (DKO4) were injected into the liver parenchyma. DLD1 cells formed liver tumors in all injected mice, but DKO4 cells were unable to form liver tumors (Figure 1A, Table 1). However, the *in vitro* proliferation rate for this pair of isogenic cells was very similar and both cell lines formed subcutaneous tumors with an incidence of 100% (Table 1). Subcutaneous DKO4 tumors did not acquire de novo mutations in the remaining wildtype allele during tumor formation (data not shown).

Table 1

Cell line	K-Ras/Kras status	Injection site	Incidence (%)	Invasion	Morbidity
DLD1	D13/wt	subcutaneous	100 (7/7)	yes	yes
DKO4	Δ/wt		100 (7/7)	no	no
C26-pLL	D12/-		100 (7/7)	yes	yes
C26-KrasKD	D12-KD/-		30 (3/10)	no	no
DLD1	D13/wt	spleen	0 (0/7)	-	-
DKO4	Δ/wt		0 (0/7)	-	-
C26-pLL	D12/-		100 (7/7)	yes	yes
C26-KrasKD	D12-KD/-		0 (0/6)	-	-
DLD1	D13/wt	liver	100 (6/6)	yes	yes
DKO4	Δ/wt		42 (3/7)*	NA	no
C26-pLL	D12/-		100 (6/6)	yes	yes
C26-KrasKD	D12-KD/-		0 (0/6)	-	-

Deletion of oncogenic K-Ras abrogates liver tumor formation but not subcutaneous tumor growth. DLD1, DKO4, C26-pLL and C26-KrasKD cells were injected either subcutaneously, into the spleen or under the liver capsule. The effect of tumor growth on health score was monitored as in[3] and post mortem analysis of skin invasion was performed by Haematoxilin and Eosin histochemistry. Subcutaneous tumor growth was measured by standard caliper measurements; liver tumor growth was measured by bioluminescence. D12-KD: Stable knockdown of the K-Ras^{D12} mRNA.[3] C26 cells have lost the wildtype K-Ras allele. *Although very low bioluminescence signals were detected in 3/7 livers injected with DKO4 cells, the tumors remained extremely small over time and had no effect on the health status of the mice (See Figure 1A). NA: not analyzed.

Next, we tested whether suppression of K-Ras^{D12} in C26 cells (C26-KrasKD) had a similar selective effect on liver tumor formation. C26 control cells formed tumors both in the liver and under the skin with 100% incidence (Figure 1B, Table 1). C26-KrasKD cells failed to form liver tumors, either when cells were injected via the spleen or directly into the liver parenchyma (Figure 1B, Table 1), but were able to form benign, non-invasive subcutaneous tumors in 30-40% of the mice (Table 1, Smakman *et al.*[16]). Intravital microscopy showed that the inability of C26-KrasKD cells to form liver tumors was

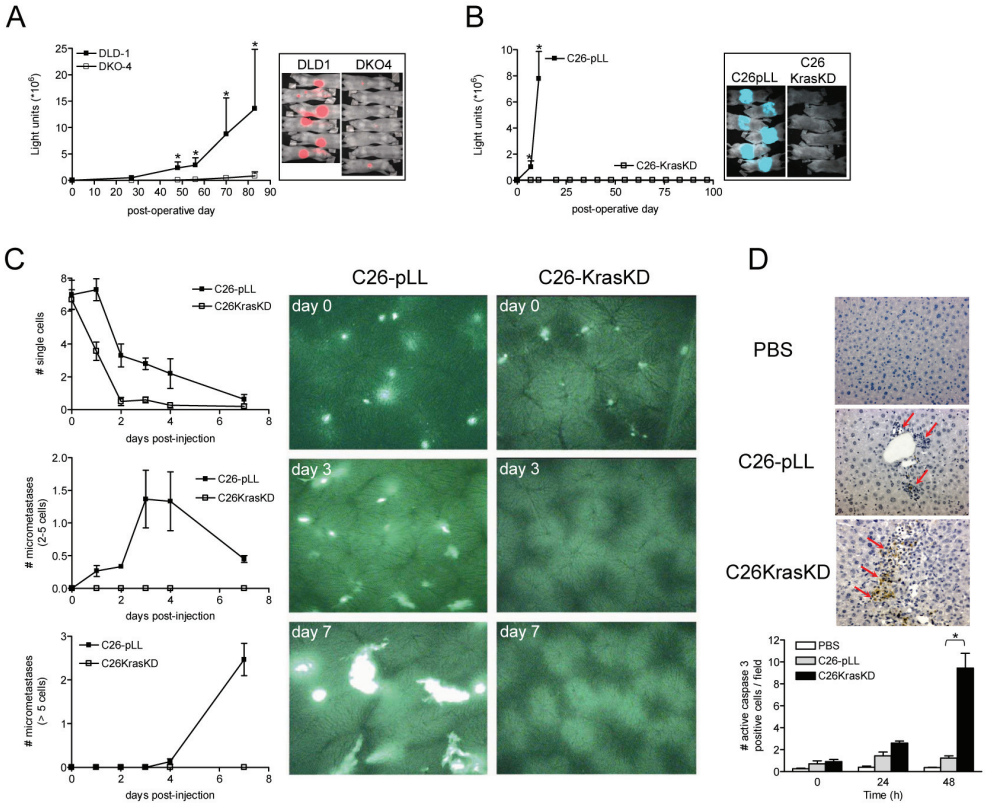

Figure 1 Oncogenic K-Ras is essential for liver metastasis formation and for tumor cell survival in the sinusoids

(A) Luciferase-expressing DLD1 and DKO4 cells were injected directly into the liver parenchyma of immune-deficient BALB/c$^{nu/nu}$ mice (n=7) and bioluminescence imaging was used to detect tumor growth over time. **(B)** Luciferase-expressing C26-pLL and C26-KrasKD cells were injected into the spleen of syngenic BALB/c mice (n=6) and liver metastasis formation was assessed over time by bioluminescence imaging. **(C)** EGFP-expressing C26-pLL and C26-KrasKD cells were injected into the spleens of BALB/c mice (n=3) and tumor cell fate in the liver sinusoids was followed by intravital microscopy. The number of single cells in the liver sinusoids and the development of micrometastases (2-5 cells and >5 cells) was then scored by off-line analysis of the generated videos. Quantification of these data is shown in the left panel. Stills from representative videos are shown in the right panel. **(D)** After intrasplenic injection of C26-pLL and C26-KrasKD cells, the livers were harvested at the indicated time points. The number of apoptotic cells was then assessed by immunohistochemistry using an antibody recognizing activated (cleaved) caspase-3 and the number of active caspase-3 positive cells was quantified as detailed in the M&M section. * $p<0.05$. All data are presented as means ± SEM.

caused by a rapid clearance of tumor cells from the liver (Figure 1C). Immunohistochemistry on liver tissue sections revealed the presence of high numbers of apoptotic (active caspase-3-positive) tumor cells in mice injected with C26-KrasKD cells but not in mice injected with control C26 cells (Figure 1D). These results suggest that endogenous oncogenic K-Ras is required for tumor cell resistance to apoptotic stimuli in the liver.

Oncogenic K-Ras provides resistance to apoptosis induced by death receptor ligands

Metastatic tumor cells have to survive the apoptotic stimulus that results from loss of adhesion (anoikis). In addition, immune cells in the liver attack tumor cells, in part by producing death receptor ligands like CD95L and TRAIL.

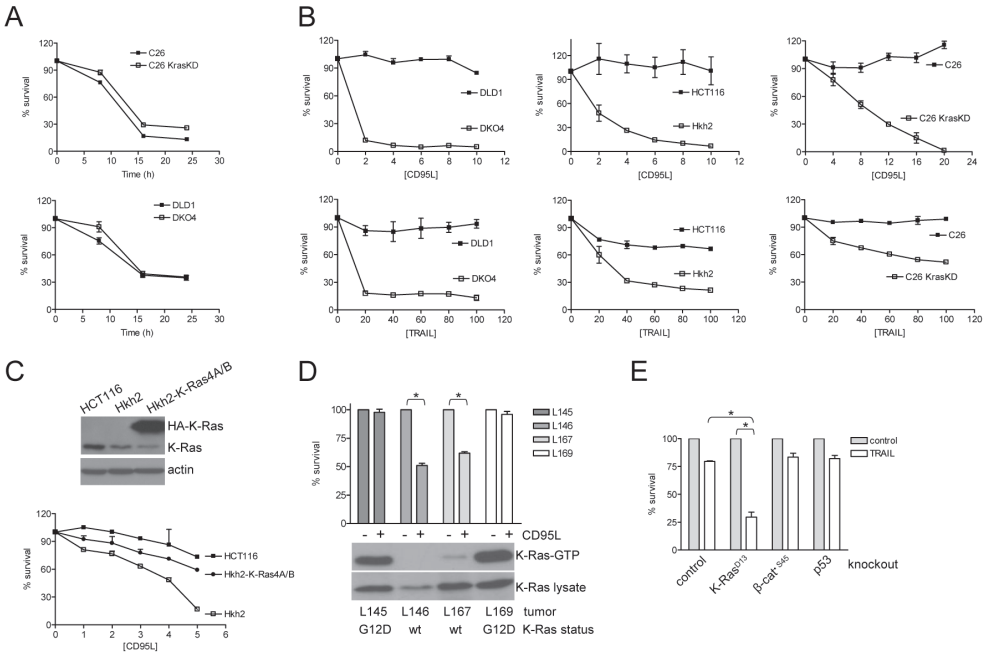

Figure 2 Oncogenic K-Ras provides resistance to apoptosis induced by death receptor ligands, but not by anoikis

(A) C26, C26-KrasKD, DLD1 and DKO4 cells were cultured under non-adherent conditions for the indicated periods of time and cell viability was then measured by MTT assays. The data shown represent means of triplicates. **(B)** DLD1 and DKO4, HCT116 and Hkh2, and C26 and C26-KrasKD cells were treated with CD95L (2-10 and 4-20 ng/ml), hisTRAIL (20-100 ng/ml) or iz-muTRAIL (20-100 ng/ml) for 24 hours. Cell viability was then assessed by MTT assays. **(C)** Hkh2 cells were transduced with lentiviral expression vectors for HA-tagged K-Ras4A and -4B. These cells were exposed to CD95L and cell viability was measured as in B. **(D)** Spheroid cultures were established from biopsies of liver metastases of 4 different colon cancer patients. Single cell suspensions were prepared and these were stimulated overnight with CD95L (6 ng/ml). Cell viability was assessed as above. The presence of active (GTP-bound) K-Ras was analyzed in parallel using lysates of the same cell lines (lower panel). K-Ras mutation status was analyzed by sequencing and is indicated at the bottom. **(E)** HCT116, Hkh2, HCT116$^{\Delta-\beta CAT\Delta S45}$ and HCT116$^{p53-/-}$ cells were treated with hisTRAIL (100 ng/ml) for 24h and cell viability was assessed as above. Data are presented as means ± SEM. * $p<0.05$.

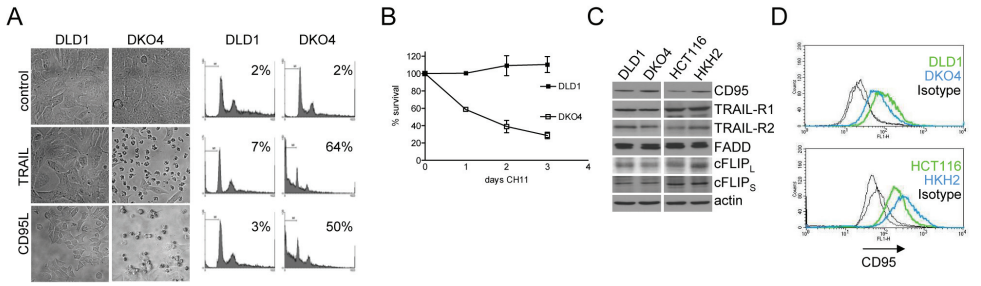

Figure 3 Oncogenic K-Ras protects colorectal cancer cells from CD95-induced apoptosis without affecting expression of DISC components
(A) DLD1 and DKO4 cells were treated with CD95L (6 ng/ml) or TRAIL (20 ng/ml) overnight. Cells were then photographed (left panels), stained with propidium iodide and analyzed by FACS (right panels). The percentage of apoptotic cells (with sub-G1 DNA content) is indicated in the graphs. **(B)** DLD1 and DKO4 cells were treated with the agonistic anti-CD95 CH11 antibody (10 ng/ml) for 3 consecutive days and cell viability was then assessed by standard MTT assays. **(C)** DLD1, DKO4, HCT116 and HKH2 cells were lysed and the steady state levels of FADD, cFLIP$_L$, and cFLIP$_S$ were analyzed by Western blotting. **(D)** Cell surface levels of CD95 on HCT116, Hkh2, DLD1 and DKO4 cells were tested by FACS analysis.

The K-Ras status had no discernable effect on anoikis in DLD1 and C26 cells (Figure 2A). However, tumor cells lacking oncogenic K-Ras (DKO4, Hkh2 and C26-KrasKD) were highly sensitive to apoptosis induction by CD95L and TRAIL and by the CD95 agonistic antibody CH11 (Figures 2B, 3A and 3B). Re-expression of oncogenic K-Ras in Hkh2 cells provided renewed resistance to CD95L-induced apoptosis (Figure 2C).
We next used four low-passage spheroid cultures that were established from freshly resected liver metastases of colorectal cancer patients. Two of these cultures expressed wildtype K-Ras and two expressed constitutively active oncogenic K-Ras (G12D) (Figure 2D). Spheroid cultures expressing wildtype K-Ras rapidly lost viability (~50%) following overnight exposure to CD95L (Figure 2D), whereas those expressing oncogenic K-Ras were resistant.

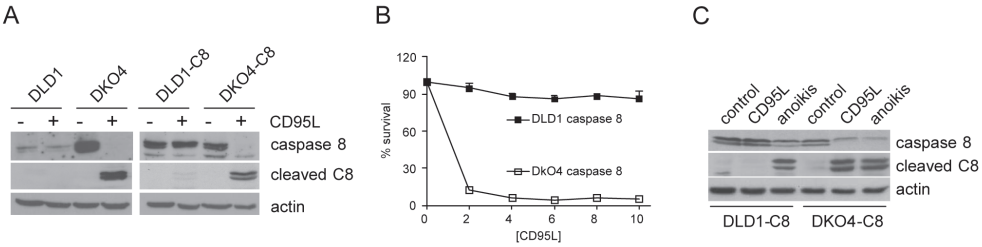

Figure 4 Oncogenic K-Ras prevents caspase-8 cleavage in response to CD95L, but not during anoikis
(A) DLD1 and DKO4 cells and DLD1 and DKO4 cells ectopically expressing caspase-8a and -8b (DLD1-C8, DKO4-C8) were either left untreated or were treated with CD95L (2 ng/ml) for 24 hours. Caspase-8 cleavage was then assessed by Western blot analysis. **(B)** DLD1-C8 and DKO4-C8 cells were exposed to CD95L (2 -10 ng/ml) for 24h. Cell viability was assessed by MTT assays and caspase-8 processing by Western blot analysis. Data are presented as means ± SEM. **(C)** DLD1-C8 and DKO4-C8 cells were either stimulated with CD95L (2 ng/ml) or were grown under non-adherent conditions to promote anoikis. Caspase-8 processing was then assessed by Western blot analysis.

Deletion of oncogenic K-Ras, but not β-catenin$^{\Delta S45}$ or p53, sensitized HCT116 cells to TRAIL-induced apoptosis (Figure 2E). Thus, of the three most common genetic alterations in colorectal tumors, only the *K-Ras* oncogene provides resistance to apoptosis induction by death receptor activation.

Deletion of oncogenic K-Ras allows caspase-8 processing by death receptor ligands

Activation of caspase-8 in the death-inducing signaling complex (DISC) is essential for apoptosis induction by CD95L[24] and TRAIL.[25] DLD1 cells express low levels of caspase-8 (Figure 4A) but re-expression of caspase-8 did not sensitize these cells to CD95L or TRAIL (Figures 4A, 4B and not shown). Resistance was accompanied by a failure to process caspase-8 in the DISC, despite expression of CD95, TRAIL-R1, TRAIL-R2, cFLIP and FADD. (Figures 3C, 3D and 4A). Deletion of oncogenic K-Ras allowed CD95L-stimulated caspase-8 processing (Figures 4A and 4B) but had no effect on caspase-8 processing during anoikis (Figure 4C).

CD95L is an attractant for tumor cells expressing oncogenic K-Ras

The apoptosis-resistant cell lines that were exposed to CD95L displayed extensive membrane ruffling but their derivatives expressing only wildtype K-Ras did not (Figure 5A and not shown). This suggests that CD95 signaling is not simply reduced in cells expressing oncogenic K-Ras, but that alternative pathways may be activated.

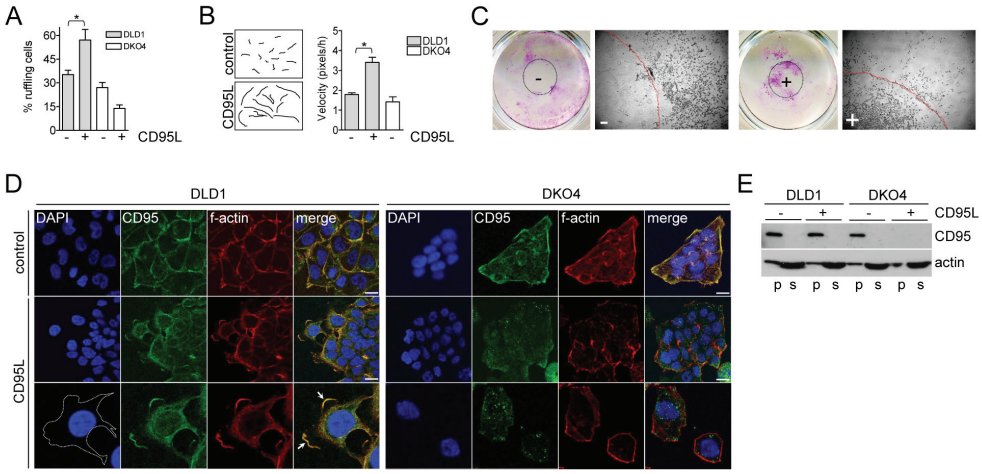

Figure 5 CD95 ligand is an attractant for tumor cells expressing oncogenic K-Ras
(A) DLD1 and DKO4 cells were stimulated with CD95L (2 ng/ml) and the number of cells with extensive ruffling was analyzed by live cell imaging. **(B)** DLD1 and DKO4 cells were treated with CD95L (2 ng/ml) for 48 hours and were analyzed by live cell imaging. The migration trails of single tumor cells are depicted in the left panel. The right panel shows a quantification of average tumor cell speed. CD95L-stimulated DKO4 cells failed to migrate but underwent apoptosis. **(C)** A droplet of Matrigel containing no (-) or 20 ng/ml CD95L (+) was allowed to set in the middle of a tissue culture dish. DLD1 cells were plated and after 24h cells were stained with crystal violet and fixed. Representative images are shown. The borders of the Matrigel drops are indicated by red dotted lines. **(D)** Immunofluorescence analysis of CD95 (green) and f-actin (red) in DLD1 cells (left panel) and DKO4 cells (right panel). Cells were left untreated or were stimulated with CD95L (2 ng/ml) for 2 hours. Arrows indicate CD95 at the leading edge in CD95L-stimulated DLD1 cells. **(E)** DLD1 and DKO4 cells were treated overnight with CD95L (6 ng/ml). Detergent lysates were prepared and cleared by high speed centrifugation. CD95 levels in the high-speed pellet (p) and sup (s) fractions were subsequently analyzed by Western blotting. * $p<0.05$.

Live cell imaging showed that exposure of DLD1 cells to CD95L increased motility by approximately two-fold (Figure 5B). In addition, CD95L stimulated the closure of monolayer wounds in scratch assays (data not shown). Directed migration assays showed that CD95L acts as an attractant for apoptosis-resistant tumor cells (Figure 5C).
Apoptosis signaling by CD95 is associated with its internalization.[26] Immunofluorescence analysis showed that CD95 is localized at the cell periphery both in DLD1 and DKO4 cells (Figure 5D). Furthermore, FACS analysis showed that cell surface expression of CD95 was unaffected by K-Ras status (Figure 3D). CD95L stimulation induced internalization of CD95 in DKO4 cells. In DLD1 cells however, activated CD95 localized to cortical f-actin-rich plasma membrane areas, including those at the leading edge of migrating cells (Figure 5D). In DKO4 cells, internalized CD95 was completely degraded after overnight stimulation, but CD95 in DLD1 cells was resistant to degradation (Figure 5E). Similar results were obtained in the HCT116/Hkh2 cell system (not shown). Thus, oncogenic K-Ras prevents CD95 from joining the classical internalization/degradation pathway.

Systemic administration of TRAIL stimulates invasion of K-Ras^{D12}-expressing micrometastases in the liver

The safety and efficacy of recombinant TRAIL or agonistic TRAIL-R2 antibodies is currently being tested in different patient groups, including those with metastatic colorectal cancer. Both CD95L and TRAIL induced invasion of C26 cells in Matrigel *in vitro* (Figure 6A). Therefore, we assessed whether systemic administration of TRAIL affected the invasive behavior of micrometastases in the liver. Micrometastases in control mice displayed a compact morphology with sharply demarcated edges (Figure 6B). In contrast, micrometastases in TRAIL-treated mice displayed a highly invasive phenotype with cells detaching from the core of the metastasis and invading the surrounding parenchyma (Figure 6B). TRAIL treatment increased the average distance between tumor cells at the extreme edges of individual metastases by approximately three-fold (Figure 6B). TRAIL treatment had no apparent effect on the number of liver metastases, nor did we observe apoptotic GFP-positive tumor cells. Thus, rather than promoting their clearance, TRAIL induced dissemination of micrometastatic tumor cells through the liver parenchyma.

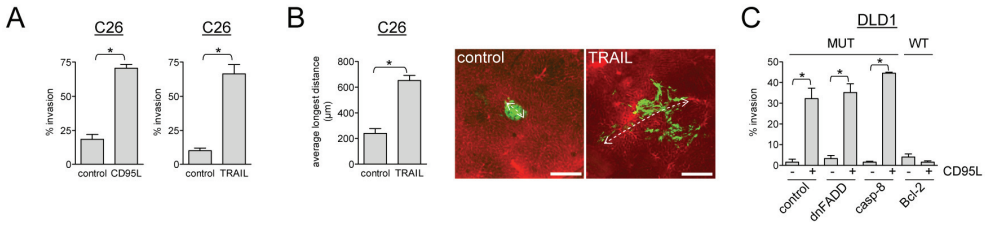

Figure 6 Oncogenic K-Ras allows death receptors to signal invasion
(A) Transwell invasion assay using C26 cells stimulated with either CD95L or TRAIL. Graphs represent means of triplicates. **(B)** C26-GFP cells were injected into the spleen and micrometastases were allowed to develop for 2 days, prior to treatment with TRAIL (6 mg/kg body weight/day), or vehicle, for 2 days. All mice were injected with Rhodamine-conjugated dextran to visualize the microvasculature. The livers were harvested and analyzed by confocal fluorescence microscopy. Representative examples of micrometastases in control-treated (left panel) and TRAIL-treated (right panel) mice are shown. (Scale bars: 150 µm). The lengths of the longest tumor cell trails in each of the metastases were measured (10 metastases per liver) and plotted. **(C)** Transwell invasion assay using DLD1 control cells, DLD1 cells expressing dnFADD or caspase-8 and DKO4 cells expressing Bcl-2. * $p<0.05$.

Invasion of apoptosis-resistant tumor cells requires oncogenic K-Ras but not caspase-8 recruitment

We next tested whether caspase-8 recruitment was required for CD95-mediated invasion. To this end, dnFADD was expressed in DLD1 and DKO4 cells. dnFADD abrogated CD95L-stimulated caspase-8 processing and apoptosis in DKO4 cells (Figures 7A and 7B). In contrast, neither dnFADD nor overexpression of capsase-8 affected CD95L-stimulated invasion of DLD1 cells (Figure 6C). Thus, caspase-8 recruitment is not required for CD95L-stimulated invasion of DLD1 cells.

The finding that CD95L causes invasion of apoptosis-resistant tumor cells raises the question whether in apoptosis-prone cells the induction of apoptosis overrides the invasion signal, or whether these are two independent modes of receptor signaling. We tested this by expressing Bcl-2 in apoptosis-prone DKO4 cells. DKO4-Bcl-2 cells were protected from CD95L-induced apoptosis (Figure 7C), but they failed to undergo invasion in response to CD95L (Figure 6C). Moreover, DKO4 cells that undergo apoptosis do not show CD95L-induced ruffling in the period preceding cell death (data not shown).

Oncogenic K-Ras requires Raf1 to prevent apoptosis induction by CD95

K-Ras signals through several distinct effector pathways. We took an RNAi- and inhibitor-based approach to assess which of these pathways mediates the switch in CD95 signaling output. Lentivirus-mediated RNAi-suppression of A-Raf, B-Raf, ERK1+ERK2, RalA, or RalB, or inhibition of MEK (with U0126) or PI(3)-kinase (with LY294002) failed to sensitize tumor cells to CD95L-stimulated apoptosis in the presence of oncogenic K-Ras (Figure 8A). However, suppression of Raf1 using 2 independent targeting sequences sensitized C26 cells to apoptosis induction by CD95L (Figures 8A and 8B). This was accompanied by activation (cleavage) of caspase-3, but not by reduced phosphorylation of ERK1 or ERK2 (Figure 8C). Raf1 suppression did not further sensitize C26-KrasKD cells to CD95L (Figure 8D). Thus, Raf1 suppression primarily affects tumor cell sensitivity to CD95L in the presence of oncogenic K-Ras.

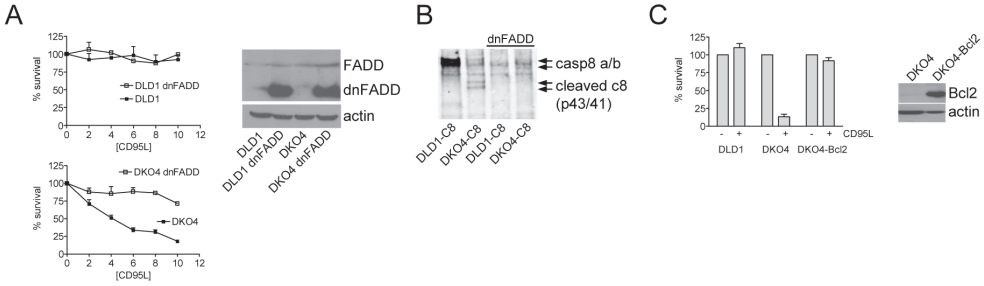

Figure 7 Protection of DKO4 cells from CD95-induced apotposis by dnFADD and Bcl2
(A) DLD1-caspase-8 and DKO4-caspase-8 cells were transduced with a lentiviral vector driving expression of dnFADD. Cells were stimulated with CD95L overnight (2 ng/ml) and cell viability was measured using MTT assays. dnFADD protected DKO4 cells from CD95L-induced apoptosis. **(B)** DLD1, DLD1-dnFADD, DKO4 and DKO4-dnFADD cells were stimulated with FLAG-TRAIL (5 µg/ml) for 15 minutes. Cell extracts were prepared and anti-Flag immunoprecipitation was performed overnight. The presence of caspase-8 in the immunocomplexes was then analyzed by Western blotting. **(C)** DKO4 cells were transfected with pREP4-Bcl2 or empty pREP4 and stable polyclonal cell lines were generated by selection in Hygromycin B medium. DLD1, DKO4-pREP4 and DKO4-pREP4-Bcl2 cells were then stimulated with CD95L overnight (2 ng/ml) and cell survival was measured by MTT assays. Bcl2 expression protected DKO4 cells from CD95L-induced apoptosis.

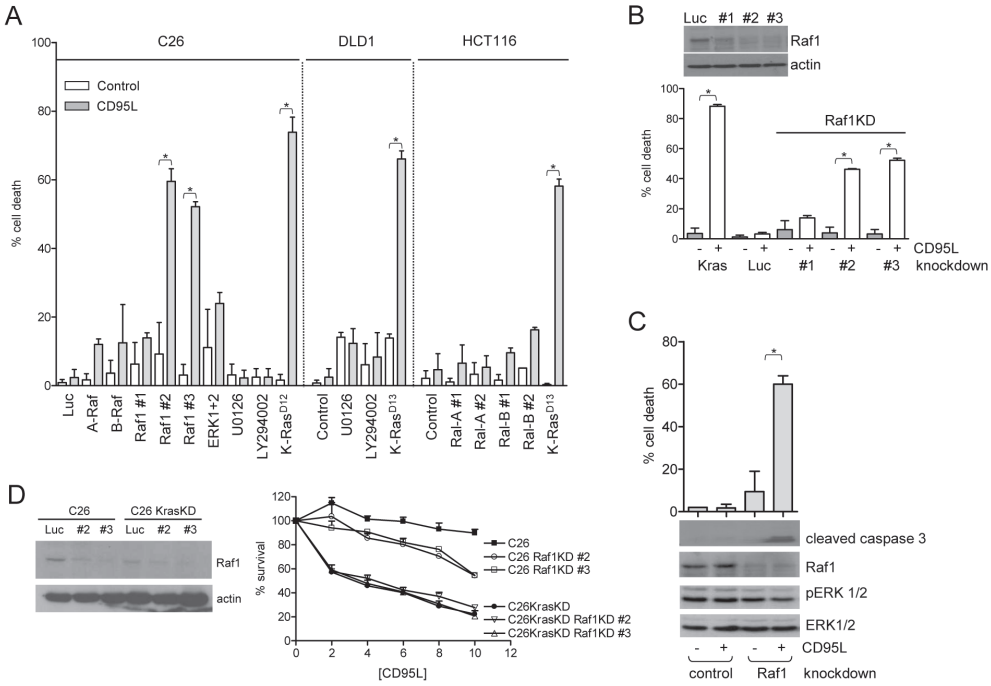

Figure 8 Raf1 mediates K-Ras-dependent apoptosis resistance
(A) C26, DLD1 and HCT116 cells were infected with lentiviral RNA-interference constructs targeting the indicated genes. In addition, cells were treated with the MEK inhibitor U0126 or with the PI(3) kinase inhibitor LY294002 as indicated. Cells were then stimulated with CD95L and cell viability was measured as in Figure 2. **(B)** C26 cells were infected with three different Raf1-targeting lentiviral RNAi constructs. Cells were stimulated with CD95L and cell viability was measured as above. Knockdown efficiency was analyzed by Western blotting. **(C)** Control and Raf1-knockdown cells were stimulated with CD95L overnight. Cells were then analyzed for viability as above. In addition, the effect of Raf1 knockdown on caspase-3 cleavage (activation) and ERK phosphorylation was assessed by Western blotting. **(D)** C26 control and C26-KrasKD cells were transduced with control (Luc) or Raf1 knockdown constructs (#2, #3) as indicated and Raf1 expression was assessed by Western blotting. Cells were stimulated with the indicated concentrations of CD95L overnight and cell viability was assessed as above. * $p<0.05$.

Raf1 is critical for K-Ras-driven invasion and liver metastasis formation

To test whether the restoration of apoptosis signaling by CD95 in Raf1-suppressed cells would be accompanied by loss of its ability to stimulate invasion, Raf1 knockdown cells were treated with the caspase inhibitor z-VAD. Raf1 knockdown cells, protected by z-VAD, displayed a greatly reduced potential to invade Matrigel in response to CD95L (Figure 9A). z-VAD had no effect on C26 control cells (Figure 9A). Thus, Raf1 knockdown switched the signaling output of activated CD95 from invasion mode back to apoptosis mode, in the presence of K-Ras^{D12}. Importantly, knockdown of Raf1 also strongly reduced the metastatic potential of C26 tumor cells, despite the continued presence of oncogenic K-Ras^{D12} (Figure 9B). This was due to massive apoptosis of tumor cells in the liver (Figure 9C), similar to K-Ras-suppressed cells (Figure 1D). These results identify Raf1 as a critical mediator of the survival of metastatic tumor cells in the liver and as a critical K-Ras effector during liver metastasis formation.

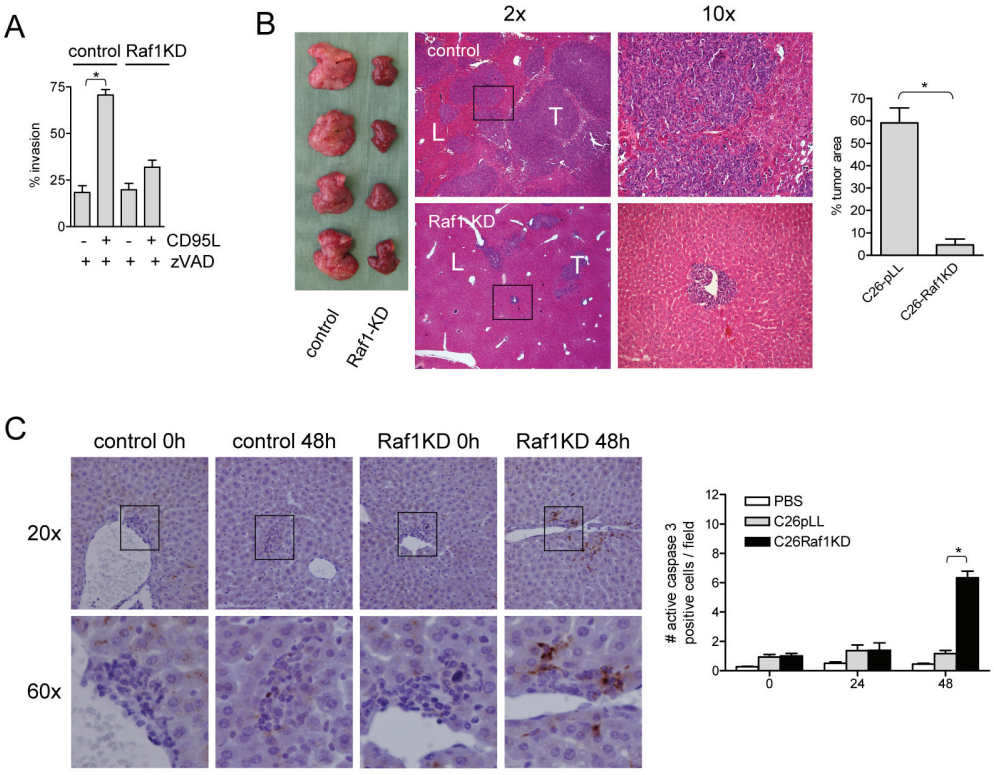

Figure 9 Raf1 is required for CD95L-stimulated invasion and K-Ras-driven metastasis formation
(A) Transwell invasion assay using C26 cells expressing shRNA's targeting luciferase or Raf1 in the presence of the apoptosis-inhibiting peptide z-VAD (20 μM). **(B)** C26 control and Raf1 knockdown cells were injected into the spleens of BALB/c mice (n=4) and liver metastasis formation was then assessed by morphometric assessment of the tumor-containing areas on liver tissue sections. Quantification of the % tumor areas are shown in the graph. **(C)** Micrometastases were established using either control (Luc knockdown) or Raf1 knockdown C26 cells. Apoptotic tumor cells were then quantified by anti-active caspase-3 immunohistochemistry as in Figure 1D. * $p<0.05$.

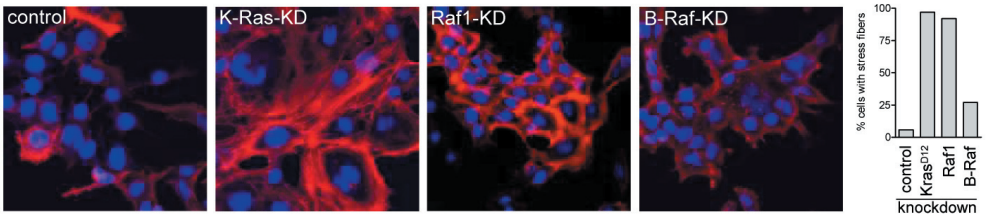

Figure 10 Stress fiber formation following K-Ras or Raf1 knockdown
C26 cells transduced with a lentiviral control shRNA (Luc) or with K-Ras-, Raf1-, or B-Raf-targeting shRNA's were grown on glass coverslips. After fixation, the actin cytoskeleton was stained with phalloidin texas-red. Nuclei were counterstained with DAPI. The % of cells with stress fibers was then quantified without knowledge of the slide's identities.

K-Ras and Raf1 subvert CD95 signaling by suppressing the Rho/ROCK/LIM kinase pathway

We noted that knockdown of K-Ras and Raf1, but not B-Raf, caused a massive increase in the number of actin stress fibers, indicating activation of the Rho/ROCK pathway (Figure 10). In fibroblasts, ROCK

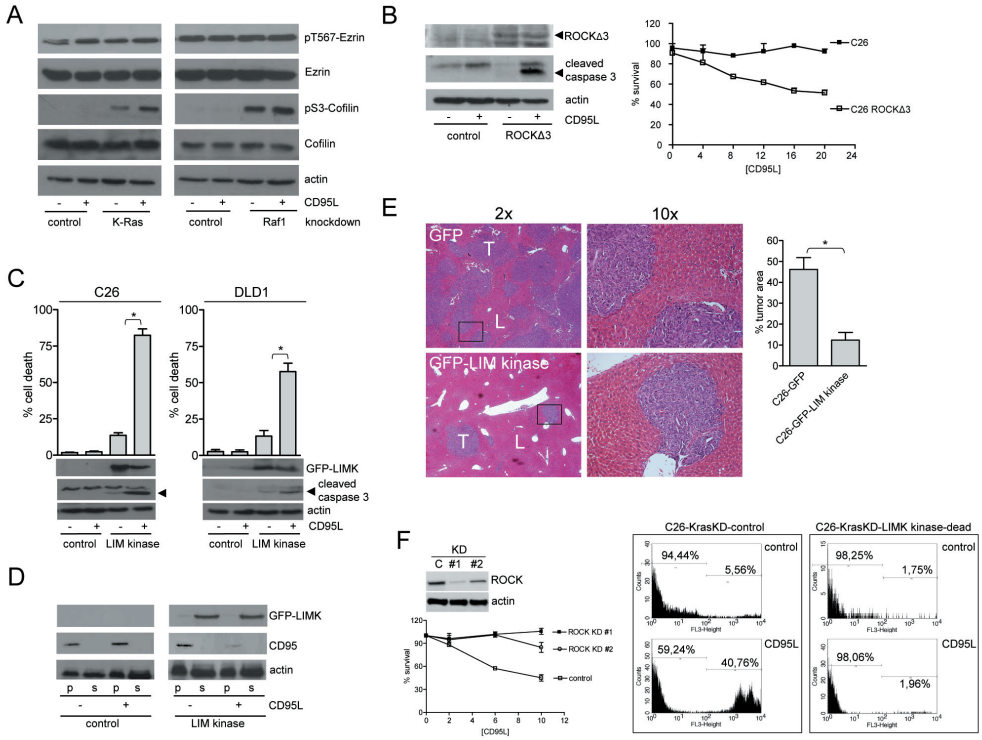

Figure 11 K-Ras-induced subversion of CD95 signaling and metastasis formation requires suppression of the Rho kinase/LIM kinase pathway

(A) Control, K-Ras knockdown and Raf1 knockdown C26 cells were either left unstimulated or were stimulated with CD95L 24h (10 ng/ml). Cell lysates were then analyzed for the presence of pT567-ezrin, ezrin, pS3-cofilin and cofilin. **(B)** C26 cells overexpressing ROCKΔ3 or a control vector were exposed to CD95L (20 ng/ml) for 24h. Caspase-3 processing and ROCKΔ3 expression was assessed by Western blot analysis. Cell viability was assessed by MTT assays. Data are presented as means ± SEM. **(C)** C26 and DLD1 cells were grown on glass coverslips (n=3), were transfected with an expression construct for GFP (control) or GFP-tagged LIMK and were stimulated 24h with CD95L (10 ng/ml). Immunofluorescence analysis for active caspase-3 was then performed to assess the number of apoptotic (a-casp3-positive) green cells under all conditions. Detergent lysates were prepared in parallel and were blotted for LIMK expression and active caspase-3. **(D)** DLD1 cells were transfected with an expression construct for GFP-tagged LIMK. Cells were stimulated 24h with CD95L (6 ng/ml). Detergent lysates were prepared and cleared by high speed centrifugation. CD95 levels in the high-speed pellet (p) and sup (s) fractions were subsequently analyzed by Western blotting. **(E)** FACS-sorted C26-GFP and C26-LIMK-GFP cells were injected into the spleens of BALB/c mice (n=4) and liver metastasis formation was then assessed as in Figure 7. (F) C26-KrasKD cells were transduced with lentiviral vectors targeting luciferase (control) or ROCK (#1 and #2). Cells were stimulated with CD95L (2-10 ng/ml) for 24 hours and cell viability was assessed by MTT assays as above. In addition, C26-KrasKD cells were transfected with an expression construct for GFP-tagged dominant negative LIMK. Cells were stimulated with CD95L for 24 hours (10 ng/ml). Cell viability of GFP-LIMK-positive and negative populations was then assessed by propidium iodide exclusion by FACS. * $p<0.05$.

facilitates apoptosis induction by CD95, possibly by phosphorylation of ezrin on T567.[27] ROCK also activates LIM kinase to phosphorylate the actin-severing protein cofilin on S3. Raf1 or K-Ras knockdown in C26 cells dramatically increased phosphorylation of cofilin S3, but did not affect ezrin T567 phosphorylation (Figure 11A). Overexpression of ROCK restored cofilin phosphorylation (data not shown) and sensitized C26 cells to CD95L-induced apoptosis (Figure 11B). Likewise, overexpression of LIM kinase sensitized both C26 and DLD1 cells to CD95L-induced apoptosis (Figure 11C). Restoration of apoptosis signaling was accompanied by stimulus-dependent degradation of CD95 (Figure 11D), similar to what was observed in K-Ras knockout cells (Figure 5E). Importantly, the metastasis-forming potential of LIM kinase-expressing C26 cells was strongly reduced (Figure 11E). Furthermore, RNAi-mediated suppression of ROCK or expression of a kinase-dead LIM kinase mutant in K-Ras knockdown cells protected these cells from CD95L-stimulated apoptosis (Figure 11F). Taken together, the results suggest that suppression of ROCK/LIM kinase by K-Ras/Raf1 is essential for altering CD95 functionality and for metastasis formation.

Discussion

The factors that determine cell fate following death receptor stimulation (i.e. apoptosis, proliferation or invasion) are poorly defined. In this manuscript we identify oncogenic K-Ras and its effector Raf1 as critical determinants of death receptor function in metastatic colorectal cancer cells. K-Ras and Raf1 do not simply suppress CD95-mediated apoptosis, but alter its signaling output to generate an invasion signal. Invasion signaling by CD95 required the continued presence of oncogenic K-Ras and Raf1 and was not secondary to apoptosis resistance. Thus, CD95 is primed to signal either apoptosis or invasion. Previous reports have uncovered death domain-dependent pathways of CD95-stimulated tumor cell invasion.[10,11] Our results show that in metastatic colorectal cancer cells CD95 retains the capacity to stimulate invasion even when its death domain is blocked. CD95 may therefore stimulate invasion via distinct pathways in distinct cell types.

The K-Ras-controlled switch in death receptor function turns one of the most potent tumor suppressor mechanisms into one stimulating tumor cell invasion. To our knowledge this is the first demonstration of such a dramatic switch in death receptor function induced by a single common oncogene. When instructed to signal invasion, CD95 and TRAIL receptors may contribute to tumor progression and metastasis formation. Indeed, components of these signaling systems are not simply lost or inactivated during tumor progression.[28-35] In fact, expression of CD95L is increased during colorectal tumorigenesis[28,31,32], is higher in metastases than in matched primary tumors[31] and is related to poor prognosis.[36] Furthermore, CD95 and CD95L are frequently co-expressed in primary colorectal tumors and liver metastases.[31,37]

CD95L could contribute to tumor progression, either by promoting the expression of pro-inflammatory cytokines from neighbouring cells, by stimulating apoptosis in hepatocytes[35,37] and/or by activating non-apoptotic CD95 signaling pathways in tumor cells that retain CD95.[12,13] The latter possibility is supported by the finding that continuous CD95 stimulation on colon carcinoma cells selects highly metastatic variants[38] and overexpression of CD95 ligand in apoptosis-resistant colorectal cancer cells promotes liver metastasis formation.[37]

An immediate implication of our finding that oncogenic K-Ras alters CD95 signaling output is that therapeutic targeting of death receptors by TRAIL or by agonistic TRAIL receptor antibodies could

have adverse effects on disease progression by promoting invasion and dissemination of micrometastases instead of clearing them. This is a major concern, at least when considering such compounds in the treatment of tumors harboring activating mutations in the *K-Ras* gene. Currently, the safety and efficacy of recombinant TRAIL and TRAIL-receptor-activating antibodies are being tested in phase I and phase II clinical trials. These include trials in patients with metastatic colorectal, pancreatic, and non-small cell lung cancer, tumor types in which activating mutations in K-Ras are frequently observed.[39] Our results provide a rationale for testing the tumors of the patients in these trials for activating mutations in K-Ras.

The physiological function of Raf1 is to suppress apoptosis.[40,41] Strikingly, this does not require Raf1 kinase activity and is independent of its ability to activate the ERK pathway.[40,41] Our results show that this function extends to the pathophysiology of metastasis formation, as Raf1 is required for the survival of metastatic colorectal cancer cells in the liver without modulating ERK phosphorylation. Rather, B-Raf is the most effective activator of the MEK/ERK pathway (reviewed Niault and Baccarini[42]). Likewise, in the colorectal cancer cells studied here, only B-Raf was essential for maintaining ERK phosphorylation (Figure 12). A-Raf is required for normal neural and intestinal development in mice[43], but it had no significant impact on the survival of colorectal cancer cells. The role of A-Raf in colorectal cancer cells is presently unknown. Taken together, the Raf kinases appear to fulfil distinct functions in colorectal cancer cells.

Raf1 suppresses apoptosis by binding and inactivating the pro-apoptotic kinases ASK1 and MST2.[44,45] CD95 activation causes disruption of the RAF1-MST2 complex, which leads to activation of MST2 and this is required for efficient apoptosis induction by CD95L[45]. A role for (disruption of) the Raf1-Ask1 complex in CD95-induced apoptosis is less clear. Raf1 also binds to and suppresses the activity of ROCK, which impairs CD95-induced apoptosis.[27] All of these studies firmly implicate Raf1 in the control of (CD95-induced) apoptosis. Our results suggest that suppression of the ROCK/LIM kinase/cofilin pathway by K-Ras/Raf1 is essential for specifying the signaling output of CD95. The cofilin pathway is a critical regulator of cortical actin dynamics, tumor cell migration, invasion and metastasis formation.[46,47] Therefore, the control of cortical actin dynamics by K-Ras/Raf1 may underlie subversion of CD95 trafficking and signaling output. Our results add a novel dimension to the control of metastatic capacity by the cofilin pathway. By keeping ROCK and LIM kinase activities suppressed, K-Ras and Raf1 turn death receptors into pro-metastatic receptors.

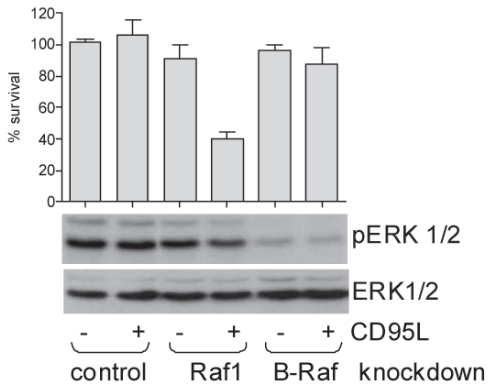

Figure 12 B-Raf, but not Raf1, is required for ERK phosphorylation
C26 cells were transduced with lentiviral RNAi vectors targeting either Raf1 or B-Raf. Cells were then stimulated with CD95L (10 ng/ml) overnight and cell viability was determined by MTT assays. Parallel samples were analyzed for the effect of Raf1 and B-Raf knockdown on the levels of phosphorylated and total ERK1 and ERK2.

References

1. Sjoblom T, Jones S, Wood LD, Parsons DW, Lin J, Barber TD, Mandelker D, Leary RJ, Ptak J, Silliman N, Szabo S, Buckhaults P, Farrell C, Meeh P, Markowitz SD, Willis J, Dawson D, Willson JK, Gazdar AF, Hartigan J, Wu L, Liu C, Parmigiani G, Park BH, Bachman KE, Papadopoulos N, Vogelstein B, Kinzler KW, Velculescu VE. The consensus coding sequences of human breast and colorectal cancers. Science 2006; 314: 268-274.
2. Wood LD, Parsons DW, Jones S, Lin J, Sjoblom T, Leary RJ, Shen D, Boca SM, Barber T, Ptak J, Silliman N, Szabo S, Dezso Z, Ustyanksky V, Nikolskaya T, Nikolsky Y, Karchin R, Wilson PA, Kaminker JS, Zhang Z, Croshaw R, Willis J, Dawson D, Shipitsin M, Willson JK, Sukumar S, Polyak K, Park BH, Pethiyagoda CL, Pant PV, Ballinger DG, Sparks AB, Hartigan J, Smith DR, Suh E, Papadopoulos N, Buckhaults P, Markowitz SD, Parmigiani G, Kinzler KW, Velculescu VE, Vogelstein B. The genomic landscapes of human breast and colorectal cancers. Science 2007; 318: 1108-1113.
3. Jones S, Chen WD, Parmigiani G, Diehl F, Beerenwinkel N, Antal T, Traulsen A, Nowak MA, Siegel C, Velculescu VE, Kinzler KW, Vogelstein B, Willis J, Markowitz SD. Comparative lesion sequencing provides insights into tumor evolution. Proc Natl Acad Sci U S A 2008; 105: 4283-4288.
4. Smakman N, Borel Rinkes IH, Voest EE, Kranenburg O. Control of colorectal metastasis formation by K-Ras. Biochim Biophys Acta 2005; 1756: 103-114.
5. Koshkina NV, Khanna C, Mendoza A, Guan H, DeLauter L, Kleinerman ES. Fas-negative osteosarcoma tumor cells are selected during metastasis to the lungs: the role of the Fas pathway in the metastatic process of osteosarcoma. Mol Cancer Res 2007; 5: 991-999.
6. Smyth MJ, Cretney E, Takeda K, Wiltrout RH, Sedger LM, Kayagaki N, Yagita H, Okumura K. Tumor necrosis factor-related apoptosis-inducing ligand (TRAIL) contributes to interferon gamma-dependent natural killer cell protection from tumor metastasis. J Exp Med 2001; 193: 661-670.
7. Takeda K, Hayakawa Y, Smyth MJ, Kayagaki N, Yamaguchi N, Kakuta S, Iwakura Y, Yagita H, Okumura K. Involvement of tumor necrosis factor-related apoptosis-inducing ligand in surveillance of tumor metastasis by liver natural killer cells. Nat Med 2001; 7: 94-100.
8. Yang D, Stewart TJ, Smith KK, Georgi D, Abrams SI, Liu K. Downregulation of IFN-gammaR in association with loss of Fas function is linked to tumor progression. Int J Cancer 2008; 122: 350-362.
9. Papenfuss K, Cordier SM, Walczak H. Death receptors as targets for anti-cancer therapy. J Cell Mol Med 2008; 12: 2566-2585.
10. Barnhart BC, Legembre P, Pietras E, Bubici C, Franzoso G, Peter ME. CD95 ligand induces motility and invasiveness of apoptosis-resistant tumor cells. EMBO J 2004; 23: 3175-3185.
11. Kleber S, Sancho-Martinez I, Wiestler B, Beisel A, Gieffers C, Hill O, Thiemann M, Mueller W, Sykora J, Kuhn A, Schreglmann N, Letellier E, Zuliani C, Klussmann S, Teodorczyk M, Grone HJ, Ganten TM, Sultmann H, Tuttenberg J, von DA, Regnier-Vigouroux A, Herold-Mende C, Martin-Villalba A. Yes and PI3K bind CD95 to signal invasion of glioblastoma. Cancer Cell 2008; 13: 235-248.
12. Peter ME, Legembre P, Barnhart BC. Does CD95 have tumor promoting activities? Biochim Biophys Acta 2005; 1755: 25-36.
13. Peter ME, Budd RC, Desbarats J, Hedrick SM, Hueber AO, Newell MK, Owen LB, Pope RM, Tschopp J, Wajant H, Wallach D, Wiltrout RH, Zornig M, Lynch DH. The CD95 receptor: apoptosis revisited. Cell 2007; 129: 447-450.
14. Trauzold A, Roder C, Sipos B, Karsten K, Arlt A, Jiang P, Martin-Subero JI, Siegmund D, Muerkoster S, Pagerols-Raluy L, Siebert R, Wajant H, Kalthoff H. CD95 and TRAF2 promote invasiveness of pancreatic cancer cells. FASEB J 2005; 19: 620-622.
15. Trauzold A, Siegmund D, Schniewind B, Sipos B, Egberts J, Zorenkov D, Emme D, Roder C, Kalthoff H, Wajant H. TRAIL promotes metastasis of human pancreatic ductal adenocarcinoma. Oncogene 2006; 25: 7434-7439.
16. Smakman N, Veenendaal LM, van DP, Bos R, Offringa R, Borel R, I, Kranenburg O. Dual effect of Kras(D12)

knockdown on tumorigenesis: increased immune-mediated tumor clearance and abrogation of tumor malignancy. Oncogene 2005; 24: 8338-8342.
17. Shirasawa S, Furuse M, Yokoyama N, Sasazuki T. Altered growth of human colon cancer cell lines disrupted at activated Ki-ras. Science 1993; 260: 85-88.
18. Smakman N, Martens A, Kranenburg O, Borel R, I. Validation of bioluminescence imaging of colorectal liver metastases in the mouse. J Surg Res 2004; 122: 225-230.
19. Grosse-Wilde A, Voloshanenko O, Bailey SL, Longton GM, Schaefer U, Csernok AI, Schutz G, Greiner EF, Kemp CJ, Walczak H. TRAIL-R deficiency in mice enhances lymph node metastasis without affecting primary tumor development. J Clin Invest 2008; 118: 100-110.
20. Reichelt P, Schwarz C, Donzeau M. Single step protocol to purify recombinant proteins with low endotoxin contents. Protein Expr Purif 2006; 46: 483-488.
21. Vantaggiato C, Formentini I, Bondanza A, Bonini C, Naldini L, Brambilla R. ERK1 and ERK2 mitogen-activated protein kinases affect Ras-dependent cell signaling differentially. J Biol 2006; 5: 14.
22. Wang W, Mouneimne G, Sidani M, Wyckoff J, Chen X, Makris A, Goswami S, Bresnick AR, Condeelis JS. The activity status of cofilin is directly related to invasion, intravasation, and metastasis of mammary tumors. J Cell Biol 2006; 173: 395-404.
23. Pirone DM, Liu WF, Ruiz SA, Gao L, Raghavan S, Lemmon CA, Romer LH, Chen CS. An inhibitory role for FAK in regulating proliferation: a link between limited adhesion and RhoA-ROCK signaling. J Cell Biol 2006; 174: 277-288.
24. Medema JP, Scaffidi C, Kischkel FC, Shevchenko A, Mann M, Krammer PH, Peter ME. FLICE is activated by association with the CD95 death-inducing signaling complex (DISC). EMBO J 1997; 16: 2794-2804.
25. Sprick MR, Weigand MA, Rieser E, Rauch CT, Juo P, Blenis J, Krammer PH, Walczak H. FADD/MORT1 and caspase-8 are recruited to TRAIL receptors 1 and 2 and are essential for apoptosis mediated by TRAIL receptor 2. Immunity 2000; 12: 599-609.
26. Lee KH, Feig C, Tchikov V, Schickel R, Hallas C, Schutze S, Peter ME, Chan AC. The role of receptor internalization in CD95 signaling. EMBO J 2006; 25: 1009-1023.
27. Piazzolla D, Meissl K, Kucerova L, Rubiolo C, Baccarini M. Raf-1 sets the threshold of Fas sensitivity by modulating Rok-alpha signaling. J Cell Biol 2005; 171: 1013-1022.
28. Bennett MW, O'Connell J, Houston A, Kelly J, O'Sullivan GC, Collins JK, Shanahan F. Fas ligand upregulation is an early event in colonic carcinogenesis. J Clin Pathol 2001; 54: 598-604.
29. Houston A, Waldron-Lynch FD, Bennett MW, Roche D, O'Sullivan GC, Shanahan F, O'Connell J. Fas ligand expressed in colon cancer is not associated with increased apoptosis of tumor cells in vivo. Int J Cancer 2003; 107: 209-214.
30. Koornstra JJ, Kleibeuker JH, van Geelen CM, Rijcken FE, Hollema H, de Vries EG, de JS. Expression of TRAIL (TNF-related apoptosis-inducing ligand) and its receptors in normal colonic mucosa, adenomas, and carcinomas. J Pathol 2003; 200: 327-335.
31. Mann B, Gratchev A, Bohm C, Hanski ML, Foss HD, Demel G, Trojanek B, Schmidt-Wolf I, Stein H, Riecken EO, Buhr HJ, Hanski C. FasL is more frequently expressed in liver metastases of colorectal cancer than in matched primary carcinomas. Br J Cancer 1999; 79: 1262-1269.
32. O'Connell J, Bennett MW, O'Sullivan GC, Roche D, Kelly J, Collins JK, Shanahan F. Fas ligand expression in primary colon adenocarcinomas: evidence that the Fas counterattack is a prevalent mechanism of immune evasion in human colon cancer. J Pathol 1998; 186: 240-246.
33. Strater J, Hinz U, Walczak H, Mechtersheimer G, Koretz K, Herfarth C, Moller P, Lehnert T. Expression of TRAIL and TRAIL receptors in colon carcinoma: TRAIL-R1 is an independent prognostic parameter. Clin Cancer Res 2002; 8: 3734-3740.
34. van Geelen CM, Westra JL, de Vries EG, Boersma-van EW, Zwart N, Hollema H, Boezen HM, Mulder NH, Plukker JT, de JS, Kleibeuker JH, Koornstra JJ. Prognostic significance of tumor necrosis factor-related apoptosis-inducing ligand and its receptors in adjuvantly treated stage III colon cancer patients. J Clin Oncol 2006; 24: 4998-5004.

35. Yoong KF, Afford SC, Randhawa S, Hubscher SG, Adams DH. Fas/Fas ligand interaction in human colorectal hepatic metastases: A mechanism of hepatocyte destruction to facilitate local tumor invasion. Am J Pathol 1999; 154: 693-703.
36. Nozoe T, Yasuda M, Honda M, Inutsuka S, Korenaga D. Fas ligand expression is correlated with metastasis in colorectal carcinoma. Oncology 2003; 65: 83-88.
37. Li H, Fan X, Stoicov C, Liu JH, Zubair S, Tsai E, Ste MR, Wang TC, Lyle S, Kurt-Jones E, Houghton J. Human and mouse colon cancer utilizes CD95 signaling for local growth and metastatic spread to liver. Gastroenterology 2009; 137: 934-944.
38. Liu K, McDuffie E, Abrams SI. Exposure of human primary colon carcinoma cells to anti-Fas interactions influences the emergence of pre-existing Fas-resistant metastatic subpopulations. J Immunol 2003; 171: 4164-4174.
39. Bos JL. ras oncogenes in human cancer: a review. Cancer Res 1989; 49: 4682-4689.
40. Huser M, Luckett J, Chiloeches A, Mercer K, Iwobi M, Giblett S, Sun XM, Brown J, Marais R, Pritchard C. MEK kinase activity is not necessary for Raf-1 function. EMBO J 2001; 20: 1940-1951.
41. Mikula M, Schreiber M, Husak Z, Kucerova L, Ruth J, Wieser R, Zatloukal K, Beug H, Wagner EF, Baccarini M. Embryonic lethality and fetal liver apoptosis in mice lacking the c-raf-1 gene. EMBO J 2001; 20: 1952-1962.
42. Niault T and Baccarini M. Targets of Raf in tumorigenesis. Carcinogenesis 2010; [Epub ahead of print].
43. Pritchard CA, Bolin L, Slattery R, Murray R, McMahon M. Post-natal lethality and neurological and gastrointestinal defects in mice with targeted disruption of the A-Raf protein kinase gene. Curr Biol 1996; 6: 614-617.
44. Chen J, Fujii K, Zhang L, Roberts T, Fu H. Raf-1 promotes cell survival by antagonizing apoptosis signal-regulating kinase 1 through a MEK-ERK independent mechanism. Proc Natl Acad Sci U S A 2001; 98: 7783-7788.
45. O'Neill E, Rushworth L, Baccarini M, Kolch W. Role of the kinase MST2 in suppression of apoptosis by the proto-oncogene product Raf-1. Science 2004; 306: 2267-2270.
46. Scott RW and Olson MF. LIM kinases: function, regulation and association with human disease. J Mol Med 2007; 85: 555-568.
47. Wang W, Eddy R, Condeelis J. The cofilin pathway in breast cancer invasion and metastasis. Nat Rev Cancer 2007; 7: 429-440.

Chapter 3

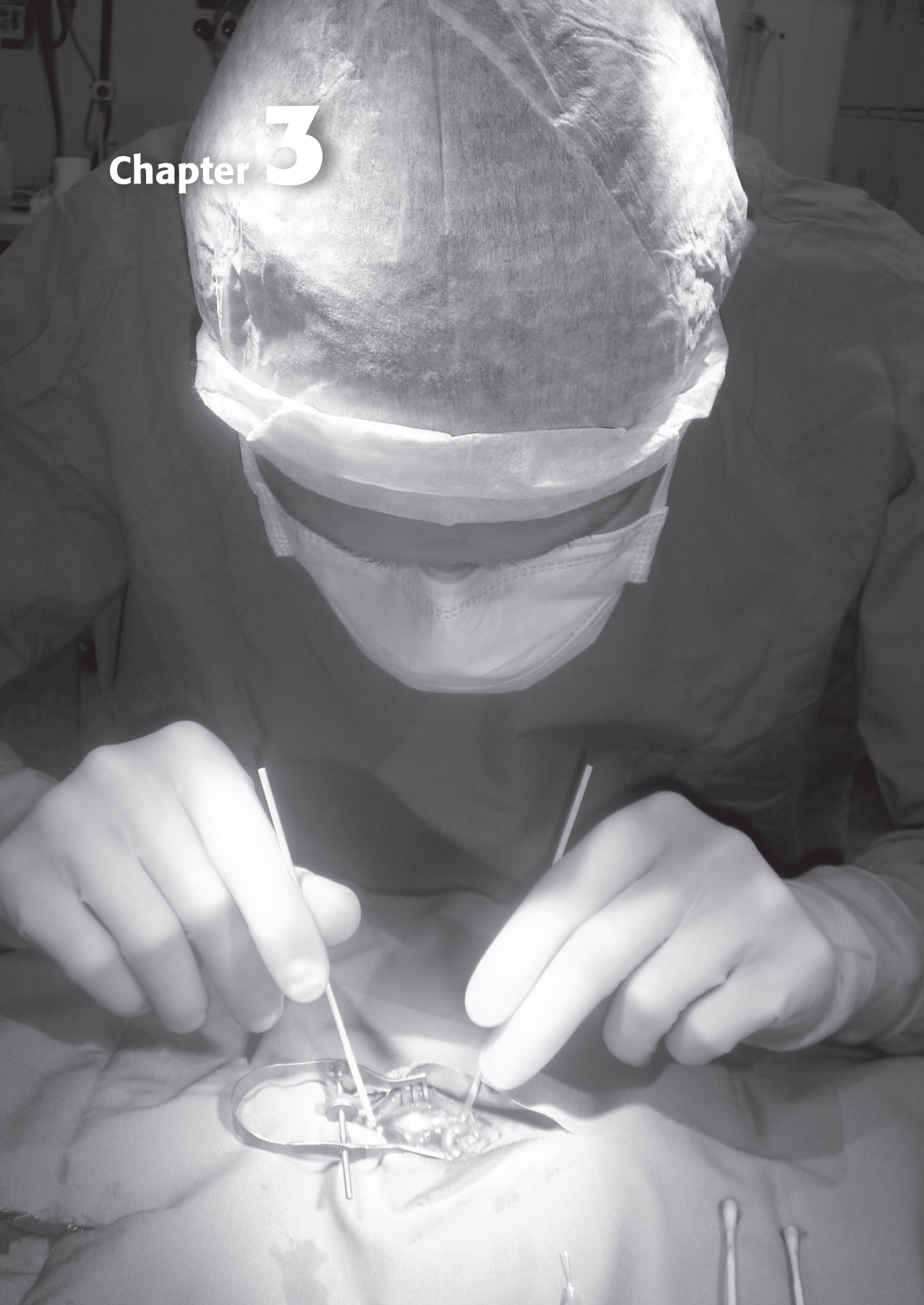

Accelerated perinecrotic outgrowth of colorectal liver metastases following radiofrequency ablation is a hypoxia-driven phenomenon

Annals of Surgery 2009; 249: 814-823

Maarten W. Nijkamp[1]
Jarmila D.W. van der Bilt[1]
Menno T. de Bruijn[1]
I. Quintus Molenaar[1]
Emile E. Voest[2]
Paul J. van Diest[3]
Onno Kranenburg[1]
Inne H.M. Borel Rinkes[1]

Departments of [1]Surgery, [2]Medical Oncology and [3]Pathology
University Medical Center Utrecht, Utrecht, The Netherlands

Abstract

Background
Thermal destruction therapies of non-resectable colorectal liver metastases, including radiofrequency ablation (RFA), can provide tumor clearance, but local recurrences are common. The aim of this study was to assess how thermal ablation of colorectal liver metastases affects the outgrowth of micrometastases in the transition zone (TZ) between ablated tissue and the unaffected reference zone (RZ) in two different murine models.

Methods
Three days after intrasplenic injection of C26 colon carcinoma cells, RFA was applied to the left liver lobe. Perinecrotic microcirculation, tissue hypoxia, HIF-1α and HIF-2α and the outgrowth of micrometastases both in the TZ and in the RZ were evaluated over time.

Results
In two different animal models, the outgrowth of micrometastases in the TZ following RFA was stimulated approximately four-fold compared to tumor growth in the reference zone. Accelerated tumor growth in the TZ was associated with microcirculatory disturbances, prolonged hypoxia and stabilization of HIF-1α and HIF-2α in the tumor cells. In addition, RFA induced the formation of new hepatic vessels that sprouted from existing sinusoids and grew into the generated necrotic lesion. Surprisingly, the accelerated tumor growth was not associated with these vessels. Treatment with 17DMAG prevented HIF-1α and HIF-2α stabilization and selectively reduced tumor growth in the TZ by ~40% without affecting tumor growth in sham-operated mice or in the RZ of RFA-treated mice. PTK787/ZK-222584, a non-selective VEGF-receptor inhibitor, reduced RFA-stimulated tumor growth and tumor growth in the RZ to a similar extent.

Conclusions
We conclude that RFA stimulates the outgrowth of tumor cells at the lesion periphery. Angiogenesis is not the driving force behind RFA-stimulated tumor growth, but other hypoxia/HIF-activated pathways are likely to be important.

Introduction

Surgical resection offers patients with colorectal liver metastases a potentially curative treatment, leading to 5-year survival rates of approximately 40%.[1] However, despite recent advances in neoadjuvant chemotherapy, surgical resection is applicable to only 15-30% of patients.[2,3] Thermal destruction therapies, such as radiofrequency ablation (RFA) and laser-induced thermotherapy (LITT), are widely used for treating non-resectable colorectal metastases confined to the liver and may provide tumor clearance and increase life-expectancy.[4,5] Recent articles on this topic revealed that local peri-lesional recurrences from colorectal metastases occur in approximately 9-18%.[5-8] Nonetheless, with increasing tumor size and during percutaneous ablation local recurrences are reported in up to 60% of cases.[7,9]

One of the major problems with thermal destruction therapies is to achieve complete tumor destruction. In the treatment of larger tumors it is difficult to reach sufficiently high temperatures further away from the heat source. This contributes to high local recurrence rates following ablative treatment of tumors with large diameters. However, as ablative devices improve, the ability to obtain satisfactory ablative margins will increase.[10]

Nonetheless, despite apparently complete tumor destruction, local recurrences may develop from residual viable tumor cells that are located at the periphery of the lesion.[11,12] The biological behavior of residual tumor cell deposits greatly determines the time to develop a recurrence, which eventually influences survival. Evidence is accumulating that the altered microenvironment after operative trauma may enhance the outgrowth of residual tumor cells.[13] Both hypoxia and hypoxia-driven angiogenesis are a consequence of surgical trauma[13-15] and these phenomena both play an important role in tumor growth.[14,16,17] Recently, we have shown that ischemia/reperfusion injury due to vascular clamping accelerates the outgrowth of pre-established micrometastases.[18] The stimulated outgrowth was mainly observed around areas of tissue necrosis and was associated with tissue hypoxia.[18,19] Based on these observations, we hypothesized that RFA may similarly affect the local outgrowth of residual tumor cells at the lesion periphery, based on induction of hypoxia and, consequently, neovascularization.

In the present work we used two pre-clinical models with pre-established colorectal micrometastases to study the effect of RFA on the outgrowth of tumor cell clusters at the lesion periphery, thereby mimicking the influence of RFA on diffuse residual disease in the liver. Furthermore, we assessed whether tumor growth in the transition zone between the central necrotic zone and the unaffected reference zone is associated with hypoxia, stabilization of Hypoxia Inducible Factor (HIF)-1αand HIF-2αand subsequent neovascularization. Finally, we tested whether intervention strategies aimed at either preventing the stabilization of HIFs in response to tissue hypoxia (by 17DMAG) or at inhibiting VEGF-signaling and angiogenesis (by PTK787/ZK-222584) would be beneficial in controlling accelerated tumor recurrence following thermal ablation of liver metastases from colonic cancer.

Materials and Methods

Animals and surgical procedures

All experiments were carried out in accordance with the guidelines of the Animal Welfare Committee of the University Medical Center Utrecht, The Netherlands. Male BALB/c mice (10-12 weeks, 20-25

gram) and male Wag/Rij rats (16-20 weeks, 200-250 gram) were purchased from Charles River (Sulzfeld, Germany) and Harlan (Horst, The Netherlands), respectively. Animals were housed under standard laboratory conditions. All surgical procedures were performed under isoflurane inhalation anesthesia. Buprenorfine was administered intramuscularly prior to surgery to provide sufficient peri-operative analgesia.

Cell culture and induction of hepatic micrometastases

The murine colon carcinoma cell line C26 was used to induce colorectal liver metastases as described previously.[18] C26 cells transduced with a lentiviral vector encoding enhanced green fluorescent protein (EGFP) were used for fluorescence microscopy analysis.

Colorectal liver metastases were induced in mice as described.[18,19] In brief, through a left lateral flank incision, $5x10^4$ C26 colon carcinoma cells were injected into the splenic parenchyma. After ten minutes, the spleen was removed to prevent intrasplenic tumor growth. Diffuse intrahepatic micrometastases were allowed to grow out for three days.

For tumor inoculation in rats, we used the CC531 colon carcinoma cell line, which was kindly provided by Dr. PJK Kuppen (Department of Experimental Surgery, Leiden University Medical Center, Leiden, The Netherlands). Through a midline incision, $1x10^6$ CC531 cells were injected into the portal vein. To prevent bleeding after injection, the puncture hole was sealed with an absorbable fibrin-collagen coated patch (Nycomed, Breda, The Netherlands). Micrometastases were allowed to develop in the ensuing six days.

Radiofrequency ablation and laser-induced thermotherapy

Radiofrequency ablation (RFA) was performed using the CELON Power System (Celon AG, Teltow, Germany). In mice, a single non-cooled bipolar electrode (outer diameter 1.0 mm, active length 10 mm, kindly provided by dr. A. Roggan, Celon AG, Teltow, Germany) was used for RFA of the left liver lobe at 2 Watts for 50 seconds, corresponding with a total energy output of 100 Joules. In rats, RFA was performed in the left liver lobe by using a bipolar electrode (Celon AG, Teltow, Germany) with a saline-cooled diffuser tip (outer diameter 1.8 mm, active length 20 mm) at 2 Watts for 150 seconds (300 Joules). Sham-operated animals underwent laparotomy without further local treatment.

To test whether the effect of RFA on perinecrotic tumor cells was based on a general phenomenon, we also used laser-induced thermotherapy (LITT) in mice. A Nd:YAG laser (Medilas 4060 N, MBB, Medizin Technik, Munchen, Germany) with a wavelength of 1064 nm was used. The laser light was delivered in a continuous wave mode through a 400 µm fiber with a diffuser tip applicator (outer diameter 1.2 mm, active length 10 mm, Trumpf Medizine Systeme, Umkirch, Germany). LITT was applied to the left liver lobe at a power setting of 3 Watts per centimeter diffuser length for 90 seconds, corresponding to a total energy output of 270 Joules.

Drug characteristics

17DMAG (InvivoGen, San Diego, USA), a heat shock protein-90 inhibitor known to destabilize HIF-1α and HIF-2α[20-22], was dissolved in saline and administered by intraperitoneal injections at a preoperative dose of 15 mg/kg body weight, followed by three postoperative doses of 7.5 mg/kg body weight every 12 hours.[23,24]

PTK787/ZK-222584 (PTK/ZK), a non-selective vascular endothelial growth factor receptor

tyrosine kinase inhibitor[25], was kindly provided by Dr. D. Laurent (Schering AG, Berlin, Germany). PTK/ZK was dissolved in polyethyleneglycol 400 and administered twice-daily by intra-gastric injections at a dose of 50 mg/kg starting prior to RFA until 48 hours after RFA.

Experimental design

The effect of RFA on perinecrotic outgrowth of micrometastases was assessed in two different animal models. Three days after intrasplenic tumor cell injection mice were subjected to either RFA or sham operation and sacrificed 7 days later (n=8 each group). In rats, micrometastases were allowed to develop for 6 days followed by RFA or sham operation. Tumor growth was assessed 9 days later (n=8 each group). The livers were harvested and fixed in 4% buffered formaldehyde and embedded in paraffin for morphological assessment of tumor growth.

For the intervention studies, mice with pre-established micrometastases underwent RFA treatment and were randomized into different treatment groups (n=8 each group). Mice received either i) 17DMAG, ii) PTK/ZK or iii) no treatment (control). Tumor growth was assessed 7 days later. The effect of these drugs on tumor growth in sham-operated mice was evaluated separately. For these control experiments, metastases were allowed to grow out for 9 days after sham operation.

Assessment of hypoxia and activation of HIF pathway

The extent and localization of hypoxia were analyzed using the hypoxia marker pimonidazole hydrochloride (Hypoxyprobe-1, 90201, Chemicon International, Temecula, CA, USA), which was injected intravenously one hour prior to termination at a dose of 60 mg/kg.[26] For this experiment, livers were harvested 2 hours, 24 hours and 7 days after RFA (n=4 each group). Pimonidazole adducts were visualized by immunohistochemistry according to instructions from the manufacturer.

Activation of the HIF-1α and HIF-2α cascade was assessed using immunohistochemistry, including the downstream markers CA-IX, Glut-1 and VEGF.[27] In addition, we evaluated the upregulation of heat shock protein 90 (hsp90), which is controlled by stresses like heat and hypoxia and regulates the HIF cascade.[22,28] Antibodies were purchased from Dako, Heverlee, Belgium (Glut-1), Novus, Littleton, USA (HIF-1α, HIF-2α, CA-IX) and Santa Cruz Biotechnology, Santa Cruz, USA (hsp90 and VEGF). As secondary antibody PowerVision+ (Immunologic, Duiven, The Netherlands) with 2% mouse serum was used. Reactions were developed using diaminobenzidine/H_2O_2 as a chromogen substrate. Primary antibody-omitted negative controls were treated with the antibody diluent alone and were all free of non-specific background staining.

Evaluation of perinecrotic microcirculation and hepatic neovascularization

The hepatic microcirculation was assessed by intravital fluorescence microscopy using a Nikon TE-300 inverted microscope (Uvikon, The Netherlands) equipped with a fluorescence filter for fluorescein isothiocyanate (FITC) (excitation 450-490 nm, emission >515 nm). For contrast enhancement, 100 µl 2% FITC-labeled dextran (MW 446.000, Sigma, Zwijndrecht, The Netherlands) in 0.9% NaCl was injected intravenously and excited with blue light (450-490 nm). After re-opening the midline incision, the mice were placed on an inverted microscopic stage, using a template to minimize tension and respiratory movement. Microcirculatory flow was assessed at two distances from the lesion edge (2 and 6 mm). For each distance ten to fifteen fields were recorded for 10 seconds per animal. Images were captured at a 40x magnification by a charge coupled device camera (Exwave HAD, Sony,

The Netherlands) and relayed to a personal computer for off-line analysis. Sinusoidal perfusion rates were analyzed by two independent observers and were calculated by dividing the number of normally perfused sinusoids by the total number of sinusoids observed (n=4 each group).
To visualize possible hepatic neovascularization in the transition zone following RFA, intravital microscopy at a 10x magnification was used as above. In non tumor-bearing mice (n=4 each group), the microcirculation in the transition zone was assessed 24 hours, 3, 5 and 7 days following RFA. To improve visualization of the hepatic neovascularization in the transition zone, we also analyzed the non tumor-bearing livers *ex vivo* with a Zeiss LSM510 Meta confocal microscope using 10x magnification (n=4 each group). At the designated time points after RFA, mice were injected intravenously with RITC-labeled dextran (MW 70.000 or MW 2.000.000, Invitrogen, Carlsbad, USA). Ten minutes after injection the mice were sacrificed, the left liver lobe was excised and placed on a coverslip using immersion oil to further improve visualization. The livers were analyzed with combined bright field/fluorescence microscopy and confocal microscopy. To visualize the vessels, the rhodamine (RITC) was excited at 561 nm using the yellow diode laser.
Finally, to evaluate the relationship between hepatic neovascularization and tumor growth, mice were injected with GFP-expressing tumor cells as above. Seven days after RFA, tumor-bearing mice were analyzed as stated in the former section (n=4 each group). In these mice, the GFP-expressing C26 tumor cells were excited at 488 nm. Vessel visualization was the same as above. Image acquisition and analysis were performed using Zeiss LSM5 Software.

Tumor analysis

Tumor load in the liver was scored as the hepatic replacement area (HRA), the percentage of liver tissue that has been replaced by tumor tissue.[18,19] HRA was measured in the transition zone, defined as the area stretching 2 mm outside the necrotic central area, and in the reference zone, i.e. the remaining part of the liver. The definition of the transition zone was based on preliminary histological data, showing transition zone characteristics being most abundant in the first 2 mm stretching from the edge of the necrosis. Analyses were performed by two independent observers, blinded to treatment, using an automated microscope with an interactive video overlay system (Leica-Q-Prodit, Leica Microsystems, Rijswijk, The Netherlands). The scar tissue induced by RFA was excluded from analysis. For analysis of treatment with 17DMAG and PTK/ZK, we also compared HRA ratios, the ratio between HRA in the transition zone versus the reference zone. Thus, HRA ratio reflects the level of tumor growth acceleration.[19]
In the rat model, the transition zone was defined as the area stretching 10 mm outside the lesion, based on the more expansive growth pattern of CC531 cells.

***In vitro* analysis of HIF-1α and HIF-2α stabilization in hypoxic C26 cells**

We assessed the expression of HIF proteins in hypoxic and normoxic C26 cells using Western blotting. Hypoxia was instantly induced by placing the C26 cells at 1% O_2 and 37°C for two hours in an Invivo$_2$ Hypoxia Workstation 1000 (Biotrace International, UK) and replacing the medium by medium equilibrated at 1% O_2. Normoxia served as a control and was represented by 21% O_2 at 37°C. For western blotting, the same antibodies were used as described above.
To determine the effect of 17DMAG on HIF protein expression *in vitro*, cells were treated with 1μM 17DMAG, 24 hours prior to hypoxia. Treated and untreated cells without hypoxia served as controls.

Statistical analysis

Statistical differences between groups were analyzed by the Student's t-test and ANOVA for parametric data. Data are expressed as mean +/- SEM.

Results

Radiofrequency ablation enhances perinecrotic outgrowth of colorectal micrometastases

Metastases in sham-operated mice were distributed equally throughout the liver lobes and covered approximately 15% of the liver tissue (Figures 1A, B, D, F and H). In RFA-treated livers, a clear necrotic zone of 7.2 ± 0.2 x 4.9 ± 0.2 mm had developed in all livers (central zone, CZ). The lesions were clearly encircled by a rim of tumor (Figures 1A, 1G and 1I). Tumor load in the transition zone (TZ) surrounding the central necrotic zone had increased three to four-fold compared to tumor load in the unaffected reference zone (RZ, 48.5 ± 3.9% vs 14.8 ± 1.1%, p=0.0002) and compared to tumor growth in the livers of sham-operated mice (48.5 ± 3.9% vs 17.9 ± 2.0%, p=0.00021, figure 1D). No differences were found between tumor growth in the reference zone of RFA-treated mice when compared to tumor growth in sham-operated mice (Figure 1D).

Laser-induced thermotherapy (LITT) stimulated the outgrowth of tumor cells in the transition zone to a similar extent (approximately four-fold) as RFA. Following LITT, tumor load in the transition zone had increased approximately four-fold compared to tumor load in the reference zone (TZ 40.1 ± 3.5% vs RZ 11.4 ± 2.3%, p=0.001, data not shown). In addition, the size of the necrotic zone formed by LITT was comparable to that induced by RFA.

Similar to the murine model, RFA in rats induced a four-fold increase in tumor tissue in the transition zone surrounding the ablated region as compared to the other non-treated reference areas (40.4 ± 6.1 vs 10.6 ± 3.9, p=0.007, figures 1C, E). Microscopically, CC531 tumors in the reference zone were well differentiated displaying glandular organization throughout the lesion (Figures 1J and 1L). However, confluent tumor masses in the transition zone displayed a disorganized and poorly differentiated phenotype with loss of glandular architecture (Figures 1K and 1M). No extrahepatic metastases were found in any of the animals.

Accelerated tumor growth is associated with perinecrotic tissue hypoxia and subsequent stabilization of hsp90, HIF-1α and HIF-2α

Histopathologically, RFA induced progressive hepatocellular injury followed by infiltration of inflammatory cells 24 hours and 7 days after RFA (Figure 2A). In control liver tissue of sham-operated mice, pimonidazole staining was exclusively observed around central venules, which are known to be characterized by relatively lower oxygen concentrations.[26] Two hours after RFA, profound diffuse tissue hypoxia was observed throughout the transition zone (Figure 2B). During the ensuing 7 days, the perinecrotic liver parenchyma remained remarkably hypoxic. Heat shock protein 90 (hsp90) showed a similar staining pattern, with maximal staining at 24 hours following RFA (Figure 2C).

Similar to the pimonidazole staining, HIF-1α was detected around central venules in control liver tissue (Figure 2D). In the transition zone, both cytoplasmic and nuclear HIF-1α and HIF-2α were observed at the lesion edge, with maximal staining at 24 hours and 2 hours after RFA, respectively (Figures 2D and 2E).

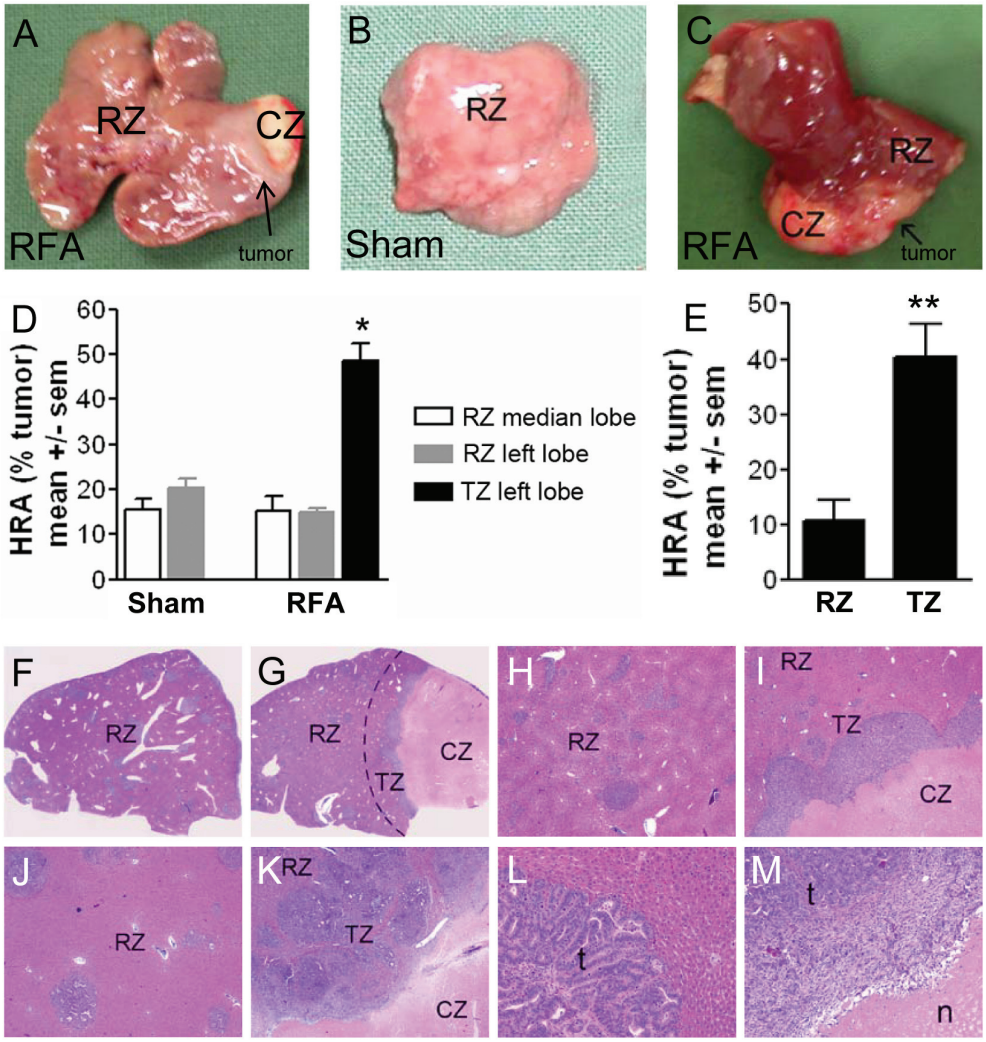

Figure 1 Accelerated peri-lesional outgrowth of pre-established micrometastases following radiofrequency ablation in BALB/c mice (A, B, D and F-I) and Wag/Rij rats (C, E and J-M)
(A, B) Mouse livers, containing C26 metastases in the reference zone (RZ) and in the transition zone (TZ, arrow) surrounding the necrotic central zone (CZ), 7 days after RFA (A) and sham-operation (B). **(C)** Rat liver, containing CC531 metastases in the reference zone (RZ) and in the transition zone (arrow) surrounding the central zone (CZ), 9 days after RFA. **(D, E)** Tumor growth, expressed as the hepatic replacement area (HRA) in the RZ and TZ, defined as the area extending 2 mm outside the necrotic lesion for RFA-treated mouse liver (D) and 10 mm outside the necrotic lesion for RFA-treated rat liver (E). *p=0.0002 TZ versus RZ in the left liver lobe and p=0.00021 TZ versus RZ sham (mouse), **p=0.007 TZ versus RZ (rat). **(F-I)** Hematoxylin and eosin (H&E)-stained sections of paraffin-embedded mouse liver containing metastases in control liver lobes (F and H) and of metastases surrounding the necrotic lesion induced by RFA (G and I) (F and G: magnification 0.5x, H and I: magnification 2x). The dotted line in G is located 2 mm outside the necrosis, the area between this dotted line and the necrosis (n) represents the transition zone. **(J-M)** H&E-stained sections of paraffin-embedded rat liver containing metastases (t) in control liver lobes (J and L) and of metastases surrounding the necrotic lesion induced by RFA (K and M) (J and K: magnification 2x, L and M: magnification 10x).

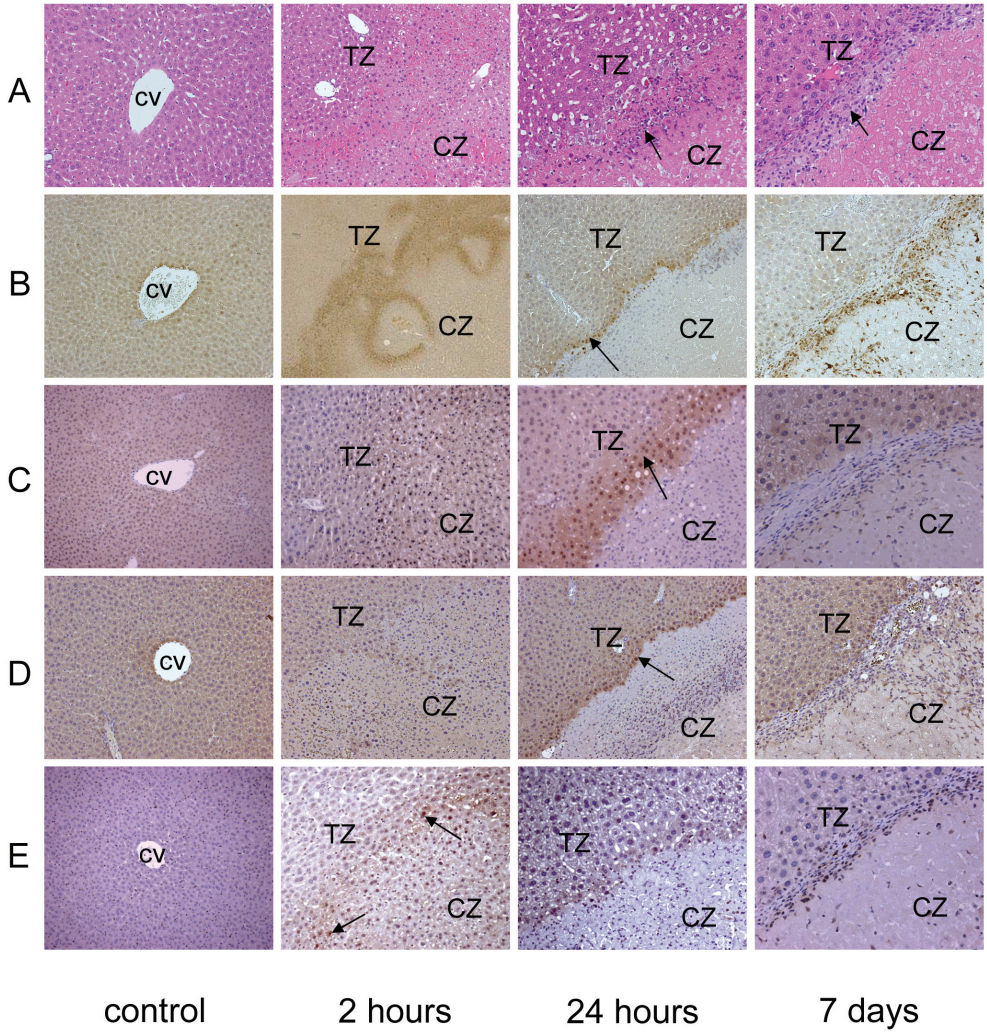

Figure 2 Hypoxia in transition zone of non tumor-bearing mice following RFA
(A) H&E-stained sections of control liver tissue and of tissue sections after RFA, showing infiltration of inflammatory cells 24 hours and 7 days after RFA (arrows). **(B)** Tissue hypoxia was detected by pimonidazole immunohistochemistry (brown) around the central veins (CV) in normal liver tissue and in the transition zone (TZ) surrounding the central necrotic zone (CZ) 2 and 24 hours and 7 days after RFA. **(C)** Heat shock protein 90 (hsp90) (brown) is upregulated in the transition zone following RFA, with a peak at 24 hours after RFA (arrow). **(D, E)** Hypoxia Inducible Factors (HIF)-1α (D) and HIF-2α (E) immunostaining (brown) in the transition zone surrounding the central necrotic zone, with highest intensities at 24 hours and 2 hours following RFA, respectively (arrows). Original magnification 10x, except pimonidazole at 2 hours (2x).

To assess the activation of HIF target genes, we stained the liver tissue for the commonly used downstream markers CA-IX, Glut-1 and VEGF. All downstream markers were upregulated in the transition zone as well, peaking at 24 hours following RFA (Figure 3).
Mice that were treated with RFA for analysis of microvascular disturbances, hepatic neovascularization or control tumor growth were analyzed for hypoxia as well. All of these mice invariably revealed the occurrence of hypoxia in the transition zone.

Accelerated tumor growth is associated with high HIF-1α and HIF-2α levels in tumor cells

As shown above, the accelerated tumor growth following RFA is predominantly located in the transition zone (Figure 4). In control tumor tissue, minimal pimonidazole staining was observed, whereas in tumor tissue located in the transition zone, pimonidazole staining was strongest at the tumor-necrosis interface (Figure 4). Neither HIF-1α nor HIF-2α staining was observed in control tumor in the reference zone. Tumor cells located in the transition zone, most notably at the hypoxic tumor-necrosis interface, displayed strong nuclear HIF-1α and HIF-2α staining (Figure 4).

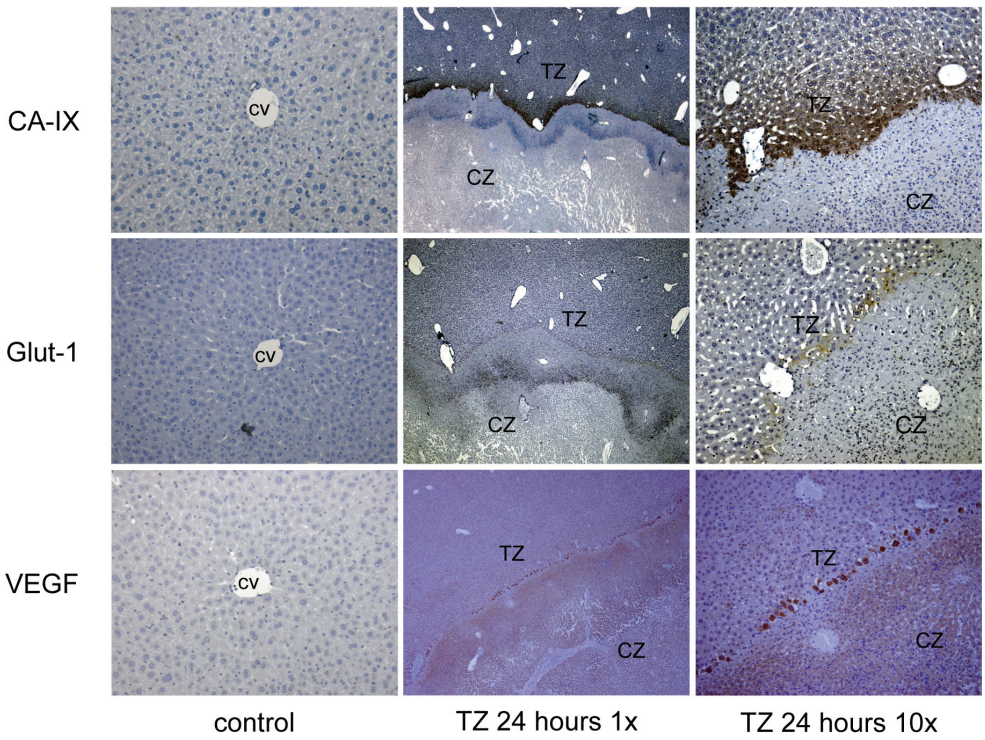

Figure 3 Upregulation of downstream markers of Hypoxia Inducible Factors
The expression of the commonly used downstream markers of HIF, carbonic anhydrase IX (CA-IX), glucose transporter-1 (Glut-1) and vascular endothelial growth factor (VEGF), is higher in the transitione zone (TZ) compared to the reference zone (RZ) at 24 hours following RFA,

RFA induces prolonged microcirculatory disturbances

We hypothesized that chronic hypoxia and HIF-stabilization could be due to prolonged local changes in the microcirculation. Extravasation of FITC-dextran was observed directly adjacent to the lesion at 2 and 24 hours following RFA, indicating loss of sinusoidal integrity. This phenomenon gradually decreased over time throughout the experiment (Figures 5B and 6). Vascular leakage was no longer observed 5-7 days following RFA (Figure 6).

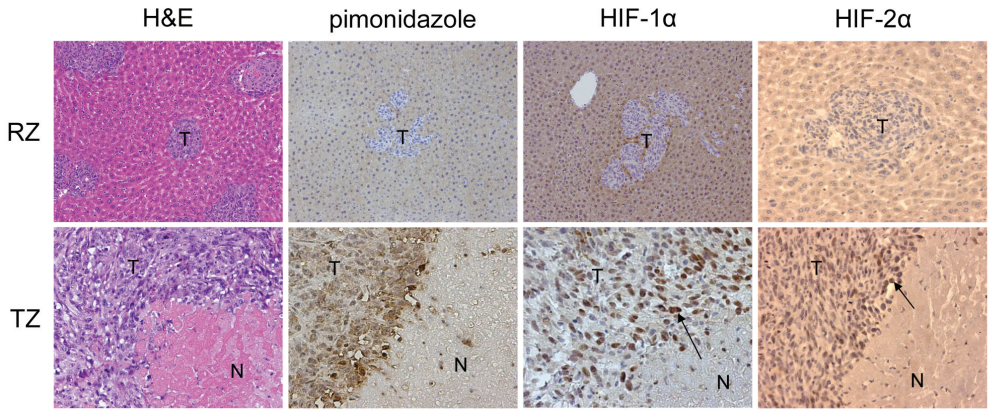

Figure 4 Hypoxia, HIF-1α and HIF-2α in control tumor tissue in the reference zone and in accelerated tumor cells in the transition zone 7 days after RFA

H&E-stained sections show control liver tissue containing tumor (t) and liver tissue sections after RFA, in which tumor is located adjacent to the necrosis (n). Pimonidazole immunohistochemistry (brown) indicates hypoxia of tumor cell deposits in the reference zone and the transition zone surrounding the central necrotic zone. HIF-1α (C) and HIF-2α (D) immunostaining shows minimal staining in control tumor tissue (blue tumor cells) and nuclear staining (brown tumor cells) in tumor tissue at the necrosis-tumor interface (arrows). Magnification RZ panel 10x, magnification TZ panel 15x.

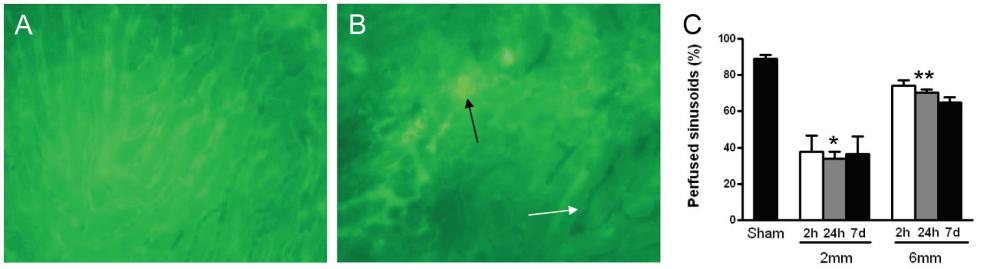

Figure 5 Peri-lesional microcirculatory flow following RFA as evaluated by intravital microscopy (IVM)

(A, B) Stills from intravital microscopy videos of the hepatic microcirculation in the reference zone (A) and in the transition zone (B), 40x magnification. **(A)** Approximately 85-90% of the identified sinusoids contain normal blood flow. **(B)** In the transition zone, extravasation of FITC-dextran (black arrow) and disturbed microcirculation (white arrow) is observed 2 hours following RFA. **(C)** Hepatic sinusoidal perfusion rates 2, 24 hours and 7 days after sham operation and RFA measured at 2 and 6 mm distance from the lesion edge. *$p<0.001$ versus untreated controls. **$p<0.05$ versus untreated controls and 2 mm.

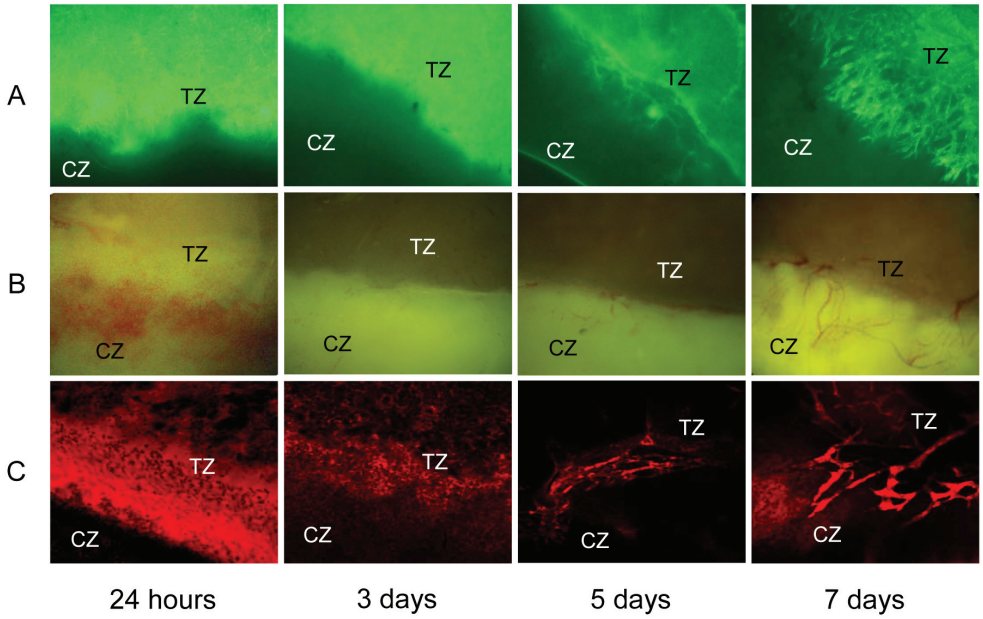

Figure 6 Microcirculation of the lesion edge of non tumor-bearing mice 24 hours, 3, 5 and 7 days after RFA
(A) Stills from intravital microscopy showing blood flow in microcirculation, while combined bright field/fluorescence microscopy **(B)** and confocal microscopy **(C)** occurred *ex vivo* to improve visualisation. At 24 hours after RFA, the transition zone is characterized by excessive vascular leakage, shown by the increased extravasation of FITC-dextran (A) and RITC-dextran (B, C), which gradually decreased throughout the experiment. Neovasvasculature was visible in the transition zone from day 5 onward. At day 7 after RFA, the neovasvasculature was more pronounced and penetrating into the necrosis. We observed blood flow and loss of vascular leakage in these vessels using intravital microscoy (A).

RFA induced severe peri-lesional sinusoidal perfusion failure, as shown by reduced sinusoidal perfusion rates within the first 2 mm outside the necrotic lesion when compared to sham-operated mice ($p<0.001$, figure 5). Sinusoidal perfusion rates gradually increased further away from the lesion edge, but were still abnormal at 6 mm from the lesion edge, when compared with sham operated mice ($p<0.05$ versus sham and 2 mm, figure 5C). Interestingly, microcirculatory disturbances surrounding the necrotic lesion did not significantly improve during the first 7 days following RFA.

Tumor cells do not co-localize with newly formed vessels in the transition zone

As angiogenesis is a physiological response to hypoxia, we hypothesized that the chronic hypoxia we observed could lead to formation of new hepatic vessels in the rim of the necrosis. In non-tumor bearing mice 24 hours and 3 days after RFA, the transition zone was characterized by vascular leakage, but we did not observe neovascularization. However, from 5 days after RFA, large vessels became visible in the rim of the necrosis (Figure 6). These vessels displayed normal blood flow, are approximately 4-5 times larger in diameter compared to the sinusoids and sprout from sinusoids (data not shown). Surprisingly, tumor cells did not co-localize with the neovasculature: the latter penetrated into the necrosis while a broad band of tumor cells was observed at the rim of the necrosis (Figure 7).

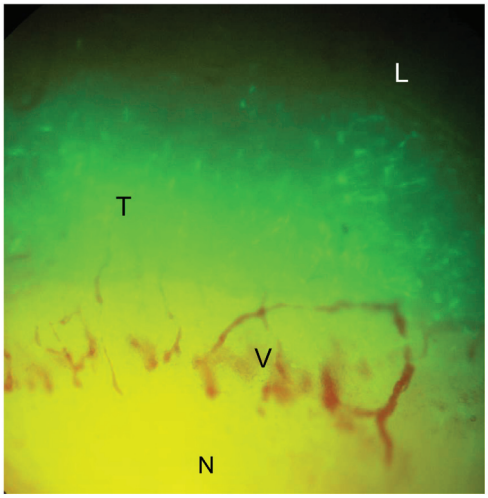

Figure 7 Combined bright field/fluorescence microscopy of the transition zone of tumor-bearing mice 7 days after RFA
From 5 days after RFA, neovasculature was observed in the transition zone (figure 5). Mark that tumor cells (T) in the transition zone do not co-localize with these vessels (V). The newly formed vessels penetrate into the necrosis (N), while a broad band of tumor cells is observed at the necrotic rim. At the top of the pictures, normal liver tissue (L) can be seen.

Treatment with 17DMAG reduces the accelerated outgrowth following RFA which is associated with reduction of HIF-1α and HIF-2α stabilization

As demonstrated above, accelerated tumor growth following RFA was associated with activation of the hypoxia/HIF cascade. 17DMAG reduced the outgrowth of micrometastases in the transition zone from 42.1 ± 1.5% to 24.6 ± 4.0% (p=0.012, figure 8A) without affecting tumor growth in the reference zone (11.2 ± 2.0% vs 12.2 ± 1.8%, p=0.68, figure 8A) or after sham operation (45.5 ± 2.9% vs 40.8 ± 6.9%, p=0.48, figure 8B). The acceleration of tumor growth, as indicated by HRA ratio, was reduced by more than 50%, from 4.6 ± 0.7 to 2.2 ± 0.3, p=0.015, figure 8C), reflecting a selective inhibitory effect of 17DMAG on hypoxia-associated stimulation of tumor growth.

To ascertain the effects of 17DMAG treatment, we evaluated its effect on HIF stabilization in C26 cells *in vitro*. Two hours of 1% hypoxia resulted in HIF-1α and HIF-2α stabilization in the tumor cells (Figure 8D). This HIF-1α and HIF-2α stabilization was counteracted by the addition of 17DMAG to the medium 24 hours before hypoxia. In addition, micrometastases in mice treated with 17DMAG failed to stabilize HIF-1α and HIF-2α in response to RFA (Figure 8F).

Treatment with the non-selective VEGF receptor inhibitor PTK/ZK clearly reduced tumor growth in the transition zone from 42.1 ± 1.5% to 23.0 ± 4.0%, (p=0.007, figure 8A). However, PTK/ZK reduced tumor growth in the reference zone (11.2 ± 2.0% vs 6.6 ± 1.2%, p=0.078, figure 8A) and in sham operated mice as well (45.5 ± 2.9% vs 24.1 ± 4.3%, p=0.008, figure 8B). Therefore, PTK/ZK, unlike 17DMAG, had no selective inhibitory effect on accelerated tumor growth following RFA, as shown by the HRA ratio when PTK/ZK treated mice were compared with control mice (4.1 ± 0.6 vs 4.6 ± 0.7 respectively, p=0.62, figure 8C).

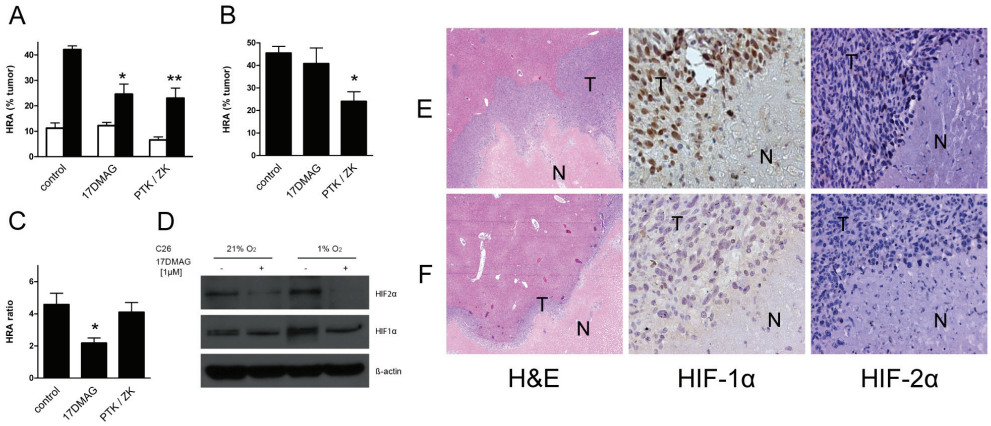

Figure 8 The effect of 17DMAG and PTK/ZK on peri-lesional outgrowth of pre-established micrometastases evaluated 7 days after RFA

(A) Tumor growth, expressed as the hepatic replacement area (HRA), in the transition zone (black bars) and reference zone (white bars). Treatment with 17DMAG (*p=0.012) and PTK/ZK (**p=0.007) reduced the tumor growth in the transition zone (p-values versus TZ of untreated controls). **(B)** Tumor growth in mice treated with 17DMAG or PTK/ZK that did not undergo RFA. 17DMAG had no significant effect (p=0.48 versus untreated controls), while PTK/ZK significantly reduced tumor load (*p=0.008 versus untreated controls). **(C)** Acceleration of tumor growth in the transition zone, expressed as HRA ratio. 17DMAG reduced the acceleration of tumor growth with >50% (*p=0.015 versus untreated controls), while PTK/ZK had no effect on the growth acceleration (p=0.62 versus untreated controls). **(D)** Western blot of normoxic and hypoxic C26 colon carcinoma cells, which were treated with 17DMAG. Hypoxia stabilized HIF-1α and HIF-2α in the C26 cells. This stabilization was prevented by incubating the cells in medium containing 1μM 17DMAG before they underwent hypoxia. **(E, F)** Microscopic appearance of tumor growth and HIF-staining in untreated mice (E) and mice treated with 17DMAG. Mark the reduction in HIF-1α and HIF-2α staining (less brown) in mice treated with 17DMAG compared with untreated mice. Magnification 2x (H&E) and 15x. T tumor; N necrosis.

Discussion

Here we show for the first time that, following RFA treatment, a highly localized hypoxia-driven acceleration of tumor growth occurs in the transition zone between necrosis induced by RFA and the normal liver tissue. Our results are in accordance with recent work from others, showing stimulatory effects of thermal ablation on recurrent tumor growth.[29,30] Moreover, we have revealed that the stimulated outgrowth of peri-lesional micrometastases is associated with profound and chronic microvascular disturbances, chronic tissue and tumor hypoxia and stabilization of HIF-1α and HIF-2α, but not with hypoxia-driven angiogenesis. This bears resemblance to the accelerated micrometastases outgrowth after ischemia/reperfusion injury which occurs following liver surgery.[19]

As illustrated by Solbiati *et al*. and others, increasing tumor size is associated with a higher rate of local recurrence.[7,9] This emphasizes the importance of obtaining satisfactory ablative margins.[31] However, even when complete tumor destruction is achieved and satisfactory ablation margins have been created, occult micrometastastatic cells can be located in the transition zone. In 26-70% of patients with colorectal liver metastases, hepatic micrometastases were detected on histological examination.[32-34] As thermal destruction therapies will unequivocally produce a transition zone, the growth of micrometastases that are located in the transition zone may be accelerated.

The observed microcirculatory disturbances are caused by a combination of at least three different phenomena. First, both hyperthermia and hypoxia have a direct detrimental effect on endothelial cells.[35,36] As a result, sinusoids become leaky, which was observed in our experiments by the extravasation of FITC-dextran in the transition zone. This is in accordance with reports describing a hyperaemic rim at the necrotic margin.[37] Second, hyperthermia leads to blood clotting in the sinusoids.[37,38] This is illustrated in our experiments by the absence of FITC-dextran in several sinusoids in the transition zone. Third, radiofrequency ablation leads to a rise in interstitial liver parenchymal pressure in the transition zone, which may aggravate the microvascular disturbances due to collapse of the sinusoids, with subsequent congestion of blood.[39] These microvascular disturbances could very well correspond to the peripheral rim of enhancement observed on post-procedural MRI or CT.[11,40] We observed that the extravasation of FITC-dextran was present in the acute phase following RFA (24 hours), which resolved within a couple of days. This is in accordance with the results of Lim *et al*., who showed the presence of peripheral rim enhancement in 79% of cases, resolving in all cases within 1 month.[40]

While prolonged periods of hypoxia are deleterious to most cells, tumor cells have adapted to survive under hypoxic conditions.[17] Subsequent HIF stabilization (both HIF-1α and HIF-2α) leads to transcription of several genes that are implicated in cancer progression, including proliferation-promoting cytokines, growth factors and glucose transporters. Moreover, the HIFs promote (tumor) neovascularization through upregulation of VEGF.[17,41] Thus, prolonged perinecrotic hypoxia as observed after RFA may provide a pro-tumorigenic microenvironment through stabilization of HIF-1α and HIF-2α. Interestingly, pimonidazole, HIF-1α and HIF-2α immunostaining were mainly localized immediately adjacent to the necrotic central zone and strong nuclear HIF-1α and HIF-2α staining was observed in tumor cells at the necrosis-tumor interface for as long as 7 days after RFA. Our finding that 17DMAG largely reduced the accelerated outgrowth of micrometastases, but did not influence tumor growth in sham-operated mice or in untreated areas, suggests that the compound may be particularly effective in selectively reducing hypoxia-associated acceleration of tumor growth. This phenomenon was supported by *in vitro* experiments showing that 17DMAG prevented stabilization of HIF-1α and HIF-2α in tumor cells by hypoxia.

The geldanamycin-analogue 17DMAG is a hsp90 inhibitor. Heat shock proteins (or stress proteins) are molecular chaperones that help other proteins fold properly. We also observed upregulation of hsp90 in the transition zone, peaking 24 hours after RFA. Hsp90 is one of the most abundant heat shock proteins that is constitutively expressed in cells.[42] Interestingly, hsp90 expression is upregulated during tumorigenesis, thereby emphasizing the role of hsp90 in tumor cell survival.[43] It is acutely upregulated in response to stresses like hypoxia and hyperthermia, followed by modulation of numerous targets aimed at promoting cell survival, including HIF.[22,28,42,44] Thus, targets other than HIF-1α or HIF-2α may have contributed to the effectiveness of 17DMAG in reducing tumor growth in the transition zone. A specific role for hsp90 and other heat shock proteins in the stimulation of tumor growth after hyperthermia requires further research.

VEGF is one of the best studied downstream effectors of HIF and plays a pivotal role in the stimulation of hypoxia-driven angiogenesis.[16] Angiogenesis has been long recognized as a prerequisite for metastatic progression[16] and has been previously implied in surgery-induced tumor growth.[14,15] Several angiogenic factors, including VEGF, are up-regulated primarily adjacent to the ablation site, comparable to our results.[29,30] Moreover, we observed neovasculature sprouting from existing sinusoids at the lesion edge starting 5 days after RFA, which corresponded with VEGF upregulation. Surprisingly,

however, tumor cells were not associated with this neovasculature.

Anti-angiogenic agents are widely investigated as anticancer treatment and are increasingly used in clinical practice. The non-selective VEGF-receptor inhibitor PTK/ZK has previously been shown to reduce the growth of solid tumors, including colorectal liver metastases.[45] Recently, two large randomized clinical trials have shown PTK/ZK to improve the progression free survival in patients with metastatic colorectal cancer, without improving the overall survival.[46,47] In the present study, anti-angiogenic treatment with PTK/ZK did not selectively suppress hypoxia-associated tumor growth in the transition zone, as was observed for 17DMAG. However, PTK/ZK reduced metastatic tumor growth in both RFA-treated and untreated liver lobes. Therefore, PTK/ZK may represent a very potent drug in the postoperative setting, as it may delay both ablation-accelerated recurrent tumor growth as well as recurrences in the remaining liver.

Until now, adjuvant treatments used in combination with thermal destruction therapies like RFA or LITT have mainly involved cytotoxic agents. In preclinical models, the combination of RFA or LITT with intravenous doxorubicin-based chemotherapy produced an increase in coagulation size and a reduction of recurrence.[48,49] Goldberg *et al*. confirmed this finding in a clinical pilot study when RFA was combined with i.v. doxorubicin in a liposome carrier (Doxil).[50] As accelerated outgrowth following RFA in our model was associated with hypoxia, hypoxia-activated pro-drugs like tirapazamine, or tirapazamine-derived analogues could be efficacious in the adjuvant treatment of metastases following RFA.[51] Using transcather arterial chemoembolization (TACE) instead of i.v. injection, higher concentrations of chemotherapeutic agents can be accomplished in tumor tissue. This resulted in significant reduction of tumor burden in rat livers treated with LITT combined with TACE.[52] Recently, it has been shown that RFA in combination with TACE increased survival in patients with hepatocellular carcinoma larger than 3 cm.[53] The added value of TACE in RFA treatment of colorectal liver metastases remains to be determined.

Alternative mechanisms other than the HIF pathways might be important in RFA-accelerated tumor growth. Necrosis and hypoxia may generate a niche for recruitment and retention of bone marrow-derived progenitor cells (BMDPC) by local secretion of cytokines, chemokines and growth factors. Recent literature emphasizes the role of BMDPCs in promoting tumor growth.[54,55] Further research will involve the role of BMDPC recruitment in RFA-accelerated tumor growth.

In addition to the local pro-tumorigenic effect described in the present study, several authors have described anti-tumorigenic effects after local ablative therapy on the outgrowth of pre-established remote tumor cell deposits.[56] Hyperthermia may elicit an anti-tumor T cell response, by presenting tumor antigens to the immune system resulting in reduced tumor growth in contralateral lobes and extrahepatic locations.[57] In our study we have not observed any anti-tumor effects in contralateral lobes. However, at the time of RFA in our model, tumor load was relatively low and, therefore, the likelihood of generating sufficient amounts of tumor-derived antigens for mounting an effective anti-tumor immune response is small.

RFA has been proposed to present an acceptable alternative in the treatment of resectable colorectal liver metastases. In a recent review, Mulier *et al*. stated that the time has come to start a randomized trial comparing RFA and resection for small resectable colorectal liver metastases.[8] In the present study we show in two pre-clinical models that RFA has a dramatic stimulatory effect on the outgrowth of pre-established microscopic tumor cell clusters at the lesion periphery. In patients, satellite lesions and residual tumor tissue due to incomplete ablation can be the source of remaining tumor cells in

the transition zone that may be stimulated to grow by RFA. Since the current imaging techniques have difficulties to visualize both phenomena, our results should be taken into consideration when plans for randomized trials are undertaken.

RFA for liver metastases of colonic cancer accelerates the outgrowth of microscopic tumor cell deposits immediately adjacent to the generated necrotic lesion. We conclude that prolonged tissue hypoxia contributes to the altered behavior of these micrometastases, possibly through stabilization of HIF-1α and HIF-2α. However, accelerated tumor growth is not associated with stimulation of tissue angiogenesis.

References

1. Simmonds PC, Primrose JN, Colquitt JL, Garden OJ, Poston GJ, Rees M. Surgical resection of hepatic metastases from colorectal cancer: a systematic review of published studies. Br J Cancer 2006; 94: 982-999.
2. Leonard GD, Brenner B, Kemeny NE. Neoadjuvant chemotherapy before liver resection for patients with unresectable liver metastases from colorectal carcinoma. J Clin Oncol 2005; 23: 2038-2048.
3. Nordlinger B, van Cutsem E., Rougier P, Kohne CH, Ychou M, Sobrero A, Adam R, Arvidsson D, Carrato A, Georgoulias V, Giuliante F, Glimelius B, Golling M, Gruenberger T, Tabernero J, Wasan H, Poston G. Does chemotherapy prior to liver resection increase the potential for cure in patients with metastatic colorectal cancer? A report from the European Colorectal Metastases Treatment Group. Eur J Cancer 2007; 43: 2037-2045.
4. Curley SA. Radiofrequency ablation of malignant liver tumors. Ann Surg Oncol 2003; 10: 338-347.
5. Siperstein AE, Berber E, Ballem N, Parikh RT. Survival after radiofrequency ablation of colorectal liver metastases: 10-year experience. Ann Surg 2007; 246: 559-567.
6. Abdalla EK, Vauthey JN, Ellis LM, Ellis V, Pollock R, Broglio KR, Hess K, Curley SA. Recurrence and outcomes following hepatic resection, radiofrequency ablation, and combined resection/ablation for colorectal liver metastases. Ann Surg 2004; 239: 818-825.
7. Mulier S, Ni Y, Jamart J, Ruers T, Marchal G, Michel L. Local recurrence after hepatic radiofrequency coagulation: multivariate meta-analysis and review of contributing factors. Ann Surg 2005; 242: 158-171.
8. Mulier S, Ni Y, Jamart J, Michel L, Marchal G, Ruers T. Radiofrequency Ablation Versus Resection for Resectable Colorectal Liver Metastases: Time for a Randomized Trial? Ann Surg Oncol 2007; 15: 144-157.
9. Solbiati L, Livraghi T, Goldberg SN, Ierace T, Meloni F, Dellanoce M, Cova L, Halpern EF, Gazelle GS. Percutaneous radio-frequency ablation of hepatic metastases from colorectal cancer: long-term results in 117 patients. Radiology 2001; 221: 159-166.
10. Ahmad A, Chen SL, Kavanagh MA, Allegra DP, Bilchik AJ. Radiofrequency ablation of hepatic metastases from colorectal cancer: are newer generation probes better? Am Surg 2006; 72: 875-879.
11. Goldberg SN, Gazelle GS, Compton CC, Mueller PR, Tanabe KK. Treatment of intrahepatic malignancy with radiofrequency ablation: radiologic-pathologic correlation. Cancer 2000; 88: 2452-2463.
12. Isbert C, Roggan A, Ritz JP, Muller G, Buhr HJ, Lehmann KS, Germer CT. Laser-induced thermotherapy: intra- and extralesionary recurrence after incomplete destruction of experimental liver metastasis. Surg Endosc 2001; 15: 1320-1326.
13. Hofer SO, Molema G, Hermens RA, Wanebo HJ, Reichner JS, Hoekstra HJ. The effect of surgical wounding on tumour development. Eur J Surg Oncol 1999; 25: 231-243.
14. Svendsen MN, Werther K, Nielsen HJ, Kristjansen PE. VEGF and tumour angiogenesis. Impact of surgery, wound healing, inflammation and blood transfusion. Scand J Gastroenterol 2002; 37: 373-379.
15. van der Bilt JD and Borel Rinkes IH. Surgery and angiogenesis. Biochim Biophys Acta 2004; 1654: 95-104.
16. Folkman J. Angiogenesis in cancer, vascular, rheumatoid and other disease. Nat Med 1995; 1: 27-31.
17. Harris AL. Hypoxia--a key regulatory factor in tumour growth. Nat Rev Cancer 2002; 2: 38-47.
18. van der Bilt JD, Kranenburg O, Nijkamp MW, Smakman N, Veenendaal LM, Te Velde EA, Voest EE, van Diest PJ, Borel Rinkes IH. Ischemia/reperfusion accelerates the outgrowth of hepatic micrometastases in a highly standardized murine model. Hepatology 2005; 42: 165-175.
19. van der Bilt JD, Soeters ME, Duyverman AM, Nijkamp MW, Witteveen PO, van Diest PJ, Kranenburg O, Borel Rinkes IH. Perinecrotic hypoxia contributes to ischemia/reperfusion-accelerated outgrowth of colorectal micrometastases. Am J Pathol 2007; 170: 1379-1388.
20. Isaacs JS, Jung YJ, Mimnaugh EG, Martinez A, Cuttitta F, Neckers LM. Hsp90 regulates a von Hippel Lindau-

independent hypoxia-inducible factor-1 alpha-degradative pathway. J Biol Chem 2002; 277: 29936-29944.
21. Mabjeesh NJ, Post DE, Willard MT, Kaur B, Van Meir EG, Simons JW, Zhong H. Geldanamycin induces degradation of hypoxia-inducible factor 1alpha protein via the proteosome pathway in prostate cancer cells. Cancer Res 2002; 62: 2478-2482.
22. Milkiewicz M, Doyle JL, Fudalewski T, Ispanovic E, Aghasi M, Haas TL. HIF-1alpha and HIF-2alpha play a central role in stretch-induced but not shear-stress-induced angiogenesis in rat skeletal muscle. J Physiol 2007; 583: 753-766.
23. Egorin MJ, Lagattuta TF, Hamburger DR, Covey JM, White KD, Musser SM, Eiseman JL. Pharmacokinetics, tissue distribution, and metabolism of 17-(dimethylaminoethylamino)-17-demethoxygeldanamycin (NSC 707545) in CD2F1 mice and Fischer 344 rats. Cancer Chemother Pharmacol 2002; 49: 7-19.
24. Hollingshead M, Alley M, Burger AM, Borgel S, Pacula-Cox C, Fiebig HH, Sausville EA. In vivo antitumor efficacy of 17-DMAG (17-dimethylaminoethylamino-17-demethoxygeldanamycin hydrochloride), a water-soluble geldanamycin derivative. Cancer Chemother Pharmacol 2005; 56: 115-125.
25. Wood JM, Bold G, Buchdunger E, Cozens R, Ferrari S, Frei J, Hofmann F, Mestan J, Mett H, O'Reilly T, Persohn E, Rosel J, Schnell C, Stover D, Theuer A, Towbin H, Wenger F, Woods-Cook K, Menrad A, Siemeister G, Schirner M, Thierauch KH, Schneider MR, Drevs J, Martiny-Baron G, Totzke F. PTK787/ZK 222584, a novel and potent inhibitor of vascular endothelial growth factor receptor tyrosine kinases, impairs vascular endothelial growth factor-induced responses and tumor growth after oral administration. Cancer Res 2000; 60: 2178-2189.
26. Arteel GE, Thurman RG, Yates JM, Raleigh JA. Evidence that hypoxia markers detect oxygen gradients in liver: pimonidazole and retrograde perfusion of rat liver. Br J Cancer 1995; 72: 889-895.
27. Bussink J, Kaanders JH, van der Kogel AJ. Tumor hypoxia at the micro-regional level: clinical relevance and predictive value of exogenous and endogenous hypoxic cell markers. Radiother Oncol 2003; 67: 3-15.
28. Katschinski DM, Le L, Heinrich D, Wagner KF, Hofer T, Schindler SG, Wenger RH. Heat induction of the unphosphorylated form of hypoxia-inducible factor-1alpha is dependent on heat shock protein-90 activity. J Biol Chem 2002; 277: 9262-9267.
29. Nikfarjam M, Muralidharan V, Christophi C. Altered growth patterns of colorectal liver metastases after thermal ablation. Surgery 2006; 139: 73-81.
30. Ohno T, Kawano K, Yokoyama H, Tahara K, Sasaki A, Aramaki M, Kitano S. Microwave coagulation therapy accelerates growth of cancer in rat liver. J Hepatol 2002; 36: 774-779.
31. Berber E and Siperstein A. Local Recurrence After Laparoscopic Radiofrequency Ablation of Liver Tumors: An Analysis of 1032 Tumors. Ann Surg Oncol 2008; 15: 2757-2764.
32. Linnemann U, Schimanski CC, Gebhardt C, Berger MR. Prognostic value of disseminated colorectal tumor cells in the liver: results of follow-up examinations. Int J Colorectal Dis 2004; 19: 380-386.
33. Nanko M, Shimada H, Yamaoka H, Tanaka K, Masui H, Matsuo K, Ike H, Oki S, Hara M. Micrometastatic colorectal cancer lesions in the liver. Surg Today 1998; 28: 707-713.
34. Yokoyama N, Shirai Y, Ajioka Y, Nagakura S, Suda T, Hatakeyama K. Immunohistochemically detected hepatic micrometastases predict a high risk of intrahepatic recurrence after resection of colorectal carcinoma liver metastases. Cancer 2002; 94: 1642-1647.
35. Minor T, Isselhard W, Berghaus K. Parenchymal and vascular endothelial cell injury in the hypoxic and reperfused rat liver. Evidence for superoxide anion generation by perfusion with ferricytochrome c. Biomed Pharmacother 1993; 47: 213-218.
36. Zhou M, Zhang A, Lin B, Liu J, Xu LX. Study of heat shock response of human umbilical vein endothelial cells (HUVECs) using cDNA microarray. Int J Hyperthermia 2007; 23: 225-258.
37. Nikfarjam M, Muralidharan V, Malcontenti-Wilson C, Christophi C. Progressive microvascular injury in liver and colorectal liver metastases following laser induced focal hyperthermia therapy. Lasers Surg Med 2005; 37: 64-73.
38. Vaezy S, Martin R, Crum L. High intensity focused ultrasound: a method of hemostasis. Echocardiography

2001; 18: 309-315.
39. Kotoh K, Morizono S, Kohjima M, Enjoji M, Sakai H, Nakamuta M. Evaluation of liver parenchymal pressure and portal endothelium damage during radio frequency ablation in an in vivo porcine model. Liver Int 2005; 25: 1217-1223.
40. Lim HK, Choi D, Lee WJ, Kim SH, Lee SJ, Jang HJ, Lee JH, Lim JH, Choo IW. Hepatocellular carcinoma treated with percutaneous radio-frequency ablation: evaluation with follow-up multiphase helical CT. Radiology 2001; 221: 447-454.
41. Carmeliet P, Dor Y, Herbert JM, Fukumura D, Brusselmans K, Dewerchin M, Neeman M, Bono F, Abramovitch R, Maxwell P, Koch CJ, Ratcliffe P, Moons L, Jain RK, Collen D, Keshert E. Role of HIF-1alpha in hypoxia-mediated apoptosis, cell proliferation and tumour angiogenesis. Nature 1998; 394: 485-490.
42. Neckers L and Ivy SP. Heat shock protein 90. Curr Opin Oncol 2003; 15: 419-424.
43. Isaacs JS, Xu W, Neckers L. Heat shock protein 90 as a molecular target for cancer therapeutics. Cancer Cell 2003; 3: 213-217.
44. Beliakoff J and Whitesell L. Hsp90: an emerging target for breast cancer therapy. Anticancer Drugs 2004; 15: 651-662.
45. Mross K, Drevs J, Muller M, Medinger M, Marme D, Hennig J, Morgan B, Lebwohl D, Masson E, Ho YY, Gunther C, Laurent D, Unger C. Phase I clinical and pharmacokinetic study of PTK/ZK, a multiple VEGF receptor inhibitor, in patients with liver metastases from solid tumours. Eur J Cancer 2005; 41: 1291-1299.
46. Hecht J, Trabasch T, Jaeger E, Hainsworth J. A randomized, double-blind, placebo-controlled, phase III study in patients (Pts) with metastatic adenocarcinoma of the colon or rectum receiving first-line chemotherapy with oxaliplatin/5-fluorouracil/leucovorin and PTK787/ZK 222584 or placebo (CONFIRM-1). Journal of Clinical Oncology, 2005 ASCO Annual Meeting Proceedings Vol 23, No 16S (June 1 Supplement): abstract #3.
47. Kohne C, Bajetta E, Lin E, Walle J. Final results of CONFIRM 2: A multinational, randomized, double-blind, phase III study in 2nd line patients (pts) with metastatic colorectal cancer (mCRC) receiving FOLFOX4 and PTK787/ZK 222584 (PTK/ZK) or placebo. Journal of Clinical Oncology, 2007 ASCO Annual Meeting Proceedings Vol 25, No 18S (June 20 Supplement): abstract# 4033.
48. Ahmed M, Liu Z, Lukyanov AN, Signoretti S, Horkan C, Monsky WL, Torchilin VP, Goldberg SN. Combination radiofrequency ablation with intratumoral liposomal doxorubicin: effect on drug accumulation and coagulation in multiple tissues and tumor types in animals. Radiology 2005; 235: 469-477.
49. Veenendaal LM, van Hillegersberg R, Smakman N, van der Bilt JD, van Diest PJ, Kranenburg O, Borel Rinkes IH. Synergistic effect of interstitial laser coagulation and doxorubicin in a murine tumor recurrence model of solitary colorectal liver metastasis. Ann Surg Oncol 2006; 13: 168-175.
50. Goldberg SN, Kamel IR, Kruskal JB, Reynolds K, Monsky WL, Stuart KE, Ahmed M, Raptopoulos V. Radiofrequency ablation of hepatic tumors: increased tumor destruction with adjuvant liposomal doxorubicin therapy. AJR Am J Roentgenol 2002; 179: 93-101.
51. Denny WA and Wilson WR. Tirapazamine: a bioreductive anticancer drug that exploits tumour hypoxia. Expert Opin Investig Drugs 2000; 9: 2889-2901.
52. Maataoui A, Qian J, Mack MG, Khan MF, Oppermann E, Roozru M, Schmidt S, Bechstein WO, Vogl TJ. Liver metastases in rats: chemoembolization combined with interstitial laser ablation for treatment. Radiology 2005; 237: 479-484.
53. Cheng BQ, Jia CQ, Liu CT, Fan W, Wang QL, Zhang ZL, Yi CH. Chemoembolization combined with radiofrequency ablation for patients with hepatocellular carcinoma larger than 3 cm: a randomized controlled trial. JAMA 2008; 299: 1669-1677.
54. Kaplan RN, Riba RD, Zacharoulis S, Bramley AH, Vincent L, Costa C, MacDonald DD, Jin DK, Shido K, Kerns SA, Zhu Z, Hicklin D, Wu Y, Port JL, Altorki N, Port ER, Ruggero D, Shmelkov SV, Jensen KK, Rafii S, Lyden D. VEGFR1-positive haematopoietic bone marrow progenitors initiate the pre-metastatic niche. Nature 2005; 438: 820-827.

55. Kitamura T, Kometani K, Hashida H, Matsunaga A, Miyoshi H, Hosogi H, Aoki M, Oshima M, Hattori M, Takabayashi A, Minato N, Taketo MM. SMAD4-deficient intestinal tumors recruit CCR1+ myeloid cells that promote invasion. Nat Genet 2007; 39: 467-475.
56. Isbert C, Boerner A, Ritz JP, Schuppan D, Buhr HJ, Germer CT. In situ ablation of experimental liver metastases delays and reduces residual intrahepatic tumour growth and peritoneal tumour spread compared with hepatic resection. Br J Surg 2002; 89: 1252-1259.
57. Isbert C, Ritz JP, Roggan A, Schuppan D, Ruhl M, Buhr HJ, Germer CT. Enhancement of the immune response to residual intrahepatic tumor tissue by laser-induced thermotherapy (LITT) compared to hepatic resection. Lasers Surg Med 2004; 35: 284-292.


M10-00343
I-1
HE 1 *
Nijkamp
M09-00052
I-1
HE 1 *
UMCU
M09-00577
I-1
HE 1
UMCU

Chapter 4

Radiofrequency ablation of colorectal liver metastases induces an inflammatory response in distant hepatic metastases but not in local accelerated outgrowth

Journal of Surgical Oncology 2010; 101: 551-556

Maarten W. Nijkamp[1]
Alie Borren[1]
Klaas M. Govaert[1]
Frederik J.H. Hoogwater[1]
I.Quintus Molenaar[1]
Paul J. van Diest[2]
Onno Kranenburg[1]
Inne H.M. Borel Rinkes[1]

Departments of [1]Surgery and [2]Pathology
University Medical Center Utrecht, Utrecht, The Netherlands

Abstract

Background
Recently, we have shown in a murine model that radiofrequency ablation (RFA) induces accelerated outgrowth of colorectal micrometastases in the transition zone (TZ) surrounding the ablated lesion. Conversely, RFA also induces an anti-tumor T-cell response that may limit tumor growth at distant sites. Here we have evaluated whether an altered density of inflammatory cells could be observed in the perinecrotic (TZ) metastases compared to hepatic metastases in the distant reference zone (RZ).

Methods
RFA-treated tumor-bearing mice (n=10) were sacrificed. The inflammatory cell density (neutrophils, macrophages, $CD4^+$ T-cells and $CD8^+$ T-cells) of tumors in the TZ (TZ-tumors) was compared to that in tumors in the RZ (RZ-tumors). Sham operated, tumor-bearing mice (n=10) were analyzed simultaneously as controls (sham-treated-tumors).

Results
In RFA-treated, tumor-bearing mice RZ-tumors contained a significantly higher density of neutrophils and $CD4^+$ T-cells, but not macrophages and $CD8^+$ T-cells compared to sham-treated-tumors. Notably, TZ-tumors had a significantly lower density of neutrophils, $CD4^+$ T-cells and $CD8^+$ T-cells, but not macrophages, when compared to RZ-tumors.

Conclusions
The accelerated perinecrotic tumor outgrowth following RFA is associated with a reduced density of neutrophils and T-cells compared to distant hepatic metastases. This may have implications for local tumor recurrence following RFA.

Introduction

Surgical resection is the only curative option in the treatment of colorectal liver metastases offering 5-year survival rates of ~45-55%.[1-4] Unfortunately, surgical resection is feasible in only 25% of these patients. For patients with non-resectable metastases confined to the liver, local tumor destruction using radiofrequency ablation (RFA) is an alternative treatment option. When RFA is used for small (<3cm) solitary colorectal metastases, it offers 5-year survival rates of ~25-50%.[5-8] However, local recurrence remains one of the major disadvantages, occurring in approximately 15% of cases.[1,9-11] Moreover, larger tumors and percutaneous RFA are associated with a worse prognosis, accompanied by local recurrence rates of up to 60%.[9,12]

Many preclinical studies have been performed to elucidate the effects of RFA on residual tumor cell deposits.[13] Some authors have shown a growth inhibitory effect of RFA on residual tumor tissue. This was caused by an anti-tumor T-cell response elicited by tumor-antigen presentation following RFA treatment.[14-16] Others have reported an increased proliferation of residing tumor cells following local ablation.[17-19] In this context, we have recently shown in two different murine models that RFA induces a four-fold acceleration of the outgrowth of colorectal micrometastases in the rim surrounding the induced necrosis (i.e. the transition zone, TZ) in comparison to tumor tissue in the remaining parts of the liver (i.e. the reference zone, RZ).[20]

Here, we tested whether this distinct response was related to an altered density of inflammatory cells in perinecrotic and distant tumor tissue. To test this, the quantity of the main inflammatory cell types was assessed in the TZ and the RZ following RFA in non-tumor-bearing and tumor-bearing mice.

Materials and Methods

Animals and surgery

Male BALB/c mice, aged 10-12 weeks, purchased from Charles River (Sulzfeld, Germany), were housed under standard laboratory conditions and received food and water *ad libitum*. All surgical procedures were performed under isoflurane inhalation anesthesia. Buprenorfine was administered intramuscularly prior to surgery to provide sufficient peri-operative analgesia. All experiments were carried out in accordance with the guidelines of the Animal Welfare Committee of the University Medical Center Utrecht, The Netherlands.

Induction of micrometastases and radiofrequency ablation

Induction of colorectal micrometastases and subsequent radiofrequency ablation were performed as previously described.[20] Briefly, through a left lateral flank incision, $5x10^4$ C26 murine colon carcinoma cells were injected into the splenic parenchyma. After ten minutes, the spleen was removed to prevent intrasplenic tumor growth. Diffuse intrahepatic micrometastases were allowed to grow out for three days. Three days after the intrasplenic injection, a single RFA treatment was performed using the CELON Power System (Celon AG, Teltow, Germany). A non-cooled bipolar electrode (outer diameter 1.0 mm, active length 10 mm, Celon AG, Teltow, Germany) was inserted into the distal part of the left liver lobe and used for 50 seconds at 2 Watts, corresponding with a total energy output of 100 Joules. Sham-operated mice underwent laparotomy without further local treatment.

Tumor analysis

Tumor load in the liver was estimated by the hepatic replacement area (HRA), i.e. the percentage of liver tissue that has been replaced by tumor tissue.[21] In brief, on hematoxylin and eosin (H&E) stained sections, at least 100 fields were selected using an interactive video overlay system, including an automated microscope (Q-Prodit; Leica Microsystems, Rijswijk, The Netherlands) at a magnification of 40x. Using a four-points grid overlay, the ratio of tumor cells versus normal hepatocytes was determined for each field. Tumor load (HRA) was expressed as the average area ratio of all fields. HRA was measured in the RZ and the TZ, defined as the area stretching 2 mm outside the necrotic central area, as previously described.[20] Both the paraffin section and frozen tissue section were used to assess HRA. Analyses were performed by two independent observers.

Histochemical stainings

After harvesting the livers, both snap frozen and paraffin embedded liver tissues were sectioned at 4µm. Tissue sections were H&E stained for standard histology and tumor analysis. Paraffin embedded tissue sections were used for the assessment of neutrophils by performing a Leder staining (Naphthol AS-D Chloroacetate, Sigma, St. Louis, MO).

Next, frozen sections were used for immunohistochemical assessment of macrophages (F4/80) and T-cells ($CD4^+$ and $CD8^+$). Sections were air-dried for 10 minutes and fixed with 4% formaldehyde (F4/80 and CD4) or acetone (CD8) for 10 minutes. After washing, samples were preincubated with 2% normal goat serum for 10 minutes to block non-specific binding and then incubated for one hour with primary antibody (FITC-conjugated rat-anti-mouse CD4 and CD8 antibody, BD Pharmingen, Breda, The Netherlands; rat-anti-mouse F4/80 antibody, Serotec, Düsseldorf, Germany). After washing, endogenous peroxidase activity was blocked with 1% hydrogen peroxide solution in methanol for 20 minutes. The secondary antibody used for F4/80 staining was HRP-conjugated rabbit-anti-rat antibody (Serotec). Secondary and tertiary antibodies for CD4 and CD8 staining were rabbit-anti-FITC (Dako, Heverlee, Belgium) and goat-anti-rabbit PowerVision+ (Immunologic, Duiven, The Netherlands) with 2% mouse serum, respectively. Reactions were developed using diaminobenzidine/H_2O_2 as chromogen substrate. Primary antibody-omitted negative controls were treated with the antibody diluent alone and were all free of non-specific background staining.

Quantitative analysis of inflammatory cells

Two independent observers took at least ten 20x-magnified photos of each area per mouse. In RFA-treated, non tumor-bearing mice both the RZ and the TZ were photographed. In RFA-treated, tumor bearing mice, pictures were taken from tumors in the RZ and from that in the TZ. In addition, pictures were also taken from sham-tumors in sham-operated mice. Pictures were stored for off-line analysis. The amount of inflammatory cells present in the zone of interest was determined by the amount of positive staining in the particular zone. For this purpose, pictures were analyzed for the percentage of positive staining per picture using Adobe Photoshop software, version 10.0 (Adobe Systems, San Jose, CA) and ImageJ software, version 1.42q (National Institutes of Health, Bethesda, MD) as previously described.[22] To check whether this semi-automatic analysis accurately represented the number of positive inflammatory cells per picture, 10 pictures with different numbers of inflammatory cells were analysed by 1) counting the number of cells and 2) using the semi-automatic analysis as described. Correlation plots were used to assess the relationship between number of cells counted and percentage positive staining as indicated by the semi-automatic analysis.

In non tumor-bearing mice, the amount of inflammatory cells (i.e. positive staining) in the TZ was compared to that in the RZ. In tumor bearing animals, the inflammatory cell density of TZ-tumors was not only compared to that of RZ-tumors, but the inflammatory cell density of RZ-tumors was also compared to that of sham-treated tumors.

Experimental design

First, the effect of RFA on the recruitment of the main inflammatory cell types to the TZ was assessed in non tumor-bearing mice. Mice (n=5 each group) were euthanized at six different time points following RFA (t=0, 4 hours, 24 hours, 3 days, 5 days and 7 days). The livers were harvested and divided in two: one part was fixed in 4% buffered formaldehyde and embedded in paraffin. The other part was snap frozen in liquid nitrogen and stored at -80˚C. Next, stainings were performed on both frozen and paraffin sections. The presence of cells in the local TZ at different time points was compared to that in distant areas in the liver of the same mouse (i.e. the RZ).

To analyze inflammatory cell density in tumor tissue following RFA treatment or sham operation, mice (n=10 each group) underwent RFA or sham operation three days after injection of C26 cells into the spleen. Seven days later, the livers were harvested as described. Tumor load in the liver was estimated by the hepatic replacement area (HRA), i.e. the percentage of liver tissue that has been replaced by tumor tissue (see tumor analysis section for further details).[21] By assessing the HRA on both frozen and paraffin section, tumor load was estimated in the local TZ and the distant RZ of RFA-treated mice and in sham operated mice. Inflammatory cell density of tumors located in the RZ (RZ-tumors) was compared to that in tumors in sham operated mice (sham-treated tumors) and to that in tumors in the TZ (TZ-tumors).

Statistical analysis

The Pearson's correlation coefficient (r) was determined to assess the degree of correlation between the number of cells and percentage positive staining. Statistical differences between the TZ and the RZ were analyzed by a paired t-test or Wilcoxon signed rank test when appropriate. Differences between sham operated mice and RFA-treated mice were analyzed by ANOVA or Kruskal-Wallis when appropriate. Normality was checked using the Kolmogorov-Smirnov test. Data are expressed as mean +/- SEM. A p-value < 0.05 was considered statistically significant. All statistical analyses were performed using GraphPad Prism® version 4 (GraphPad Software, La Jolla, CA).

Results

The transition zone following RFA in non-tumor-bearing mice is characterized by influx of inflammatory cells

Graphs plotting the number of positive cells versus the percentage positive staining showed significant correlations for all cell types with Pearson's $r > 0.85$ in all cases (data not shown).

Next, the presence of the different inflammatory cell types was evaluated in RFA-treated liver tissue of non-tumor-bearing mice at different time points. The presence of neutrophils (Leder) in the TZ increased four-fold compared to that in the RZ at 4 hours following RFA (p=0.055). This rise was maintained until 24 hours post-RFA (p=0.0078), whereafter a gradual decline to normal values was observed over the ensuing days (Figures 1 and 2). The influx of macrophages (F4/80) into the TZ

started at later time points following RFA. Three, five and seven days post-RFA, macrophage content was approximately nine-fold higher in the TZ when compared to the RZ (p=0.0028, p=0.0009 and p=0.0067, respectively, figures 1 and 2). Influx of $CD4^+$ T-cells into the TZ was first observed 3 days after RFA, with a three-fold increase compared to the RZ (p=0.018) which was sustained until 7 days post-RFA (Figures 1 and 2). A higher amount of $CD8^+$ T-cells was observed in the TZ compared to the RZ 3 days after RFA, although this was not statistically significant (p=0.068). At five days following RFA, a three-fold higher $CD8^+$ T-cell content was observed in the TZ compared to the RZ (p=0.029), followed by a gradual decline (Figures 1 and 2).

Radiofrequency ablation induces perinecrotic growth acceleration of colorectal micrometastases

Following RFA, the necrotic lesions were encircled by a clear rim of tumor (Figure 3). Tumor load in the TZ surrounding the central necrotic zone had increased approximately three-fold compared to tumor load in the RZ (52.3 ± 5.7% vs 17.8 ± 2.4%, p=0.002). No differences were found between tumor growth in the RZ of RFA-treated mice and that in sham-operated mice (p=0.28) (Figure 3).

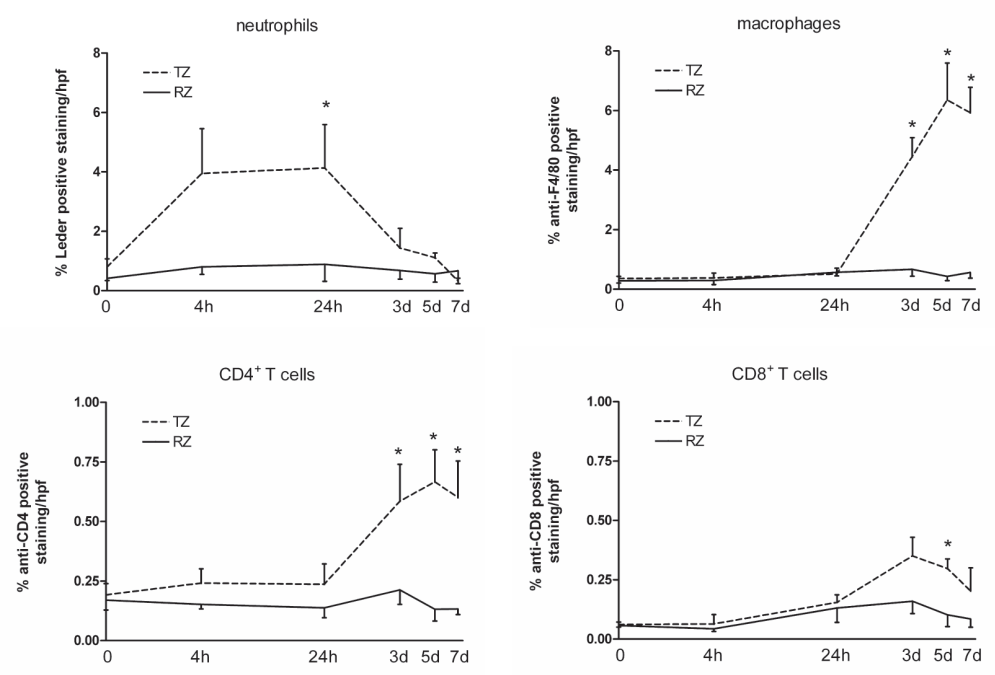

Figure 1 Semi-automatic quantification of inflammatory cell staining in RFA-treated, non-tumor-bearing murine livers

Influx into the transition zone (TZ) is observed for all inflammatory cell types, where neutrophils (4-24 hours) precede macrophages and T-cells (3-7 days). Number of inflammatory cells in the TZ is compared to that in the reference zone (RZ). * p<0.05, hpf = high power field.

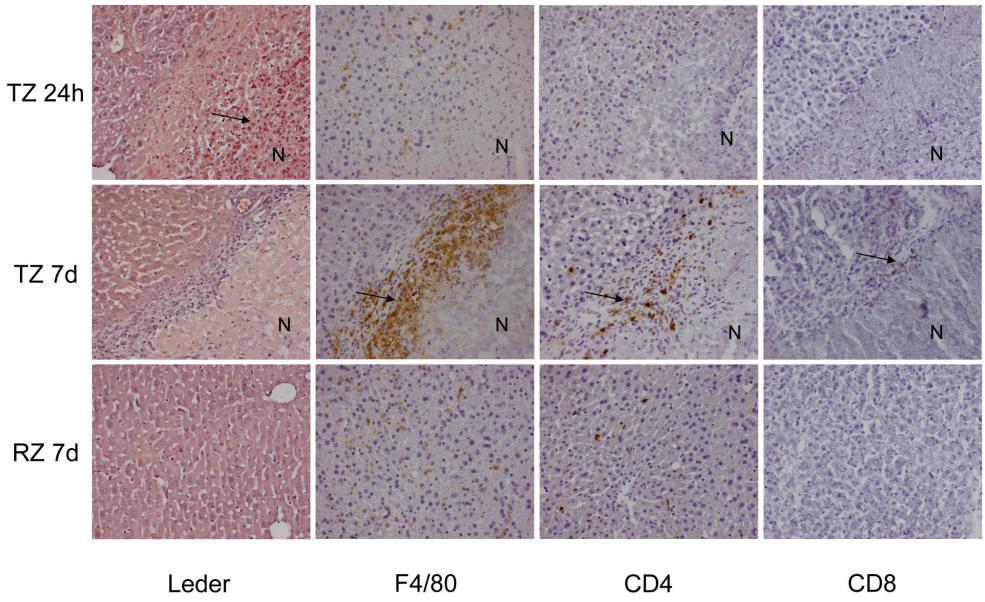

Figure 2 Histochemical stainings of RFA-treated, non tumor-bearing mouse livers
In the reference zone (RZ) some positive inflammatory cells are observed (arrows). In the transition zone (TZ) at 24 hours following RFA, intense Leder-positive cell staining can be observed, indicating an influx of neutrophils (arrow). Seven days following RFA, intense staining of F4/80 positive cells (macrophages) is visible in the TZ (arrow). Similarly intense staining is seen for $CD4^+$ and $CD8^+$ T-cells in the TZ (arrows). n=necrosis, induced by RFA treatment. Leder = neutrophils, F4/80 = macrophages, CD4 = $CD4^+$ T-cells, CD8 = $CD8^+$ T-cells.

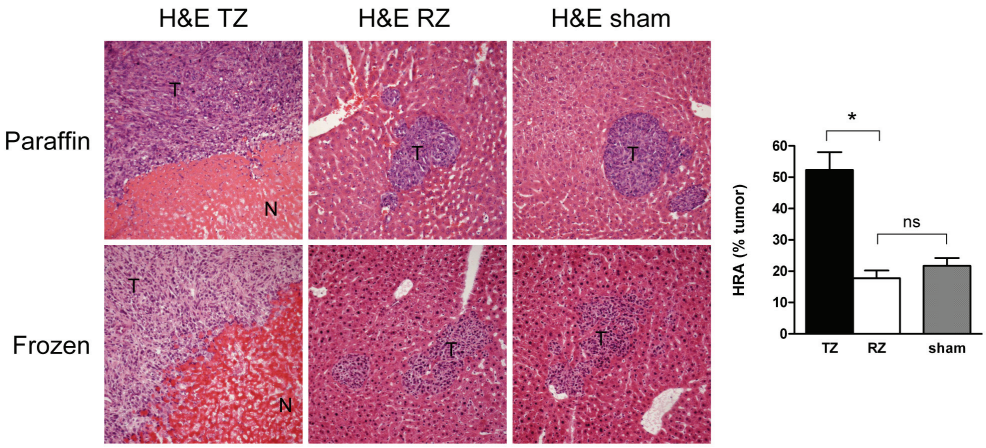

Figure 3 Tumor load as estimated by the hepatic replacement area (HRA) in RFA-treated (transition zone and reference zone) and sham-operated mice
Three days after intrasplenic tumor cell injection, mice underwent either RFA (upper 2 panels) or sham operation (lower panel). Figures show histology 7 days later. H&E staining of paraffin-embedded and frozen liver tissue (40x magnification) were used to assess the HRA. A broad rim of tumor (t) surrounds the necrosis (n) induced by RFA (upper panel). * p=0.002

RFA induces an influx of neutrophils and CD4$^+$ T-cells into distant metastases in the reference zone

The neutrophil density of RZ-tumors of RFA-treated mice was approximately three-fold higher than that of sham-treated tumors (p=0.002, figures 4 and 5). In contrast, the macrophage density of RZ-tumors did not significantly differ from that of sham-treated tumors (p=0.26, figures 4 and 5). Furthermore, the CD4$^+$ T-cell density of RZ-tumors was approximately three-fold higher compared to that of sham-treated tumors (p=0.015, figures 4 and 5). Finally, the CD8$^+$ T-cell density of RZ-tumors did not differ significantly from that of sham-treated tumors (p=0.41, figures 4 and 5).

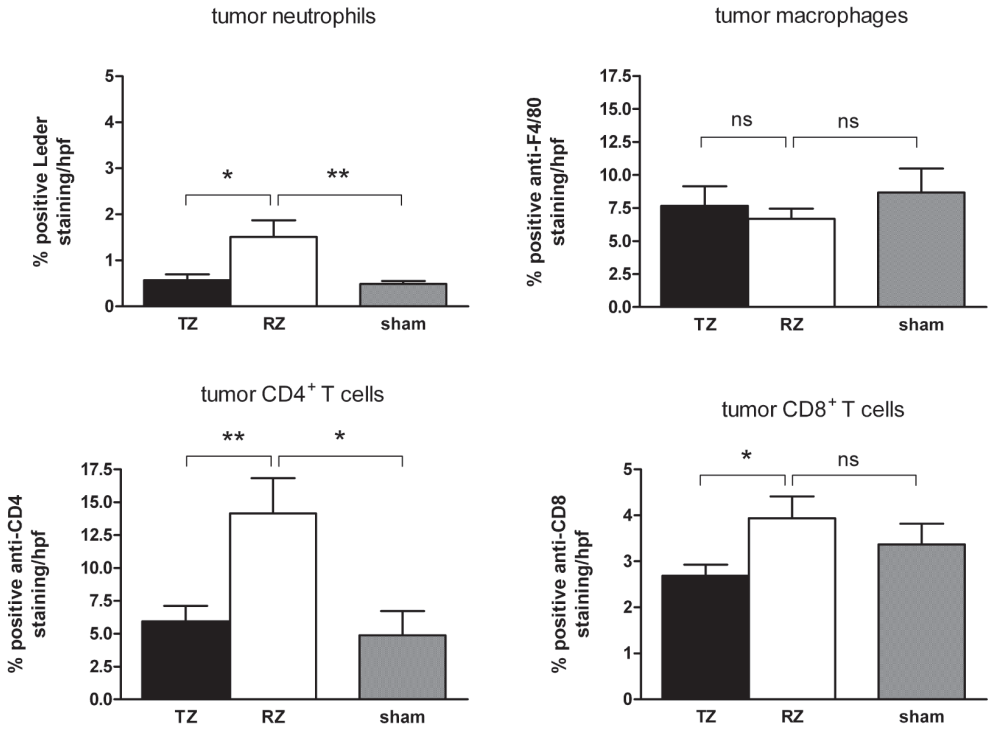

Figure 4 Semi-automatic quantification of inflammatory cells in tumor tissue of the transition zone (TZ) or reference zone (RZ) in RFA-treated mice or tumor tissue in livers from sham-operated mice

Mice were sacrificed 7 days following RFA-treatment or sham-operation. Density of inflammatory cells is compared between RZ-tumors and TZ-tumors and RZ-tumors and sham-treated tumors. TZ-tumors have a significantly lower density of neutrophils (Leder), as well as CD4$^+$ and CD8$^+$ T-cells. In addition, sham-treated tumors contain significantly less neutrophils and CD4$^+$ T-cells compared to RZ-tumors. No differences are observed for macrophage (F4/80) density of the different tumors. Leder = neutrophils, F4/80 = macrophages, CD4 = CD4$^+$ T-cells, CD8 = CD8$^+$ T-cells, hpf = high power field. * $p<0.05$; ** p=0.002; ns not significant.

Tumor tissue in the transition zone is characterized by a reduction of neutrophils and T-cells

The neutrophil density in TZ-tumors was two- to three-fold reduced compared to that of RZ-tumors (p=0.033). The macrophage density of TZ-tumors was not significantly different from that of RZ-tumors (p=0.61). The $CD4^+$ T-cell density of tumor tissue showed a two- to three-fold reduction of $CD4^+$ T-cells in TZ-tumors compared to that in RZ-tumors (p=0.002). Finally, also the $CD8^+$ T-cell density of TZ-tumors was significantly lower when compared to that of RZ-tumors (p=0.044).

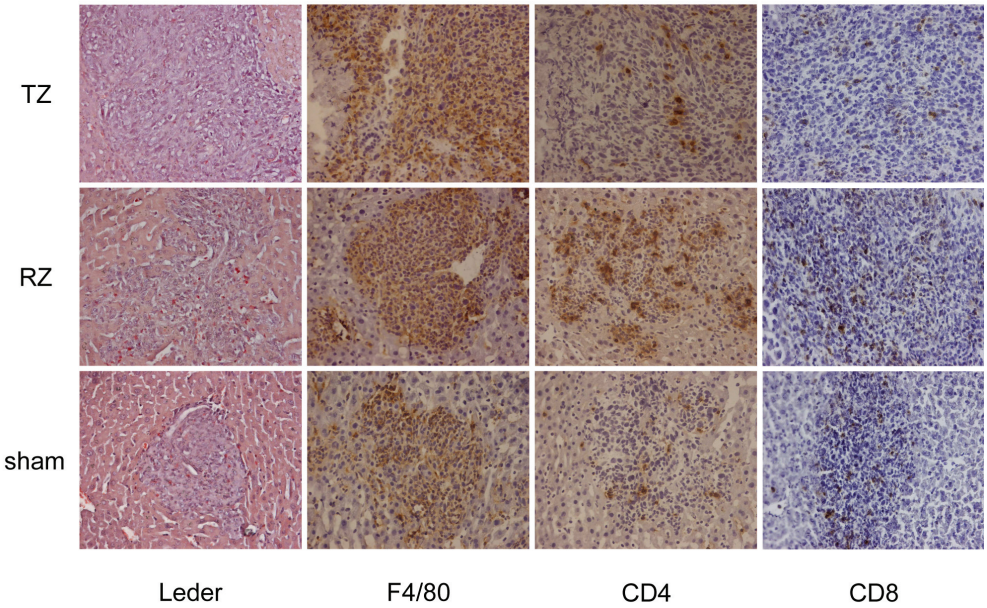

Figure 5 Histochemical stainings of tumor-bearing mouse livers 7 days following RFA or sham operation
TZ-tumors have a lower density of neutrophils (Leder), as well as $CD4^+$ and $CD8^+$ T-cells. In addition, sham-treated tumors contain significantly less neutrophils and $CD4^+$ T-cells compared to RZ-tumors. No clear differences are observed in F4/80 staining between the TZ-, RZ- and sham-treated tumors. n=necrosis, induced by RFA treatment. Leder = neutrophils, F4/80 = macrophages, CD4 = $CD4^+$ T-cells, CD8 = $CD8^+$ T-cells.

Discussion

Many studies have been performed showing that local ablative therapies induce an inflammatory response.[14,15,23-25] In this study we show that the inflammatory reaction induced by RFA is primarily observed in distant hepatic metastases, but not in perinecrotic metastases. The reduced inflammatory reaction in perinecrotic tumor tissue might contribute to tumor growth acceleration. The low quantity of leucocytes in TZ-tumors, compared to RZ-tumors, could be due to differences in the cytokine profiles produced at these different tumor sites. In addition, increased apoptosis of leucocytes present in TZ-tumors might also result in a reduced density of leucocytes. Interestingly, colorectal cancer cells are capable of creating a counterattack by the Fas-FasL system[26,27], causing apoptosis of tumor infiltrating leucocytes.[27,28]

Until now, data concerning the effects of local ablative therapies on residual tumor deposits either express pro-tumorigenic or anti-tumorigenic effects. However, the available data suggest that local ablative therapies induce both a local pro-tumorigenic and a distant anti-tumorigenic effect on residual tumor deposits. The different observations can be based on the tumor model used. Studies reporting an anti-tumor T-cell response following local ablative therapy often use a tumor implantation model. In these models, a relatively large bulk of tumor is ablated. This will result in a massive generation of tumor-specific antigens against which an anti-tumor T-cell response can be elicited. Rechallenge of these animals with tumor cells resulted in reduced tumor outgrowth.[14,16,29,30] Additionally, Isbert *et al*. have demonstrated a growth delay of a synchronically implanted but untreated metastasis in the right liver lobe based on an anti-tumor T-cell response induced by local ablation of another metastasis in the left liver lobe.[15] These preclinical results have been corroborated in the clinical setting by reported formation of tumor specific T-cells in patients treated with RFA for liver tumors.[31-33]

Translating the results obtained from this study to the clinical setting is rather difficult. Experiments using a micrometastases model in which a relatively small bulk of tumor is ablated compared to implantation models[17,19,20], will result in considerably less tumor-specific antigens. The low amount of tumor antigens generated in these models may therefore be too low to induce a significant anti-tumor immune response. In addition, the time of sacrifice (7 days post-RFA in this study) might also be too short to induce an effective anti-tumor T-cell response. Therefore, more research is needed to show whether comparable results are obtained using tumor implantation models.

It is known that a higher amount of T-cells in colorectal liver metastases is associated with a better survival.[34] Although it is not clear whether the reduced density of inflammatory cells is causally involved in local acceleration of tumor growth in the TZ following RFA, it is tempting to postulate that approaches aimed at augmenting local inflammation in perinecrotic tumor tissue might be beneficial. Recent articles about the effect of inflammation-stimulating agents, such as anti-CTLA-4, in conjunction with RFA treatment, show an increased anti-tumor response[14,35] and promising results concerning recurrence following thermal ablation.[35,36] Further research should elucidate whether these agents increase the inflammatory cell density in TZ-tumors as well and can thereby reduce the local tumor recurrence following RFA.

References

1. Abdalla EK, Vauthey JN, Ellis LM, Ellis V, Pollock R, Broglio KR, Hess K, Curley SA. Recurrence and outcomes following hepatic resection, radiofrequency ablation, and combined resection/ablation for colorectal liver metastases. Ann Surg 2004; 239: 818-825.
2. de Jong MC, Pulitano C, Ribero D, Strub J, Mentha G, Schulick RD, Choti MA, Aldrighetti L, Capussotti L, Pawlik TM. Rates and patterns of recurrence following curative intent surgery for colorectal liver metastasis: an international multi-institutional analysis of 1669 patients. Ann Surg 2009; 250: 440-448.
3. Gleisner AL, Choti MA, Assumpcao L, Nathan H, Schulick RD, Pawlik TM. Colorectal liver metastases: recurrence and survival following hepatic resection, radiofrequency ablation, and combined resection-radiofrequency ablation. Arch Surg 2008; 143: 1204-1212.
4. Zakaria S, Donohue JH, Que FG, Farnell MB, Schleck CD, Ilstrup DM, Nagorney DM. Hepatic resection for colorectal metastases: value for risk scoring systems? Ann Surg 2007; 246: 183-191.
5. Aloia TA, Vauthey JN, Loyer EM, Ribero D, Pawlik TM, Wei SH, Curley SA, Zorzi D, Abdalla EK. Solitary colorectal liver metastasis: resection determines outcome. Arch Surg 2006; 141: 460-466.
6. Berber E, Tsinberg M, Tellioglu G, Simpfendorfer CH, Siperstein AE. Resection Versus Laparoscopic Radiofrequency Thermal Ablation Of Solitary Colorectal Liver Metastasis. J Gastrointest Surg 2008; 12: 1967-1972.
7. Hur H, Ko YT, Min BS, Kim KS, Choi JS, Sohn SK, Cho CH, Ko HK, Lee JT, Kim NK. Comparative study of resection and radiofrequency ablation in the treatment of solitary colorectal liver metastases. Am J Surg 2009; 197: 728-736.
8. Lee WS, Yun SH, Chun HK, Lee WY, Kim SJ, Choi SH, Heo JS, Joh JW, Choi D, Kim SH, Rhim H, Lim HK. Clinical outcomes of hepatic resection and radiofrequency ablation in patients with solitary colorectal liver metastasis. J Clin Gastroenterol 2008; 42: 945-949.
9. Mulier S, Ni Y, Jamart J, Ruers T, Marchal G, Michel L. Local recurrence after hepatic radiofrequency coagulation: multivariate meta-analysis and review of contributing factors. Ann Surg 2005; 242: 158-171.
10. Mulier S, Ni Y, Jamart J, Michel L, Marchal G, Ruers T. Radiofrequency Ablation Versus Resection for Resectable Colorectal Liver Metastases: Time for a Randomized Trial? Ann Surg Oncol 2007; 15: 144-157.
11. Siperstein AE, Berber E, Ballem N, Parikh RT. Survival after radiofrequency ablation of colorectal liver metastases: 10-year experience. Ann Surg 2007; 246: 559-567.
12. Solbiati L, Livraghi T, Goldberg SN, Ierace T, Meloni F, Dellanoce M, Cova L, Halpern EF, Gazelle GS. Percutaneous radio-frequency ablation of hepatic metastases from colorectal cancer: long-term results in 117 patients. Radiology 2001; 221: 159-166.
13. Gravante G, Sconocchia G, Ong SL, Dennison AR, Lloyd DM. Immunoregulatory effects of liver ablation therapies for the treatment of primary and metastatic liver malignancies. Liver Int 2009; 29: 18-24.
14. den Brok MH, Sutmuller RP, van der Voort R, Bennink EJ, Figdor CG, Ruers TJ, Adema GJ. In situ tumor ablation creates an antigen source for the generation of antitumor immunity. Cancer Res 2004; 64: 4024-4029.
15. Isbert C, Boerner A, Ritz JP, Schuppan D, Buhr HJ, Germer CT. In situ ablation of experimental liver metastases delays and reduces residual intrahepatic tumour growth and peritoneal tumour spread compared with hepatic resection. Br J Surg 2002; 89: 1252-1259.
16. van Duijnhoven FH, Tollenaar RA, Terpstra OT, Kuppen PJ. Locoregional therapies of liver metastases in a rat CC531 coloncarcinoma model results in increased resistance to tumour rechallenge. Clin Exp Metastasis 2005; 22: 247-253.
17. Nikfarjam M, Muralidharan V, Christophi C. Altered growth patterns of colorectal liver metastases after thermal ablation. Surgery 2006; 139: 73-81.
18. Ohno T, Kawano K, Yokoyama H, Tahara K, Sasaki A, Aramaki M, Kitano S. Microwave coagulation therapy

accelerates growth of cancer in rat liver. J Hepatol 2002; 36: 774-779.
19. von Breitenbuch P, Kohl G, Guba M, Geissler E, Jauch KW, Steinbauer M. Thermoablation of colorectal liver metastases promotes proliferation of residual intrahepatic neoplastic cells. Surgery 2005; 138: 882-887.
20. Nijkamp MW, van der Bilt JD, de Bruijn MT, Molenaar IQ, Voest EE, van Diest PJ, Kranenburg O, Borel Rinkes IH. Accelerated perinecrotic outgrowth of colorectal liver metastases following radiofrequency ablation is a hypoxia-driven phenomenon. Ann Surg 2009; 249: 814-823.
21. van der Bilt JD, Kranenburg O, Nijkamp MW, Smakman N, Veenendaal LM, Te Velde EA, Voest EE, van Diest PJ, Borel Rinkes IH. Ischemia/reperfusion accelerates the outgrowth of hepatic micrometastases in a highly standardized murine model. Hepatology 2005; 42: 165-175.
22. Turk T, Leeuwis JW, Gray J, Torti SV, Lyons KM, Nguyen TQ, Goldschmeding R. BMP signaling and podocyte markers are decreased in human diabetic nephropathy in association with CTGF overexpression. J Histochem Cytochem 2009; 57: 623-631.
23. Isbert C, Ritz JP, Roggan A, Schuppan D, Ruhl M, Buhr HJ, Germer CT. Enhancement of the immune response to residual intrahepatic tumor tissue by laser-induced thermotherapy (LITT) compared to hepatic resection. Lasers Surg Med 2004; 35: 284-292.
24. Ivarsson K, Myllymaki L, Jansner K, Stenram U, Tranberg KG. Resistance to tumour challenge after tumour laser thermotherapy is associated with a cellular immune response. Br J Cancer 2005; 93: 435-440.
25. Wissniowski TT, Hansler J, Neureiter D, Frieser M, Schaber S, Esslinger B, Voll R, Strobel D, Hahn EG, Schuppan D. Activation of tumor-specific T lymphocytes by radio-frequency ablation of the VX2 hepatoma in rabbits. Cancer Res 2003; 63: 6496-6500.
26. O'Connell J, O'Sullivan GC, Collins JK, Shanahan F. The Fas counterattack: Fas-mediated T cell killing by colon cancer cells expressing Fas ligand. J Exp Med 1996; 184: 1075-1082.
27. Ryan AE, Shanahan F, O'Connell J, Houston AM. Addressing the "Fas counterattack" controversy: blocking fas ligand expression suppresses tumor immune evasion of colon cancer in vivo. Cancer Res 2005; 65: 9817-9823.
28. Liles WC, Kiener PA, Ledbetter JA, Aruffo A, Klebanoff SJ. Differential expression of Fas (CD95) and Fas ligand on normal human phagocytes: implications for the regulation of apoptosis in neutrophils. J Exp Med 1996; 184: 429-440.
29. den Brok MH, Sutmuller RP, Nierkens S, Bennink EJ, Frielink C, Toonen LW, Boerman OC, Figdor CG, Ruers TJ, Adema GJ. Efficient loading of dendritic cells following cryo and radiofrequency ablation in combination with immune modulation induces anti-tumour immunity. Br J Cancer 2006; 95: 896-905.
30. Kuang M, Liu SQ, Saijo K, Uchimura E, Huang L, Leong KW, Lu MD, Huang JF, Ohno T. Microwave tumour coagulation plus in situ treatment with cytokine-microparticles: induction of potent anti-residual tumour immunity. Int J Hyperthermia 2005; 21: 247-257.
31. Hansler J, Wissniowski TT, Schuppan D, Witte A, Bernatik T, Hahn EG, Strobel D. Activation and dramatically increased cytolytic activity of tumor specific T lymphocytes after radio-frequency ablation in patients with hepatocellular carcinoma and colorectal liver metastases. World J Gastroenterol 2006; 12: 3716-3721.
32. Napoletano C, Taurino F, Biffoni M, De Majo A., Coscarella G, Bellati F, Rahimi H, Pauselli S, Pellicciotta I, Burchell JM, Gaspari LA, Ercoli L, Rossi P, Rughetti A. RFA strongly modulates the immune system and anti-tumor immune responses in metastatic liver patients. Int J Oncol 2008; 32: 481-490.
33. Zerbini A, Pilli M, Penna A, Pelosi G, Schianchi C, Molinari A, Schivazappa S, Zibera C, Fagnoni FF, Ferrari C, Missale G. Radiofrequency thermal ablation of hepatocellular carcinoma liver nodules can activate and enhance tumor-specific T-cell responses. Cancer Res 2006; 66: 1139-1146.
34. Katz SC, Pillarisetty V, Bamboat ZM, Shia J, Hedvat C, Gonen M, Jarnagin W, Fong Y, Blumgart L, 'Angelica M, Dematteo RP. T cell infiltrate predicts long-term survival following resection of colorectal cancer liver metastases. Ann Surg Oncol 2009; 16: 2524-2530.
35. Chen Z, Shen S, Peng B, Tao J. Intratumoural GM-CSF microspheres and CTLA-4 blockade enhance the antitumour immunity induced by thermal ablation in a subcutaneous murine hepatoma model. Int J Hyperthermia 2009; 25: 374-382.

36. Johnson EE, Yamane BH, Buhtoiarov IN, Lum HD, Rakhmilevich AL, Mahvi DM, Gillies SD, Sondel PM. Radiofrequency Ablation Combined with KS-IL2 Immunocytokine (EMD 273066) Results in an Enhanced Antitumor Effect against Murine Colon Adenocarcinoma. Clin Cancer Res 2009; 15: 4875-4884.

Chapter 5

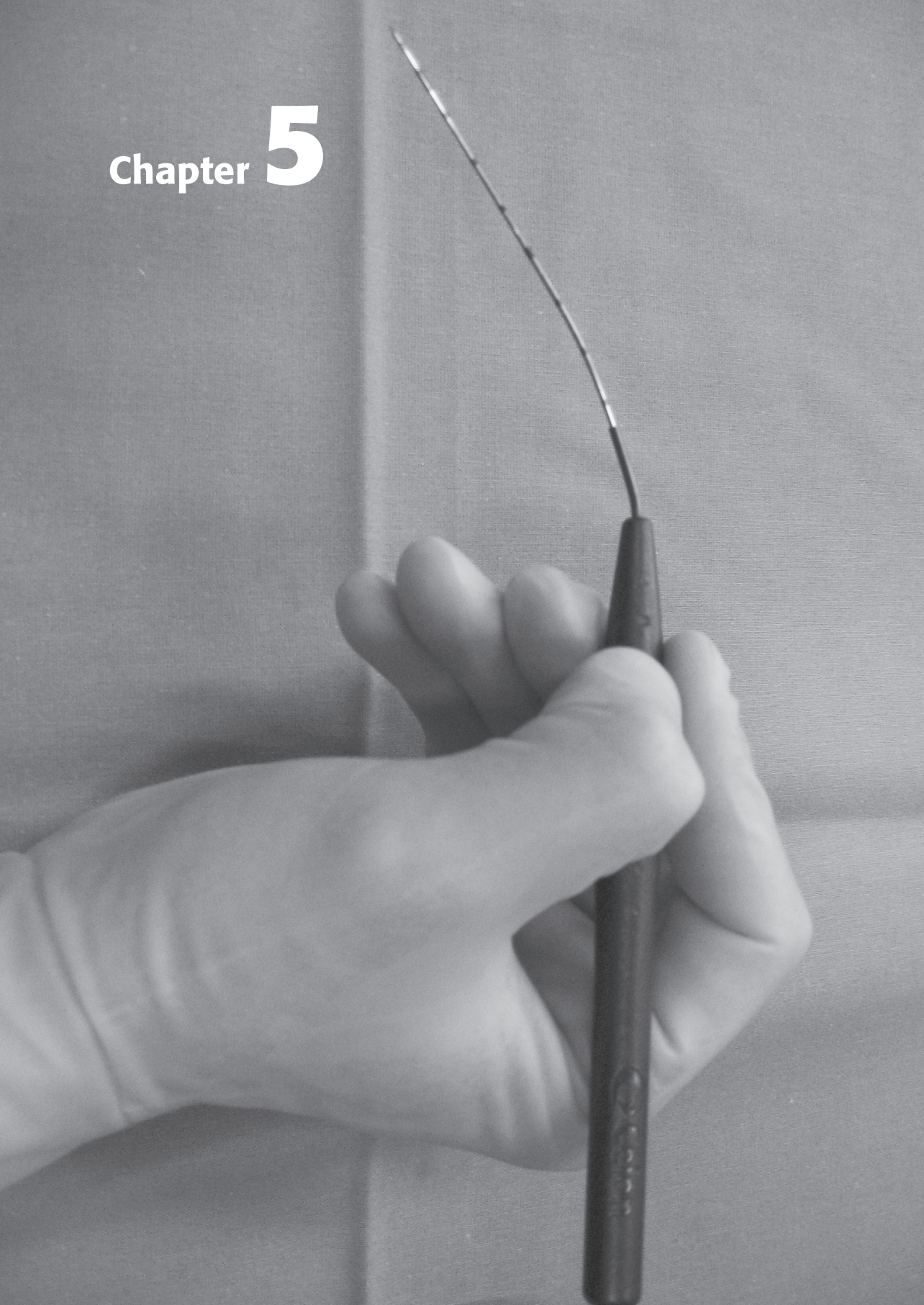

CD95 is a key mediator of invasion and accelerated outgrowth of colorectal liver metastases following radiofrequency ablation

Journal of Hepatology, in press

Maarten W. Nijkamp*
Frederik J.H. Hoogwater*
Ernst J.A. Steller
B. Florien Westendorp
Taco A. van der Meulen
Martijn W.H. Leenders
Inne H.M. Borel Rinkes
Onno Kranenburg

* these authors contributed equally

Department of Surgery
University Medical Center Utrecht, Utrecht, The Netherlands

Abstract

Background
Recently, we have shown that micrometastases in the hypoxic transition zone surrounding lesions generated by radiofrequency ablation (RFA) display strongly accelerated outgrowth. CD95 is best known for its ability to induce apoptosis but can also promote tumorigenesis in apoptosis-resistant tumor cells. Therefore, we tested whether CD95 signaling plays a role in accelerated outgrowth of colorectal liver metastases following RFA.

Methods
Hypoxia-induced invasion was assessed in three-dimensional EGFP-expressing C26 tumor cell cultures by confocal microscopy. CD95 localization was tested by immunofluorescence. Invasion and outgrowth of liver metastases following RFA was analyzed by post-mortem confocal microscopy and by morphometric assessment of tumor load. Neutralization of CD95L was performed by using antibody MFL4. CD95 was suppressed by lentiviral RNA interference. The role of host CD95L was assessed using *gld*-mice.

Results
Micrometastases in the hypoxic transition zone following RFA displayed a highly invasive phenotype and increased expression of CD95 and CD95L. Hypoxia induced tumor cell invasion *in vitro*, increased expression of CD95 and CD95L and induced translocation of CD95 to the invasive front. *In vitro* invasion, metastasis invasion and accelerated tumor growth in the transition zone were strongly suppressed by neutralizing CD95L or by suppressing tumor cell CD95. In contrast, metastasis invasion and outgrowth were unaffected in *gld*-mice.

Conclusions
Hypoxia causes autocrine activation of CD95 on colorectal tumor cells, thereby promoting local invasion and accelerated metastasis outgrowth in the hypoxic transition zone following RFA. Further pre-clinical work is needed to assess the role of CD95L neutralization, either alone or in combination with chemotherapy, in limiting aggressive recurrence of liver metastases following RFA.

Introduction

Radiofrequency ablation (RFA) is a local thermal destruction therapy that is used as an alternative treatment option for patients with non-resectable colorectal liver metastases. Local tumor recurrence following RFA treatment occurs in approximately 15% of all cases. However, with increased tumor size, or when a percutaneous approach is used, local recurrence rates of up to 60% are reported.[1-4]

Recently, we have shown in two murine models that RFA can stimulate the outgrowth of colorectal liver metastases. The RFA-generated necrotic lesion is surrounded by a rim of chronically hypoxic liver tissue which is usually referred to as the 'transition zone' (TZ). Micrometastases that happen to be present in the transition zone grow out approximately three to four times faster than those in the normoxic reference zone (RZ) further away from the lesion.[5] Interestingly, up to 70% of patients with colorectal liver metastases contain micrometastases that may result in (local) tumor recurrence.[6]

Hypoxia can contribute to tumor cell invasion and metastatic progression and is generally associated with a more aggressive tumor phenotype.[7,8] Several genes and receptor systems have been implicated in hypoxia-stimulated invasion and metastasis formation, including hepatocyte growth factor receptor (c-Met), vascular endothelial growth factor receptors (VEGFR) and increased expression of proteolytic enzymes.[8-10] Additionally, hypoxia can cause activation of the CD95 death receptor system, leading to CD95-induced apoptosis.[11-13] However, in apoptosis-resistant cells, CD95 can activate alternative signaling pathways which may cause invasion, differentiation, survival or proliferation.[14-18]

In colorectal cancer, the expression of CD95 ligand (CD95L) is correlated with metastasis formation.[19] Recent evidence shows that enforced expression of CD95L promotes the metastatic capacity of apoptosis-resistant colorectal cancer cells.[20] In addition, we have recently shown that stimulation of CD95 on such cells predominantly leads to tumor cell invasion and that signaling by the K-Ras oncogene is a critical determinant of CD95 signaling output.[15]

The combined observations that i) CD95 signaling is regulated by hypoxia and that ii) CD95L can promote invasion and metastatic capacity, prompted us to assess whether activation of the CD95 system contributes to local outgrowth of liver metastases following RFA. We found that CD95 and CD95L were selectively and strongly upregulated in the hypoxic transition zone following RFA and that this was correlated with a dramatic invasive tumor phenotype. *In vitro* hypoxia was sufficient to cause autocrine CD95 activation and CD95-dependent tumor cell invasion. Autocrine CD95 activation also mediated invasion and outgrowth of micrometastases following RFA. Our results identify CD95 as a major participant in local tumor cell invasion and accelerated outgrowth of micrometastases following RFA.

Materials and Methods

Cell lines and cell culture

C26 mouse colon carcinoma cells were obtained from the American Type Tissue Culture Collection (ATCC, Rockville, MD). C26-EGFP cells were generated by lentiviral transduction using pWPT-GFP (kindly provided by Professor Didier Trono). A panel of five lentiviral pLKO1 constructs targeting CD95 (Open Biosystems; Huntsville, AL, USA) was tested. Of these five, two gave the best knockdown and

were used for generating stable C26-CD95-knockdown cell lines (TCRN0000012328 (#1) and (TCRN0000012331 (#2)). As a control, C26 cells were transduced with luciferase-targeting lentiviral shRNA vectors (C26-Luc-kd). All cells were cultured in Dulbecco's Modified Eagle's Medium (DMEM; Dulbecco, ICN Pharmaceuticals, Costa Mesa, CA, USA) supplemented with 5% (v/v) fetal calf serum, 2 mM glutamine, 0.1 mg/ml steptomycin and 100 U/ml penicillin. Cells were kept at 37°C in a humidified atmosphere containing 5% CO_2.

Antibodies and reagents

The following primary antibodies were used: anti-mouse CD95 (clone M-20, #sc-716) Santa Cruz Biotechnology, Inc., Santa Cruz, CA, USA. Anti-CD95 Ligand (ab15285), Abcam, Cambridge, MA, USA. Anti-HIF-1 alpha (NB100-449) and anti-Beta-Actin (AC-15, NB600-501), Novus Biologicals, LLC, Littleton, CO, USA. Secondary antibodies were anti-rabbit IgG, HRP-linked (#7074), Cell Signaling, Danvers, MA, USA. Polyclonal rabbit anti-mouse immunoglobulins, HRP (p0260), DAKO, Glostrup, Denmark. Goat anti-hamster IgG-HRP (sc2493), Santa Cruz Biotechnology, Inc., Santa Cruz, CA, USA. The following reagents were used in this study: CD95 Ligand (FasL), membrane bound (#01-210) from Upstate Cell Signaling Solutions (now Millipore), Lake Placid, NY, USA. Functional Grade purified anti-mouse CD95 Ligand (Fas Ligand, CD178), clone MFL4 (#16-5912), from eBioscience, Inc., San Diego, CA, USA.

MTT assay

To test the neutralizing effect of MFL4 on CD95L, C26 cells and apoptosis-prone C26KrasKD cells[15] were plated at a density of 5000 cells/well in 96-well plates. Cells were either pre-treated with MFL4 (6 ng/ml) for 2h or directly stimulated with increasing concentrations of CD95L (2 ng/ml to 10 ng/ml). Mitochondrial activity in each well was analyzed after 24h stimulation by standard 3- (4,5 dimethylthiazolyl-2)-2,5-diphenyltetrazoleumbromide (MTT) assays (Roche Diagnostics) according to the manufacturer's instructions.

Invasion (colony scatter) assay under hypoxia

To investigate the phenotype of cells under normoxic and hypoxic conditions $3.5x10^4$ C26-EGFP cells were plated on coverslips with matrigel. Micro-colonies were allowed to form for 72 hours under normoxic (21% O_2) or hypoxic (1% O_2 $Invivo_2$ Hypoxia Workstation 1000 (Biotrace International, UK)) conditions in a humidified atmosphere at 37°C. Coverslips were mounted using Vectashield mounting fluid (H-1200, Vectorlabs). Confocal images were then acquired on a Zeiss Axiovert 200M. Image acquisition and analysis were performed using Zeiss LSM 510 Software. The length of the longest diameter of each colony was measured in 10 randomly chosen fields per coverslip. All assays were performed in duplicate and repeated twice.

Confocal microscopy

Control cells and cells treated with CD95L and MFL4 (isotype control with IgG; 6 ng/ml) were fixed in 3.7% formaldehyde for 10 minutes and were subsequently permeabilized with 0.05% Triton X-100 in 1% PBS/BSA. Coverslips were then blocked in PBS with 3% BSA for 1 hour. Anti-CD95 primary antibody (isotype control with IgG, 10 ng/ml) was incubated at room temperature for 1 hour and secondary antibodies (FITC and Alexa-568-conjugated phalloidin) were incubated for 30 minutes at room temperature. Coverslips were mounted using Vectashield mounting fluid (H-1200, Vectorlabs)

with DAPI. Confocal images were acquired on a Zeiss Axiovert 200M microscope. Image acquisition and analysis were performed using Zeiss LSM-510 software.

Animals and surgery

Male BALB/c mice (10-12 weeks) were purchased from Charles River (Sulzfeld, Germany). BALB/c-*gld/gld* (CPt.C3-*Fasl*^{gld}/J) mice carrying homozygous loss-of-function mutation in CD95L (hereafter referred to as *gld*-mice) were purchased from The Jackson Laboratory (Bar Harbor, USA). In experiments using *gld*-mice, control BALB/c mice were also from The Jackson Laboratory. Mice were housed under standard laboratory conditions and received food and water *ad libitum*. All surgical procedures were performed under isoflurane inhalation anesthesia. Prior to surgery, buprenorfine was administered intramuscularly to provide sufficient peri-operative analgesia. All experiments were carried out in accordance with the guidelines of the Animal Welfare Committee of the University Medical Center Utrecht, The Netherlands.

Induction of micrometastases and radiofrequency ablation

Induction of colorectal micrometastases and subsequent radiofrequency ablation were performed as previously described.[5] In brief, through a left lateral flank incision, $5x10^4$ C26 murine colon carcinoma cells were injected into the splenic parenchyma, followed by removal of the spleen after ten minutes to prevent intrasplenic tumor growth. For tumor cell invasion experiments, EGFP-expressing C26 cells were used. This resulted in a homogeneous spread of diffuse intrahepatic micrometastases, which were allowed to grow out for three days. Three days after the intrasplenic injection, RFA was performed using the CELON Power System (Celon AG, Teltow, Germany). A single non-cooled bipolar electrode (outer diameter 1.0 mm, active length 10 mm, Celon AG, Teltow, Germany) was used for RFA of the left liver lobe at 2 Watts for 50 seconds (100 Joules), resulting in a lesion of approximately 8 by 15 mm. Since RFA was performed in a liver containing homogeneous spread of numerous diffuse micrometastases, the effect of RFA on residual tumor cells could be investigated.

Assessment of the tumor cell phenotype in the transition zone following RFA

Mice bearing EGFP-expressing tumor cells were sacrificed at t=0, t=6 hours, t=12 hours, t=24 hours and t=7 days following RFA of the left liver lobe (n=4 mice each group). The liver was excised and placed on a coverslip using immersion oil to improve visualization. The livers were visualized using combined bright field/fluorescence settings on the confocal microscope to localize the transition zone, using a 10x magnification.[5] To visualize the tumor cells, EGFP was excited at 488nm. Tumor cell invasiveness was assessed by creating confocal image stacks in axial dimension. At least 15 randomly chosen tumor cell clusters in the transition zone and the reference zone were visualized and relayed to a personal computer for off line analysis using Zeiss LSM 510 Software. Tumor cell invasion was assessed by creating a two-dimensional stack projection and was defined as the average longest distance between cells making up a single cluster/metastasis. Analysis of tumor cell invasion was performed by two independent observers on liver tissue 24 hours following RFA.

Immunohistochemistry

Tumor-bearing and non-tumor-bearing mice were sacrificed 24 hours and 7 days after RFA (n=4 each group). To visualize hypoxia, these mice were injected intravenously with 60mg/kg pimonidazole

hydrochloride (Hypoxyprobe-1,90201; Chemicon International, Temecula, CA) prior to their sacrifice. After harvesting, the livers were fixed in formaldehyde and embedded in paraffin. Tissue sections (4µm) were used for the immunohistochemical staining of CD95L, using a rabbit polyclonal antibody to CD95L (Abcam, Cambridge, USA). As secondary antibody PowerVision+ (Immunologic, Duiven, The Netherlands) with 2% mouse serum was used. Hypoxia was visualized using anti-pimonidazole, according to the manufacturer's instructions. Reactions were developed using diaminobenzidine/ H_2O_2 as a chromogen substrate. Negative controls were treated with isotype control antibody and were all free of nonspecific background staining.

Analysis of tumor load

Tumor load in the liver was scored as hepatic replacement area (HRA), i.e. the percentage of liver tissue that had been replaced by tumor tissue. HRA was measured in the reference zone and the transition zone, defined as the area stretching 2 mm outside the necrotic central area, as previously described.[5] In brief, on hematoxylin and eosin (H&E) stained sections, at least 100 fields were selected using an interactive video overlay system, including an automated microscope (Q-Prodit; Leica Microsystems, Rijswijk, The Netherlands) at a 40x magnification. Using a four-points grid overlay, the ratio of tumor cells versus normal hepatocytes was determined for each field. Tumor load (HRA) was expressed as the average area ratio of all fields.

Experimental design of *in vivo* studies

First, the effects of RFA on the tumor cell phenotype in the transition zone were assessed. Mice (n=4 each group) were euthanized at five different time points following RFA (t=0, 6 hours, 12 hours, 24 hours and 7 days) and analyzed for tumor cell phenotype as mentioned. Next, the role of CD95/ CD95L system in RFA-induced tumor cell invasion was assessed 24 hours post-RFA by using MFL4 as CD95L neutralizing antibody or IgG isotype control (2 intraperitoneal doses of 20mg/kg, 12 hours before and 12 hours after RFA), CD95 knockdown (KD) cells using shRNA-interference or *gld*-mice that lack functional CD95L. Finally, the influence of CD95 interference on accelerated outgrowth of micrometastases following RFA was investigated using CD95KD cells or *gld*-mice. For mice injected with C26-CD95kd cells, mice injected with C26 shRNA luc served as controls.

Statistical analysis

Statistical differences between the transition zone and the reference zone were analyzed by a paired t-test or Wilcoxon signed rank test when appropriate. Differences between groups were analyzed by ANOVA or Kruskal-Wallis test when appropriate. Data are expressed as mean +/- SEM. A p-value $<$ 0.05 was considered statistically significant.

Results

Micrometastases in the hypoxic transition zone following RFA rapidly acquire an invasive phenotype

Metastases in the reference zone grew as compact spherical tumor cell clusters. However, micrometastases in the transition zone displayed a characteristic invasive growth pattern which was first observed 6 hours post-RFA and which further increased over time (Figure 1A). At 24 hours after

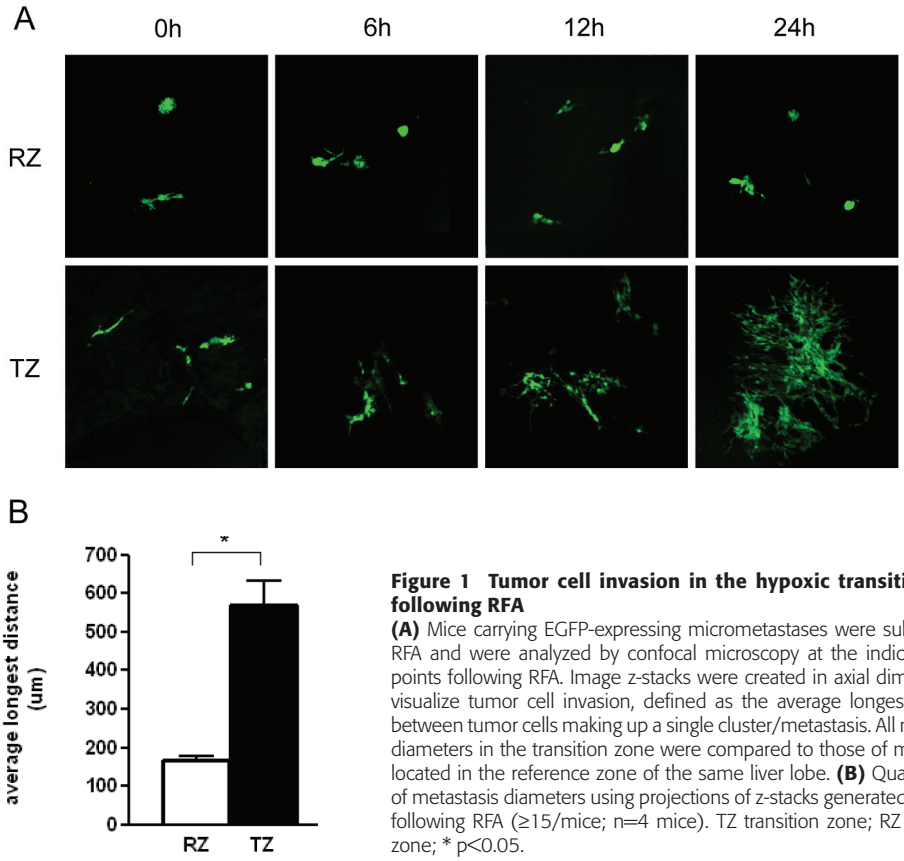

Figure 1 Tumor cell invasion in the hypoxic transition zone following RFA
(A) Mice carrying EGFP-expressing micrometastases were subjected to RFA and were analyzed by confocal microscopy at the indicated time points following RFA. Image z-stacks were created in axial dimension to visualize tumor cell invasion, defined as the average longest distance between tumor cells making up a single cluster/metastasis. All metastasis diameters in the transition zone were compared to those of metastases located in the reference zone of the same liver lobe. **(B)** Quantification of metastasis diameters using projections of z-stacks generated 24 hours following RFA (≥15/mice; n=4 mice). TZ transition zone; RZ reference zone; * $p<0.05$.

RFA, the average longest distance of tumor cells making up a single scattered micrometastasis in the transition zone (569 ± 62 µm) was significantly longer when compared to micrometastases in the reference zone (166 ± 13 µm; p=0.0007) (Figure 1B). During the ensuing 7 days, micrometastases in the reference zone grew but retained their compact phenotype with sharply demarcated edges. In contrast, micrometastases in the transition zone eventually formed a confluent rim of invasive tumor tissue (Figure 2A). To asses the relationship between the invasive phenotype of the micrometastases and tissue hypoxia, we made use of pimonidazole staining. Interestingly, tumor cell invasion was primarily observed at the hypoxic side of the tumor rim facing the necrosis, while tumor cells facing the normoxic reference zone were relatively non-invasive (Figures 2B and 2C).

Hypoxia promotes matrix invasion of C26 cells *in vitro*

In vitro hypoxia for 24 hours was sufficient to induce a drastic change in the growth pattern of tumor cell clusters. Normoxic clusters remained spherical and compact, but hypoxic clusters grew in a scattered fashion with tumor cells detaching from the center of the cluster and invading the surrounding matrix, resulting in a 3.8 fold increase of longest tumor diameter (p=0.0001, figure 3A).

Hypoxia stimulates expression of CD95 and CD95L and causes translocation of CD95 to cell protrusions

Hypoxia induced the expression of HIF1α, CD95 and CD95L *in vitro* (Figure 3B). Immunofluorescence analysis showed that upon CD95L stimulation a subpopulation of CD95 was associated with the leading edges of migrating C26 cells (Figure 3C), similar to what was shown for CD95L-stimulated DLD1 cells.[15] Interestingly, hypoxia-induced tumor cell invasion was also associated with translocation of CD95 to the leading edges of migrating cells (Figure 3C). Neutralization of CD95L with MFL4 completely blocked CD95 translocation. The ability of MFL4 to neutralize CD95L was validated in a control experiment using apoptosis-prone cells stimulated with CD95L (data not shown).

Neutralization of CD95L or suppression of CD95 reduces hypoxia-induced invasion

Using lentiviral shRNA constructs we generated two stable CD95 knockdown cell lines and a control cell line expressing luciferase-targeting shRNAs (shLuc) (Figure 4A). When exposed to hypoxia, control (shLuc) cells displayed the scatter-like growth pattern as expected (Figures 4B and 4C). However,

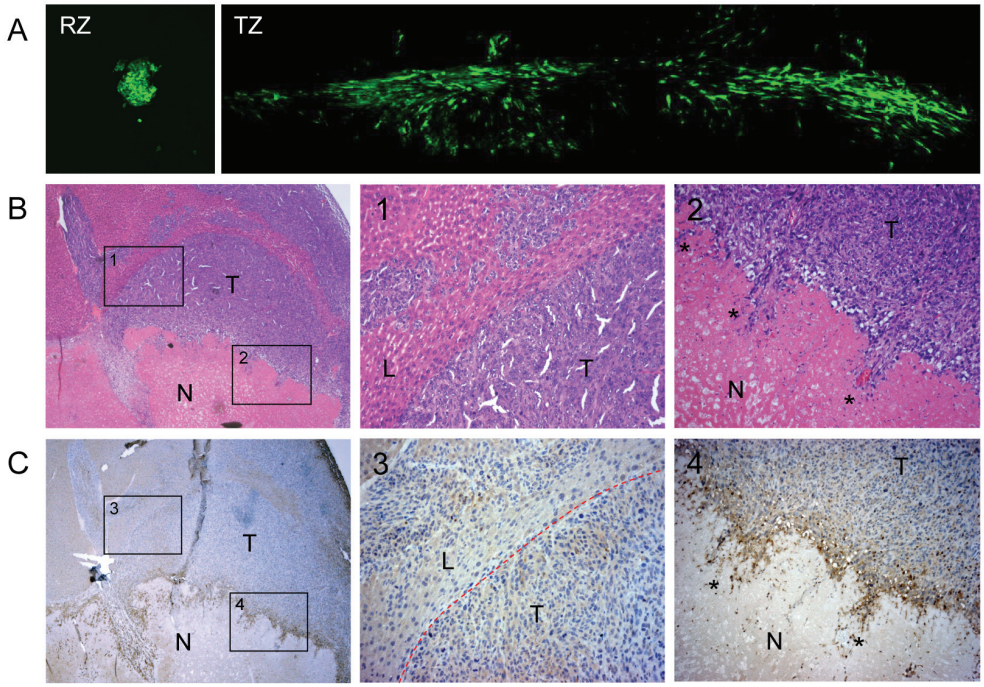

Figure 2 Hypoxia in the transition zone is associated with tumor cell invasion

Mice carrying EGFP-expressing liver metastases were subjected to RFA and the livers were harvested seven days later. To visualize hypoxia, all mice received pimonidazole 60 minutes prior to sacrifice. The growth pattern of metastases in the reference zone and the transition zone was analyzed **(A)** by confocal microscopy on non-fixed livers, and **(B)** by haematoxylin and eosin staining and **(C)** anti-pimonidazole immunohistochemistry on formalin-fixed paraffin-embedded tissue. The right panels show higher magnifications of the normoxic tumor-liver border (1 and 3) and the hypoxic tumor-necrosis border (2 and 4). Invasive tumor cell clusters at the hypoxic tumor-necrosis border are indicated by asterisks. TZ transition zone; RZ reference zone; T tumor; L liver; N necrosis;

neutralization of CD95L using MFL4 or knockdown of tumor cell CD95 was sufficient to completely prevent the scatter response (Figures 4B and 4C).

Increased expression of CD95 and CD95L in the transition zone following RFA

In tumor-bearing mice, Western blotting showed a clear increase in the levels of CD95L and CD95 in the transition zone of all mice when compared to the reference zone (Figure 5A). However, this difference could not be observed in non-tumor-bearing mice (Figure 5B).

Next, to analyze the localization of CD95L, immunohistochemistry was performed on liver tissue sections of tumor-bearing mice 24 hours and 7 days following RFA. At 24 hours after RFA, CD95L

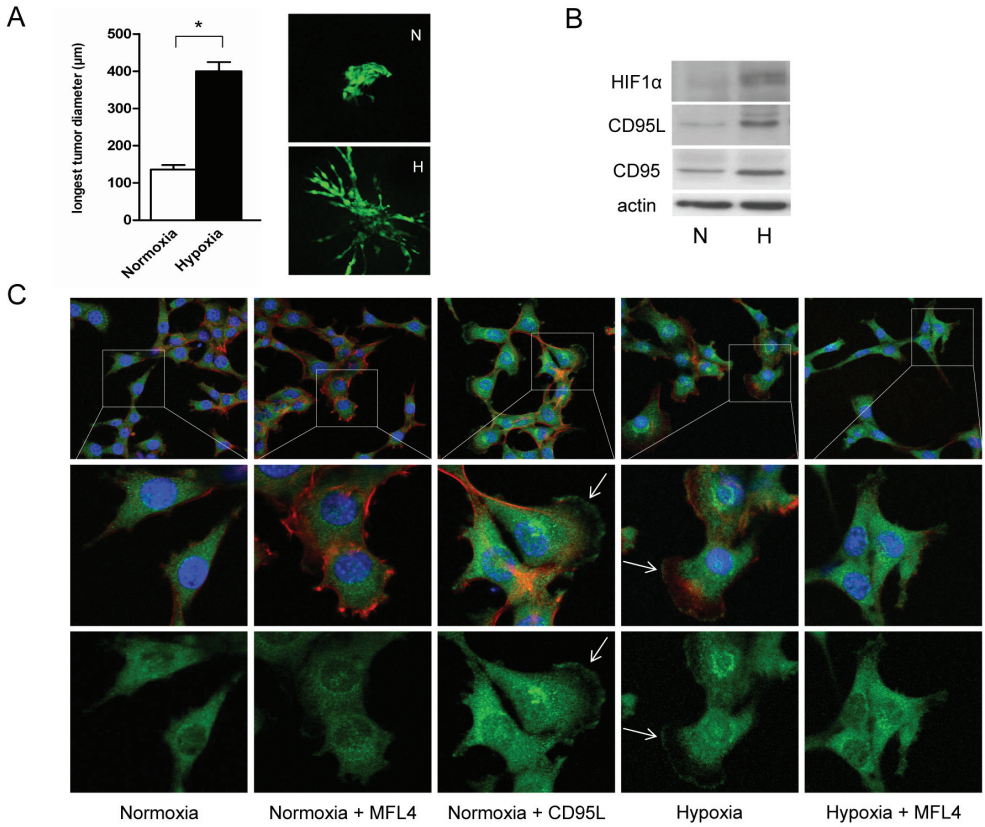

Figure 3 Hypoxia stimulates expression of CD95 and CD95L and causes activation of CD95

(A) EGFP-expressing tumor cells were cultured as three-dimensional clusters in Matrigel and were exposed to normoxia or hypoxia for 24 hours. Confocal microscopy was used to analyze the longest diameter of all tumor cell clusters. The bar graph shows a quantification of the results. **(B)** C26 cells were incubated under normoxia or hypoxia for 24 hours and cell lysates were analyzed by Western blotting for HIF1a, CD95 and CD95L. **(C)** C26 cells were grown on glass coverslips under normoxia or hypoxia for 24 hours either in the presence or absence of MFL4 (6 ng/ml). Stimulation under normoxia with CD95L (10ng/ml for 1h) was used as a positive control. Cells were then fixed and processed for immunofluorescence using anti-CD95 (green) and Alexa568-phalloidin (filamentous actin). Stained coverslips were then analyzed by confocal microscopy. N normoxia; H hypoxia; * $p<0.05$. Arrows indicate the leading edges of migrating cells.

levels were below detection level for immunohistochemistry (data not shown). Interestingly, 7 days after RFA CD95L was strongly expressed in the transition zone in tumor-bearing mice, but was hardly detectable in non tumor-bearing mice (Figure 5C). These results suggest that tumor cells could be the source of CD95L. CD95L was selectively localized at the invasive hypoxic side of the tumor rim facing the generated lesion, but not in the non-invasive normoxic side facing the liver parenchyma. This is in line with a potential role for this cytokine in local, hypoxia-associated, tumor cell invasion (Figure 5C central panel, see also pimonidazole staining for hypoxia at the tumor-necrosis interface in figure 2). No immunohistochemical differences could be observed for CD95 at the mentioned time points (data not shown).

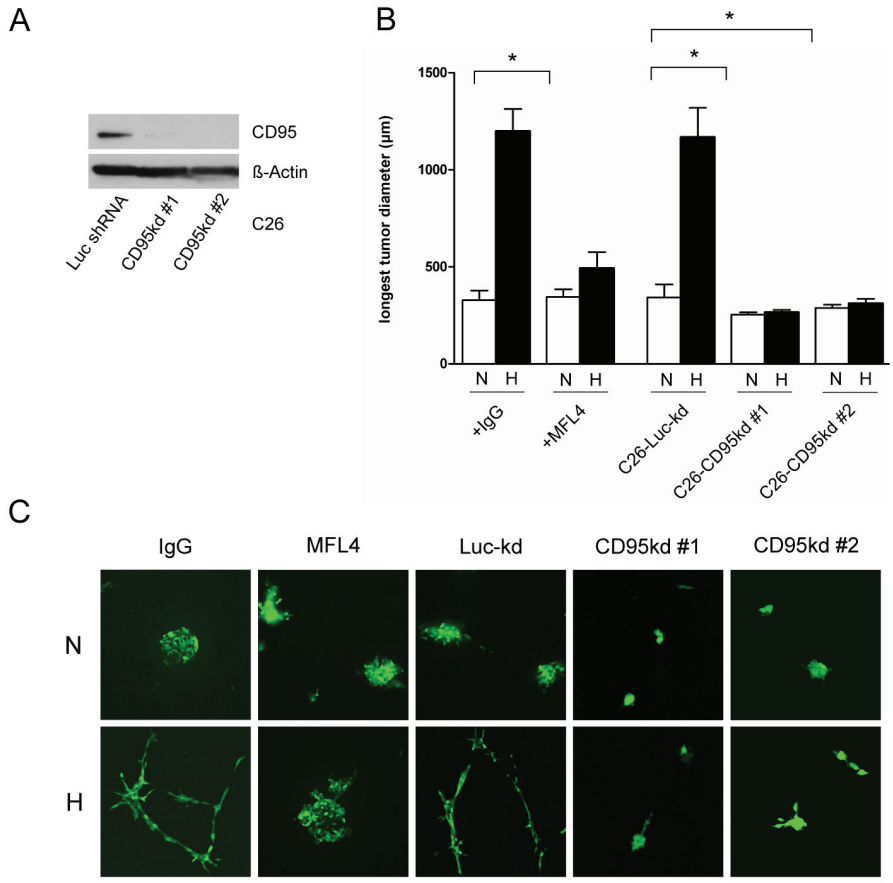

Figure 4 CD95 is required for hypoxia-induced tumor cell invasion
(A) Western blot showing efficient CD95 knockdown by two independent constructs. **(B)** EGFP-expressing tumor cells were cultured as three-dimensional clusters in Matrigel and were exposed to normoxia or hypoxia for 24 hours. Cultures were incubated either with IgG (6ng/ml), or with MFL4 (6ng/ml) for 24 hours. In addition, C26 cells stably expressing shRNA's targeting either Luciferase (Luc) or CD95 were used. Confocal microscopy was used to analyze the longest diameter of all tumor cell clusters. The bar graph shows means and SEM of 10 tumor cell clusters in three independent cultures. **(C)** Representative confocal microscopic images of tumor cell clusters. N normoxia; H hypoxia; * $p<0.05$

Autocrine CD95 signaling is required for tumor cell invasion in the transition zone following RFA

Neutralizing CD95L using MFL4 caused an impressive (~60%) reduction in tumor cell invasion in the transition zone when compared to mice treated with isotype IgG (230 ± 35 µm versus 570 ± 55 µm; p=0.007, figure 6). Additionally, CD95 knockdown (C26-CD95kd, figure 4A) had a strong suppressive effect on metastasis invasion in the transition zone, when compared to control metastases (C26-Luc-kd, 232 ± 34 µm versus 586 ± 64 µm, respectively; p=0.0012, figure 6). Thus, both CD95L neutralization and knockdown of CD95 in tumor cells prevented RFA-induced invasion of micrometastases in the transition zone. This indicates that the tumor cell invasion is based on a direct effect of CD95L on tumor cells rather than an indirect effect by, for instance, suppressing hepatocyte apoptosis or local inflammation.

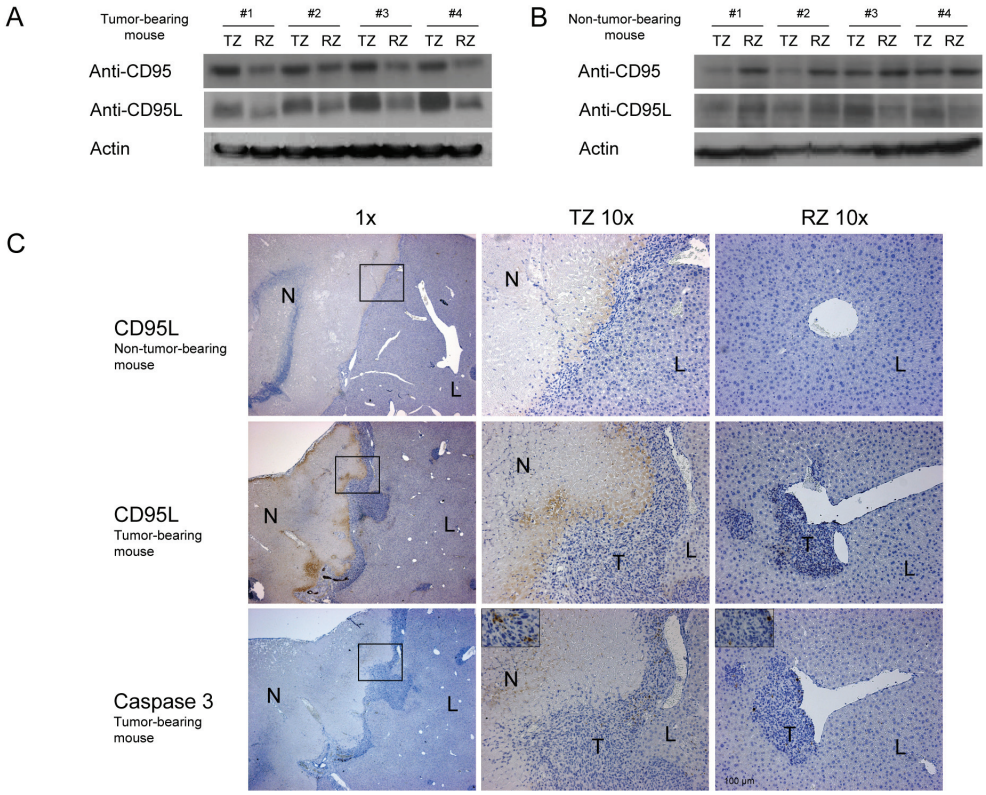

Figure 5 Upregulation of CD95 and CD95L in the transition zone following RFA

TZ-tissue and RZ-tissue were separated from frozen **(A)** tumor-bearing and **(B)** non-tumor-bearing livers 24 hours after RFA using a dissection microscope. Tissue (TZ and RZ) lysates were prepared and were analyzed by Western blotting using specific antibodies directed against CD95, CD95L and actin as a loading control. **(C)** Immunohistochemistry of tumor bearing livers and non-tumor bearing livers 7 days following RFA, using anti-CD95L and anti-active caspase-3. TZ transition zone; RZ reference zone; T tumor; L liver; N necrosis.

To analyze the contribution of host CD95L, we made use of mice lacking functional CD95L (*gld*). Invasion of micrometastases in the transition zone following RFA was not significantly different between *gld*-mice and control mice (491 ± 58 µm versus 554 ± 56 µm; p=0.53, figure 6). This suggests that tumor cell invasion following RFA is most likely due to autocrine activation of CD95 on tumor cells.

Suppression of CD95 signaling reduces accelerated tumor outgrowth in the transition zone following RFA

In mice carrying C26-Luc control metastases, tumor growth in the transition zone was stimulated 3.1-fold when compared to tumor growth in the reference zone (18± 3% versus 47± 5%; p<0.0001, figures 7A-C). However, in mice carrying C26-CD95kd metastases, tumor load in the transition zone was strongly and significantly reduced when compared to C26-Luc metastases (16 ± 3% versus 47± 5%, p<0.0001 respectively). The acceleration of tumor growth, as indicated by the ratio between HRA values of transition zone and reference zone, was significantly reduced by ~60% from 3.1 for C26-Luc cells to 1.7 for C26-CD95kd cells (p=0.0048, figure 7B).

Finally, we tested whether host CD95L was instrumental in accelerating transition zone tumor growth

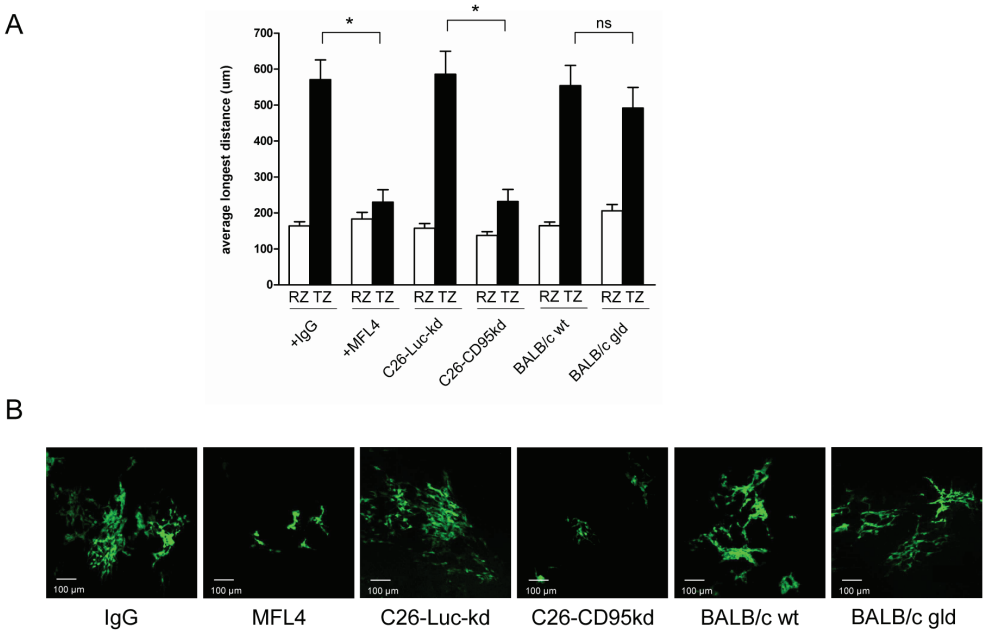

Figure 6 Metastasis invasion in the transition zone requires autocrine CD95 signaling

Mice carrying EGFP-expressing C26 micrometastases were treated either with the CD95L-neutralizing antibody MFL4 or with control IgG prior to the RFA procedure. In addition, RFA was performed on mice carrying C26-Luc-kd or C26-CD95kd metastases. Finally, EGFP-expressing C26 cells were allowed to form metastases in control mice and in mice lacking functional CD95L (*gld*). **(A)** Metastasis diameters in the RZ (white bars) and the TZ (black bars) were then determined 24 hours following RFA, as in Figure 1 (n≥15 metastases). **(B)** Representative confocal microscopic images of transition zone metastases. TZ transition zone; RZ reference zone; kd knock down; * p<0.05; ns not significant

following RFA. Tumor load in the transition zone was not significantly different in *gld*-mice lacking functional CD95L when compared to control mice (44 ± 6% versus 43± 5%, p=0.91, respectively). Consequently, tumor growth acceleration, as measured by HRA ratios, was similar in both genetic backgrounds (2.8 ± 0.3 versus 3.0 ± 0.35; p=0.75, figures 7A-C).

Discussion

In the present study, we show that RFA results in rapid CD95-dependent invasion and accelerated outgrowth of micrometastases in the hypoxic transition zone. These results couple hypoxia-activated CD95 signaling to invasive tumor recurrence in the liver following RFA.

Expression of both CD95 and CD95L is increased in the brain and in the heart following ischemia. In these post-ischemic tissues CD95 is instrumental in inducing apoptosis.[11,13,21] Similarly, hypoxia induces CD95 expression in colorectal cancer cells, which can result in CD95-dependent apoptosis.[12]

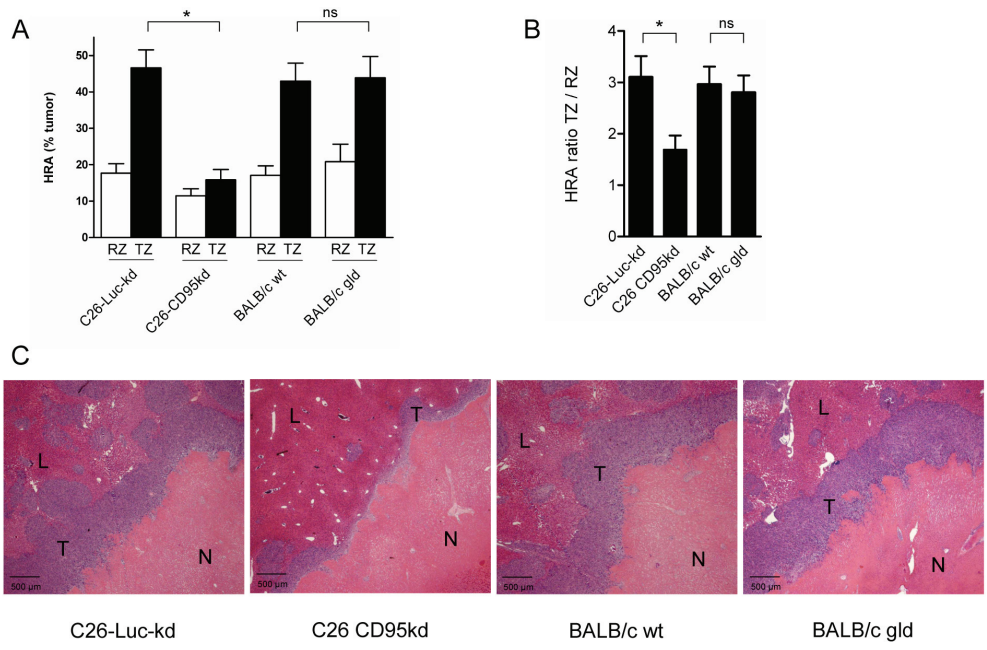

Figure 7 Tumor cell CD95 mediates accelerated outgrowth of liver metastases following RFA
RFA was performed on mice carrying C26-Luc-kd or C26-CD95kd metastases. In addition, RFA was performed on tumor-bearing control mice and on mice lacking functional CD95L (*gld*). All mice were sacrificed 7 days after the RFA procedure. **(A)** The livers were harvested and tumor load in the reference zone (RZ) (white bars) and in the transition zone (TZ) (black bars) was analyzed by morphometric measurement of the hepatic replacement areas (HRA). **(B)** HRA ratio values were determined and plotted. These values indicate the acceleration of tumor growth in the transition zone relative to the reference zone. CD95kd reduced growth acceleration by ~ 60%. **(C)** Representative microscopic images of tumor growth in the transition zone by H&E histochemistry. TZ transition zone; RZ reference zone; T tumor; L liver; N necrosis; * p<0.05; ns not significant

However, many colorectal tumor cells display inherent resistance to apoptosis induction by CD95. In recent years it has become clear that CD95 can activate a number of non-apoptotic pathways that stimulate proliferation and invasion.[14-18]

Although CD95 is expressed on the majority of colonic epithelial cells, its primary function in these cells does not appear to be apoptosis induction.[22,23] Remarkably, it was shown in a recent study that CD95 on intestinal epithelial cells is cytoprotective rather than cytotoxic.[23] The non-apoptotic function of CD95 may therefore be conserved in colon tumors. Indeed, chronic CD95 stimulation of colorectal tumor cells selects for highly metastatic variants.[24] Moreover, forced expression of CD95L in apoptosis-resistant tumor cells can promote liver metastasis formation.[20] During colorectal cancer progression, expression of CD95L increases and correlates with metastasis formation.[19,25] In addition, we have shown recently that the *K-Ras* oncogene, which is present in approximately 40% of all colorectal tumors, is a major determinant of CD95 signaling output and forces it to signal invasion, rather than apoptosis.[15] In the present study, we demonstrate that hypoxia, generated following the RFA procedure, stimulates CD95-dependent outgrowth of colorectal micrometastases. Taken together, it appears that CD95 activation on colorectal tumor cells promotes tumor progression rather than tumor clearance. Our data suggest that this is especially relevant during conditions of hypoxia, which causes autocrine activation of the CD95 system and CD95-dependent invasion.

High levels of tumor-produced CD95L in the hypoxic transition zone could affect tumor progression in different ways. First, it can cause apoptosis of infiltrating lymphocytes (a phenomenon known as the 'tumor counterattack').[26] Second, it can induce apoptosis in surrounding hepatocytes, which could lead to facilitated tumor cell invasion.[27] Third, our results (based on the use of CD95 knockdown tumor cells and CD95L-deficient mice) strongly suggest that autocrine activation of the CD95 system on tumor cells mediates aggressive outgrowth of liver metastases following RFA.

It has recently been demonstrated that hypoxia leads to reduced cell proliferation and increased survival of colorectal cancer cells. This was due to HIF-1α stabilization followed by the formation of a HIF1-ß-catenin complex at the expense of the TCF-ß-catenin complex.[28] However, hypoxia is generally associated with metastatic spread and poor prognosis.[7,29] Also in colorectal tumors, expression of different HIF targets is associated with disease progression and poor patient prognosis.[30,31] It therefore seems unlikely that hypoxia-induced cell cycle arrest plays an important role during aggressive tumor recurrence in the transition zone following RFA. In accordance with our findings, pre-clinical studies have shown that tumor cell proliferation is increased, not decreased, following local ablative therapies like RFA.[32,33]

Many surgical procedures generate tissue hypoxia. We have recently shown that vascular clamping, which is frequently applied to prevent excessive blood loss during partial liver resection, generates chronically hypoxic liver tissue that is associated with aggressive tumor recurrence in pre-clinical mouse models.[34,35] In colorectal cancer patients, prolonged clamping times during liver surgery were significantly associated with decreased time to tumor progression in the liver.[36] In addition, we have recently found that the levels of circulating CD95L were significantly increased following RFA treatment of liver metastases in CRC patients (FJHH, ms in preparation). Taken together, we propose that CD95 signaling may contribute to tumor recurrence in livers treated with hypoxia-generating (surgical) procedures.

Patient selection for RFA of colorectal liver metastases is essential for optimal response to the treatment, making it a potentially curative treatment option. The mechanistic understanding of local recurrences might be important for making RFA applicable to more patients with colorectal liver

metastases. Currently, clinical observations show highly aggressive local tumor recurrence in patients treated with local ablative therapies.[37,38] In the present study we have demonstrated that the hypoxic rim of RFA-generated lesions is characterized by aggressive CD95-dependent outgrowth of colorectal micrometastases. Although neutralization of CD95L would not kill remaining tumor cells, it could be of therapeutic benefit in patients with colorectal liver metastases treated with RFA by reducing tumor cell invasion and outgrowth. Prolonged treatment with CD95L-neutralizing agents holds the potential danger of inducing lymphoproliferative disorders and autoimmunity[39,40], short-term peri-operative treatment however may prove to be feasible. Whether CD95L-neutralizing agents, either alone or in combination with chemotherapy, can be of added value in preventing aggressive tumor recurrence following RFA requires further pre-clinical work. This work should initially focus on tumors with mutant K-Ras as such tumors are prone to respond aggressively to CD95L.[15]

References

1. Abdalla EK, Vauthey JN, Ellis LM, Ellis V, Pollock R, Broglio KR, Hess K, Curley SA. Recurrence and outcomes following hepatic resection, radiofrequency ablation, and combined resection/ablation for colorectal liver metastases. Ann Surg 2004; 239: 818-825.
2. Mulier S, Ni Y, Jamart J, Ruers T, Marchal G, Michel L. Local recurrence after hepatic radiofrequency coagulation: multivariate meta-analysis and review of contributing factors. Ann Surg 2005; 242: 158-171.
3. Siperstein AE, Berber E, Ballem N, Parikh RT. Survival after radiofrequency ablation of colorectal liver metastases: 10-year experience. Ann Surg 2007; 246: 559-567.
4. Solbiati L, Livraghi T, Goldberg SN, Ierace T, Meloni F, Dellanoce M, Cova L, Halpern EF, Gazelle GS. Percutaneous radio-frequency ablation of hepatic metastases from colorectal cancer: long-term results in 117 patients. Radiology 2001; 221: 159-166.
5. Nijkamp MW, van der Bilt JD, de Bruijn MT, Molenaar IQ, Voest EE, van Diest PJ, Kranenburg O, Borel Rinkes IH. Accelerated perinecrotic outgrowth of colorectal liver metastases following radiofrequency ablation is a hypoxia-driven phenomenon. Ann Surg 2009; 249: 814-823.
6. Yokoyama N, Shirai Y, Ajioka Y, Nagakura S, Suda T, Hatakeyama K. Immunohistochemically detected hepatic micrometastases predict a high risk of intrahepatic recurrence after resection of colorectal carcinoma liver metastases. Cancer 2002; 94: 1642-1647.
7. Harris AL. Hypoxia--a key regulatory factor in tumour growth. Nat Rev Cancer 2002; 2: 38-47.
8. Semenza GL. Targeting HIF-1 for cancer therapy. Nat Rev Cancer 2003; 3: 721-732.
9. Pouyssegur J, Dayan F, Mazure NM. Hypoxia signalling in cancer and approaches to enforce tumour regression. Nature 2006; 441: 437-443.
10. Wey JS, Fan F, Gray MJ, Bauer TW, McCarty MF, Somcio R, Liu W, Evans DB, Wu Y, Hicklin DJ, Ellis LM. Vascular endothelial growth factor receptor-1 promotes migration and invasion in pancreatic carcinoma cell lines. Cancer 2005; 104: 427-438.
11. Jeremias I, Kupatt C, Martin-Villalba A, Habazettl H, Schenkel J, Boekstegers P, Debatin KM. Involvement of CD95/Apo1/Fas in cell death after myocardial ischemia. Circulation 2000; 102: 915-920.
12. Liu T, Laurell C, Selivanova G, Lundeberg J, Nilsson P, Wiman KG. Hypoxia induces p53-dependent transactivation and Fas/CD95-dependent apoptosis. Cell Death Differ 2007; 14: 411-421.
13. Martin-Villalba A, Herr I, Jeremias I, Hahne M, Brandt R, Vogel J, Schenkel J, Herdegen T, Debatin KM. CD95 ligand (Fas-L/APO-1L) and tumor necrosis factor-related apoptosis-inducing ligand mediate ischemia-induced apoptosis in neurons. J Neurosci 1999; 19: 3809-3817.
14. Barnhart BC, Legembre P, Pietras E, Bubici C, Franzoso G, Peter ME. CD95 ligand induces motility and invasiveness of apoptosis-resistant tumor cells. EMBO J 2004; 23: 3175-3185.
15. Hoogwater FJ, Nijkamp MW, Smakman N, Steller E.J., Emmink B.L., B.F.Westendorp, Raats D.A., Sprick M.R., Schaeffer U., van Houdt WJ, de Bruijn MT, Schackmann R.C., Derksen P.W., Medema J.P., Walczak H, Borel Rinkes I.H., Kranenburg O. Oncogenic K-Ras Turns Death Receptors Into Metastasis-Promoting Receptors in Human and Mouse Colorectal Cancer Cells. Gastroenterology 2010; 137: 2357-2367.
16. Kleber S, Sancho-Martinez I, Wiestler B, Beisel A, Gieffers C, Hill O, Thiemann M, Mueller W, Sykora J, Kuhn A, Schreglmann N, Letellier E, Zuliani C, Klussmann S, Teodorczyk M, Grone HJ, Ganten TM, Sultmann H, Tuttenberg J, von DA, Regnier-Vigouroux A, Herold-Mende C, Martin-Villalba A. Yes and PI3K bind CD95 to signal invasion of glioblastoma. Cancer Cell 2008; 13: 235-248.
17. Trauzold A, Roder C, Sipos B, Karsten K, Arlt A, Jiang P, Martin-Subero JI, Siegmund D, Muerkoster S, Pagerols-Raluy L, Siebert R, Wajant H, Kalthoff H. CD95 and TRAF2 promote invasiveness of pancreatic cancer cells. FASEB J 2005; 19: 620-622.
18. Wisniewski P, Ellert-Miklaszewska A, Kwiatkowska A, Kaminska B. Non-apoptotic Fas signaling regulates invasiveness of glioma cells and modulates MMP-2 activity via NFkappaB-TIMP-2 pathway. Cell Signal 2010; 22: 212-220.

19. Nozoe T, Yasuda M, Honda M, Inutsuka S, Korenaga D. Fas ligand expression is correlated with metastasis in colorectal carcinoma. Oncology 2003; 65: 83-88.
20. Li H, Fan X, Stoicov C, Liu JH, Zubair S, Tsai E, Ste MR, Wang TC, Lyle S, Kurt-Jones E, Houghton J. Human and mouse colon cancer utilizes CD95 signaling for local growth and metastatic spread to liver. Gastroenterology 2009; 137: 934-44, 944.
21. Sairanen T, Karjalainen-Lindsberg ML, Paetau A, Ijas P, Lindsberg PJ. Apoptosis dominant in the periinfarct area of human ischaemic stroke--a possible target of antiapoptotic treatments. Brain 2006; 129: 189-199.
22. Abreu-Martin MT, Palladino AA, Faris M, Carramanzana NM, Nel AE, Targan SR. Fas activates the JNK pathway in human colonic epithelial cells: lack of a direct role in apoptosis. Am J Physiol 1999; 276: G599-G605.
23. Park SM, Chen L, Zhang M, Ashton-Rickardt P, Turner JR, Peter ME. CD95 is cytoprotective for intestinal epithelial cells in colitis. Inflamm Bowel Dis 2010; 16: 1063-1070.
24. Liu K, McDuffie E, Abrams SI. Exposure of human primary colon carcinoma cells to anti-Fas interactions influences the emergence of pre-existing Fas-resistant metastatic subpopulations. J Immunol 2003; 171: 4164-4174.
25. Mann B, Gratchev A, Bohm C, Hanski ML, Foss HD, Demel G, Trojanek B, Schmidt-Wolf I, Stein H, Riecken EO, Buhr HJ, Hanski C. FasL is more frequently expressed in liver metastases of colorectal cancer than in matched primary carcinomas. Br J Cancer 1999; 79: 1262-1269.
26. O'Connell J, O'Sullivan GC, Collins JK, Shanahan F. The Fas counterattack: Fas-mediated T cell killing by colon cancer cells expressing Fas ligand. J Exp Med 1996; 184: 1075-1082.
27. Yoong KF, Afford SC, Randhawa S, Hubscher SG, Adams DH. Fas/Fas ligand interaction in human colorectal hepatic metastases: A mechanism of hepatocyte destruction to facilitate local tumor invasion. Am J Pathol 1999; 154: 693-703.
28. Kaidi A, Williams AC, Paraskeva C. Interaction between beta-catenin and HIF-1 promotes cellular adaptation to hypoxia. Nat Cell Biol 2007; 9: 210-217.
29. Gort EH, Groot AJ, van der Wall E., van Diest PJ, Vooijs MA. Hypoxic Regulation of Metastasis via Hypoxia-Inducible Factors. Curr Mol Med 2008; 8: 60-67.
30. Chung FY, Huang MY, Yeh CS, Chang HJ, Cheng TL, Yen LC, Wang JY, Lin SR. GLUT1 gene is a potential hypoxic marker in colorectal cancer patients. BMC Cancer 2009; 9: 241.
31. Koukourakis MI, Giatromanolaki A, Sivridis E, Gatter KC, Harris AL. Lactate dehydrogenase 5 expression in operable colorectal cancer: strong association with survival and activated vascular endothelial growth factor pathway--a report of the Tumour Angiogenesis Research Group. J Clin Oncol 2006; 24: 4301-4308.
32. Ohno T, Kawano K, Yokoyama H, Tahara K, Sasaki A, Aramaki M, Kitano S. Microwave coagulation therapy accelerates growth of cancer in rat liver. J Hepatol 2002; 36: 774-779.
33. von Breitenbuch P, Kohl G, Guba M, Geissler E, Jauch KW, Steinbauer M. Thermoablation of colorectal liver metastases promotes proliferation of residual intrahepatic neoplastic cells. Surgery 2005; 138: 882-887.
34. van der Bilt JD, Kranenburg O, Nijkamp MW, Smakman N, Veenendaal LM, Te Velde EA, Voest EE, van Diest PJ, Borel Rinkes IH. Ischemia/reperfusion accelerates the outgrowth of hepatic micrometastases in a highly standardized murine model. Hepatology 2005; 42: 165-175.
35. van der Bilt JD, Soeters ME, Duyverman AM, Nijkamp MW, Witteveen PO, van Diest PJ, Kranenburg O, Borel Rinkes IH. Perinecrotic hypoxia contributes to ischemia/reperfusion-accelerated outgrowth of colorectal micrometastases. Am J Pathol 2007; 170: 1379-1388.
36. Nijkamp MW, van der Bilt JD, Snoeren N, Hoogwater FJ, van Houdt WJ, Molenaar IQ, Kranenburg O, van Hillegersberg R, Borel Rinkes IH. Prolonged portal triad clamping during liver surgery for colorectal liver metastases is associated with decreased time to hepatic tumour recurrence. Eur J Surg Oncol 2009; 36: 182-188.
37. Portolani N, Tiberio GA, Ronconi M, Coniglio A, Ghidoni S, Gaverini G, Giulini SM. Aggressive recurrence after radiofrequency ablation of liver neoplasms. Hepatogastroenterology 2003; 50: 2179-2184.
38. Ruzzenente A, Manzoni GD, Molfetta M, Pachera S, Genco B, Donataccio M, Guglielmi A. Rapid progression

of hepatocellular carcinoma after Radiofrequency Ablation. World J Gastroenterol 2004; 10: 1137-1140.
39. Cohen PL and Eisenberg RA. Lpr and *gld*: single gene models of systemic autoimmunity and lymphoproliferative disease. Annu Rev Immunol 1991; 9:243-69.: 243-269.
40. Jackson CE and Puck JM. Autoimmune lymphoproliferative syndrome, a disorder of apoptosis. Curr Opin Pediatr 1999; 11: 521-527.

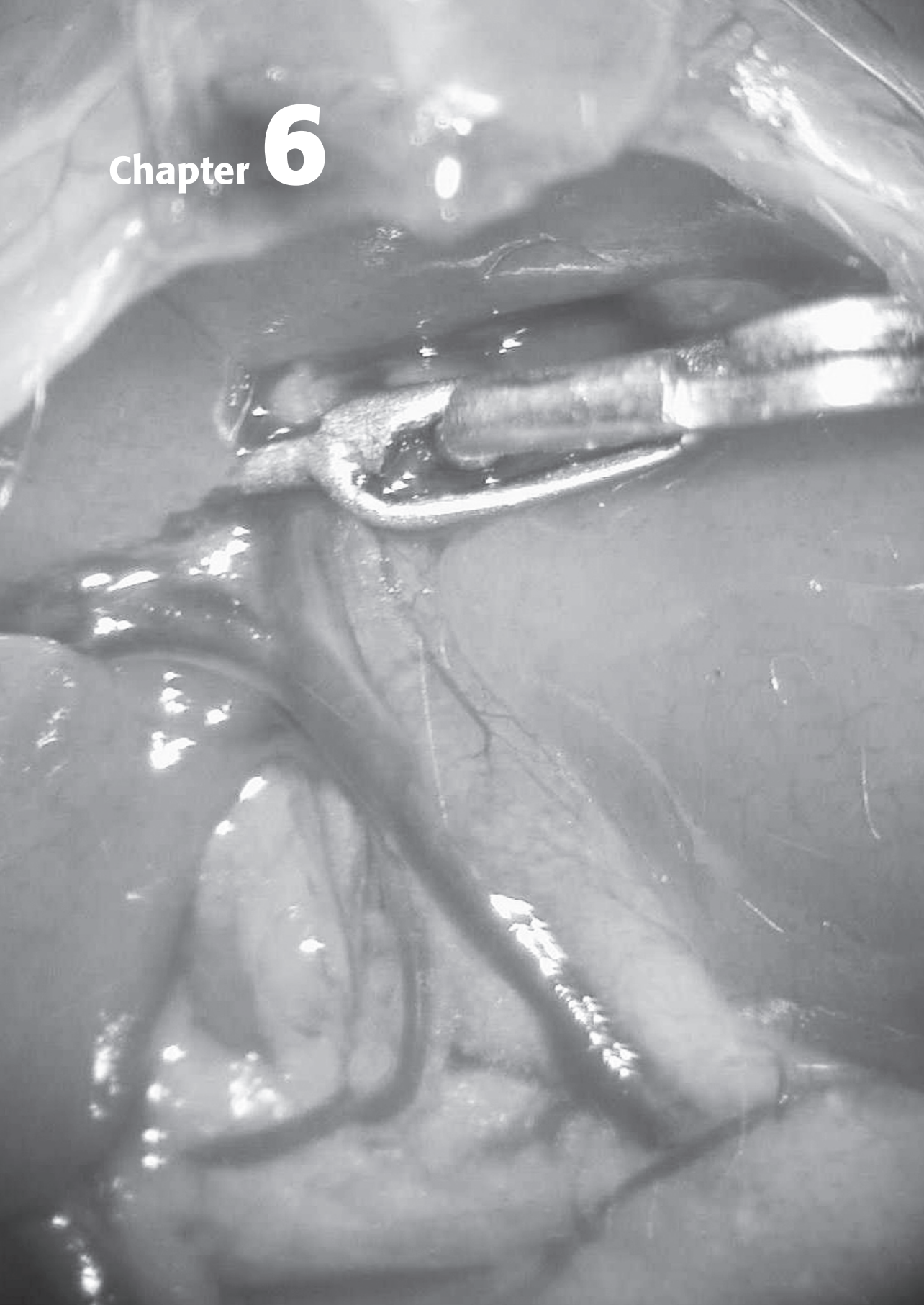
Chapter 6

A role for CD95 signaling in ischemia/reperfusion-stimulated invasion and accelerated outgrowth of colorectal liver metastases

Submitted for publication

Maarten W. Nijkamp
Frederik J.H. Hoogwater
Klaas M. Govaert
Ernst J.A. Steller
Andre Verheem
Onno Kranenburg
Inne H.M. Borel Rinkes

Department of Surgery
University Medical Center Utrecht, Utrecht, The Netherlands

Abstract

Background
Ischemia/reperfusion (I/R) injury is frequently caused by hepatic surgery due to clamping of the vascular inflow of the liver. I/R injury generates hepatocellular damage but is also associated with accelerated outgrowth of micrometastases. Recently, we demonstrated that CD95 is a key mediator of tumor cell invasion and outgrowth following radiofrequency ablation. Here, we tested whether CD95 signaling plays a role in accelerated outgrowth of colorectal liver metastases following I/R.

Methods
Mice underwent vascular clamping five days after induction of colorectal liver metastases. Invasion and outgrowth of micrometastases following I/R were analyzed by post-mortem confocal microscopy (36 hours post-I/R) and by morphometric assessment of tumor load (5 days post-I/R), respectively. Tumor cell CD95 was suppressed by lentiviral RNA interference. The contribution of host CD95L was assessed by using *gld*-mice lacking functional CD95L.

Results
I/R induced invasion of micrometastases selectively in the perinecrotic regions. CD95 knockdown in tumor cells strongly reduced invasion and largely prevented accelerated outgrowth of perinecrotic liver metastases following I/R. I/R-induced liver necrosis and necrosis-associated accelerated tumor growth were reduced in *gld*-mice. However, the remaining perinecrotic tumor cell clusters in *gld*-mice still displayed an invasive phenotype.

Conclusions
I/R induces invasion and accelerated outgrowth of pre-established metastases in a CD95-dependent manner. Activation of the CD95 system following I/R not only contributes to liver injury, but may also promote aggressive tumor recurrence.

Introduction

Approximately 50% of colorectal cancer patients develop liver metastases. For these patients, partial liver resection is the only curative treatment option, leading to a 5-year survival of approximately 40-60%.[1,2] Nonetheless, tumor recurrence following partial liver resection is observed in ~60% of cases.[2,3] Vascular clamping is frequently applied to limit excessive blood loss during hepatic resection and can cause ischemia/reperfusion (I/R) injury to the liver. I/R not only causes tissue injury, but also has a growth-stimulatory effect on residual tumor tissue in the liver.[4-6] Indeed, in colorectal cancer patients receiving liver surgery for colorectal liver metastases, prolonged vascular clamping is associated with a reduced time to tumor recurrence in the liver.[7]

I/R in the liver generates long-term microcirculatory disturbances and chronic hypoxia, which play an important role in accelerated tumor outgrowth following hepatic I/R.[8] Hypoxia can stimulate motility and invasion of tumor cells through induction of matrix-metalloproteinases (MMPs), urokinase plasminogen activator receptor (uPAR) and/or c-Met.[9-11] Recently, we demonstrated that hypoxia also activates the CD95/CD95L system in apoptosis-resistant colorectal tumor cells and that this mediates tumor cell invasion.[12] Moreover, radiofrequency ablation (RFA) resulted in invasion and accelerated outgrowth of tumor cells in the hypoxic tissue areas surrounding RFA lesions and this could be abrogated by suppressing the CD95/CD95L system.[12] CD95 is also activated during liver I/R and mediates tissue injury.[13,14] This is most likely due to the fact that hepatocytes express CD95 and are highly sensitive to CD95-mediated apoptosis.[15] However, CD95 was not a critical mediator of liver injury following I/R in another study.[16]

Based on these observations, we hypothesized that CD95 activation during I/R may contribute to invasion and outgrowth of hepatic micrometastases. In the present study we demonstrate that CD95 and CD95L are upregulated following hepatic I/R and that this contributes to invasion and outgrowth of micrometastases. Our results identify CD95 as an important participant in local tumor cell invasion and accelerated outgrowth of micrometastases following liver I/R.

Materials and Methods

Animals and surgery

All experiments were performed in accordance with the guidelines of the Animal Welfare Committee of the University Medical Center Utrecht, The Netherlands. Male BALB/c mice (10-12 weeks) were purchased from Charles River (Sulzfeld, Germany). BALB/c-*gld*/*gld* (CPt.C3-*Fasl*^{gld}/J) mice carrying a homozygous loss-of-function mutation in CD95L (hereafter referred to as *gld*-mice) were purchased from The Jackson Laboratory (Bar Harbor, ME, USA). When *gld*-mice were used, control BALB/c mice were purchased from The Jackson Laboratory as well. Mice were housed under standard laboratory conditions and received food and water *ad libitum*. All surgical procedures were performed under isoflurane inhalation anesthesia. Prior to surgery, buprenorfine was administered intramuscularly to provide sufficient peri-operative analgesia. During surgery, body temperature was maintained at 36,5˚C to 37,5˚C by placing the mice on a heated table and covering them with aluminium foil.

Induction of micrometastases and ischemia/reperfusion injury

C26 mouse colon carcinoma cells and its derivatives, including Green Fluorescent Protein (GFP)-

expressing C26 cells, C26-CD95 knockdown cells and C26-Luciferase-knockdown control cells were cultured exactly as previously described.[12] For tumor cell invasion experiments, GFP-expressing C26 cells were used. When C26-CD95 knockdown (kd) cells were used, cells expressing shRNA's directed at firefly luciferase (sh-Luc) were used as control cells. For induction of colorectal micrometastases we used our previously described mouse model.[5,8] In brief, through a left lateral flank incision, $5x10^4$ routinely cultured C26 colon carcinoma cells were injected into the splenic parenchyma, followed by removal of the spleen after ten minutes to prevent intrasplenic tumor growth.
Diffuse intrahepatic micrometastases were allowed to grow out for five days, followed by partial hepatic ischemia. After laparotomy, the liver hilus was exposed and the vascular inflow to the left lateral lobe was clamped for 45 minutes. Tumor cell invasion was assessed 36 hours later in both the clamped and non-clamped lobes. Tumor outgrowth was assessed 5 days following I/R. Sham-operated animals underwent laparotomy with subsequent exposure of the liver hilus, but without clamping the hepatic blood inflow.

Liver enzymes
Early liver damage was assessed by plasma alanine aminotransferase (ALT) and aspartate aminotransferase (AST) levels. Blood was drawn from mice 6 hours following surgery and centrifuged at 14000 rpm for 10 minutes (n=8 I/R groups, n=4 sham groups). Plasma levels of ALT and AST were automatically analyzed (Beckman Coulter UniCel® DxC 600, Beckman Coulter B.V. Woerden, The Netherlands) and were expressed as units per liter (U/L).

Assessment of the perinecrotic tumor cell phenotype following I/R
Mice bearing GFP-expressing tumor cells were sacrificed at 36 hours following I/R of the left liver lobe. Prior to sacrifice, mice were injected intravenously with rhodamine(RITC)-labeled dextran (MW 2.000.000; Invitrogen, Carlsbad, CA) to identify the perinecrotic region. The non-clamped and clamped liver lobes were harvested and placed on a coverslip using immersion oil to improve visualization. The livers were imaged with a Zeiss LSM510 Meta confocal microscope using 10x magnification (n=4 mice each group). As previously described, the perinecrotic region is characterized by microcirculatory disturbances[8,17], which could be visualized by exciting RITC at 561 nm. GFP was excited at 488nm to visualize the tumor cells. Tumor cell invasion was assessed using confocal image stacks in axial dimension and was defined as the average longest distance between cells making up a single cluster metastasis, exactly as previously described.[12] At least 15 randomly chosen tumor cell clusters in clamped and non-clamped liver lobes were visualized and relayed to a personal computer for off line analysis. Analysis of tumor cell invasion was performed by two independent observers.

Western blot analysis of tissue extracts
Tumor-bearing mice (n=4) were sacrificed 36 hours following surgery. After harvesting the livers, the clamped and non-clamped liver lobes were divided. Next, the liver sections were minced and homogenized. Homogenized tissue samples were then lysed in a buffer containing 20 mM HEPES pH 7.4, 1% NP40, 150 mM NaCl, 5 mM $MgCl_2$ and 10% glycerol. Lysates were cleared by centrifugation (Eppendorf, 13.000 rpm) and analyzed by Western blotting using anti-CD95 (clone M-20, #sc-716, Santa Cruz Biotechnology Inc., Santa Cruz, CA, USA), anti-CD95L (ab15285, Abcam, Cambridge, MA, USA) and anti-ß-actin (AC-15, NB600-501, Novus Biologicals, Littleton, CO, USA).

Immunohistochemistry

Tumor-bearing mice (n=4 each time point) were sacrificed 36 hours and 5 days after I/R. After harvesting, livers were fixed in formaldehyde and embedded in paraffin. Tissue sections (4µm) were used for the immunohistochemical staining of CD95L (ab15285, Abcam, Cambridge, MA, USA). As secondary antibody PowerVision+ (Immunologic, Duiven, The Netherlands) with 2% mouse serum was used. Reactions were developed using diaminobenzidine/H_2O_2 as a chromogen substrate. Negative controls were stained with isotype control antibody and were all free of nonspecific background staining.

Analysis of tumor load and hepatocellular necrosis

Tumor load in the liver was assessed in both the clamped and the non-clamped liver lobes. Tumor load was scored as hepatic replacement area (HRA), i.e. the percentage of liver tissue that had been replaced by tumor tissue.[5,8] In brief, on hematoxylin and eosin (H&E) stained sections, at least 100 fields were selected using an interactive video overlay system, including an automated microscope (Q-Prodit; Leica Microsystems, Rijswijk, The Netherlands) at a 40x magnification. Using a four-points grid overlay, the ratio of tumor cells versus normal hepatocytes plus necrotic cells was determined for each field. Tumor load (HRA) was expressed as the average area ratio of all fields.
The percentage of hepatocellular necrosis was scored simultaneously with tumor HRA analysis. The ratio of necrotic cells versus normal hepatocytes plus tumor cells was determined for each field. The percentage of hepatocellular necrosis was expressed as the average area ratio of all fields.

Statistical analysis

Statistical differences between the clamped and the unclamped lobes were analyzed by a paired t-test or Wilcoxon signed rank test when appropriate. Differences between groups were analyzed by ANOVA or Kruskal-Wallis test when appropriate. Data are expressed as mean +/- SEM. A p-value $<$ 0.05 was considered statistically significant.

Results

Hepatic I/R induces scattering of micrometastases in perinecrotic liver tissue

Micrometastases in the livers from sham-operated mice grew non-invasively, both in the median and left liver lobe (Figure 1). Necrotic tissue areas had formed in the clamped but not in the non-clamped liver lobes 36 hours following I/R. Micrometastases surrounding these necrotic tissue areas displayed a characteristic scatter response, which is indicative of tumor cell invasion. Quantification of the average longest distance between tumor cells making up a single metastasis revealed that peri-necrotic 'scattered' metastases in the clamped (left) liver lobes had an average diameter of 949 ± 81 µm. This was significantly longer than the diameter of metastases in the unclamped median lobes (241 ± 18 µm; p=0.0008, figure 1) and in the left lobe of sham-operated mice (256 ± 15 µm; p=0.0001, figure 1).

Induction of CD95 and CD95L following hepatic I/R

At 36 hours following I/R, the liver lobes were harvested, lysed and analyzed for expression of CD95 and CD95L by Western blotting. CD95 was induced in the clamped liver lobes compared to the

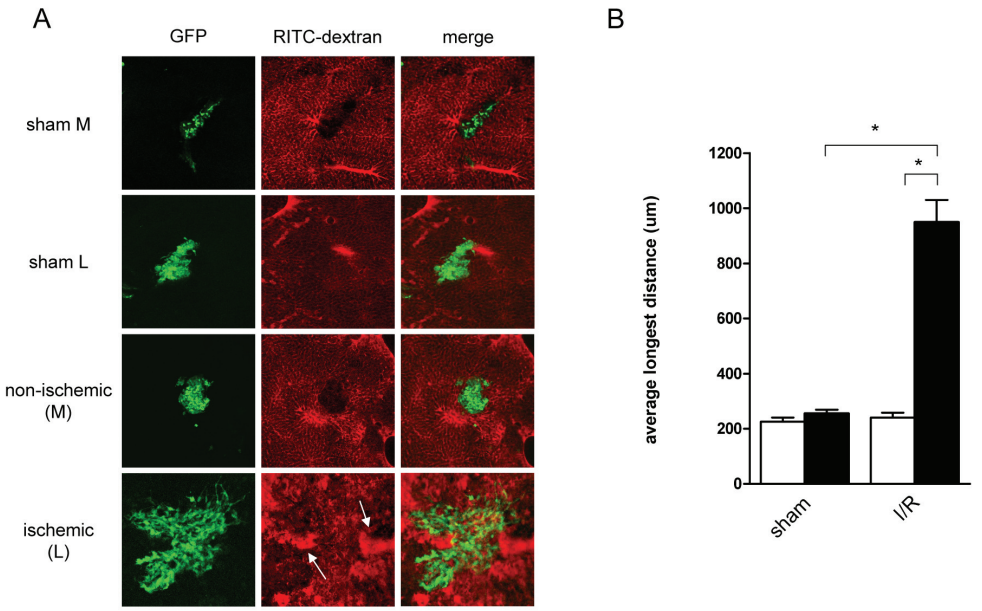

Figure 1 Perinecrotic tumor cell invasion in the clamped liver lobes following I/R
(A) Mice carrying EGFP-expressing micrometastases were subjected to I/R or sham operation and were analyzed by confocal microscopy 36 hours later. The perinecrotic area was identified by microcirculatory disturbances (arrow). Image z-stacks were created in axial dimension to visualize tumor cell invasion, defined as the average longest distance between tumor cells making up a single cluster/metastasis. **(B)** Quantification of metastasis diameters in mice that underwent sham operation or I/R (≥15/mice; n=4 mice each group). In I/R mice, black bars represent clamped (ischemic) liver lobes, white bars represent unclamped (non-ischemic) liver lobes. In sham-operated mice, black bars represent left liver lobes, white bars represent median liver lober. M median liver lobe; L left liver lobe; * $p<0.05$.

unclamped liver lobes in 3 out of 4 mice. Moreover, CD95L was induced in the clamped liver lobes of all 4 mice (Figure 2A). Next, immunohistochemistry was performed on liver tissue sections of tumor-bearing mice 36 hours and 5 days following I/R. The induction of CD95L in the clamped liver lobes 36 hours following I/R, as it was observed on the Western blots, could not be detected by immunohistochemistry (data not shown). However, 5 days following I/R, CD95L was strongly expressed in the rim of invasive tumor tissue facing the areas of I/R-induced necrosis (Figure 2B).

I/R-injury is reduced in *gld*-mice

In wildtype mice, I/R induced early hepatocelular damage as evidenced by elevated plasma ALT and AST levels (Figures 3A and 3B). *Gld*-mice, however, were partly protected from I/R-induced liver damage as plasma ALT levels were reduced by ~55% (3145 ± 864 U/L versus 6891 ± 1310 U/L in wildtype mice, p=0.036, figure 3A) and plasma AST levels were reduced by ~35% (2124 ± 412 U/L versus 3241 ± 446 U/L in wildtype mice, p=0.083, figure 3B). In addition, the formation of necrotic tissue areas 5 days post-I/R was also significantly reduced in *gld*-mice when compared to wildtype mice (9.1 ± 4.3% vs 22.8 ± 3.8%, p=0.035, figure 3C).

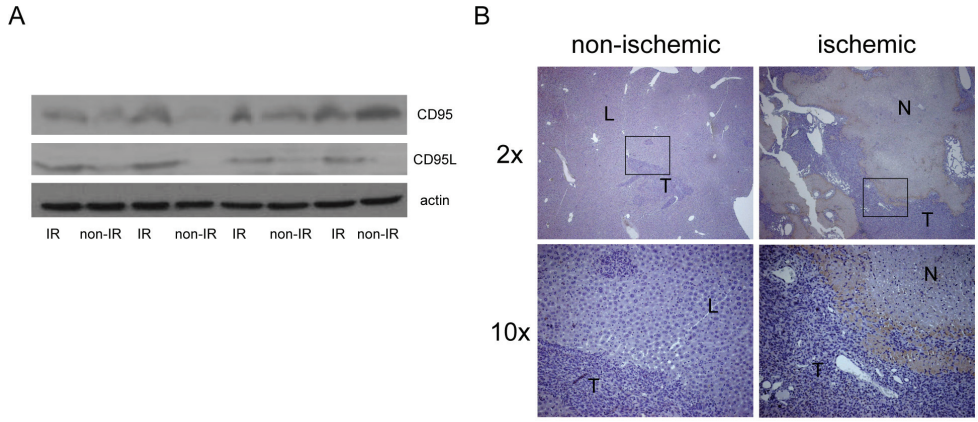

Figure 2 Upregulation of CD95 and CD95L in the clamped liver lobes following I/R
(A) Tissue lysates were prepared from clamped (ischemic)- and unclamped (non-ischemic) liver lobes 36 hours after I/R and were analyzed by Western blotting using specific antibodies directed against CD95 and CD95L. Actin was used as a loading control. **(B)** Immunohistochemichal staining of clamped (ischemic)- and unclamped (non-ischemic) tumor-bearing liver lobes 5 days following I/R, using anti-CD95L antibody. IR ischemic liver lobe; non-IR non-ischemic liver lobe; T tumor; L liver; N necrosis.

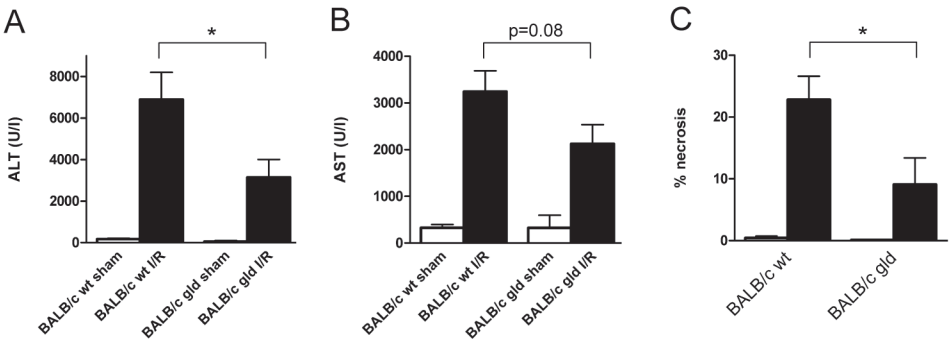

Figure 3 I/R-injury is reduced in gld-mice
Plasma levels of **(A)** alanine aminotransferase (ALT) and **(B)** aspartate aminotransferase (AST) from wildtype (wt) mice and *gld*-mice 6 hours after I/R or sham operation. **(C)** Percentage of liver tissue necrosis in wildtype mice and gld-mice 5 days after I/R. White bars indicate unclamped liver lobe, black bars indicate clamped liver lobe. * $p<0.05$.

CD95 knockdown prevents invasion of perinecrotic metastases following I/R

Since I/R-injury was reduced in *gld*-mice, we investigated whether tumor cell invasion following I/R would also be reduced in these mice. However, micrometastases surrounding the necrotic regions in *gld*-mice still displayed the invasive phenotype that was also observed in wildtype mice (1043 ± 124 µm versus 867 ± 92 µm p=0.29, respectively; figure 4).

Next, we tested whether tumor cell CD95 was essential for the invasive phenotype of perinecrotic metastases. The diameter of perinecrotic metastases in clamped liver lobes was significantly

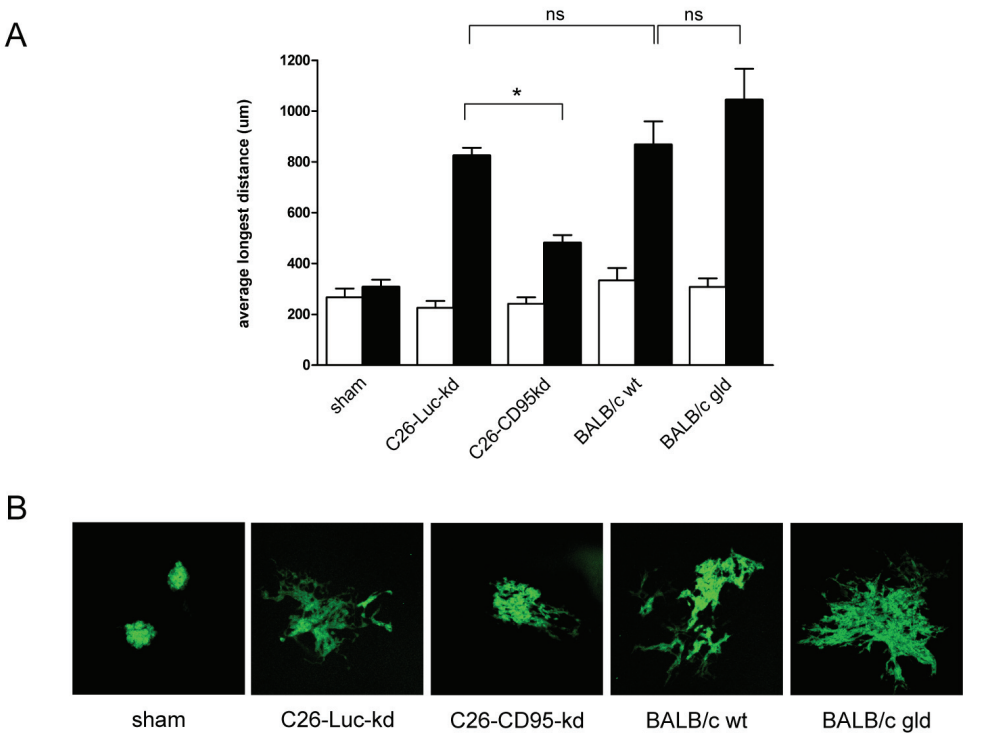

Figure 4 Metastasis invasion following I/R requires autocrine CD95 signaling
I/R was performed in mice carrying C26-Luc-kd or C26-CD95kd metastases. Additionally, EGFP-expressing C26 cells were allowed to form metastases in control mice and in *gld*-mice lacking functional CD95L. **(A)** Metastasis diameters in the unclamped non-ischemic (white bars) and the clamped ischemic liver lobes (black bars) determined 36 hours following I/R, as in Figure 1 (n≥15 metastases). **(B)** Representative confocal microscopic images of metastases located in the clamped liver lobes. kd knock down; * $p<0.05$; ns not significant

reduced from 824 ± 31 µm in mice bearing C26 shRNA-luc control cells to 481 ± 31 µm in mice bearing C26-CD95kd cells (p=0.0003, figure 4).

CD95 signaling is required for accelerated tumor outgrowth following I/R

Following I/R in control mice, increased tumor load (expressed as the hepatic replacement area (HRA)) was observed in the clamped liver lobes compared to unclamped lobes, as expected (Figures 5A and 5C).[5,8] In *gld*-mice, the increased tumor load in the clamped lobes was reduced when compared to that in wildtype mice, although this did not reach statistical significance (26.8 ± 4.9% vs 38.4 ± 6.0% p=0.14, respectively; figures 5A and 5C). However, the acceleration of tumor growth, as expressed by the ratio of HRA values in the clamped versus the non-clamped lobes, was significantly reduced in *gld*-mice (HRA ratio 4.9 ± 1.9 for *gld*-mice versus 8.3 ± 1.4 for control mice, p=0.035; figure 5B).

Next, we tested whether the accelerated tumor growth in clamped liver lobes 5 days following I/R

was reduced when interfering with CD95 signaling in tumor cells (CD95kd cells). The increase in tumor load in clamped liver lobes of mice bearing C26-CD95kd cells was significantly lower when compared to that of mice bearing C26 shRNA-luc control cells (21.1 ± 6.2% versus 34.5 ± 3.2% p=0.049, respectively; figure 5A and 5C). In addition, tumor growth acceleration (HRA ratio) was significantly reduced using CD95kd cells, from 7.8 ± 1.1 for C26 shRNA-luc control cells to 4.7 ± 0.6 for C26-CD95kd cells (p=0.0081, figure 5B).

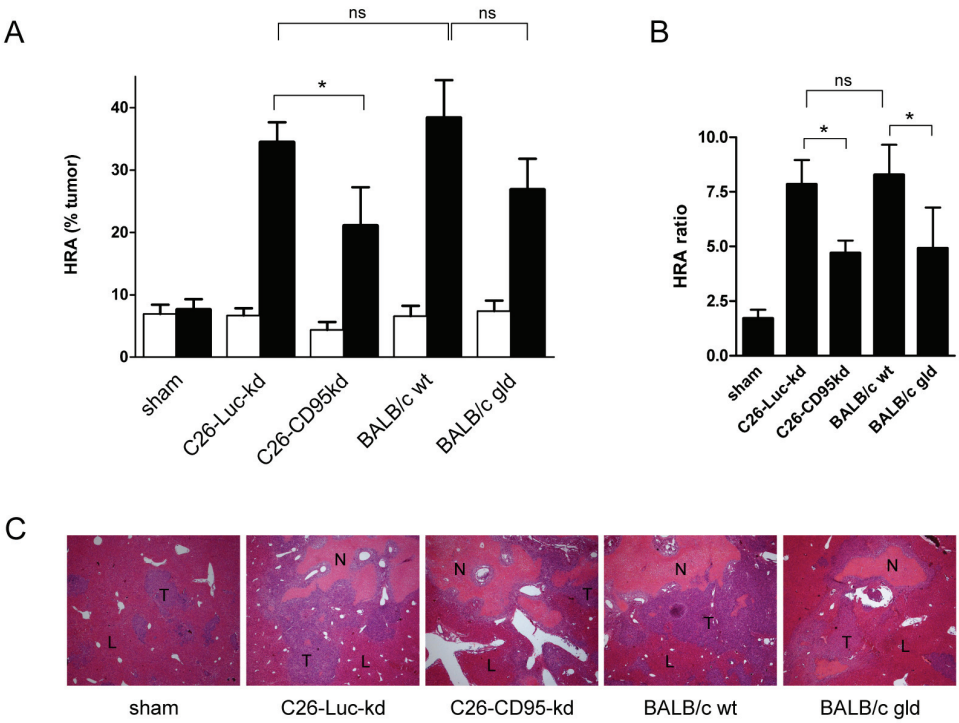

Figure 5 Accelerated outgrowth of liver metastases following I/R is reduced by inhibiting CD95 signaling in tumor cells

I/R was performed on mice carrying C26-Luc-kd or C26-CD95kd metastases. Additionally, I/R was performed on tumor-bearing control mice and on *gld*-mice. All mice were sacrificed 5 days following I/R. **(A)** The livers were harvested and tumor load in unclamped non-ischemic (white bars) and in the clamped ischemic liver lobes (black bars) was analyzed by morphometric measurement of the hepatic replacement areas (HRA). **(B)** HRA ratio values were determined and plotted. These values indicate the acceleration of tumor growth in the clamped ischemic liver lobe relative to the unclamped non-ischemic liver lobe. **(C)** Representative microscopic images of tumor growth in the clamped ischemic liver lobe by H&E histochemistry. wt wildtype; kd knockdown; T tumor; L liver; N necrosis; * $p<0.05$; ns not significant

Discussion

In the present study we have demonstrated that CD95 signaling in tumor cells contributes to I/R-induced invasion and outgrowth of micrometastases. These results are in accordance with our

previous results demonstrating that tumor cell CD95 mediates accelerated invasive outgrowth of liver metastases in the hypoxic transition zone surrounding radiofrequency ablation (RFA)-generated lesions.[12] Likewise, accelerated tumor outgrowth following I/R is exclusively observed in areas of prolonged microcirculatory disturbances and chronic hypoxia.[8]

Tumor growth may be stimulated by CD95/CD95L signaling in several ways. First, CD95 may induce apoptosis in hepatocytes, thereby facilitating tumor cell invasion and outgrowth.[18] Second, CD95 may cause apoptosis of infiltrating cytotoxic lymphocytes, resulting in a reduction of the anti-tumor immune response. This phenomenon is known as the 'tumor counterattack'.[19] Third, CD95 may activate non-apoptotic pro-tumorigenic signaling pathways in tumor cells. Evidence is accumulating that CD95 signaling can promote tumor cell invasion.[20-22] We have recently demonstrated that the *K-Ras* oncogene switches CD95 from a death receptor into an invasion-inducing receptor.[22] Interestingly, *in vitro* hypoxia alone was sufficient to induce CD95-dependent invasion.[12]

In the present study, mice lacking functional CD95L (*gld*-mice) showed reduced I/R injury as demonstrated by reduced post-operative ALT and AST plasma levels and reduced tissue necrosis following I/R. These results are in accordance with those of other investigators[13,14] and suggest that hepatocyte cell death following I/R is partly mediated by CD95. Whether post-I/R hepatocytes die by apoptosis, by necrosis or by an intermediate form of cell death is still a matter of debate.[15,23] In the present study we have referred to the post-IR lesions of cell debris that were identified by histology as 'necrotic'. Nevertheless, the initial type of hepatocyte cell death that caused the formation of these lesions is at least in part apoptotic since it is characterized by the presence of active caspase 3-positive cells[5] and it is partly dependent on CD95L (present study). In contrast,

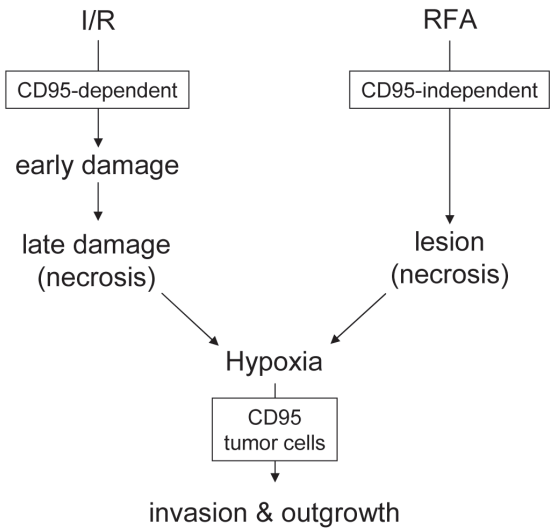

Figure 6 Schematic overview of surgery-induced, CD95-dependent tumor invasion and outgrowth in the liver

CD95 signaling in tumor cells plays a key role in I/R- and RFA-stimulated invasion and outgrowth of micrometastases in the liver. In addition, host CD95L has an indirect effect on outgrowth of micrometastases due to its role in necrosis formation following I/R.

another study showed that I/R-induced liver injury was CD95/CD95L-independent.[16] Possibly, differences in the genetic backgrounds of the mice (C57Bl/6 *versus* BALB/c) may underlie these different dependencies on CD95.

Interestingly, accelerated outgrowth, but not perinecrotic invasion of micrometastases was reduced in *gld*-mice following I/R. Accelerated tumor growth following I/R is exclusively observed in perinecrotic hypoxic tissue areas.[5,8] Since CD95L contributes to I/R injury and necrosis formation, the reduced tumor outgrowth following I/R in *gld*-mice is most likely the result of reduced formation of necrotic tissue, although a direct stimulatory effect of host CD95L on tumor cells cannot be excluded. Nonetheless, the observation that tumor cell invasion in perinecrotic tissue following I/R is similar in *gld*-mice and wildtype mice, but is strongly reduced when using CD95 knockdown tumor cells, strongly suggests that autocrine CD95 signaling in tumor cells mediates this response. This is in line with our previous study showing that autocrine CD95 signaling mediates tumor cell invasion and accelerated outgrowth in hypoxic tissue surrounding RFA-generated lesions.[12] In this study, tumor outgrowth was not affected in the *gld*-mice, most likely because RFA-generated tissue necrosis, unlike that generated by I/R, does not depend on CD95L. Together, these results are in line with a model in which host CD95L contributes to I/R-induced (but not RFA-induced) tissue necrosis and thereby indirectly affects tumor outgrowth. Secondly, autocrine CD95 signaling on tumor cells in hypoxic perinecrotic tissue contributes to the aggressive invasive behaviour of micrometastases in these areas following both surgical procedures (Figure 6).

The mechanisms by which I/R may accelerate the outgrowth of tumour cell deposits are incompletely understood. Nicoud *et al*. showed that vascular clamping was associated with upregulation of matrix-metalloprotease (MMP)-9 and MMP-9 inhibition resulted in reduced tumor outgrowth.[4] MMP-9 is frequently upregulated in colorectal tumor cells and induces invasion of tumor cells by degrading the extracellular matrix.[24,25] Interestingly, CD95 induces MMP-9 expression to mediate invasion of gliomas.[20] Further research should elucidate whether MMP-9 expression following I/R depends on CD95 activation.

Hypoxia is an unavoidable consequence of wound healing and surgery. Here, we demonstrate that hepatic I/R injury due to vascular clamping induces aggressive tumor outgrowth which depends on CD95 signaling in tumor cells. Interestingly, prolonged vascular clamping during liver surgery for colorectal liver metastases was significantly associated with decreased time to hepatic tumor recurrence in patients.[7] In addition, high preoperative levels of circulating CD95L were significantly associated with a reduced period of disease free survival following liver surgery in colorectal cancer patients (FJHH, submitted). Taken together, we propose that CD95 signaling may contribute to hepatic tumor recurrence following surgery for colorectal liver metastases. As such, it may form a potential therapeutic target in these patients.

References

1. Choti MA, Sitzmann JV, Tiburi MF, Sumetchotimetha W, Rangsin R, Schulick RD, Lillemoe KD, Yeo CJ, Cameron JL. Trends in long-term survival following liver resection for hepatic colorectal metastases. Ann Surg 2002; 235: 759-766.
2. de Jong MC, Pulitano C, Ribero D, Strub J, Mentha G, Schulick RD, Choti MA, Aldrighetti L, Capussotti L, Pawlik TM. Rates and patterns of recurrence following curative intent surgery for colorectal liver metastasis: an international multi-institutional analysis of 1669 patients. Ann Surg 2009; 250: 440-448.
3. Simmonds PC, Primrose JN, Colquitt JL, Garden OJ, Poston GJ, Rees M. Surgical resection of hepatic metastases from colorectal cancer: a systematic review of published studies. Br J Cancer 2006; 94: 982-999.
4. Nicoud IB, Jones CM, Pierce JM, Earl TM, Matrisian LM, Chari RS, Gorden DL. Warm Hepatic Ischemia-Reperfusion Promotes Growth of Colorectal Carcinoma Micrometastases in Mouse Liver via Matrix Metalloproteinase-9 Induction. Cancer Res 2007; 67: 2720-2728.
5. van der Bilt JD, Kranenburg O, Nijkamp MW, Smakman N, Veenendaal LM, Te Velde EA, Voest EE, van Diest PJ, Borel Rinkes IH. Ischemia/reperfusion accelerates the outgrowth of hepatic micrometastases in a highly standardized murine model. Hepatology 2005; 42: 165-175.
6. Man K, Ng KT, Lo CM, Ho JW, Sun BS, Sun CK, Lee TK, Poon RT, Fan ST. Ischemia-reperfusion of small liver remnant promotes liver tumor growth and metastases--activation of cell invasion and migration pathways. Liver Transpl 2007; 13: 1669-1677.
7. Nijkamp MW, van der Bilt JD, Snoeren N, Hoogwater FJ, van Houdt WJ, Molenaar IQ, Kranenburg O, van Hillegersberg R., Borel Rinkes IH. Prolonged portal triad clamping during liver surgery for colorectal liver metastases is associated with decreased time to hepatic tumour recurrence. Eur J Surg Oncol 2009; 36: 182-188.
8. van der Bilt JD, Soeters ME, Duyverman AM, Nijkamp MW, Witteveen PO, van Diest PJ, Kranenburg O, Borel Rinkes IH. Perinecrotic hypoxia contributes to ischemia/reperfusion-accelerated outgrowth of colorectal micrometastases. Am J Pathol 2007; 170: 1379-1388.
9. Harris AL. Hypoxia--a key regulatory factor in tumour growth. Nat Rev Cancer 2002; 2: 38-47.
10. Semenza GL. Targeting HIF-1 for cancer therapy. Nat Rev Cancer 2003; 3: 721-732.
11. Pouyssegur J, Dayan F, Mazure NM. Hypoxia signalling in cancer and approaches to enforce tumour regression. Nature 2006; 441: 437-443.
12. Nijkamp MW, Hoogwater FJ, Steller EJ, Westendorp BF, van der Meulen TA, Leenders MW, Borel Rinkes IH, Kranenburg O. CD95 is a key mediator of invasion and accelerated outgrowth of mouse colorectal liver metastases following radiofrequency ablation. J Hepatol 2010; in press.
13. Cursio R, Filippa N, Miele C, Colosetti P, Auberger P, Van OE, Gugenheim J. Fas ligand expression following normothermic liver ischemia-reperfusion. J Surg Res 2005; 125: 30-36.
14. Nakajima H, Mizuta N, Fujiwara I, Sakaguchi K, Ogata H, Magae J, Yagita H, Koji T. Blockade of the Fas/Fas ligand interaction suppresses hepatocyte apoptosis in ischemia-reperfusion rat liver. Apoptosis 2008; 13: 1013-1021.
15. Malhi H, Gores GJ, Lemasters JJ. Apoptosis and necrosis in the liver: a tale of two deaths? Hepatology 2006; 43: S31-S44.
16. Rudiger HA and Clavien PA. Tumor necrosis factor alpha, but not Fas, mediates hepatocellular apoptosis in the murine ischemic liver. Gastroenterology 2002; 122: 202-210.
17. Nijkamp MW, van der Bilt JD, de Bruijn MT, Molenaar IQ, Voest EE, van Diest PJ, Kranenburg O, Borel Rinkes IH. Accelerated perinecrotic outgrowth of colorectal liver metastases following radiofrequency ablation is a hypoxia-driven phenomenon. Ann Surg 2009; 249: 814-823.
18. Yoong KF, Afford SC, Randhawa S, Hubscher SG, Adams DH. Fas/Fas ligand interaction in human colorectal hepatic metastases: A mechanism of hepatocyte destruction to facilitate local tumor invasion. Am J Pathol

1999; 154: 693-703.
19. O'Connell J, O'Sullivan GC, Collins JK, Shanahan F. The Fas counterattack: Fas-mediated T cell killing by colon cancer cells expressing Fas ligand. J Exp Med 1996; 184: 1075-1082.
20. Kleber S, Sancho-Martinez I, Wiestler B, Beisel A, Gieffers C, Hill O, Thiemann M, Mueller W, Sykora J, Kuhn A, Schreglmann N, Letellier E, Zuliani C, Klussmann S, Teodorczyk M, Grone HJ, Ganten TM, Sultmann H, Tuttenberg J, von DA, Regnier-Vigouroux A, Herold-Mende C, Martin-Villalba A. Yes and PI3K bind CD95 to signal invasion of glioblastoma. Cancer Cell 2008; 13: 235-248.
21. Barnhart BC, Legembre P, Pietras E, Bubici C, Franzoso G, Peter ME. CD95 ligand induces motility and invasiveness of apoptosis-resistant tumor cells. EMBO J 2004; 23: 3175-3185.
22. Hoogwater FJ, Nijkamp MW, Smakman N, Steller EJ, Emmink BL, BF Westendorp, Raats DA, Sprick MR, Schaeffer U, van Houdt WJ, de Bruijn MT, Schackmann RC, Derksen PW, Medema JP, Walczak H, Borel Rinkes IH, Kranenburg O. Oncogenic K-Ras Turns Death Receptors Into Metastasis-Promoting Receptors in Human and Mouse Colorectal Cancer Cells. Gastroenterology 2010; 137: 2357-2367.
23. Massip-Salcedo M, Rosello-Catafau J, Prieto J, Avila MA, Peralta C. The response of the hepatocyte to ischemia. Liver Int 2007; 27: 6-16.
24. Waas ET, Wobbes T, Lomme RM, DeGroot J, Ruers T, Hendriks T. Matrix metalloproteinase 2 and 9 activity in patients with colorectal cancer liver metastasis. Br J Surg 2003; 90: 1556-1564.
25. Zucker S and Vacirca J. Role of matrix metalloproteinases (MMPs) in colorectal cancer. Cancer Metastasis Rev 2004; 23: 101-117.

Chapter 7

Prolonged portal triad clamping during liver surgery for colorectal liver metastases is associated with reduced time to hepatic tumor recurrence

European Journal of Surgical Oncology 2010; 36: 182-188

Maarten W. Nijkamp
Jarmila D.W. van der Bilt
Nikol Snoeren
Frederik J.H. Hoogwater
Winan J. van Houdt
I. Quintus Molenaar
Onno Kranenburg
Richard van Hillegersberg
Inne H.M. Borel Rinkes

Department of Surgery
University Medical Center Utrecht, Utrecht, The Netherlands

Abstract

Background
During liver surgery, portal triad clamping is frequently applied to minimize blood loss, but causes liver ischemia/reperfusion (I/R) injury. Recently, it was shown that I/R accelerates the outgrowth of pre-established micrometastases in a murine model. The aim of this study was to evaluate the oncological outcome of portal triad clamping during hepatectomy in colorectal cancer patients.

Methods
160 patients with colorectal liver metastases underwent a partial hepatectomy with curative intent. Data were collected in a prospective database and were retrospectively analyzed for time to liver recurrence (TTLiR) and time to overall recurrence (TTR). The prognostic significance of portal triad clamping of any type and severe ischemia due to prolonged portal triad clamping was determined by Cox regression models.

Results
TTLiR was reduced after clamping of any type, although not statistically significant (p=0.061). Severe ischemia due to prolonged portal triad clamping significantly decreased TTLiR (p=0.022), but not TTR. Furthermore, severe ischemia independently predicted TTLiR in a multivariable analysis (p= 0.038).

Conclusions
Severe ischemia due to prolonged portal triad clamping during hepatic resection for colorectal liver metastases appears to be associated with decreased TTLiR. Further research remains necessary to determine the causative effect of prolonged vascular clamping on liver tumor recurrence.

Introduction

Surgical resection is the most effective treatment for patients with colorectal liver metastases, offering 5-year and 10-year survival rates between 36-58% and 23-26%, respectively.[1-4] However, even after an apparently complete resection, approximately 50% of patients ultimately present with recurrent disease, usually within the first year following resection.[1,3] The most likely source for recurrences are microscopic tumor residues that are undetectable at the time of surgery.[5,6] Furthermore, recurrence may also develop from circulating tumor cells that are shed into the circulation during surgery.[7,8] In the past decades, many prognostic factors of recurrence and survival after hepatectomy for metastatic colorectal cancer have been documented, including both preoperative[9,10] and peri-operative variables.[11-14]

Temporary clamping of the vascular inflow of the liver is frequently applied in liver surgery. It is predominantly used to reduce peri-operative blood loss during hepatic resections.[15] A major disadvantage of vascular inflow occlusion is that it causes ischemia/reperfusion injury (I/R) to the liver, which may lead to postoperative liver dysfunction. The adverse effects of I/R on hepatocellular damage and liver function have been well documented.[16] Nonetheless, Rahbari *et al*. showed recently in a meta-analysis that portal triad clamping had no effect on postoperative overall morbidity and mortality when compared to no portal triad clamping.[17] However, nothing is known about the effects of vascular clamping during liver surgery on long-term oncological outcome. We have recently shown in a murine model of partial hepatic I/R by temporary blood flow occlusion that the outgrowth of pre-existing colorectal micrometastases in occluded liver lobes was accelerated five- to six-fold compared to non-occluded lobes.[18] Based on these results, portal triad clamping during partial hepatectomy may adversely affect oncological outcome in colorectal cancer patients by accelerating the outgrowth of pre-existent hepatic micrometastases.

The aim of the present study was therefore to evaluate the prognostic significance of portal triad clamping and of severe ischemia due to prolonged clamping, on long-term oncological outcome in patients after partial hepatectomy for colorectal liver metastases.

Methods and Patients

Patients and surgical management

All consecutive patients who underwent a partial hepatectomy for colorectal liver metastases with curative intent (1998-2008) at the University Medical Center Utrecht in The Netherlands were selected from a prospectively collected liver database. Selection criteria for entering the study were: no signs of extrahepatic disease on preoperative imaging by routine liver contrast-enhanced four phase CT and thoraco-abdominal spiral CT scan, no untreatable lesions as determined by intraoperative ultrasonography, no gross residual disease (R2) at laparotomy and no simultaneous focal heat destruction by radiofrequency ablation, laser induced thermotherapy or any other local ablative treatment. In addition, patients who had died within 30 days after the hepatic resection were excluded from further analysis. Following these selection criteria, 160 patients were identified from the database and were further analysed.

Three expert hepatic surgeons performed the operations. Portal triad clamping was used consistently by the hepatic surgeons, without specific preoperative indications. As in many other institutions, portal

triad clamping was applied only when the surgeons expected, during surgery, that the peri-operative blood loss would exceed 1000 ml in total. When portal triad clamping was applied, intermittent clamping of maximally 15 minutes per cycle was preferred. Blood loss was minimized by maintaining central venous pressure below 5 cm H_2O.

Prognostic factors

Patient and operation characteristics were prospectively collected. Besides clamping type and duration, various factors were extracted from the database for each patient, including age at the time of liver resection, gender, location of the primary tumor, nodal status of the primary tumor, disease free interval between resection of the primary tumor and detection of the liver metastases and synchronicity of metastases, the number, maximal size and distribution of the hepatic metastases, preoperative carcinoembryonic antigen (CEA), duration of operation, usage of (neo)adjuvant chemotherapy, extent (major defined as 3 segments or more) and type of the resection (anatomical or non-anatomical), aspect of liver parenchyma, resection margins, blood loss and the amount of packed red blood cells transfused.

First, we analyzed the influence of clamping of any type compared to no vascular clamping on outcome. Second, patients were classified according to severity of ischemia during hepatectomy. The first group consisted of patients who had no vascular clamping during liver surgery. The second group of patients had minor ischemia during hepatectomy. This was defined as portal triad clamping for 20 minutes continuously or intermittent clamping of not more than 3 cycles of maximally 15 minutes ischemia time each. The third group, i.e. the severe ischemia group, consisted of patients in whom clamping times exceeded those mentioned for the minor ischemia group. The cut-off points regarding clamping times are based on preclinical observations.[18,19]

Follow-up

Routine follow-up included at least liver contrast-enhanced four phase CT-scan of the liver, chest X-ray and CEA levels every 6 months, which were prospectively collected in the database. Follow-up data were updated by letters and telephone calls to referring physicians and general practitioners. The duration of the follow-up and the time between hepatectomy and the detection of recurrence were obtained, as well as the site of recurrence and survival data. The end-points of this analysis were the time to develop liver recurrence (TTLiR) and the time to develop recurrence in general (TTR). The influence on overall survival was also determined.

Statistical analysis

Kaplan-Meier survival curves were compared by log rank test statistics. Comparison between groups for the different variables was performed by ANOVA, Kruskal-Wallis test or Pearson Chi-square test when appropriate. Hazard ratios (HR) of decreased TTLiR, decreased TTR and overall survival were computed for all variables to estimate relative risks and 95% confidence intervals using Cox proportional hazards regression analysis. Multivariable analysis was performed to determine the independent prognostic impact of severity of ischemia on TTLiR, TTR and overall survival while adjusting for possible confounders simultaneously. Therefore, covariables that significantly affected outcome by univariable analysis entered into a multivariable regression analysis. A 95% confidence interval or $p<0.050$ was considered significant. All statistical analyses were performed using SPSS® for Windows® version 15.0 (SPSS, Chicago, Illinois, USA).

Results

Patient characteristics

During the study period, 160 patients who underwent a partial hepatectomy for colorectal liver metastases with curative intent were identified from the liver database. Twenty patients with initially non-resectable metastases were down-staged by neo-adjuvant chemotherapy. Three patients had preoperative portal vein embolisation to allow regeneration of the future remnant liver. Two patients had a two-staged resection (because of excessive intraoperative blood loss or R2 resection) and were evaluated for recurrence and survival from the second operation.

Table 1. Base-line characteristics of patients according to the severity of ischemia

Variable	No ischemia (n=72)	Minor ischemia (n=38)	Severe ischemia (n=50)	P-value
Age (years)				
Median (range)	64.5 (32.7-81.9)	59.7 (40.4-78.7)	62.5 (33.0-75.5)	0.173*
< 63[a]	30	22	26	
≥ 63	42	16	24	0.121#
Gender				
Female	22	13	20	
Male	50	25	30	0.558#
Location of primary				
Colon	44	24	32	
Rectum	28	14	18	0.944#
Nodal status of primary				
Negative	33	19	18	
Positive	39	19	32	0.294#
Disease free interval (months)				
Median (range)	9.0 (0.0-109.0)	9.0 (0.0-76.0)	8.5 (0-81.0)	0.784†
≥ 12	28	14	20	
< 12	44	24	30	0.955#
Preoperative CEA (ng/mL)[b]				
Median (range)	14.0 (0.8-1992.0)	6.9 (0.5-500.0)	6.4 (1.2-235.0)	0.647†
< 200	47	26	37	
≥ 200	5	5	5	0.804#
Tumour number				
Solitary	38	22	23	
Multiple	34	16	27	0.531#
Maximum tumour size (cm)				
Median (range)	4.0 (0.4-18.0)	3.7 (0.8-16.0)	3.8 (1.3-19.5)	0.938†
< 3.0	26	13	18	
3.0-5.0	24	13	19	
≥ 5.0	22	12	13	0.972#
Tumour distribution				
Unilobar	48	26	29	

Table 1. *continued*

Variable	No ischemia (n=72)	Minor ischemia (n=38)	Severe ischemia (n=50)	P-value
Bilobar	24	12	21	0.182#
Duration of operation (min)				
Median (range)	226 (75-390)	245 (80-534)	235 (100-465)	0.209*
Extent of resection				
Minor (< 3 segments)	27	14	19	
Major (≥ 3 segments)	45	24	31	0.994#
Type of resection				
Anatomical	40	23	30	
Non-anatomical	32	15	20	0.836#
Blood loss (ml)				
Median (range)	950 (40-7500)	1100 (100-11000)	930 (100-10600)	0.518†
< 1000	38	19	28	
≥ 1000	34	19	22	0.853#
Red blood cell transfusion				
No	32	21	25	
Yes	40	17	25	0.546#
≤ 2 units	50	24	38	
> 2 units	22	14	12	0.474#
Liver parenchyma				
Normal	48	22	29	
Abnormal	24	16	21	0.529#
Resection margin				
R0	63	34	45	
R1	9	4	5	0.900#
Chemotherapy				
None	59	26	36	
Neoadjuvant	7	6	7	
Adjuvant	6	6	8	0.458#

[a]Median age of the whole population was used as a cut-off point; [b]Pre-operative carcinoembryonic antigen (CEA) 20 missing values in no ischemia group, 7 missing values in minor ischemia group and 8 missing values in severe ischemia group; *Oneway ANOVA; #Pearson Chi square test; †Kruskal-Wallis test.

Vascular clamping was used in 88 patients. All patients had an inflow occlusion (Pringle Maneuver). Inflow occlusion was performed continuously in 53 patients and intermittently in 35 patients. Ischemic preconditioning was not performed. Median total ischemia time was 21 (range 2 - 69) minutes for continuous clamping and 40 (range 20-90) minutes for intermittent clamping. The "minor ischemia" group was formed by 38 patients. The remaining 50 patients comprised the "severe ischemia" group.

As the indication for vascular clamping is influenced by several factors, the ischemia groups were compared concerning their baseline values. No significant differences concerning the (baseline) prognostic factors were observed between the ischemia groups, including factors influencing the choice for vascular clamping, such as blood loss, extent and type of resection (Table 1).

Long-term outcome

Median follow-up was 2.5 years. Altogether, 112 patients had a recurrence within the study period, of whom 66 had a liver recurrence. Median TTR was 1.3 years, with 38.3% and 23.3% of patients being disease free after 2 and 5 years, respectively. Seven patients underwent repeat hepatectomy for liver recurrence, 10 patients underwent local ablation of hepatic recurrent disease and 4 had lung resection for pulmonary metastases. Adjuvant chemotherapy was given to 20 patients after hepatic resection. 91 patients died during follow-up. Overall 5- and 10-year survival was 36.5% and 22.3 %, respectively.

Effect of vascular clamping and severe ischemia on patterns of recurrence and survival

Decreased time to liver recurrence was observed in patients subjected to vascular clamping of any type (p=0.061, figure 1A). Vascular clamping of any type did not affect TTR or overall survival (data not shown). In patients with severe ischemia, TTLiR was significantly shorter when compared to patients undergoing no clamping (p=0.022, figure 1B). In the minor ischemia group, TTLiR was not significantly different when compared to both other groups. TTR and overall survival were not affected by either minor or severe liver ischemia (Figure 1C and data not shown, respectively).

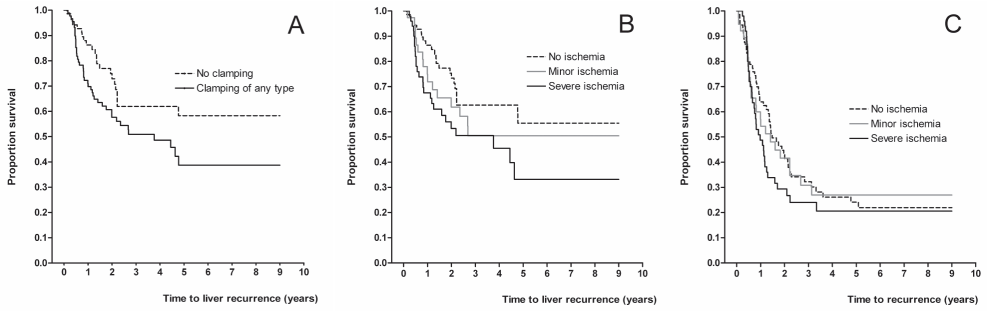

Figure 1 Kaplan-Meier curves illustrating the effects of any type of clamping on liver free survival (**A**, p=0.061, log rank test), the effect of severe ischemia on liver free survival (**B**, p=0.022, log rank test) and disease free survival (**C**, p=0.173, log rank test). Severe ischemia is compared to no ischemia.

Severe ischemia is an independent predictor of tumor recurrence in the liver

To evaluate the effect of severe ischemia on tumor recurrence, patients who had severe ischemia due to prolonged vascular clamping were compared to patients who had no clamping at all during hepatectomy. Univariable analysis among all variables examined revealed that synchronous disease, bilobar tumor distribution, positive resection margin and severe ischemia were inversely correlated to TTLiR (Table 2). TTR was inversely correlated to positive lymph nodes of the primary tumor, synchronous disease, the use of neoadjuvant chemotherapy and type of resection. Overall survival was inversely affected by disease free interval between primary tumor and hepatic metastases of less than 12 months and a preoperative CEA value ≥ 200ng/mL. None of the other prognostic variables examined were correlated to TTLiR, TTR or overall survival (Table 2).

Subsequent analysis using multivariable regression analysis revealed that positive resection margin and severe ischemia were independent predictors for decreased TTLiR (p=0.040 and p=0.038

Table 2. Univariable analysis for liver recurrence, overall recurrence and overall survival in patients with no ischemia or severe ischemia

Variable	#	Hazard Ratio (95% confidence interval)		
		Liver recurrence	Overall recurrence	Overall survival
Age (years)				
< 64[a]	61			
≥ 64	61	0.63 (0.35-1.13)	0.94 (0.62-1.44)	1.44 (0.90-2.30)
Gender				
Female	42			
Male	80	1.17 (0.63-2.17)	1.13 (0.72-1.78)	0.95 (0.57-1.58)
Location				
Colon	76			
Rectal	46	0.88 (0.50-1.59)	0.73 (0.47-1.14)	0.91 (0.56-1.47)
N-stadium				
Negative	51			
Positive	71	1.76 (0.97-3.17)	**1.81 (1.16-2.82) ***	1.48 (0.91-2.40)
Disease free interval (m)				
≥ 12	48			
< 12	74	1.67 (0.92-3.04)	1.53 (0.98-2.38)	**1.81 (1.09-3.01) ***
Metachronous	53			
Synchronous	69	**2.03 (1.12-3.68) ***	**1.67 (1.14-2.45) ***	1.42 (0.93-2.18)
Preoperative CEA (ng/mL)[b]				
< 200	84			
≥ 200	10	0.97 (0.90-1.05)	1.02 (0.97-1.08)	**1.06 (1.00-1.12) ***
Number				
Solitary	77			
Multiple	45	1.50 (0.85-2.66)	1.11 (0.73-1.70)	1.00 (0.63-1.60)
Maximum size (cm)				
≥ 3.0	78	0.81 (0.46-1.44)	0.96 (0.62-1.50)	1.08 (0.66-1.77)
≥ 5.0	25	1.03 (0.53-1.97)	1.23 (0.77-1.97)	1.62 (0.98-2.69)
Distribution				
Unilobar	77			
Bilobar	45	**1.91 (1.09-3.34) ***	1.33 (0.87-2.05)	0.96 (0.59-1.55)
Chemotherapy[c,d]				
None	95			
Neoadjuvant	14	1.92 (0.99-3.71)	**2.34 (1.25-4.37) ***	1.89 (0.97-3.79)
Duration of operation (min)				
< 231[e]	61			
≥ 231	61	1.25 (0.71-2.18)	1.13 (0.74-1.73)	0.96 (0.60-1.54)
Extent				
Minor (< 3 segments)	46			
Major (≥ 3 segments)	76	1.56 (0.85-2.86)	1.16 (0.75-1.80)	1.31 (0.79-2.15)
Type				
Anatomical	70			
Non-anatomical	52	1.26 (0.72-2.20)	**1.53 (1.00-2.34) ***	0.99 (0.62-1.58)
Blood loss (ml)				
< 1000	66			
≥ 1000	56	1.36 (0.77-2.39)	0.93 (0.61-1.43)	1.31 (0.82-2.11)

Table 2. *continued*

Variable	#	Hazard Ratio (95% confidence interval)		
		Liver recurrence	**Overall recurrence**	**Overall survival**
Red blood cell transfusion				
No	57			
Yes	65	0.99 (0.56-1.73)	0.83 (0.54-1.28)	1.34 (0.82-2.19)
< 2 units	88			
≥ 2 units	34	1.07 (0.61-1.87)	0.81 (0.53-1.24)	1.31 (0.81-2.12)
Liver parenchyma				
Normal	77			
Abnormal	45	0.96 (0.53-1.73)	0.97 (0.63-1.51)	0.82 (0.50-1.33)
Resection margin				
R0	108			
R1	14	**1.94 (1.00-3.96) ***	1.79 (0.97-3.30)	1.85 (0.92-3.74)
Vascular clamping				
No ischemia	72			
Severe ischemia	50	**1.38 (1.04-1.83) ***	1.16 (0.94-1.44)	0.99 (0.78-1.27)

*significant prognostic factor in univariable regression model ($p<0.05$). [a]Median age was used as a cut-off point; [b]CEA 28 (23%) missing values; [c] 14 patients received adjuvant chemotherapy; [d] 1 patient received both neoadjuvant and adjuvant chemotherapy; [e]Median operating time was used as a cut-off point.

Table 3. Multivariable analysis for liver recurrence, overall recurrence and overall survival

	Liver recurrence		**Overall recurrence**		**Overall survival**	
Variable	HR (95% CI)	P-value	HR (95% CI)	P-value	HR (95% CI)	P-value
Positive nodal status primary	-	-	**1.84 (1.11-3.05)**	**0.011**	-	-
Disease free interval < 12 months	-	-	-	-	**1.70 (1.01-2.84)**	**0.045**
Synchronous disease	1.83 (0.99-3.38)	0.053	1.36 (0.85-2.17)	0.202	-	-
Preoperative CEA ≥ 200 ng/mL	-	-	-	-	1.05 (0.98-1.11)	0.117
Bilobar distribution	1.72 (0.93-3.16)	0.084	-	-	-	-
Neoadjuvant chemotherapy	-	-	1.63 (0.85-3.15)	0.144	-	-
Resection type	-	-	1.25 (0.94-1.74)	0.182	-	-
Positive margin	**2.25 (1.04-4.86)**	**0.040**	-	-	-	-
Severe ischemia	**1.37 (1.02-1.85)**	**0.038**	-	-	-	-

respectively (Table 3). In addition, positive lymph nodes of the primary tumor independently predicted decreased TTR (p=0.017). Finally, overall survival was independently predicted by a disease free interval between primary tumor and hepatic metastases of less than 12 months (p=0.045).

Discussion

In the past decades, many prognostic factors of (hepatic) recurrence and survival after hepatectomy for metastatic colorectal cancer have been documented.[9,11,20] Although the majority of these studies focused on preoperative criteria for selecting patients with liver metastases that may benefit from surgery, several studies hypothesized a correlation between accelerated tumor recurrence and peri-operative factors, including hypotension[14], blood transfusion[12], portal vein embolisation[21] and morbidity.[13,22] Surprisingly, very little is known about the effects of vascular occlusion on tumor recurrence and survival. Vascular clamping methods have been traditionally analyzed as a predictor of postoperative morbidity and mortality. Recently, Rahbari *et al*. showed in a meta-analysis that portal triad clamping had no effect on postoperative overall morbidity and mortality when compared to no portal triad clamping.[17] However, the studies analyzed did not provide any data on long-term (oncological) outcome. Recently, Wong *et al*. reported that time to recurrence and overall survival in patients who received a hepatectomy with or without intermittent clamping of the portal triad were not significantly different.[23] However, time to *liver* recurrence was not addressed by Wong *et al*., which was the focus of the present study.

A significantly shorter time to liver recurrence was observed in colorectal cancer patients who had been subjected to prolonged periods of portal triad clamping, which appeared to be irrespective of the clamping method used. This is in accordance with our preclinical results, showing that vascular clamping induces a five- to six-fold growth acceleration of pre-established colorectal micrometastases.[18] Furthermore, comparable results were demonstrated by Ito *et al*., showing that prolonged ischemia time during liver resection for colorectal liver metastases was associated with reduced progression free survival.[24]

A disadvantage of the present study is its retrospective nature. As a consequence, one can not entirely exclude the possibility of indication bias. However, as in many other institutions, portal triad clamping was used without specific preoperative indications and applied only when the surgeons expected, during surgery, that the peri-operative blood loss would exceed 1000 ml in total. *No* differences between the groups were observed in extent and type of the resection, in tumor characteristics, blood loss or red blood cell transfusion (see Table 1). This suggests that the groups may be considered similar concerning the base-line characteristics. As such, the present study enhances our hypothesis that severe hepatic ischemia provides a local tumor growth stimulatory micro-environment.

Nonetheless, a retrospective study is not designed to provide data on the mechanisms for this phenomenon; therefore we can only conclude that the severe ischemia during liver surgery is associated with a shorter time to hepatic recurrence, rather than a causative mechanism. A large randomized controlled trial would be necessary to determine the causative effect of prolonged vascular clamping on liver tumor recurrence. However, in most hospitals, vascular clamping is not a standard procedure, but is only applied in case of (impending) excessive blood loss. Randomization between clamping and no clamping would therefore imply that some patients would unnecessarily

be subjected to a procedure which is potentially harmful and on the other hand some patients with accelerating blood loss would be withheld from a maneuver which may be needed to perform a safe resection. A randomized controlled trial on clamping versus no clamping could therefore be considered unethical. Since the data presented here is the only data available until now, it may be advisable to keep the ischemia times as short as possible, whenever clamping during liver surgery is warranted.

Since inhibition of hypoxia following I/R resulted in decreased tumor acceleration in a preclinical mouse model[25], liver *ischemia* was used as a predicting variable, rather than clamping type (continuous versus intermittent) or clamping duration. The cut-off points between minor and severe ischemia were based on preclinical findings. Concerning continuous clamping, clamping for 30 minutes or 45 mintues resulted in accelerated outgrowth of micrometastases in a murine model, while ischemia up to 20 minutes did not show any difference in tumor growth acceleration.[19] Furthermore, when the 45 minutes of clamping was performed intermittently by three cycles of 15 minutes, no growth acceleration of the micrometastases was observed as well. Therefore, patients undergoing continuous clamping up to 20 minutes or intermittent clamping for not more than 3 cycles of maximally 15 minutes ischemia time each were designated as patients with minor ischemia.

With the introduction of approaches that reduce blood loss during hepatic resection, such as the maintenance of low venous pressure[26], precoagulation devices[27,28] and hemostatic biologicals[29], portal triad clamping can be avoided more frequently.[30] However, when vascular control is needed in case of excessive hemorrhage, intermittent clamping is preferred and total clamping times should be kept to a minimum. When ischemia times are inevitably long, future strategies that counteract the adverse effects of surgery-induced I/R on tumor growth may include drugs that improve post-operative hypoxia, post-ischemic microcirculation, anti-angiogenic therapies or anti-inflammatory agents. Adjuvant chemotherapy destructing possible residual tumor deposits combined with strategies that protect against accelerated tumor growth may hopefully result in further improvement in long term outcome.

In conclusion, both in pre-clinical mouse models and in this series of colorectal cancer patients, severe liver ischemia due to prolonged vascular clamping during liver resection for colorectal liver metastases *appears to be associated* with decreased time to liver recurrence. In case of inevitable clamping, total ischemia time should be kept to a minimum. In light of the study characteristics, further research remains necessary to determine the causative effect of prolonged vascular clamping on liver tumor recurrence. Meanwhile, it may be advisable to keep total ischemia times as short as possible whenever vascular inflow occlusion is warranted.

References

1. Abdalla EK, Vauthey JN, Ellis LM, Ellis V, Pollock R, Broglio KR, Hess K, Curley SA. Recurrence and outcomes following hepatic resection, radiofrequency ablation, and combined resection/ablation for colorectal liver metastases. Ann Surg 2004; 239: 818-825.
2. Choti MA, Sitzmann JV, Tiburi MF, Sumetchotimetha W, Rangsin R, Schulick RD, Lillemoe KD, Yeo CJ, Cameron JL. Trends in long-term survival following liver resection for hepatic colorectal metastases. Ann Surg 2002; 235: 759-766.
3. Pawlik TM, Scoggins CR, Zorzi D, Abdalla EK, Andres A, Eng C, Curley SA, Loyer EM, Muratore A, Mentha G, Capussotti L, Vauthey JN. Effect of surgical margin status on survival and site of recurrence after hepatic resection for colorectal metastases. Ann Surg 2005; 241: 715-722.
4. Rees M, Tekkis PP, Welsh FK, O'Rourke T, John TG. Evaluation of long-term survival after hepatic resection for metastatic colorectal cancer: a multifactorial model of 929 patients. Ann Surg 2008; 247: 125-135.
5. Linnemann U, Schimanski CC, Gebhardt C, Berger MR. Prognostic value of disseminated colorectal tumor cells in the liver: results of follow-up examinations. Int J Colorectal Dis 2004; 19: 380-386.
6. Yokoyama N, Shirai Y, Ajioka Y, Nagakura S, Suda T, Hatakeyama K. Immunohistochemically detected hepatic micrometastases predict a high risk of intrahepatic recurrence after resection of colorectal carcinoma liver metastases. Cancer 2002; 94: 1642-1647.
7. Koch M, Kienle P, Hinz U, Antolovic D, Schmidt J, Herfarth C, von Knebel DM, Weitz J. Detection of hematogenous tumor cell dissemination predicts tumor relapse in patients undergoing surgical resection of colorectal liver metastases. Ann Surg 2005; 241: 199-205.
8. Vlems FA, Diepstra JH, Punt CJ, Ligtenberg MJ, Cornelissen IM, van Krieken JH, Wobbes T, van Muijen GN, Ruers TJ. Detection of disseminated tumour cells in blood and bone marrow samples of patients undergoing hepatic resection for metastasis of colorectal cancer. Br J Surg 2003; 90: 989-995.
9. Fong Y, Fortner J, Sun RL, Brennan MF, Blumgart LH. Clinical score for predicting recurrence after hepatic resection for metastatic colorectal cancer: analysis of 1001 consecutive cases. Ann Surg 1999; 230: 309-318.
10. Nagashima I, Takada T, Matsuda K, Adachi M, Nagawa H, Muto T, Okinaga K. A new scoring system to classify patients with colorectal liver metastases: proposal of criteria to select candidates for hepatic resection. J Hepatobiliary Pancreat Surg 2004; 11: 79-83.
11. Figueras J, Burdio F, Ramos E, Torras J, Llado L, Lopez-Ben S, Codina-Barreras A, Mojal S. Effect of subcentimeter nonpositive resection margin on hepatic recurrence in patients undergoing hepatectomy for colorectal liver metastases. Evidences from 663 liver resections. Ann Oncol 2007; 18: 1190-1195.
12. Kooby DA, Stockman J, Ben-Porat L, Gonen M, Jarnagin WR, Dematteo RP, Tuorto S, Wuest D, Blumgart LH, Fong Y. Influence of transfusions on perioperative and long-term outcome in patients following hepatic resection for colorectal metastases. Ann Surg 2003; 237: 860-869.
13. Laurent C, Sa CA, Couderc P, Rullier E, Saric J. Influence of postoperative morbidity on long-term survival following liver resection for colorectal metastases. Br J Surg 2003; 90: 1131-1136.
14. Younes RN, Rogatko A, Brennan MF. The influence of intraoperative hypotension and perioperative blood transfusion on disease-free survival in patients with complete resection of colorectal liver metastases. Ann Surg 1991; 214: 107-113.
15. Smyrniotis V, Farantos C, Kostopanagiotou G, Arkadopoulos N. Vascular control during hepatectomy: review of methods and results. World J Surg 2005; 29: 1384-1396.
16. Jaeschke H. Molecular mechanisms of hepatic ischemia-reperfusion injury and preconditioning. Am J Physiol Gastrointest Liver Physiol 2003; 284: G15-G26.
17. Rahbari NN, Wente MN, Schemmer P, Diener MK, Hoffmann K, Motschall E, Schmidt J, Weitz J, Buchler MW. Systematic review and meta-analysis of the effect of portal triad clamping on outcome after hepatic resection. Br J Surg 2008; 95: 424-432.

18. van der Bilt JD, Kranenburg O, Nijkamp MW, Smakman N, Veenendaal LM, Te Velde EA, Voest EE, van Diest PJ, Borel Rinkes IH. Ischemia/reperfusion accelerates the outgrowth of hepatic micrometastases in a highly standardized murine model. Hepatology 2005; 42: 165-175.
19. van der Bilt JD, Kranenburg O, Borren A, van Hillegersberg R, Borel Rinkes IH. Ageing and hepatic steatosis exacerbate ischemia/reperfusion-accelerated outgrowth of colorectal micrometastases. Ann Surg Oncol 2008; 15: 1392-1398.
20. Simmonds PC, Primrose JN, Colquitt JL, Garden OJ, Poston GJ, Rees M. Surgical resection of hepatic metastases from colorectal cancer: a systematic review of published studies. Br J Cancer 2006; 94: 982-999.
21. Kokudo N, Tada K, Seki M, Ohta H, Azekura K, Ueno M, Ohta K, Yamaguchi T, Matsubara T, Takahashi T, Nakajima T, Muto T, Ikari T, Yanagisawa A, Kato Y. Proliferative activity of intrahepatic colorectal metastases after preoperative hemihepatic portal vein embolization. Hepatology 2001; 34: 267-272.
22. Vigano L, Ferrero A, Lo TR, Capussotti L. Liver surgery for colorectal metastases: results after 10 years of follow-up. Long-term survivors, late recurrences, and prognostic role of morbidity. Ann Surg Oncol 2008; 15: 2458-2464.
23. Wong KH, Hamady ZZ, Malik HZ, Prasad R, Lodge JP, Toogood GJ. Intermittent Pringle manoeuvre is not associated with adverse long-term prognosis after resection for colorectal liver metastases. Br J Surg 2008; 95: 985-989.
24. Ito H, Gonen M, Alley M, D'Angelica M, Dematteo RP, Fong Y, Blumgart LH, Jarnagin WR. Reappraisal of Pringle maneuver: effect of ischemic time on late oncological outcomes following hepatic resection for metastastic colorectal cancer. 9th AHPBA congress 2009: abstract #67
25. van der Bilt JD, Soeters ME, Duyverman AM, Nijkamp MW, Witteveen PO, van Diest PJ, Kranenburg O, Borel Rinkes IH. Perinecrotic hypoxia contributes to ischemia/reperfusion-accelerated outgrowth of colorectal micrometastases. Am J Pathol 2007; 170: 1379-1388.
26. Smyrniotis V, Kostopanagiotou G, Theodoraki K, Tsantoulas D, Contis JC. The role of central venous pressure and type of vascular control in blood loss during major liver resections. Am J Surg 2004; 187: 398-402.
27. Fioole B, van der Bilt JD, Elias SG, de Hoog J, Borel Rinkes IH. Precoagulation minimizes blood loss during standardized hepatic resection in an experimental model. Br J Surg 2005; 92: 1409-1416.
28. Scatton O, Massault PP, Dousset B, Houssin D, Bernard D, Terris B, Soubrane O. Major liver resection without clamping: a prospective reappraisal in the era of modern surgical tools. J Am Coll Surg 2004; 199: 702-708.
29. Frilling A, Stavrou GA, Mischinger HJ, de HB, Rokkjaer M, Klempnauer J, Thorne A, Gloor B, Beckebaum S, Ghaffar MF, Broelsch CE. Effectiveness of a new carrier-bound fibrin sealant versus argon beamer as haemostatic agent during liver resection: a randomised prospective trial. Langenbecks Arch Surg 2005; 390: 114-120.
30. Descottes B, Lachachi F, Durand-Fontanier S, Geballa R, Atmani A, Maisonnette F, Sodji M, Valleix D. Right hepatectomies without vascular clamping: report of 87 cases. J Hepatobiliary Pancreat Surg 2003; 10: 90-94.

Chapter 8

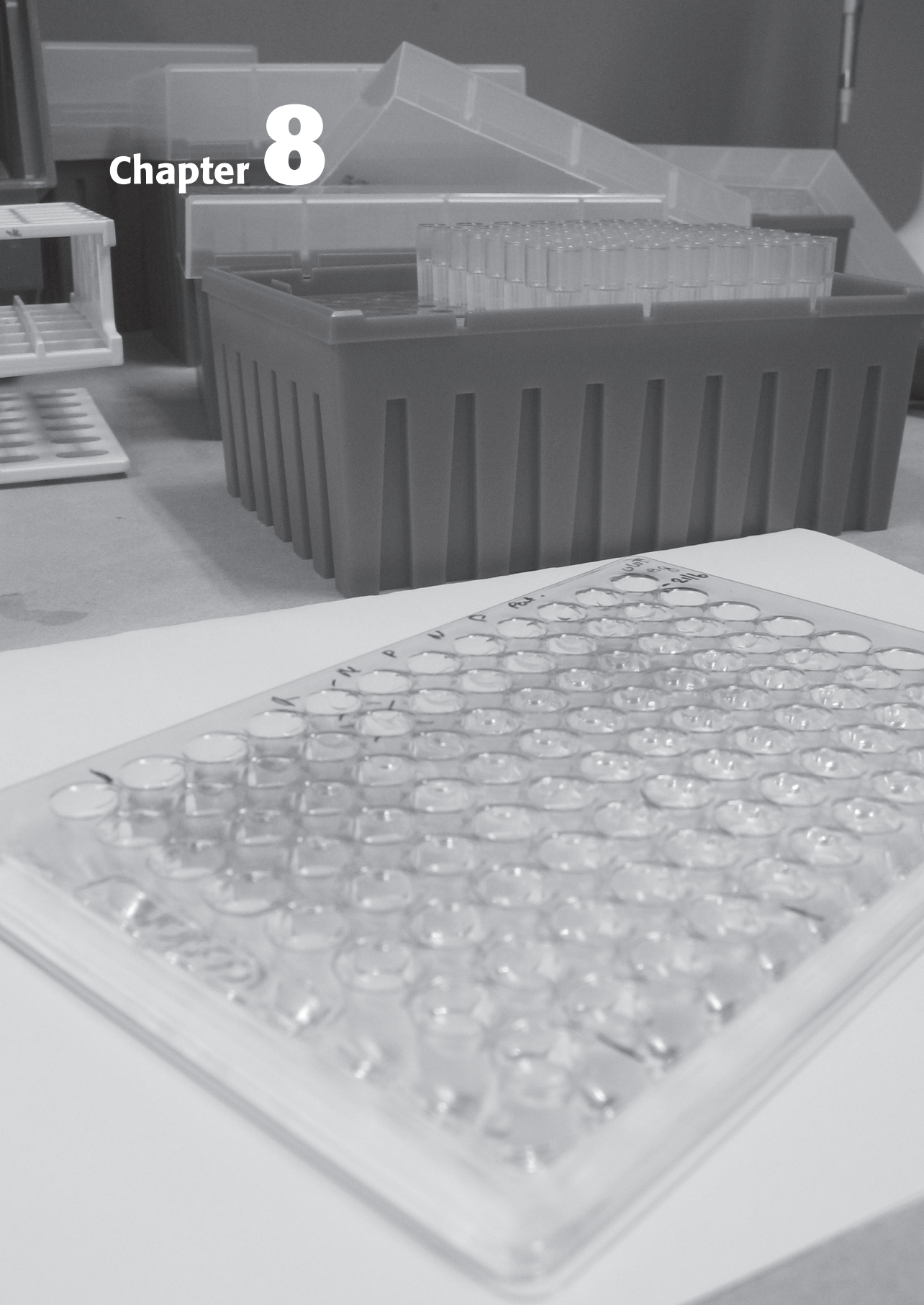

Liver surgery induces an immediate mobilization of progenitor cells in liver cancer patients- a potential role for G-CSF

Cancer Biology and Therapy 2010; 9: 742-747

Marlies H.G. Langenberg[1]
Maarten W. Nijkamp[2]
Jeanine M.L. Roodhart[1]
Nikol Snoeren[2]
Terence Tang[3]
Yuval Shaked[4]
Richard van Hillegersberg[2]
Petronella O. Witteveen[1]
Joost S.P. Vermaat[1]
Onno Kranenburg[2]
Robert S. Kerbel[3]
Rene H. Medema[2]
Inne H.M. Borel Rinkes[2]
Emile E. Voest[1]

Departments of [1]Medical Oncology and [2]Surgery, University Medical Center Utrecht, Utrecht, The Netherlands
[3]Molecular and Cell Biology, Sunnybrook Health Science Centre, University of Toronto, Ontario, Canada
[4]Department of Molecular Pharmacology, Rappaport Faculty of Medicine, Technion-Israel Institute of Technology; Israel

Abstract

Background
In preclinical models recruitment of bone-marrow derived (endothelial) progenitor cells (BD(E)PCs) contributes to tumor growth and metastasis formation. Here we investigated whether these (E)PCs and mobilizing cytokines are released after partial hepatectomy or radiofrequency ablation (RFA) for liver tumors. In addition, we tested whether G-CSF could play a role in EPC mobilization in mice and in human volunteers.

Methods
Before, during and after liver surgery plasma and mononuclear cells were collected from 12 patients undergoing partial hepatectomy or RFA. To explore the role of G-CSF C57Bl/6 mice and 20 human volunteers received G-CSF (0.3 or 3 μg). In all individuals, (E)PC numbers were determined by flow cytometry at predefined timepoints shortly after therapy. Plasma levels of G-CSF, VEGF and SDF-1α were measured by ELISA.

Results
Patients undergoing partial hepatectomy or RFA showed a instantaneous release of EPCs following laparotomy and mobilization of the liver. Elevated EPC levels were maintained during the entire procedure, but dropped to near-baseline levels 4 hours after completion of the procedure. Plasma G-CSF levels showed a five- to ten-fold increase after the procedure and low-dose G-CSF administration to mice or healthy volunteers was sufficient to induce an immediate release of EPCs. Surgery also caused an increase in the plasma levels of VEGF, but not SDF1.

Conclusions
Compliant with previous published data concerning VDA and chemotherapy treatment, liver surgery induces an instantaneous release of EPCs, conceivably in response to elevated G-CSF levels. This suggests the value of exploring therapeutic avenues to prevent this process.

Introduction

The liver is the most common site of metastases from colorectal carcinoma. Surgery is for patients with hepatic metastases a potentially curative treatment option, leading to 5-year survival rates of approximately 30-40%.[1] As resection is only applicable in a small number of cases, local destructive therapies like radiofrequency ablation (RFA) is an alternative treatment option. RFA generates heat in the tumor tissue and results in immediate necrosis. In small liver tumors, RFA shows comparable survival rates.[2,3] A major problem of liver surgery is the high recurrence rates: in approximately 60-70% of cases the tumor will recur.[1-3] As angiogenesis is important in both tissue repair and tumor growth, this biologic process has been suggested to play a role in tumor regrowth following surgery.[4] Local activation and proliferation of endothelial cells are thought to drive angiogenesis, but recruited bone marrow derived progenitor cells (BMDPCs) are also shown to contribute to this process.[5,6] Moreover, it is now becoming clear that several different lineages of supporting cells can egress from the bone marrow which can potentially support the growth of tumors.[6-9] Although some preclinical studies have demonstrated the incorporation of endothelial progenitor cells (EPCs) in the neovascularization of tumors, controversy exists regarding the relative contribution of these cells to the actual growth of the tumor, especially in patients.[6,10-14] Based on observations in patients who underwent a sex mismatched allogeneic bone marrow transplantation, it was estimated that approximately 5% of the endothelial cells of the tumor vasculature was derived from bone marrow progenitor cells.[15] However, these studies were performed on patients who had not recently received any therapy. There is recent evidence that when a host is challenged (e.g., with a vascular disruptive agent (VDA) or with chemotherapy) EPCs are mobilized within hours after start of treatment, which subsequently home to the tumor and reduce necrosis.[16] Interestingly, this phenomenon could be inhibited by an antibody against the VEGF-receptor 2. These preclinical studies are supported by results of early clinical studies showing an increase in EPCs in cancer patients treated with VDAs and chemotherapy.[17-19] The biological relevance of the BMDPC is further illustrated by the observation that these cells appear to play an important role in metastasis formation, especially during the transition of micrometastasis to macrometastasis.[20,21] The mechanism by which certain stress signals and mediators evoke acute egression of (E)PCs from the bone marrow is not well understood. Granulocyte-colony stimulating factor (G-CSF) is well known for its mobilization of hematopoietic stem cells and more recently other cytokines such as stroma cell-derived factor 1 alpha (SDF-1α) and vascular endothelial growth factor (VEGF) also have been implicated in this trafficking process.[9,22-25] Recently we reported that VDA treatment induced a rapid increase in circulating EPC levels, host derived VEGF, SDF-1α and G-CSF in wild type mice, but not in G-CSF-R -/- mice.[26] Further, our unpublished data show that chemotherapy induced a rapid increase in circulating EPC levels in wild type mice and once again not in G-CSF-/- mice (Shaked Y, unpublished data). These findings suggest that G-CSF plays an essential role in the chemotherapy-induced instantaneous release of EPCs. Here, we hypothesize that liver surgery also induces a release of EPCs from the bone marrow shortly after the procedure as a host repair response and that G-CSF could be an important mediator in this trafficking process.

Materials and Methods

Study subjects and procedures

To test this hypothesis blood samples were collected from twelve patients with hepatic malignancies who underwent surgery: six patients with liver metastases of colorectal cancer treated by partial hepatectomy and six patients with liver metastases of colorectal cancer or carcinoid treated with radiofrequency ablation (RFA). Blood was withdrawn at five different timepoints: preoperatively (baseline), postmobilisation (after laparotomy and mobilisation of the liver, just prior to the procedure) and 20 minutes, 4 hours and 24 hours after the procedure. Blood was immediately transferred to our laboratory for further processing. To explore the role of G-CSF in this immediate EPC recruitment, fifteen 8 weeks old C57Bl/6 mice (Jackson Laboratory-West, Sacramento, USA) divided in five groups were treated with 0.04, 4.3, 8.6 and 20 mg/kg recombinant murine G-CSF (Peprotech) or vehicle by intraperitoneal injection and were bled by retro-orbital sinus 4 hours after treatment. Additionally, 4 groups of 5 human healthy volunteers were treated with G-CSF (filgrastim, Amgen) by subcutaneous injection in three different dose levels of 0.3, 3 and 300 µg G-CSF and placebo (0.9% saline). Blood sampling was performed at baseline (before G-CSF administration) and 2, 4 and 6 hours after administration of G-CSF. The subjects' characteristics are displayed in Table 1. All patients and volunteers were included in Institutional Ethics Committee approved protocols conform the principles embodied in the Declaration of Helsinki and all animal studies were performed according to the Sunnybrook Health Sciences Centre Animal Care Committee (Toronto) and the Canadian Council on Animal Care.

Table 1. Subjects' baseline characteristics of all treatment groups RFA: radiofrequency ablation, NA: not applicable

Subject group	RFA	Resection	Volunteers
number included	6	6	20
median age (range)	59 (35-76)	68 (47-80)	29.5 (23-48)
gender			
male	2	1	14
female	4	5	6
tumortype			
colorectal	4	6	NA
hepatocellular	0	0	NA
carcinoid	2	0	NA

B(E)DPC analysis by flowcytometry

For the clinical samples, the mononuclear cell fraction was isolated from whole blood using a cell preparation tube with a density gradient gel (8 ml CPT tube, BD Biosciences) and frozen in RPMI 1640 / 10% DMSO / 20% Fetal Calf Serum and stored at -80°C until further analysis. At time of analysis, samples were thawed and washed two times in PBS-BSA 1%-EDTA 5 mM buffer. Circulating (endothelial) progenitor cells were analyzed by fluorescence-activated cell sorting (FACS)

by a four colour flow cytometer (Becton Dickinson FACScalibur) using peridin chlorophyll protein (PerCP)-conjugated anti-CD45 (Becton Dickinson), isothiocyanate (FITC)-conjugated anti-CD31 (Becton Dickinson Pharmingen), fluorescein, phycoerythin (PE)-conjugated anti-CD146 (MAB 16985H, Chemicon International) and allophycocyanin (APC)-conjugated anti-CD133 (Miltenyl Biotec) as antibodies as previously reported.[27-29] Negative controls for each sample were stained with appropriate isotype controls to exclude atypical binding/staining. Immortalized human microvascular endothelial cells (HMEC-1) and human teratocarcinoma (NT2) cells were used as positive controls for CD146 and CD133, respectively. Cells of interest were defined as $CD45^-$, $CD31^+$ and $CD133^+$ for the circulating endothelial progenitor cells (EPC), $CD45^-$, $CD31^+$ and $CD146^+$ for the circulating endothelial cells (CEC) and $CD133^+$ for the progenitor cells in general (PC). In mice, a few minutes before and 2 to 4 hours after administration of G-CSF, blood was collected in EDTA tubes. The cell suspension samples were immediately evaluated by flow cytometry after red cell lysis and labelling with CD13-FITC, CD45-PerCP, CD117-APC and VEGFR-2-PE (all from Becton Dickinson Pharmingen). EPCs were defined as $CD45^-$, $CD13^+$, VEGFR-2^+ and $CD117^+$. For all samples, accurately defined gates were used to exclude platelets, dead cells and debris. Analyses were considered informative when adequate numbers of gated events (i.e., >100,000) were collected. Measurements of EPCs were expressed in fold increase as compared to baseline values. All samples were measured in duplo.

Measurement of various growth factors and cytokines

Plasma G-CSF, SDF-1α and VEGF levels were measured using commercially available sandwich ELISA kits (R&D Systems) following the manufacturer's instructions, using EDTA plasma. For the RFA/surgery patients and higher doses G-CSF treated volunteers normal sensitivity G-CSF assays (R&D, DCS50) were used and for the low dose G-CSF treated volunteers high sensitivity assays (R&D, HSC0B) were performed. All samples were measured in duplo.

Statistical analysis and data interpretation

Statistical comparisons were performed using the Student's t-test when data were normally distributed and the nonparametric analyses of Wilcoxon when data were not normally distributed. All tests were 2-sided. P-values lower than 0.05 were considered as statistically significant. All statistical calculations were performed using commercially available statistical software (Graphpad prism 4.0/SPSS version 15).

Results

Immediate increase in EPC levels in patients undergoing liver surgery

In patients undergoing either partial hepatectomy or RFA we observed an immediate rise in the levels of circulating EPCs following laparotomy and mobilization of the liver, just prior to the start of the procedure (partial liver resection or RFA) ($p=0.03$ compared to baseline values, figure 1). The increase in circulating EPCs was maintained during the procedure, but rapidly dropped to near-baseline levels 4 and 24 hours after completion of the procedure. No significant changes were observed in circulating PC or CEC levels during or after surgery.

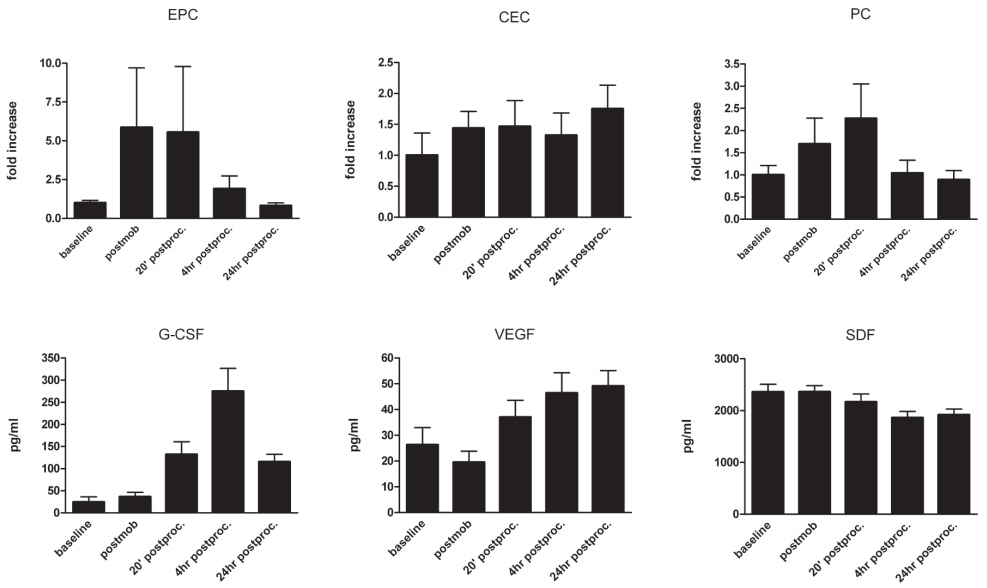

Figure 1 Increase in levels of circulating (endothelial) (progenitor) cells C(E)(P)C (EPC: $CD45^-/CD31^+/CD133^+$, PC: $CD133^+$ and CEC: $CD45^-/CD31^+/CD146^+$) as compared to baseline and plasma levels of G-CSF, VEGF and SDF-1α measured in 12 liver cancer patients before treatment and at various timepoints after surgery, represented as means ± SEM. * 0.05>P>0.01; ** 0.01>P>0.001; *** P≤0.001 (Wilcoxon rank analysis as compared to baseline value) Abbreviations: postmob: post-mobilization; postproc: post-procedure.

Increased plasma G-CSF and VEGF levels in patients undergoing liver surgery

In patients undergoing liver surgery we observed a five- to ten-fold increase in plasma G-CSF levels from 20 minutes to 4 hours after the procedure (p=0.0093 and p=0.001, respectively). In addition, we observed a two-fold increase in VEGF levels from 4-24 hours after the procedure (p=0.0024 and p=0.0068, respectively, figure 1). SDF-1α levels did not change within the period of sampling.

G-CSF administration to C57Bl/6 mice results in an immediate increase in EPCs

Next, in order to investigate the mobilizing potential of the observed G-CSF peaks in the plasma of the liver surgery treated patients, we tested whether administration of comparable doses G-CSF to mice or healthy volunteers was sufficient to cause the release of EPCs from the bone marrow. To this end, fifteen C57Bl/6 mice received G-CSF (0.04–20 mg/kg) via intraperitoneal injection. These doses are within the range observed in the plasma of the surgery treated patients. We found a three- to five-fold increase in circulating EPCs 4 hours after injection, indicating that G-CSF alone was sufficient to mobilize EPCs from the bone marrow. (0.04 and 4.3 μg/kg: p=0.0038 and p=0.0008, respectively, as compared to the vehicle, figure 2A).

Elevated levels of EPCs in human volunteers treated with low-dose G-CSF

Subsequently, 20 healthy human volunteers were injected with G-CSF (0.3, 3 and 300 μg) or placebo

(saline 0.9%). Pharmacokinetic analysis of G-CSF in the volunteers confirmed that the concentrations of G-CSF given were in the range of those seen after surgery. At lower doses, G-CSF stimulated the mobilization of EPCs although this did not reach statistical significance (range p-values 0.17 to 0.30, figure 2B).

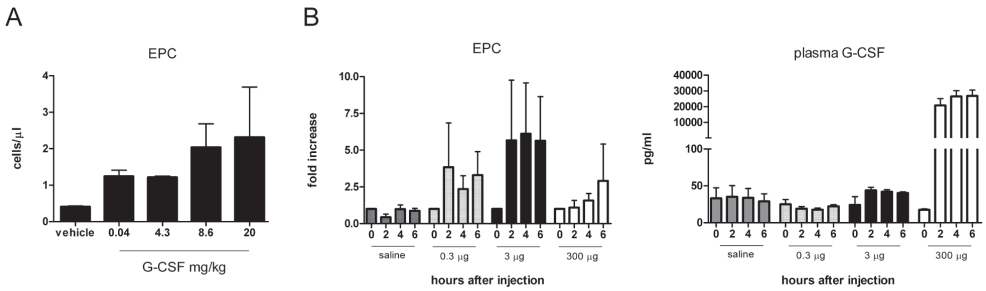

Figure 2 Effects of an injection of G-CSF on EPC levels in C57Bl/6 mice **(A)** treated with 4 different doses G-CSF or vehicle intraperitoneally and in human volunteers **(B)** treated with 3 different doses G-CSF or placebo subcutaneously and corresponding plasma levels of G-CSF after injection. All data represented as means ± SEM. ** 0.01>P>0.001; *** P≤0.001 (Student's t-test as compared to baseline value).

Discussion

Recently, it has been demonstrated that vascular disruptive agents and certain forms of chemotherapy induce acute mobilization of progenitor cells.[16,18,19] Here, we show that a similar phenomenon is seen during and immediately after surgery. Although there are reports showing a mobilization of EPCs within days following surgery[30,31], this is the first study showing a mobilization of EPCs already after laparotomy and mobilization of the liver but prior to initiation of resection or RFA. This suggests that the incision and/or the process of liver mobilization are sufficient to induce release of EPCs from the bone marrow. The observed peri-operative increased G-CSF concentrations were sufficient to induce an EPC release in mice and to a lesser extent in human subjects when administered as single agent. In the patients undergoing liver surgery, circulating EPCs were detected prior to the increase in plasma G-CSF levels. We propose that a minor increase in the concentration of G-CSF during the earlier timepoints could be sufficient to induce EPC release, potentially aided by an active dopaminergic system in patients undergoing surgery. This may help explain this apparent contradictory result. Taken together, our findings support the concept that the host bone marrow responds to certain stress signals in an immediate '*seek and repair*' manner, presumably in order to support tissue regeneration. The bone marrow response consists of the release of progenitor cells from the endothelial cell lineages but is certainly not limited to these cells. As a matter of fact, several other progenitor cells have now been implicated in tumor growth or tissue repair. Indeed, in our mouse experiment and volunteer study, G-CSF administration resulted in an immediate increase in EPCs. However, the results from the volunteer study are less consistent than those from patients undergoing surgery and the mouse experiment. This may indicate that there is an intricate regulation of this process by G-CSF

and other cytokines. VEGF, matrix metalloproteinase 9 (MMP-9), CXCR4 receptor and its ligand SDF-1α, placental growth factor (PlGF), RANTES (CCL5) and many other factors are reported to be involved in the release and trafficking process of BMDPCs, many of which may be upregulated during surgery.[9] Depending on the interplay of these cytokines, the release of certain cell types may be regulated. Additionally, it has been shown recently that the release and function of progenitor cells could be induced through catecholaminergic neurotransmitters, modulated via G-CSF by upregulation of dopamine receptors.[32-36] Besides that, certain anesthetics have been shown to increase the number of colony forming units of EPCs in healthy volunteers.[37] This may also provide an alternative explanation for the differences between the volunteers and surgical patients where the latter may have a more active catecholaminergic system during surgery. Altogether, it is tempting to speculate that tumors may benefit from the influx of progenitor cells after perturbation by treatment modalities. Recurrence or stimulated tumor growth following liver surgery may potentially be explained by this phenomenon. The progenitor cells may support neovascularization, prevent apoptosis and facilitate tumor recurrence and metastasis formation.[20] Inhibiting the influx of these BD(E)PC in the short time period during or following liver surgery may constitute a beneficial adjuvant treatment for patients with liver metastasis. Interestingly, in preclinical models the mobilization of progenitor cells could be prevented through various approaches, such as VEGF/VEGF-receptor inhibiting agents, anti-G-CSF treatment and inhibitors of the SDF/CXCR4 pathway.[16,38,39] Additionally, Ferrara *et al*. show that G-CSF might mediate refractoriness to anti-VEGF therapy in mouse models and that anti-GCSF treatment resulted in responsiveness to anti VEGF treatment in previous refractory tumors.[40] Alternatively, exploiting the regulatory capacity of the catecholaminergic system peri-operatively and the effect of anesthesia on these pathways may also be worthwhile.

Lately, several groups have expressed their reserve towards CE(P)C enumeration and using these cells as surrogate biomarkers. The major concern is the inability to exactly identify the 'endothelial progenitor cell'. This problem is reflected in the fact that several research groups report CEC levels in healthy and cancer subjects in very different ranges.[41] This controversy could be very well caused by different methods of enumeration, but could also be an expression of differences in identification of cells of interest.[42] In addition, some groups showed that CE(P)Cs indicated with our phenotype, did not show endothelial differentiation potential.[43] Although it was not the purpose of our manuscript to address this identification issue, we are very well aware that characterization of the origin of these cells is of great biological importance. As it was recently shown that CE(P)Cs play an important role in tumor biology and therefore could not only serve as a surrogate biomarker, but also as a target for therapy, further critical exploration of the true identity and capacity of these cells is necessary.

In conclusion, this study reveals that liver surgery induces a release of EPCs within minutes to hours after initiation of the surgical procedure and that G-CSF may play a modulatory role in the releasing and trafficking process. In terms of clinical relevance, this could imply that these cells and also the inducing or guiding factors like G-CSF can constitute a new target of therapy. Future studies should be aimed at investigating the role of this immediate EPC release in tumor recurrence following liver surgery and the surplus value of combination therapy in the immediate moments after surgery, starting already during the surgical procedure, in order to reduce tumor recurrences following liver surgery.

References

1. Simmonds PC, Primrose JN, Colquitt JL, Garden OJ, Poston GJ, Rees M. Surgical resection of hepatic metastases from colorectal cancer: a systematic review of published studies. Br J Cancer 2006; 94: 982-999.
2. Berber E, Tsinberg M, Tellioglu G, Simpfendorfer CH, Siperstein AE. Resection Versus Laparoscopic Radiofrequency Thermal Ablation Of Solitary Colorectal Liver Metastasis. J Gastrointest Surg 2008; 12: 1967-1972.
3. Mulier S, Ni Y, Jamart J, Michel L, Marchal G, Ruers T. Radiofrequency Ablation Versus Resection for Resectable Colorectal Liver Metastases: Time for a Randomized Trial? Ann Surg Oncol 2007; 15: 144-157.
4. van der Bilt JD and Borel Rinkes IH. Surgery and angiogenesis. Biochim Biophys Acta 2004; 1654: 95-104.
5. Carmeliet P. VEGF as a key mediator of angiogenesis in cancer. Oncology 2005; 69 Suppl 3: 4-10.
6. Lyden D, Hattori K, Dias S, Costa C, Blaikie P, Butros L, Chadburn A, Heissig B, Marks W, Witte L, Wu Y, Hicklin D, Zhu Z, Hackett NR, Crystal RG, Moore MA, Hajjar KA, Manova K, Benezra R, Rafii S. Impaired recruitment of bone-marrow-derived endothelial and hematopoietic precursor cells blocks tumor angiogenesis and growth. Nat Med 2001; 7: 1194-1201.
7. Asahara T, Takahashi T, Masuda H, Kalka C, Chen D, Iwaguro H, Inai Y, Silver M, Isner JM. VEGF contributes to postnatal neovascularization by mobilizing bone marrow-derived endothelial progenitor cells. EMBO J 1999; 18: 3964-3972.
8. Hattori K, Heissig B, Wu Y, Dias S, Tejada R, Ferris B, Hicklin DJ, Zhu Z, Bohlen P, Witte L, Hendrikx J, Hackett NR, Crystal RG, Moore MA, Werb Z, Lyden D, Rafii S. Placental growth factor reconstitutes hematopoiesis by recruiting VEGFR1(+) stem cells from bone-marrow microenvironment. Nat Med 2002; 8: 841-849.
9. Rafii S, Avecilla S, Shmelkov S, Shido K, Tejada R, Moore MA, Heissig B, Hattori K. Angiogenic factors reconstitute hematopoiesis by recruiting stem cells from bone marrow microenvironment. Ann N Y Acad Sci 2003; 996: 49-60.
10. Asahara T, Murohara T, Sullivan A, Silver M, van der ZR, Li T, Witzenbichler B, Schatteman G, Isner JM. Isolation of putative progenitor endothelial cells for angiogenesis. Science 1997; 275: 964-967.
11. Duda DG, Cohen KS, Kozin SV, Perentes JY, Fukumura D, Scadden DT, Jain RK. Evidence for incorporation of bone marrow-derived endothelial cells into perfused blood vessels in tumors. Blood 2006; 107: 2774-2776.
12. Purhonen S, Palm J, Rossi D, Kaskenpaa N, Rajantie I, Yla-Herttuala S, Alitalo K, Weissman IL, Salven P. Bone marrow-derived circulating endothelial precursors do not contribute to vascular endothelium and are not needed for tumor growth. Proc Natl Acad Sci U S A 2008; 105: 6620-6625.
13. Ruzinova MB, Schoer RA, Gerald W, Egan JE, Pandolfi PP, Rafii S, Manova K, Mittal V, Benezra R. Effect of angiogenesis inhibition by Id loss and the contribution of bone-marrow-derived endothelial cells in spontaneous murine tumors. Cancer Cell 2003; 4: 277-289.
14. Seandel M, Butler J, Lyden D, Rafii S. A catalytic role for proangiogenic marrow-derived cells in tumor neovascularization. Cancer Cell 2008; 13: 181-183.
15. Peters BA, Diaz LA, Polyak K, Meszler L, Romans K, Guinan EC, Antin JH, Myerson D, Hamilton SR, Vogelstein B, Kinzler KW, Lengauer C. Contribution of bone marrow-derived endothelial cells to human tumor vasculature. Nat Med 2005; 11: 261-262.
16. Shaked Y, Ciarrocchi A, Franco M, Lee CR, Man S, Cheung AM, Hicklin DJ, Chaplin D, Foster FS, Benezra R, Kerbel RS. Therapy-induced acute recruitment of circulating endothelial progenitor cells to tumors. Science 2006; 313: 1785-1787.
17. Beerepoot LV, Radema SA, Witteveen EO, Thomas T, Wheeler C, Kempin S, Voest EE. Phase I clinical evaluation of weekly administration of the novel vascular-targeting agent, ZD6126, in patients with solid

tumors. J Clin Oncol 2006; 24: 1491-1498.
18. Nathan PD, Judson I, Padhani A, Harris A, Carden CP, Smythe J, Collins D, Leach M, Walicke P, Rustin GJ. A phase I study of combretastatin A4 phosphate (CA4P) and bevacizumab in subjects with advanced solid tumors. Journal of Clinical Oncology, 2008 ASCO Annual Meeting Proceedings Vol 26, No 15S (May 20 Supplement): abstract# 3550.
19. Shaked Y, Henke E, Roodhart JM, Mancuso P, Langenberg MH, Colleoni M, Daenen LG, Man S, Xu P, Emmenegger U, Tang T, Zhu Z, Witte L, Strieter RM, Bertolini F, Voest EE, Benezra R, Kerbel RS. Rapid chemotherapy-induced acute endothelial progenitor cell mobilization: implications for antiangiogenic drugs as chemosensitizing agents. Cancer Cell 2008; 14: 263-273.
20. Gao D, Nolan DJ, Mellick AS, Bambino K, McDonnell K, Mittal V. Endothelial progenitor cells control the angiogenic switch in mouse lung metastasis. Science 2008; 319: 195-198.
21. Kaplan RN, Riba RD, Zacharoulis S, Bramley AH, Vincent L, Costa C, MacDonald DD, Jin DK, Shido K, Kerns SA, Zhu Z, Hicklin D, Wu Y, Port JL, Altorki N, Port ER, Ruggero D, Shmelkov SV, Jensen KK, Rafii S, Lyden D. VEGFR1-positive haematopoietic bone marrow progenitors initiate the pre-metastatic niche. Nature 2005; 438: 820-827.
22. Du R, Lu KV, Petritsch C, Liu P, Ganss R, Passegue E, Song H, Vandenberg S, Johnson RS, Werb Z, Bergers G. HIF1alpha induces the recruitment of bone marrow-derived vascular modulatory cells to regulate tumor angiogenesis and invasion. Cancer Cell 2008; 13: 206-220.
23. Grunewald M, Avraham I, Dor Y, Bachar-Lustig E, Itin A, Jung S, Chimenti S, Landsman L, Abramovitch R, Keshet E. VEGF-induced adult neovascularization: recruitment, retention, and role of accessory cells. Cell 2006; 124: 175-189.
24. Petit I, Szyper-Kravitz M, Nagler A, Lahav M, Peled A, Habler L, Ponomaryov T, Taichman RS, renzana-Seisdedos F, Fujii N, Sandbank J, Zipori D, Lapidot T. G-CSF induces stem cell mobilization by decreasing bone marrow SDF-1 and up-regulating CXCR4. Nat Immunol 2002; 3: 687-694.
25. Shi Q, Bhattacharya V, Hong-De WM, Sauvage LR. Utilizing granulocyte colony-stimulating factor to enhance vascular graft endothelialization from circulating blood cells. Ann Vasc Surg 2002; 16: 314-320.
26. Shaked Y, Tang T, Woloszynek J, Daenen LG, Man S, Xu P, Cai SR, Arbeit JM, Voest EE, Chaplin DJ, Smythe J, Harris A, Nathan P, Judson I, Rustin G, Bertolini F, Link DC, Kerbel RS. Contribution of granulocyte colony-stimulating factor to the acute mobilization of endothelial precursor cells by vascular disrupting agents. Cancer Res 2009; 69: 7524-7528.
27. Duda DG, Cohen KS, Scadden DT, Jain RK. A protocol for phenotypic detection and enumeration of circulating endothelial cells and circulating progenitor cells in human blood. Nat Protoc 2007; 2: 805-810.
28. Mancuso P, Antoniotti P, Quarna J, Calleri A, Rabascio C, Tacchetti C, Braidotti P, Wu HK, Zurita AJ, Saronni L, Cheng JB, Shalinsky DR, Heymach JV, Bertolini F. Validation of a standardized method for enumerating circulating endothelial cells and progenitors: flow cytometry and molecular and ultrastructural analyses. Clin Cancer Res 2009; 15: 267-273.
29. Norden-Zfoni A, Desai J, Manola J, Beaudry P, Force J, Maki R, Folkman J, Bello C, Baum C, DePrimo SE, Shalinsky DR, Demetri GD, Heymach JV. Blood-based biomarkers of SU11248 activity and clinical outcome in patients with metastatic imatinib-resistant gastrointestinal stromal tumor. Clin Cancer Res 2007; 13: 2643-2650.
30. Gehling UM, Willems M, Dandri M, Petersen J, Berna M, Thill M, Wulf T, Muller L, Pollok JM, Schlagner K, Faltz C, Hossfeld DK, Rogiers X. Partial hepatectomy induces mobilization of a unique population of haematopoietic progenitor cells in human healthy liver donors. J Hepatol 2005; 43: 845-853.
31. Lemoli RM, Catani L, Talarico S, Loggi E, Gramenzi A, Baccarani U, Fogli M, Grazi GL, Aluigi M, Marzocchi G, Bernardi M, Pinna A, Bresadola F, Baccarani M, Andreone P. Mobilization of bone marrow-derived hematopoietic and endothelial stem cells after orthotopic liver transplantation and liver resection. Stem Cells 2006; 24: 2817-2825.
32. Asada M, Ebihara S, Numachi Y, Okazaki T, Yamanda S, Ikeda K, Yasuda H, Sora I, Arai H. Reduced tumor

growth in a mouse model of schizophrenia, lacking the dopamine transporter. Int J Cancer 2008; 123: 511-518.
33. Chakroborty D, Chowdhury UR, Sarkar C, Baral R, Dasgupta PS, Basu S. Dopamine regulates endothelial progenitor cell mobilization from mouse bone marrow in tumor vascularization. J Clin Invest 2008; 118: 1380-1389.
34. Katayama Y, Battista M, Kao WM, Hidalgo A, Peired AJ, Thomas SA, Frenette PS. Signals from the sympathetic nervous system regulate hematopoietic stem cell egress from bone marrow. Cell 2006; 124: 407-421.
35. Mendez-Ferrer S, Lucas D, Battista M, Frenette PS. Haematopoietic stem cell release is regulated by circadian oscillations. Nature 2008; 452: 442-447.
36. Sarkar C, Chakroborty D, Chowdhury UR, Dasgupta PS, Basu S. Dopamine increases the efficacy of anticancer drugs in breast and colon cancer preclinical models. Clin Cancer Res 2008; 14: 2502-2510.
37. Lucchinetti E, Zeisberger SM, Baruscotti I, Wacker J, Feng J, Zaugg K, Dubey R, Zisch AH, Zaugg M. Stem cell-like human endothelial progenitors show enhanced colony-forming capacity after brief sevoflurane exposure: preconditioning of angiogenic cells by volatile anesthetics. Anesth Analg 2009; 109: 1117-1126.
38. Redjal N, Chan JA, Segal RA, Kung AL. CXCR4 inhibition synergizes with cytotoxic chemotherapy in gliomas. Clin Cancer Res 2006; 12: 6765-6771.
39. Shojaei F, Wu X, Qu X, Kowanetz M, Yu L, Tan M, Meng YG, Ferrara N. G-CSF-initiated myeloid cell mobilization and angiogenesis mediate tumor refractoriness to anti-VEGF therapy in mouse models. Proc Natl Acad Sci U S A 2009; 106: 6742-6747.
40. Ferrara N. Role of myeloid cells in vascular endothelial growth factor-independent tumor angiogenesis. Curr Opin Hematol 2010; 17: 219-224.
41. Strijbos MH, Kraan J, Lamers CH, Sleijfer S, Gratama JW. Quantification of circulating endothelial cells by flow cytometry. Clin Cancer Res 2009; 15: 3640-3641.
42. Bertolini F, Shaked Y, Mancuso P, Kerbel RS. The multifaceted circulating endothelial cell in cancer: towards marker and target identification. Nat Rev Cancer 2006; 6: 835-836.
43. Case J, Mead LE, Bessler WK, Prater D, White HA, Saadatzadeh MR, Bhavsar JR, Yoder MC, Haneline LS, Ingram DA. Human CD34+AC133+VEGFR-2+ cells are not endothelial progenitor cells but distinct, primitive hematopoietic progenitors. Exp Hematol 2007; 35: 1109-1118.

Chapter 9

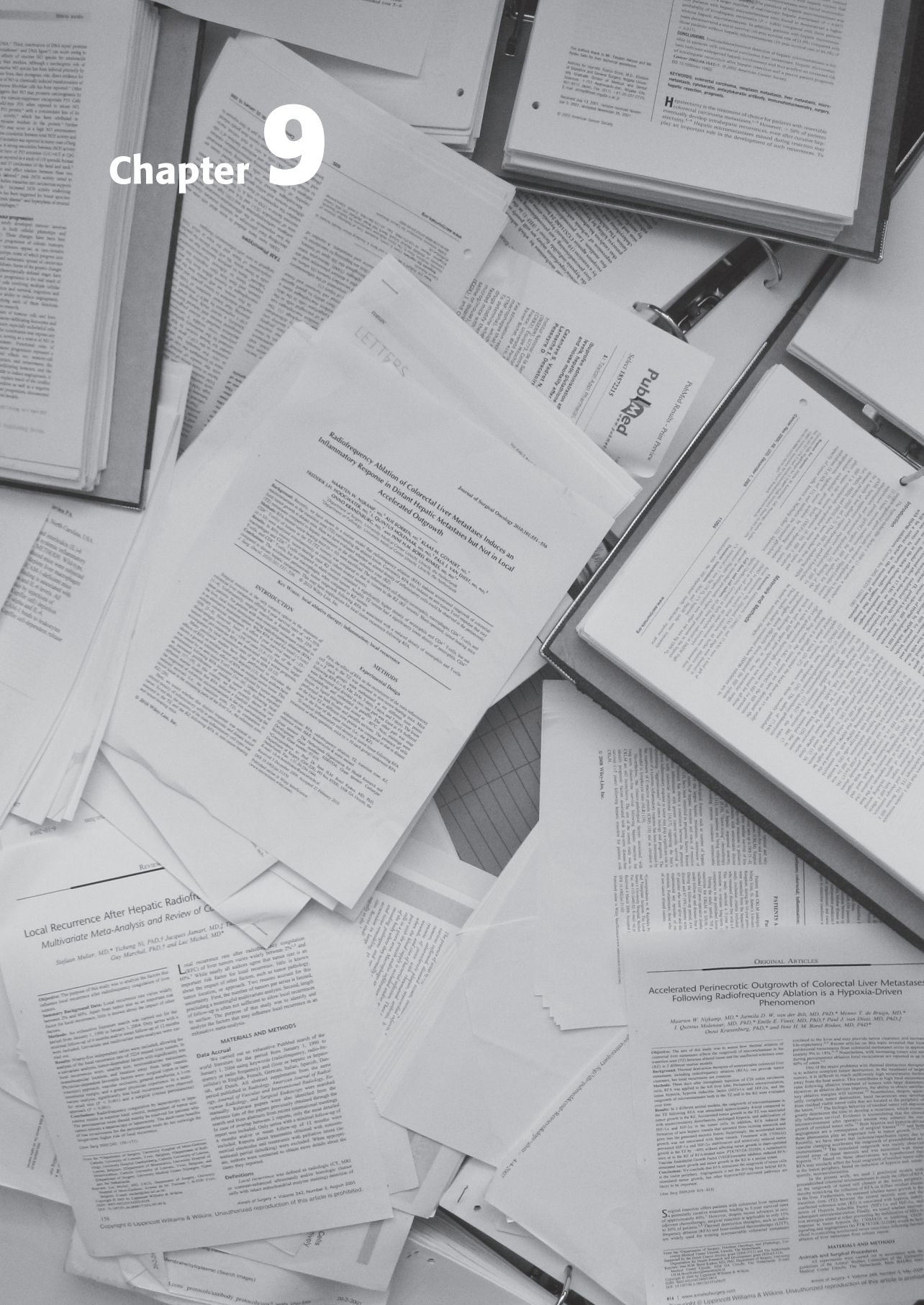

General discussion

Surgical treatment of colorectal liver metastases includes partial liver resection and radiofrequency ablation (RFA). Vascular clamping of the hepatic inflow during liver surgery is often applied during both surgical interventions, either to control blood loss (partial liver resection) or to increase lesion size (RFA). Surgery can offer cure in patients with colorectal liver metastases. However, tumor recurrence occurs in approximately 60-70% of cases and may develop from i) circulating tumor cells possibly induced by the surgical procedure or ii) residual tumor deposits remaining after surgery. This thesis describes factors that contribute to survival (**chapter 2**) and outgrowth of colorectal cancer cells in the liver. It investigates the effects of liver surgery on residual micrometastases (**chapters 3-6**) and tumor recurrence (**chapters 7 and 8**). In our preclinical studies, standardized RFA and selective vascular inflow clamping were regarded as representative surgical interventions in the liver.

Mouse models in cancer research

To investigate the effects of liver surgery on the outgrowth of colorectal tumor cells, we used a mouse model of pre-established micrometastases in the liver. This mouse model mimics micrometastatic disease in patients and has several advantages. First, micrometastases are induced in a relatively simple manner by injecting tumor cells into the spleen. Similar to the development of colorectal metastases in the human liver, tumor cells will reach the liver via the portal circulation. Second, metastases develop rapidly (within several days) and in a highly reproducible fashion.

However, this mouse model also has several disadvantages. First, the murine colon carcinoma cell line used in most experiments described in this thesis (the Colon Tumor 26 or C26) is an aggressive tumor cell line which forms undifferentiated carcinomas.[1] Using the C26 cell line, the effects of surgery on residual micrometastases may be overemphasized. Therefore, it is unclear whether the obtained results are relevant for colorectal liver metastases in patients. Second, the mouse livers only contain multiple micrometastases, without a single (or multiple) large metastasis as seen in patients. It has been demonstrated that primary tumors may produce anti-angiogenic factors that suppress distant metastatic growth, which is followed by metastatic growth induction after removal of the primary tumor.[2,3] Indeed, it has been demonstrated that the removal of the primary colorectal tumor in patients induced an increase in vascular density and outgrowth of its liver metastases.[4,5] A similar effect on micrometastases may be present after the removal of a colorectal liver metastases. Conversely, local thermal ablation of a large metastasis will result in a massive generation of tumor-specific antigens against which an anti-tumor T-cell response can be elicited. However, the influence that a large metastasis has on the outgrowth of micrometastases was not considered in our mouse model. Third, micrometastases in patients may rather act as dormant or senescent micrometastases that may cause tumor recurrence after many years. In our mouse model however, injected tumor cells form actively growing micrometastases rather than dormant metastases. Whether liver surgery can act as a wake up call for dormant metastases is difficult to answer using the C26-BALB/c model employed in our studies. Interestingly, the first mouse model for colorectal cancer with spontaneous liver metastasis formation was recently published and may be better suited to study the biology of dormant spontaneous liver metastases.[6]

K-Ras-induced survival of colorectal tumor cells in the liver

Research on the role of K-Ras in metastasis formation has focused primarily on the first phase of the metatatic cascade, including local tumor cell invasion, migration and anoikis-resistance.[7] In **chapter**

2 we focus on survival of K-Ras-mutated colon carcinoma cells in the hepatic environment. Survival of infiltrating tumor cells in the liver is primarily determined by overcoming the hepatic defense mechanism, which involves cytotoxic lymphocytes. Cytotoxic lymphocytes can kill tumor cells in part by excreting cytokines like TNF-α, TNF-related apoptosis-inducing ligand (TRAIL) and CD95 ligand (CD95L). These cytokines bind to death receptors to induce tumor cell apoptosis.[8,9] However, we show in **chapter 2** that K-Ras-mutated colon carcinoma cells do not die in response to TRAIL or CD95 ligand. Alternative signaling of CD95 has been reported previously, including tumor cell proliferation and invasion, due to the increased expression of matrix metalloproteinases (MMPs)[10,11] and/or urokinase plasminogen activator (uPA).[11,12] We demonstrate that mutant K-Ras and its effector Raf1 switch the death receptor signaling of CD95 into invasion-inducing signaling by suppressing the Rho/ROCK/Lim kinase/cofilin pathway. Our results imply that targeting death receptors in K-Ras-mutated cells would result in tumor progression rather than tumor kill. Currently, clinical trials are conducted to evaluate the safety and efficacy of TRAIL and agonistic death receptor-targeting antibodies, aiming to induce apoptosis in tumor cells.[13,14] Of note, the trials contain patients with metastatic colorectal, pancreatic, and non-small cell lung cancer. These tumor types frequently harbour activating K-Ras mutations in 40%, 95% and 35% respectively.[15] Therefore, testing the K-Ras mutation status in tumors of patients in these trials may predict tumor resistance to TRAIL-receptor-activating therapeutics. In addition, one might hypothesize that re-activation of the Rho/ROCK/Lim kinase/cofilin pathway in K-Ras-mutated cells by Lim kinase-activating agents would result in apoptosis upon treatment with death receptor-targeting agents. However, such agents have not been developed yet. Future research aiming to find such agents would be worthwhile.

K-Ras-mutated colon carcinoma cells were able to survive in the hepatic microenvironment and form metastases (**chapter 2**). The driving force(s) behind metastasis formation in colorectal cancer are presently unknown. Acquisition of mutations in 'metastasis genes' or 'metastasis-suppressor genes' has long been thought to be required for an invasive primary carcinoma to gain metastatic potential. However, such 'metastasis(-suppressor) genes' have not been identified in colorectal cancer.[16] Alternatively, mutated genes that drive the formation of a primary tumor may also drive the formation of its metastases. Thus, the genetic blueprint of the primary tumor may explain the ability of tumor cells to metastasize. K-Ras could represent such a gene. However, the K-Ras mutation frequency in metastases is similar to that found in primary tumors.[17,18]

Colorectal cancer is characterized by an enormous genetic heterogeneity. A total of 69 mutated genes have been identified in this disease, of which a highly variable combination of 3-18 genes drives tumorigenesis in individual tumors.[19] Similarly, the combination of (many different) mutations in the primary tumor may determine whether tumor cells are able to metastasize. This concept is supported by the observation that very few additional mutations are identified in metastases when compared to the carcinoma from which they originated.[16] Therefore, the contribution of K-Ras to metastasis formation may depend on the collection of additional mutations present in each individual tumor. The exact function of K-Ras in colorectal metastasis formation remains to be elucidated. Future research on this topic should focus on the effects of different combinations of mutations, including K-Ras. In addition, mutational differences between metastasized primary tumors and non-metastasized primary tumors should be investigated. Finally, since gene mutation analysis comparing primary colorectal tumors with their paired metastases was only comprised of candidate cancer genes[16], a whole genome analysis should be performed to address all mutational differences between primary colorectal tumors with their paired metastases to assess its role in metastasis formation.

Liver surgery & inflammation

In addition to the pro-tumorigenic micro-environment produced by inflammatory cells during surgery and wound healing, anti-tumorigenic effects by inflammatory cells have been reported as well.[20] Local thermal ablation of liver tumors induces a specific anti-tumor immune response in patients due to circulating tumor antigens following tumor destruction.[21,22] Interestingly, we demonstrate in **chapter 4** that the local accelerated tumor outgrowth following RFA contain a reduced density of neutrophils, $CD4^+$ and $CD8^+$ T-cells compared to tumor tissue that is located in the untreated liver. Hypothetically, increasing the inflammatory cell density in the perinecrotic tumor tissue may result in reduced local tumor outgrowth following RFA. Indeed, adjuvant treatment of tumors with inflammation-stimulating agents following RFA seems to lead to an increased anti-tumor response and a reduction of tumor recurrence.[23,24] Since a higher amount of T-cells in colorectal liver metastases is associated with improved patient survival[25], increasing the immune response following liver surgery for colorectal liver metasasases may be an appealing novel treatment strategy. Currently, clinical trials are conducted in patients with liver tumors to explore the safety and toxicity of RFA combined with inflammation-stimulating agents.[26]

Liver surgery & hypoxia

Aggressive tumor behaviour can be caused by hypoxia in numerous ways, including the induction of tumor cell survival, invasion and angiogenesis. Hypoxia Inducible Factors (HIF)-1α and HIF-2α are key players in these modifications.[27] Indeed, hypoxia and HIF expression are associated with tumor progression and poor patient survival in different types of cancer, including colorectal cancer.[28,29] In **chapter 3** we demonstrate that radiofrequency ablation induces a three- to four-fold growth acceleration of tumor cells surrounding the generated lesion. This area is characterized by hypoxia and subsequent upregulation of HIF-1α and HIF-2α. Using an hsp90-inhibitor which is known to destabilize HIF-1α and HIF-2α, the perinecrotic accelerated tumor outgrowth can be reduced by more than 60%. These results are in accordance with our previous observations that ischemia/reperfusion-accelerated outgrowth of micrometastases is associated with prolonged perinecrotic microcirculatory disturbances, hypoxia and subsequent stabilization of HIF-1α.[30] The exact mechanism of action by which the hsp90-inhibitor reduce the perinecrotic tumor outgrowth is unclear. Although it is known for its destabilizing effect on HIF-1α and HIF-2α, experiments using tumor cells in which HIFs are selectively silenced by RNA interference should reveal their specific role in this phenomenon.

Tumor cell survival under hypoxia may be caused by inducing apoptosis resistance.[31] In general, activation of the apoptosis-inducing death receptor CD95 results in activation of the extrinsic apoptotic pathway. However, alternative CD95 signaling in tumor cells may result in invasion, as was demonstrated in **chapter 2**. In **chapter 5**, we find that hypoxia-induced invasion could be abrogated by inhibiting CD95 *in vitro*. In addition, we demonstrate in **chapters 5** (RFA) and **6** (IR) that tumor cells located in hypoxic areas following liver surgery adapted a highly invasive phenotype when compared to tumor cells elsewhere in the liver. Accordingly, interfering with CD95 signaling reduces the invasion and outgrowth of tumor cells in the hypoxic areas. It is unknown whether the hypoxia-induced activation of CD95 is HIF-dependent. However, the hsp90 inhibitor used in **chapter 3** did not decrease the tumor cell invasion in the hypoxic transition zone following RFA *in vivo* (unpublished data). This might suggest HIF-independency. When this is sustained in further research, HIF

destabilizing agents combined with CD95 inhibition might further antagonize the accelerated outgrowth following liver surgery.
In line with the results demonstrating the importance of hypoxia in accelerated tumor growth, we show in **chapter 7** that severe ischemia due to prolonged vascular clamping during liver surgery is associated with a reduced time to hepatic tumor recurrence in patients with colorectal liver metastases. Treatment modalities aimed at reducing hypoxia-induced signaling during or following surgical treatment of colorectal liver metastases may be beneficial in reducing tumor recurrence. Clinical trials exploring the effects of such compounds should be conducted in the future. In addition, other relevant hypotheses need to be tested in hypoxia-induced tumor outgrowth following liver surgery. First, cytotoxic agents that are activated by hypoxia may be valuable in reducing tumor outgrowth. These hypoxia-activated pro-drugs are only active in hypoxic areas and may be used peri-operatively without inducing extensive side-effects compared to regular cytotoxic agents. Furthermore, cancer stem cells are believed to be essential in tumor recurrence following cancer treatment due to drug resistance. Interestingly, hypoxia has been demonstrated to induce cancer stemness.[32] Exploring the effect of surgery-induced hypoxia on cancer stem cell expansion or de-differentiation of tumor cells to a stem-like state would further augment our understanding of surgery-stimulated tumor growth.

Liver surgery & angiogenesis
Tumor recurrence following liver surgery depends on angiogenesis.[33] Besides activation and proliferation of local endothelial cells, bone marrow derived (endothelial) progenitor cells (EPCs) contribute to this process.[34] The contribution of EPCs to tumor growth appears to be especially relevant when the tumor is challenged with chemotherapy or vascular disrupting agents.[35] Interestingly, it has been demonstrated that Granolocyte-Colony Stimulating Factor (G-CSF) receptor knockout mice did not show a rapid increase of EPCs in the blood combined with tumor regrowth following treatment with a vascular disrupting agent.[36] In **chapter 8** we find that liver surgery induces a rapid release of EPCs in conjunction with an upregulation of G-CSF. Also, administration of G-CSF to mice and volunteers induces an increase of EPCs. Although these results suggest a role for G-CSF in surgery-induced EPC release, its exact function herein remains to be elucidated. Using the G-CSF receptor knockout mice in our mouse model, we could explore whether G-CSF is important in liver surgery-induced EPC release and whether these cells contribute to the accelerated tumor outgrowth. Insights in the mechanisms responsible for EPC release following liver surgery may lead to potential therapeutic targets for reducing its release. However, to what extent EPCs contribute to tumor recurrence following liver surgery needs to be explored first.

In conclusion, our results increase the understanding how liver surgery affects residual tumor tissue. We demonstrate the association of hypoxia with surgery-stimulated tumor outgrowth. In addition, CD95 activation upon hypoxia is important for tumor cell invasion and outgrowth following liver surgery in our model. Nonetheless, despite CD95 inhibition in tumor cells, tumor cell invasion as well as tumor outgrowth were still increased in the hypoxic areas compared to that in the normoxic areas in the liver. Other hypoxia-induced or inflammation-induced factors may play an additional role in the accelerated outgrowth following liver surgery. In addition, whether the obtained results are applicable to liver tumors irrespective of their origin should be further elucidated.
Several suggestions for daily clinical practice can be made based on the results presented in this thesis. First, testing the K-Ras mutation status in tumors of patients treated with TRAIL-receptor-

activating therapeutics should be performed in order to test whether possible tumor resistance is associated with the presence of activating mutations in K-Ras. Second, liver ischemia due to clamping of the heptic inflow during partial hepatectomy for colorectal liver metastases should be omitted when it is not obligatory or should be kept to an absolute minimum in case of (impending) excessive blood loss. Furthermore, a debate is ongoing in literature whether RFA should be used as a replacement for resection of small colorectal liver metastases.[37] Although (local) recurrences and therefore re-interventions occur more often in patients with colorectal liver metastases treated with RFA compared to patients treated with resection, overall survival is similar between these patient groups.[38] Our results may -in part- explain the high incidence of local recurrences following RFA. In addition, this thesis forms the basis for performing clinical trials in surgical patients with colorectal liver metastases in which the efficacy will be tested of therapeutics that reduce hypoxia-induced signaling including HIF and CD95.

References

1. Corbett TH, Griswold DP, Jr., Roberts BJ, Peckham JC, Schabel FM, Jr. Tumor induction relationships in development of transplantable cancers of the colon in mice for chemotherapy assays, with a note on carcinogen structure. Cancer Res 1975; 35: 2434-2439.
2. O'Reilly MS, Holmgren L, Shing Y, Chen C, Rosenthal RA, Moses M, Lane WS, Cao Y, Sage EH, Folkman J. Angiostatin: a novel angiogenesis inhibitor that mediates the suppression of metastases by a Lewis lung carcinoma. Cell 1994; 79: 315-328.
3. O'Reilly MS, Boehm T, Shing Y, Fukai N, Vasios G, Lane WS, Flynn E, Birkhead JR, Olsen BR, Folkman J. Endostatin: an endogenous inhibitor of angiogenesis and tumor growth. Cell 1997; 88: 277-285.
4. Peeters CF, de Waal RM, Wobbes T, Ruers TJ. Metastatic dormancy imposed by the primary tumor: does it exist in humans? Ann Surg Oncol 2008; 15: 3308-3315.
5. Peeters CF, Westphal JR, de Waal RM, Ruiter DJ, Wobbes T, Ruers TJ. Vascular density in colorectal liver metastases increases after removal of the primary tumor in human cancer patients. Int J Cancer 2004; 112: 554-559.
6. Hung KE, Maricevich MA, Richard LG, Chen WY, Richardson MP, Kunin A, Bronson RT, Mahmood U, Kucherlapati R. Development of a mouse model for sporadic and metastatic colon tumors and its use in assessing drug treatment. Proc Natl Acad Sci U S A 2010; 107: 1565-1570.
7. Smakman N, Borel Rinkes IH, Voest EE, Kranenburg O. Control of colorectal metastasis formation by K-Ras. Biochim Biophys Acta 2005; 1756: 103-114.
8. Wiltrout RH. Regulation and antimetastatic functions of liver-associated natural killer cells. Immunol Rev 2000; 174: 63-76.
9. Smyth MJ, Crowe NY, Pellicci DG, Kyparissoudis K, Kelly JM, Takeda K, Yagita H, Godfrey DI. Sequential production of interferon-gamma by NK1.1(+) T cells and natural killer cells is essential for the antimetastatic effect of alpha-galactosylceramide. Blood 2002; 99: 1259-1266.
10. Kleber S, Sancho-Martinez I, Wiestler B, Beisel A, Gieffers C, Hill O, Thiemann M, Mueller W, Sykora J, Kuhn A, Schreglmann N, Letellier E, Zuliani C, Klussmann S, Teodorczyk M, Grone HJ, Ganten TM, Sultmann H, Tuttenberg J, von DA, Regnier-Vigouroux A, Herold-Mende C, Martin-Villalba A. Yes and PI3K bind CD95 to signal invasion of glioblastoma. Cancer Cell 2008; 13: 235-248.
11. Trauzold A, Roder C, Sipos B, Karsten K, Arlt A, Jiang P, Martin-Subero JI, Siegmund D, Muerkoster S, Pagerols-Raluy L, Siebert R, Wajant H, Kalthoff H. CD95 and TRAF2 promote invasiveness of pancreatic cancer cells. FASEB J 2005; 19: 620-622.
12. Barnhart BC, Legembre P, Pietras E, Bubici C, Franzoso G, Peter ME. CD95 ligand induces motility and invasiveness of apoptosis-resistant tumor cells. EMBO J 2004; 23: 3175-3185.
13. Trarbach T, Moehler M, Heinemann V, Kohne CH, Przyborek M, Schulz C, Sneller V, Gallant G, Kanzler S. Phase II trial of mapatumumab, a fully human agonistic monoclonal antibody that targets and activates the tumour necrosis factor apoptosis-inducing ligand receptor-1 (TRAIL-R1), in patients with refractory colorectal cancer. Br J Cancer 2010; 102: 506-512.
14. Mom CH, Verweij J, Oldenhuis CN, Gietema JA, Fox NL, Miceli R, Eskens FA, Loos WJ, de Vries EG, Sleijfer S. Mapatumumab, a fully human agonistic monoclonal antibody that targets TRAIL-R1, in combination with gemcitabine and cisplatin: a phase I study. Clin Cancer Res 2009; 15: 5584-5590.
15. Bos JL. ras oncogenes in human cancer: a review. Cancer Res 1989; 49: 4682-4689.
16. Jones S, Chen WD, Parmigiani G, Diehl F, Beerenwinkel N, Antal T, Traulsen A, Nowak MA, Siegel C, Velculescu VE, Kinzler KW, Vogelstein B, Willis J, Markowitz SD. Comparative lesion sequencing provides insights into tumor evolution. Proc Natl Acad Sci U S A 2008; 105: 4283-4288.
17. Loupakis F, Pollina L, Stasi I, Ruzzo A, Scartozzi M, Santini D, Masi G, Graziano F, Cremolini C, Rulli E, Canestrari E, Funel N, Schiavon G, Petrini I, Magnani M, Tonini G, Campani D, Floriani I, Cascinu S, Falcone A. PTEN expression and K-Ras mutations on primary tumors and metastases in the prediction of benefit from

cetuximab plus irinotecan for patients with metastatic colorectal cancer. J Clin Oncol 2009; 27: 2622-2629.
18. Santini D, Loupakis F, Vincenzi B, Floriani I, Stasi I, Canestrari E, Rulli E, Maltese PE, Andreoni F, Masi G, Graziano F, Baldi GG, Salvatore L, Russo A, Perrone G, Tommasino MR, Magnani M, Falcone A, Tonini G, Ruzzo A. High concordance of K-Ras status between primary colorectal tumors and related metastatic sites: implications for clinical practice. Oncologist 2008; 13: 1270-1275.
19. Sjoblom T, Jones S, Wood LD, Parsons DW, Lin J, Barber TD, Mandelker D, Leary RJ, Ptak J, Silliman N, Szabo S, Buckhaults P, Farrell C, Meeh P, Markowitz SD, Willis J, Dawson D, Willson JK, Gazdar AF, Hartigan J, Wu L, Liu C, Parmigiani G, Park BH, Bachman KE, Papadopoulos N, Vogelstein B, Kinzler KW, Velculescu VE. The consensus coding sequences of human breast and colorectal cancers. Science 2006; 314: 268-274.
20. Zitvogel L, Tesniere A, Kroemer G. Cancer despite immunosurveillance: immunoselection and immunosubversion. Nat Rev Immunol 2006; 6: 715-727.
21. Hansler J, Wissniowski TT, Schuppan D, Witte A, Bernatik T, Hahn EG, Strobel D. Activation and dramatically increased cytolytic activity of tumor specific T lymphocytes after radio-frequency ablation in patients with hepatocellular carcinoma and colorectal liver metastases. World J Gastroenterol 2006; 12: 3716-3721.
22. Zerbini A, Pilli M, Laccabue D, Pelosi G, Molinari A, Negri E, Cerioni S, Fagnoni F, Soliani P, Ferrari C, Missale G. Radiofrequency thermal ablation for hepatocellular carcinoma stimulates autologous NK-cell response. Gastroenterology 2010; 138: 1931-1942.
23. den Brok MH, Sutmuller RP, van der Voort R, Bennink EJ, Figdor CG, Ruers TJ, Adema GJ. In situ tumor ablation creates an antigen source for the generation of antitumor immunity. Cancer Res 2004; 64: 4024-4029.
24. Johnson EE, Yamane BH, Buhtoiarov IN, Lum HD, Rakhmilevich AL, Mahvi DM, Gillies SD, Sondel PM. Radiofrequency Ablation Combined with KS-IL2 Immunocytokine (EMD 273066) Results in an Enhanced Antitumor Effect against Murine Colon Adenocarcinoma. Clin Cancer Res 2009; 15: 4875-4884.
25. Katz SC, Pillarisetty V, Bamboat ZM, Shia J, Hedvat C, Gonen M, Jarnagin W, Fong Y, Blumgart L, D'Angelica M, Dematteo RP. T cell infiltrate predicts long-term survival following resection of colorectal cancer liver metastases. Ann Surg Oncol 2009; 16: 2524-2530.
26. Ma H, Zhang Y, Wang Q, Li Y, He J, Wang H, Sun J, Pan K, Chen M, Xia J. Therapeutic safety and effects of adjuvant autologous RetroNectin activated killer cell immunotherapy for patients with primary hepatocellular carcinoma after radiofrequency ablation. Cancer Biol Ther 2010; 9:
27. Semenza GL. Targeting HIF-1 for cancer therapy. Nat Rev Cancer 2003; 3: 721-732.
28. Rajaganeshan R, Prasad R, Guillou PJ, Poston G, Scott N, Jayne DG. The role of hypoxia in recurrence following resection of Dukes' B colorectal cancer. Int J Colorectal Dis 2008; 23: 1049-1055.
29. Baba Y, Nosho K, Shima K, Irahara N, Chan AT, Meyerhardt JA, Chung DC, Giovannucci EL, Fuchs CS, Ogino S. HIF1A Overexpression Is Associated with Poor Prognosis in a Cohort of 731 Colorectal Cancers. Am J Pathol 2010;
30. van der Bilt JD, Soeters ME, Duyverman AM, Nijkamp MW, Witteveen PO, van Diest PJ, Kranenburg O, Borel Rinkes IH. Perinecrotic hypoxia contributes to ischemia/reperfusion-accelerated outgrowth of colorectal micrometastases. Am J Pathol 2007; 170: 1379-1388.
31. Harris AL. Hypoxia--a key regulatory factor in tumour growth. Nat Rev Cancer 2002; 2: 38-47.
32. Heddleston JM, Li Z, Lathia JD, Bao S, Hjelmeland AB, Rich JN. Hypoxia inducible factors in cancer stem cells. Br J Cancer 2010; 102: 789-795.
33. van der Bilt JD and Borel Rinkes IH. Surgery and angiogenesis. Biochim Biophys Acta 2004; 1654: 95-104.
34. Lyden D, Hattori K, Dias S, Costa C, Blaikie P, Butros L, Chadburn A, Heissig B, Marks W, Witte L, Wu Y, Hicklin D, Zhu Z, Hackett NR, Crystal RG, Moore MA, Hajjar KA, Manova K, Benezra R, Rafii S. Impaired recruitment of bone-marrow-derived endothelial and hematopoietic precursor cells blocks tumor angiogenesis and growth. Nat Med 2001; 7: 1194-1201.
35. Shaked Y, Ciarrocchi A, Franco M, Lee CR, Man S, Cheung AM, Hicklin DJ, Chaplin D, Foster FS, Benezra R,

Kerbel RS. Therapy-induced acute recruitment of circulating endothelial progenitor cells to tumors. Science 2006; 313: 1785-1787.
36. Shaked Y, Tang T, Woloszynek J, Daenen LG, Man S, Xu P, Cai SR, Arbeit JM, Voest EE, Chaplin DJ, Smythe J, Harris A, Nathan P, Judson I, Rustin G, Bertolini F, Link DC, Kerbel RS. Contribution of granulocyte colony-stimulating factor to the acute mobilization of endothelial precursor cells by vascular disrupting agents. Cancer Res 2009; 69: 7524-7528.
37. Mulier S, Ruers T, Jamart J, Michel L, Marchal G, Ni Y. Radiofrequency ablation versus resection for resectable colorectal liver metastases: time for a randomized trial? An update. Dig Surg 2008; 25: 445-460.
38. Otto G, Duber C, Hoppe-Lotichius M, Konig J, Heise M, Pitton MB. Radiofrequency Ablation as First-Line Treatment in Patients With Early Colorectal Liver Metastases Amenable to Surgery. Ann Surg 2010; 251: 796-804.

Chapter 10


LABORATORIUM VOOR
EXPERIMENTELE HEELKUNDE
BIJ ROOD LICHT
NIET STOREN A.U.B.
Laboratorium voor
Experimentele Heelkunde
Experimentlokaal
254

Summary in Dutch - Nederlandse samenvatting

Dikkedarmkanker en uitzaaiingen naar de lever

Alle organen en weefsels in het menselijk lichaam zijn opgebouwd uit miljarden cellen. De cellen bevatten in hun kernen het erfelijke materiaal, het DNA. In het DNA liggen de erfelijke eigenschappen opgeslagen. Ieder stukje DNA dat de code bevat voor één van de vele eiwitten waaruit het lichaam is opgebouwd wordt een gen genoemd. In iedere cel treden er continu beschadigingen en fouten (mutaties) op in het DNA. De cel kan deze beschadiging onschadelijk maken met behulp van bepaalde verdedigings- en reparatiemechanismen. Helaas komt het voor dat deze herstelmechanismen tekort schieten. Als een aaneenschakeling van dergelijke mutaties zich bevinden op zeer belangrijke plekken (genen) in het DNA, dan kan kanker ontstaan. Eén van de genen die vaak gemuteerd is in het geval van dikkedarmkanker (colorectaal carcinoom), is het K-Ras gen (in ongeveer 40% van de gevallen). Het K-Ras gen bevat de erfelijke code voor een eiwit dat betrokken is bij de signaaloverdracht van groeistimulerende stoffen. Normaal kan dit eiwit aan- of uit worden gezet, maar indien er een mutatie is opgetreden staat het eiwit altijd 'aan'. Hierdoor kan het groeisignaal voortdurend worden doorgegeven, wat leidt tot ongeremde celdeling, een belangrijk kenmerk van kanker.

Dikkedarmkanker is een van de meest voorkomende vormen van kanker in de westerse wereld. Jaarlijks wordt de diagnose bij ongeveer 12.000 nieuwe patiënten in Nederland gesteld en overlijden er ongeveer 5.000 mensen aan. Meestal overlijden patiënten aan dikkedarmkanker omdat de ziekte is uitgezaaid, wat meestal naar de lever gebeurt. Hoewel de rol van het K-Ras in het ontwikkelen van dikkedarmkanker uitgebreid is onderzocht, is de rol in de vorming van uitzaaiingen onduidelijk. In **hoofdstuk 2** van dit proefschrift hebben wij gekeken naar de rol van een K-Ras mutatie in het vormen van leveruitzaaiingen van dikkedarmkanker.

Chirurgische behandeling van leveruitzaaiingen van dikkedarmkanker

Ongeveer de helft van alle patiënten met dikkedarmkanker krijgt leveruitzaaiingen (levermetastasen). Met alleen chemotherapie kan het leven van deze patiënten verlengd worden van ongeveer 10 naar 20 maanden, maar patiënten kunnen nog niet genezen worden. Het wegsnijden van de uitzaaiing (leverresectie) biedt tot op heden de enige kans op genezing. Omdat de lever anatomisch gezien uit 8 kleine 'sub-levers' bestaat is het mogelijk dat deel van de lever weg te snijden waar de uitzaaiing in zit. Na 5 jaar is ongeveer 35-60% van de patiënten die geopereerd zijn nog in leven, na 10 jaar is dat ongeveer 25%. Echter, de leveruitzaaiingen kunnen maar bij een kwart van de patiënten weggesneden worden. Voor patiënten bij wie de leveruitzaaiing niet weggesneden kan worden, is het soms mogelijk deze te vernietigen met behulp van hitte. Radiofrequente ablatie (RFA) wordt tegenwoordig in deze techniek het meest toegepast. Met behulp van een dikke naald die in de uitzaaiing wordt gestoken, wordt een wisselstroom teweeg gebracht. De ionen in de uitzaaiing worden door deze wisselstroom zo snel heen en weer bewogen dat frictiehitte ontwikkeld wordt. De temperatuur wordt hierbij zo hoog (boven de 60ºC) dat de uitgezaaide kankercellen sterven. De resultaten van deze techniek zijn veelbelovend en sommigen claimen zelfs dat het in bepaalde gevallen het wegsnijden van de uitzaaiing zou kunnen vervangen.

Recidief van chirurgisch behandelde uitzaaiingen: rol van micrometastasen

Een groot probleem van kanker is het terugkomen van de ziekte (recidief) nadat deze in eerste instantie succesvol is behandeld. Ook na leverchirurgie voor uitzaaiingen van dikkedarmkanker komen recidieven vaak voor, in maar liefst 60-70% van de gevallen. De meest waarschijnlijke bron voor deze recidieven zijn kleine onzichtbare uitzaaiingen (micrometastasen) die al ten tijde van de

leveroperatie aanwezig waren in de lever. Omdat we deze micrometastasen nog niet in beeld kunnen brengen, weten we niet waar deze zich bevinden in het lichaam. Het komt dus vaak voor dat deze overblijvende micrometastasen zich in het achterblijvende deel van de lever bevinden, waardoor zich weer een nieuwe uitzaaiing kan vormen. Veelal wordt de prognose van een patiënt bepaald door het terugkomen van de kanker.
De RFA behandeling heeft naast een recidief elders in de lever ook kans op een lokaal recidief. Dit houdt in dat er nieuwe kanker groeit in de rand van het met de hitte gedode weefsel. Naast de aanwezigheid van deze micrometastasen ten tijde van de operatie is bij de RFA sprake van een tweede bron van achterblijvende kankercellen. Normaliter wordt geprobeerd al het uitgezaaide kankerweefsel én een klein stukje gezond leverweefsel met de hitte te vernietigen om een zekerheidsmarge te creëren. Maar men kan zich voorstellen dat de hitte die ontwikkeld wordt bij de RFA behandeling het grootst is dicht bij de dikke naald en dat deze afneemt met de afstand ten opzichte van de naald. Het kan dus voorkomen dat in de rand van het gedode weefsel waar de hitte niet hoog genoeg geworden is nog kankercellen leven die de hitte hebben overleefd. Deze cellen kunnen ook de bron zijn van een lokaal recidief, dat in ongeveer 15% van de gevallen voorkomt.

Chirurgie-gestimuleerde tumorgroei
Micrometastasen kunnen jarenlang in een soort slapende toestand verkeren zonder dat deze uitgroeien tot een grote uitzaaiing. In de vakliteratuur wordt gesteld dat weefselschade de micrometastasen wakker zou kunnen schudden waardoor ze uitgroeien tot grote uitzaaiingen. Al in 1927 toonde een Groningse professor in een diermodel aan dat wondgenezing tumorgroei stimuleerde. Aangezien chirurgie -logischerwijs- gepaard gaat met wondgenezing zijn er sindsdien veel onderzoeken verschenen over chirurgie-gestimuleerde tumorgroei. Groeifactoren die belangrijk zijn bij wondgenezing zouden een rol kunnen spelen, maar de oorzaak van de groeistimulatie is niet volledig duidelijk. In dit proefschrift hebben wij onderzocht wat de invloed is van leverchirurgie op micrometastasen. Hiervoor hebben wij gebruik gemaakt van twee verschillende procedures die vaak gebruikt worden in de leverchirurgie: de eerder genoemde radiofrequente ablatie (RFA) en het afklemmen van de bloedtoevoer naar de lever.

Afklemmen van de bloedtoevoer naar de lever en ischemie/reperfusie schade
Het doel van leverchirurgie voor leveruitzaaiingen is het volledig verwijderen van alle uitzaaiingen zonder (veel) bloedverlies. Bloedverlies tijdens het wegsnijden van de uitzaaiing treedt regelmatig op omdat de lever zeer goed doorbloed is. Het is aangetoond dat bloedverlies erge complicaties en zelfs overlijden tot gevolg kan hebben. Tijdens de operatie wordt dan ook vaak de bloedtoevoer naar de lever afgeklemd om zo het bloedverlies te verminderen. Bovendien wordt ook tijdens de RFA behandeling de bloedtoevoer afgeklemd. Men kan zich voorstellen dat de hitte die nodig is om al het kankerweefsel te vernietigen wordt weggevoerd door de bloedstroom, zoals een hete pan onder de koude kraan. Om dit te voorkomen wordt ook tijdens de RFA behandeling de bloedtoevoer naar de lever (tijdelijk) afgeklemd.
Het tijdelijk afklemmen van de bloedtoevoer naar de lever heeft ook een nadelig effect. Door het tijdelijk afklemmen van de bloedtoevoer naar de lever ontstaat zuurstoftekort in de levercellen (ischemie). Wanneer de klem verwijderd wordt en de zuurstoftoevoer naar de lever is hersteld, spreekt men van reperfusie. Het is bekend dat ischemie gevolgd door reperfusie schade (ischemie/reperfusie schade) aan de levercellen veroorzaakt. Daarnaast heeft onze onderzoeksgroep aangetoond

dat micrometastasen in de levers van muizen harder uitgroeien na het tijdelijk afklemmen van de bloedtoevoer naar de lever. Het werkingsmechanisme hierachter is echter niet bekend.

K-Ras & leveruitzaaiingen van dikkedarmkanker

Voordat een kankercel van dikkedarmkanker een leveruitzaaiing kan vormen, moet het een reeks van gebeurtenissen doorstaan. Al deze opeenvolgende gebeurtenissen moeten succesvol worden uitgevoerd voordat een uitzaaiing kan ontstaan. Ten eerste moeten de kankercellen los komen van de dikkedarmkanker. De kankercellen moeten daarna het basale membraan afbreken dat de kankercellen omringt en vervolgens naar een bloedvat bewegen om de bloedbaan binnen te dringen (intravasatie). Hier moeten de kankercellen alleen (dus niet ondersteund door andere cellen) kunnen overleven. De kankercellen bereiken via de darmvenen en de poortader de lever, waar ze vastlopen in kleine leverbloedvaatjes. Door uit deze bloedvaatjes te treden bereiken ze het leverweefsel. Hier kunnen ze alleen overleven door het immuunsysteem van de lever te overwinnen. Om vervolgens verder uit te groeien tot een grote uitzaaiing moeten de kankercellen nieuwe bloedvaten vormen om zuurstof en voedingsstoffen te krijgen. In **hoofdstuk 2** hebben wij gekeken naar de rol van de K-Ras mutatie in het uitzaaien van dikkedarmkankercellen. Wij hebben hierin specifiek gekeken naar de rol van K-Ras in het overleven van de kankercellen in de lever. Zoals gezegd moeten kankercellen het immuunsysteem van de lever overwinnen om uit te groeien tot een grote uitzaaiing. Een manier van immuuncellen in de lever om binnendringende kankercellen te vernietigen is het activeren van het zogenaamde 'death receptor' systeem. Door dit systeem te activeren wordt in normale gevallen een (kanker)cel gestimuleerd om dood te gaan, eigenlijk om zelfmoord te plegen (apoptose). Hierbij wordt de receptor (CD95) geactiveerd door zijn overeenkomende ligand (CD95-Ligand), zoals een sleutel een bepaald slot kan openen. Naast het CD95-Ligand (ook wel Fas-Ligand genoemd) is TRAIL een ander 'death receptor' ligand. Dit laatste eiwit wordt ook in kankerpatiënten gebruikt om te testen of het de kanker kan laten doodgaan. Uit de resultaten van **hoofdstuk 2** bleek echter dat wanneer K-Ras gemuteerde kankercellen gestimuleerd werden met deze liganden, zij niet dood gingen maar juist een invasief karakter aannamen. Bovendien waren kankercellen met een K-Ras mutatie in staat om leveruitzaaiingen in muizen te vormen, terwijl kankercellen zonder de K-Ras mutatie dat niet konden. Dus, een K-Ras mutatie in dikkedarmkankercellen zorgt voor een switch van het signaal van de 'death-receptors': van zelfmoord plegen naar invasief worden. Door een brede screen uit te voeren onder de eiwitten die K-Ras kan aansturen, bleek dat het Raf1 eiwit hiervoor verantwoordelijk was doordat het de cascade Rho-ROCK-LIM kinase-cofillin blokkeert waardoor onder andere de beweeglijkheid van de tumorcellen beïnvloed wordt.

Concluderend betekent dit dat dikkedarmkankercellen met een K-Ras mutatie niet doodgaan van eiwitten die de 'death receptors' activeert, maar dat ze dat signaal kunnen overleven en zelfs invasiever worden. De eiwitten die 'death receptors' activeren die aan patiënten worden gegeven om de kanker te vernietigen zouden dus wel eens averechts kunnen werken wanneer de kanker een K-Ras mutatie heeft. Vandaar dat patiënten die dergelijke medicijnen krijgen getest zouden moeten worden op de aanwezigheid van een K-Ras mutatie.

Onderzoeken van chirurgie-gestimuleerde tumorgroei

Om het effect van leverchirurgie op het uitgroeien van micrometastasen te onderzoeken hebben wij gebruik gemaakt van een muizenmodel. Muizen kregen dikkedarmkankercellen ingespoten in de milt. De milt is verbonden met de lever via de poortader, die ook de darmen met de lever verbindt.

Zo wordt de totstandkoming van een uitzaaiing nagebootst. Door de kankercellen een aantal dagen te laten uitgroeien ontstaan er micrometastasen die zich gelijkmatig verspreid door de lever bevinden. Na enkele dagen worden de muizen aan de lever geopereerd. Ofwel met RFA waarbij een klein stukje lever wordt weggebrand, ofwel door de bloedtoevoer naar de lever af te klemmen. In beide gevallen sterft een stukje leverweefsel af (necrose). Vergelijkbaar aan het effect van het afklemmen, bleek in **hoofdstuk 3** dat tumorcellen in de rand van het dode leverweefsel sneller uitgroeiden dan kankercellen elders in de lever. Wij hebben vervolgens geprobeerd te achterhalen hoe dit komt.

Leverchirurgie & hypoxie (laag zuurstof gehalte)

De versnelde kankergroei na leverchirurgie was specifiek gelegen in de rand van het dode leverweefsel, na zowel RFA als na het afklemmen van de bloedtoevoer naar de lever. In het geval van het afklemmen heeft onze onderzoeksgroep eerder aangetoond dat de rand van het gedode leverweefsel zich kenmerkt door een verlaagd zuurstofgehalte (hypoxie). Het is bekend dat kankercellen agressief gaan groeien van een verlaagd zuurstofgehalte. Ze gaan als het ware hard op zoek naar een bloedvat waar zuurstof is. Belangrijke eiwitten die ervoor zorgen dat kankercellen kunnen overleven onder een verlaagd zuurstofgehalte zijn de Hypoxia Inducible Factors HIF-1α en HIF-2α. Het bleek in **hoofdstuk 3** dat beide eiwitten in verhoogde mate aanwezig en actief waren in de rand van het gedode leverweefsel nadat de muizen een RFA behandeling ondergaan hadden. Door deze eiwitten te remmen met een geneesmiddel waren wij in staat de versnelde uitgroei na RFA te verminderen.

Het lage zuurstofgehalte bleek al in een vroeg stadium (enkele uren) na de leveroperaties aanwezig te zijn. Daarom wilden wij weten wat het vroege effect van de operaties op de micrometastasen zou zijn. Met speciale lichtgevende kankercellen die we zichtbaar konden maken met een speciale microscoop konden we de kankercellen volgen. Het bleek dat zowel RFA (**hoofdstuk 5**) en afklemmen van de bloedtoevoer naar de lever (**hoofdstuk 6**) er voor zorgden dat de kankercellen een invasief karakter aannamen. Omdat de kankercellen die wij hiervoor gebruikten dezelfde waren als in **hoofdstuk 2** (waarin wij aantoonden dat het activeren van de 'death receptor' CD95 de kankercellen invasief maakten in plaats van dood te laten laten gaan) wilden wij weten of deze receptor misschien geactiveerd werd door leverchirurgie. Wij toonden in **hoofdstuk 5** aan dat een verlaagd zuurstofgehalte het CD95 in de kankercellen activeerde. Het bleek ook dat in de muizen het CD95 en het bijbehorende CD95-Ligand meer aanwezig waren in de rand van het gedode leverweefsel na de RFA behandeling. Vervolgens hebben wij op drie verschillende manieren het CD95/CD95-Ligand systeem geremd en gekeken wat het effect hiervan was op het invasieve karakter en de uitgroei van de kankercellen na RFA. Ten eerste hebben we de muizen behandeld met een geneesmiddel dat het CD95-Ligand neutraliseert. We zagen dat hierdoor het invasieve karakter afnam. Vervolgens hebben we kankercellen gebruikt waarin het CD95 genetisch geremd was. Ook hierbij was de invasiviteit en ook de uitgroei van de kankercellen verminderd, waardoor een direct effect van het CD95/CD95-Ligand systeem op de kankercellen aangetoond werd. Om tenslotte te kijken wat de bijdrage van het CD95-Ligand van de muis was in de invasiviteit en uitgroei van de kankercellen na RFA, hebben we gekeken naar het effect in muizen die een genetische mutatie hadden ondergaan waardoor zij geen CD95-Ligand hadden. In deze muizen bleek de invasiviteit en uitgroei van de kankercellen na RFA *níet* verminderd te zijn. Daarom denken wij dat de kankercellen zelf verantwoordelijk zijn voor het CD95-Ligand en de daarop volgende CD95 activatie, zonder dat de muis hier invloed op heeft.

Zoals bekend gaat ook het afklemmen van de bloedtoevoer naar de lever gepaard met een verlaagd zuurstofgehalte en versnelde uitgroei van kanker. Daarom hebben wij in **hoofdstuk 6** gekeken naar de rol van het CD95 in invasiviteit en versnelde uitgroei van kankercellen na afklemmen. Wij zagen vergelijkbare resultaten als na RFA, zoals in **hoofdstuk 5** beschreven. De invasiviteit en uitgroei van kankercellen na het afklemmen van de bloedtoevoer bleek ook verminderd te zijn als wij kankercellen gebruikten waarin het CD95 genetisch geremd was. Als wij vervolgens de muizen gebruikten die geen CD95-Ligand hadden dan bleek de invasiviteit *niet* verminderd, wat weer doet vermoeden dat het CD95-Ligand van de kankercellen zelf belangrijk is en niet zo zeer het CD95-Ligand van de muis. Interessant genoeg was de uitgroei van de kankercellen in deze muizen juist *wel* verminderd. Omdat deze muizen ook een verminderde schade (minder dood leverweefsel) lieten zien na het afklemmen vergeleken met normale muizen, denken wij dat dit de oorzaak is van de verminderde kanker uitgroei.

Het belang van een verlaagd zuurstofgehalte bij het sneller uitgroeien van de kanker na leverchirurgie is dus onmiskenbaar. In **hoofdstuk 7** hebben wij vervolgens gekeken bij 160 patiënten met leveruitzaaiingen van dikkedarmkanker wat de invloed was van het afklemmen van de bloedtoevoer naar de lever op het terugkeren van de kanker. Hierbij deelden wij patiënten in naar heftigheid van leverischemie (dat een verlaagd zuurstofgehalte tot gevolg heeft). De drie groepen van leverischemie werden gedefinieerd op basis van de duur en de techniek van het afklemmen van de bloedtoevoer: geen ischemie (niet afgeklemd), matige ischemie en ernstige ischemie. De grens tussen matige en ernstige leverischemie was gebaseerd op onderzoek in muizen dat wij eerder uitgevoerd hadden. Het bleek dat de patiënten die veel leverischemie ondergingen de kanker eerder terug kregen in de lever dan patiënten die geen leverischemie kregen. Na enkele statistische berekeningen konden we zelfs aantonen dat de ernstige leverischemie een onafhankelijke correlatie had met het terugkeren van de ziekte. Echter, door de studieopzet was het niet mogelijk een causaal verband aan te tonen. Desalniettemin zou het afklemmen van de bloedtoevoer naar de lever bij patiënten die een leveroperatie ondergaan voor uitzaaiingen van dikkedarmkanker zo veel mogelijk vermeden moeten worden.

Leverchirurgie & angiogenese (vaatnieuwvorming)

Een belangrijk gevolg van zuurstoftekort is vaatnieuwvorming (angiogenese). Kankercellen proberen op deze manier hun zuurstofgehalte te verhogen zodat ze verder kunnen uitgroeien. Alle kankers zijn hiervan afhankelijk, zo ook leveruitzaaiingen van dikkedarmkanker en ook het recidief van de uitzaaiing nadat deze is weggesneden of weggebrand. Deze nieuwe bloedvaatjes kunnen opgebouwd worden uit andere bloedvatcellen (endotheelcellen) maar ook voorloper (progenitor) cellen uit het beenmerg kunnen hieraan bijdragen, de zogenaamde endotheliale progenitor cellen (EPC). De bijdrage van de EPC's aan de vaatnieuwvorming in de tumor blijkt vooral van belang als de kanker terugkomt (recidiveert) nadat deze behandeld is met bepaalde soorten chemotherapie. Hierbij blijkt het eiwit Granulocyte-Colony Stimulating Factor (G-CSF) een belangrijke rol te spelen, dat er voor zorgt dat de EPC's uit het beenmerg via het bloed naar de kanker gaan. In **hoofdstuk 8** wilden wij weten of leverchirurgie ook zorgt voor een stijging van de EPC's in het bloed en wat de rol van G-CSF hierin was. Het bloed werd onderzocht van 12 patiënten die ofwel RFA ofwel leverresectie ondergingen. Een acute stijging van EPC's kon worden waargenomen direct nadat de buik van de patiënt was geopend. Deze stijging bleef aanwezig tot 20 minuten na de ingreep, waarna het weer daalde.

Ondanks dat het G-CSF pas later een stijging in het bloed van de patiënten liet zien, bleek dat wanneer G-CSF aan muizen of vrijwilligers werd gegeven dit wel een stijging van de EPC's veroorzaakte. De exacte rol van G-CSF in de patiënten is echter niet duidelijk. Toekomstig onderzoek zou zich hierop kunnen concentreren. Ook zou duidelijk moeten worden wat de bijdrage is van de EPC's aan het kankerrecidief na leverchirurgie.

Leverchirurgie & ontsteking (inflammatie)

Een belangrijk bijverschijnsel van de RFA behandeling van leveruitzaaiingen is de aanwakkering van het immuunsysteem. Doordat de kankercellen vernietigd worden door de hitte, maar wel achterblijven in het lichaam, kunnen kleine stukjes eiwit van de kanker in de bloedstroom komen. Deze kleine stukjes kankereiwit hebben een zelfde soort werking als een vaccinatie: het kan de patiënt niet meer ziek maken, maar er wordt wel een ontstekingsreactie (immuunrespons) tegen aangemaakt. Als de immuunrespons sterk genoeg is, kan het vervolgens ook de achterblijvende kankercellen gaan tegenwerken en vernietigen. In **hoofdstuk 4** wilden wij weten hoe de ontstekingsreactie eruit zag in de versneld uitgroeiende kanker in de rand van het gedode leverweefsel na RFA. Wij zagen dat de ontstekingsreactie in de versnelde kankergroei juist minder was dan in kanker die elders in de lever was gelegen. We weten niet of de verminderde ontstekingsreactie de oorzaak of het gevolg is van de versneld uitgroeiende kanker. Het zou kunnen zijn dat het verhoogde CD95-Ligand aldaar (uit **hoofdstuk 5**) er voor zorgt dat de ontstekingscellen dood gaan (zelfmoord plegen). Toekomstig onderzoek zou moeten uitwijzen of het versterken van de lokale ontstekingsreactie de versnelde kankeruitgroei zou kunnen verminderen.

Conclusies

De resultaten van dit proefschrift breiden ons inzicht uit hoe leverchirurgie achterblijvende micrometastasen beïnvloedt. De CD95 activatie in de kankercellen door het verlaagde zuurstofgehalte dat ontstaat door de leverchirurgie blijkt een deel van het werkingsmechanisme te zijn waarom de kanker sneller uitgroeit. Andere factoren die te maken hebben met het verlaagde zuurstofgehalte of met de ontstekingsreactie zouden ook een rol kunnen spelen. Het combineren van medicijnen, bijvoorbeeld die uit **hoofdstuk 3** en **hoofdstuk 5**, zou de effectiviteit van de therapie kunnen verhogen. In toekomstig onderzoek zou ook gekeken moeten worden of dezelfde resultaten bereikt kunnen worden wanneer andere soorten cellen gebruikt worden, zodat de resultaten makkelijker naar de patiënt vertaald kunnen worden.


Chapter 11

Als ik ook maar enigszins de indruk heb gewekt dat dit proefschrift tot stand is gekomen door mijzelf, en door mijzelf alleen, dan is dat een misvatting die ik graag wil rechtzetten. Er zijn namelijk veel mensen geweest die hebben bijgedragen aan alle studies die beschreven zijn in dit proefschrift en/of aan de verdere ontwikkeling ervan. Een aantal personen wil ik hiervoor expliciet bedanken.

Prof. dr. I.H.M. Borel Rinkes, beste Inne. Translationeel onderzoek en muizen opereren, wat een schitterende combinatie! Dat jij mij deze plek hebt aangeboden zie ik als een enorm voorrecht. Ik ben je veel dank verschuldigd voor het vertrouwen dat je de afgelopen jaren in mij hebt getoond, ondanks de momenten dat mijn tact weleens te wensen over liet. De combinatie van je (wetenschappelijke) stimuleringsvermogen met je ijzersterke crisis-management maakt je tot een ideale begeleider. Het heeft me gevormd, op zowel wetenschappelijk als sociaal gebied.

Dr. O. Kranenburg, beste Onno. Al snel nadat ik op het lab kwam heb jij je hard gemaakt voor mijn aanstelling. Daar sprak een bijzonder groot vertrouwen uit. Je onuitputtelijke inzet bij het aanvragen van verschillende subsidies bleek niet voor niets en heeft er uiteindelijk toe geleid dat er rust in de tent kwam. Je blik was immer kritisch, maar ik wist (uiteindelijk) dat het de kwaliteit ten goede zou komen. Jij hebt mijn onderzoek naar een hoger plan weten te stuwen en daar ben ik je zeer dankbaar voor.

Dr. I.Q. Molenaar, beste Quintus. Een terechte plek voor jou direct na promotor en co-promotor. Voornamelijk op het morele vlak heb je een grote bijdrage geleverd aan dit proefschrift. Onze wegen kruisten bij het aanvragen van 'de Catharijne Stichting', maar je echte waarde toonde je bij het schrijven van mijn eerste paper. Jij maakte duidelijk dat op dat moment alles moest wijken voor het schrijven, ondanks de hoeveelheid projecten en de geplande experimenten. Daarna liet je me telkens de andere kant van de munt zien: als het onderzoek naar mijn idee nog niet goed genoeg was, maakte je duidelijk dat er nog wat op stapel stond, namelijk chirurg worden. Het zorgde voor een juist evenwicht tussen enerzijds gedegen onderzoek doen, maar aan de andere kant realistisch kijken naar de mogelijkheden en de toekomst. Daar hoop ik over een aantal jaren weer met je aan te werken.

Prof. dr. E.E. Voest, beste Emile. Translationeel onderzoek heeft geen basis zonder uitzicht op een klinische trial. Jij verstaat dat als geen ander. Jouw kunst om translationeel onderzoek te vertalen naar klinisch onderzoek (en vice versa) heeft dan ook een grote bijdrage geleverd aan mijn proefschrift. Ik dank je voor al je adviezen, in de breedste zin van het woord.

Prof. dr. R. Medema, beste René. Op de retraite tot diep in de nacht met een theekopje bier praten over 'belangrijke' niet-onderzoek-gerelateerde zaken. Met ontzag heb ik naar je gekeken hoe messcherp je de volgende ochtend weer op je 'troon' plaatsnam. Knallen als het moet, maar ontspannen als het kan. Dank voor je 'focussing-adviezen' in mijn AIO-commissie en je mooie verhalen van het Italiaanse voetbal.

Prof. dr. P.J. van Diest, beste Paul, wat heb jij me enthousiast weten te maken voor de pathologie! Door je hartstochtelijke betogen achter de microscoop (beginnend of eindigend met '*This is awesome!!*') is het simpelweg onmogelijk om zelf niet mee te gaan in de euforie. Maar juist als

dingen niet liepen zoals gehoopt toonde jij je kracht. Met pragmatische oplossingen zorgde je ervoor dat ik met frisse moed weer aan de slag kon. Toch blijft het voor mij een wonder dat jij in die eerste poepbruine HIF-1 kleuringen werkelijk een hoopgevend positief resultaat zag…

Prof. dr. R. van Hillegersberg, beste Richard. Ondanks dat jouw focus meer ligt op het klinische dan het preklinische onderzoek heb je je altijd zeer geïnteresseerd opgesteld ten opzichte van mijn onderzoek. Je hebt een enorme drive bij het doen van onderzoek die zich uit in de absolute wil om ons chirurgisch kunnen te vergroten. Dat zie ik als een voorbeeld. In de toekomst hoop ik ook klinisch veel van je op te mogen steken.

De overige leden van de beoordelingscommissie, prof. dr. C.H.C. Dejong, prof.dr. T.M. van Gulik en prof.dr. P.D. Siersema, u wil ik bedanken voor het kritisch beoordelen van het manuscript. Prof. dr. L.M.A. Akkermans, altijd was u geïnteresseerd als wij elkaar tegenkwamen op de gang. Ik wil u bedanken dat u op uw 'laatste werkdag' in de oppositie plaats wilt nemen!

Dr. A. Pronk, beste Apollo. Dank voor je interesse tijdens de woensdagmiddagen, je klinische visie in mijn AIO-commissie en je hulp bij de toekomst. Ik kijk er erg naar uit.

Alle medewerkers van het GDL, in het bijzonder Anja van der Sar, Jan Smits, Jannico den Breejen, Joyce Visser, Hans Vosmeer, Helma Avezaat, Hester de Bruin, Nico Attevelt, Romy van Geffen en Sabine Versteeg, altijd bereid voor een helpende hand. Jullie hulp was vaak onmisbaar bij het uitvoeren van de operaties en alles wat daarbij komt kijken. Proefdierdeskundigen dr. Harry Blom en dr. Fred Poelma, dank dat jullie deur altijd open stond voor overleg.

André Verheem, alleskunnend microchirurgisch analist. Eerst alle kastjes open trekken, dan pas gaan nadenken wat ik ook al weer nodig heb…. Hoewel ik alle CD's van Ramstein nu tegen wil en dank kan meeschreeuwen, altijd een toptijd in café *Chez-André*! Dank voor alle momenten dat je klaarstond.

De koningen en koningin van de Biobank: Jan Willem van Ginkel, Martijn van Osch en Natalie ter Hoeve. Wat hebben jullie een werk verzet voor al mijn coupes. Uiteraard op het allerlaatste moment bellen dat ze gisteren klaar moesten zijn…. Het was jullie nooit teveel.

Alle medewerkers van de afdeling Pathologie, in het bijzonder Amélie Dendooven, Annette Gijsbers-Bruggink, Cathy Moelans, Dick van Wichen, Dionne van der Giezen, Domenico Castigliego, Dorine van den Brink, Gladys Mancipe, Harry Lammers, Helga Steenbergen, Jan Beekhuis, Jan Willem Leeuwis, John de Pinth, Kevin van der Ven, Petra van der Groep (mijn IHC-juf!), Petra Homoet, Remco Radersma, Sabrina Elshof en Willy van Bragt. Dank voor al jullie hulp. Zonder jullie waren de immunohistochemische plaatjes nooit zo mooi geworden.

Alle (oud-)secretaresses van de afdeling Heelkunde, Annet van Esser, Cobie van Veen, Fatiha Asnnosi, Gioya Soós, Ingrid Norder, Kootje Custers, Marianne van Leeuwerden, Mariëlle Hoefakker, Marjolein de Vries, Romy Liesdek en Susan Hora Siccama. Ik wil jullie bedanken voor jullie geestelijke ondersteuning, die niet te onderschatten valt!

Alle collega's van de Medische Oncologie (Annelieke Jaspers, Doris Mans, Eva Vlug, Jeanine Roodhart, Joost Vermaat, Laura Daenen, Marlies Langenberg, Martijn Lolkema, Miranda van Amersfoort, Patrick Derksen, Rachel Giles, Rhandy Eman, Ron Schackmann, Sander Basten) en van de Urologie (Judith Jans en Stephanie Kroeze) together with all colleagues of the Experimental Oncology Department, many thanks for your interest and input during the work discussions, but also for the good times during other activities.

Het Kranenburg-Borel Rinkes lab: Benjamin Emmink, Daniëlle Raats, Ernst Steller, Jamila Laoukili en Menno de Bruijn. Jullie, of eigenlijk wij, zijn het bewijs dat het bundelen van krachten resulteert in een hogere uitkomst: het '1+1=3' principe. Dank voor alle hulp bij het uitvoeren van de experimenten, maar uiteraard ook voor alle dingen daar omheen!

Mijn voorgangers, Jarmila van der Bilt, Liesbeth Veenendaal en Niels Smakman, de fijne kneepjes van het doen van onderzoek heb ik van jullie geleerd. Jar, dankzij jou kon ik een vliegende start maken!

Mijn student-onderzoekers, Alie Borren, Florien Westendorp, Martijn Leenders en Taco van der Meulen. Jullie hebben me geholpen op verschillende vlakken en op verschillende manieren, maar jullie hebben één ding gemeen: dankzij jullie was het aanzienlijk makkelijker dit proefschrift zo te krijgen zoals het is.

Klaas Govaert, mijn opvolger. Via één of andere obscure instelling aan de andere kant van Woerden kwam je in aanraking met een onderzoeksleider in het UMCU… Maar, eerlijk is eerlijk, vanaf dag 1 heb je laten zien een verrijking te zijn voor onze onderzoeksgroep. Niet alleen op werktechnisch gebied, maar ook vanuit sociaal oogpunt. Kritisch als je was bij het maken van je 3700 foto's, om daarna '*nog even een paar pintjes te doen*'. Ga zo door, jouw tijd komt ook. Daar heb ik alle vertrouwen in.

Mijn homies van Isengard en ik heb er als antiek meubelstuk heel wat meegemaakt. Van de oude garde met Bob Bloemendaal, Eline van Hattum, Falco Hietbrink, Judith Boone, Nikol Snoeren, Stijn van Esser en Tjaakje Visser tot de jonge garde met Anne den Hartog, Charlotte van Kessel, Emily Postma, Jasper van Keulen, Klaas Govaert en Roy Verhage. Iedere dag met een glimlach naar je werk gaan als onderzoeker, dat is vrij uitzonderlijk. Maar discussiëren over onderzoek en elkaar hierin stimuleren, gecombineerd met het zo nu en dan zo slap ouwehoeren dat je er niet goed van wordt (en uiteraard een potje clippen: NOUCAMP bovenaan!!), het zijn essentiële ingrediënten die Isengard biedt als fundament voor het doen van goed onderzoek. Veel dank voor alles.

Alle andere (oud) mede-onderzoekers van de Heelkunde, Claire Pennekamp, Daphne de Groot, Dave Koole, Erik Tournoy, Femke Lutgendorff, Guus van Lammeren, Herman Zandvoort, Hjalmar van Santvoort, Janesh Pillay, Joffrey van Prehn, Joris Broeders, Kathelijne Groeneveld, Okan Bastian, Olaf Bakker, Peter Paul Wisman, Ralf Sprengers, Rian Nijmeijer, Rob Hurks, Sander Schouten, Siegrid de Meer, Stefaan Tytgat, Usama Ahmed Ali, Vincent Scholtens, Willem Hellings, Wouter Derksen en Wouter Peeters, jullie wil ik bedanken voor de vele mooie momenten!

Mijn paranimfen, Frederik Hoogwater en Winan van Houdt. Wat mooi dat jullie naast mij staan op de 30e. Als collega's op het lab begonnen, maar ik koester de vriendschappen die eruit ontstaan zijn. Freek, als broers (Fokke en Sukke…?) haast onafscheidelijk op het lab. Mooi hoe scherp wij elkaar kunnen krijgen voor experimenten om vervolgens elkaar in de kroeg nog even gek te draaien: '*dos mas, por favor…!*' Winan, je bent een soort evenbeeld met je nuchtere en relativerende blik op zaken. Zonder enig probleem leg jij de vinger precies op de zere plek om vervolgens met oplossingen of advies te komen. Ik kijk er erg naar uit om weer met je samen te werken.

Peter (en Noor) en Lien (en Koen), *geschwister*. Hoewel ik mij vaak heb afgezet tegen de titel 'broertje van…' ben ik er maar wat trots op dat ik het ben. Het is heel fijn om te weten dat er mensen op deze aardbol rondlopen die er onvoorwaardelijk voor je (zullen) zijn.

Lucas en Eva, jullie zijn twee toppers die voor de nodige afleiding hebben gezorgd. Met jullie capriolen maken jullie me altijd vrolijk!

Lieve pap en mam, als jongste telg wilde ik het altijd net even iets anders doen, waar jullie alle begrip voor hadden. Door al vroeg verantwoordelijkheid te geven hebben jullie ervoor gezorgd dat er drie grote mensen op de wereld zijn gezet. Daar heb ik diepe bewondering voor. Het heeft zonder enige twijfel de basis gevormd van dit boek. Lieve pap, ik heb je de laatste jaren intens gemist als *sparring partner*. Wat vind ik het moeilijk dat je er niet meer bij kunt zijn. Lieve mam, de sterkste rots in de zwaarste branding. Jouw trots maakt mij sterk. En vergeet nooit, drie keer vijftig is honderdvijftig.

Lieve, lieve Meriam. Sommige dingen zijn pas echt belangrijk en jij laat me dat elke dag weer zien. X

List of publications

Nijkamp MW*, Hoogwater FJH*, Steller EJA, Westendorp BF, van der Meulen TA, Leenders MW, Borel Rinkes IHM, Kranenburg O.
CD95 is a key mediator of invasion and accelerated outgrowth of colorectal liver metastases following radiofrequency ablation.
Journal of Hepatology, in press

van Houdt WJ, Hoogwater FJH, de Bruijn MT, Emmink BL, Nijkamp MW, Raats DA, van der Groep P, van Diest PJ, Borel Rinkes IHM, Kranenburg O.
Oncogenic K-Ras desensitizes colorectal tumor cells to epidermal growth factor receptor inhibition and activation.
Neoplasia 2010; 12: 443-452

Nijkamp MW, Borren A, Govaert KM, Hoogwater FJ, Molenaar IQ, van Diest PJ, Kranenburg O, Borel Rinkes IHM.
Radiofrequency ablation of colorectal liver metastases induces an inflammatory response in distant hepatic metastases but not in local accelerated outgrowth.
Journal of Surgical Oncology 2010; 101: 551-556

Langenberg MH, Nijkamp MW, Roodhart JM, Snoeren N, Tang T, Shaked Y, van Hillegersberg R, Witteveen PO, Vermaat JS, Kranenburg O, Kerbel RS, Medema RH, Borel Rinkes IHM, Voest EE.
Liver surgery induces an immediate mobilization of progenitor cells in liver cancer patients: A potential role for G-CSF.
Cancer Biology & Therapy 2010; 9: 742-747

Hoogwater FJH, Nijkamp MW*, Smakman N*, Steller EJ, Emmink BL, Westendorp BF, Raats DA, Sprick MR, Schaefer U, Van Houdt WJ, De Bruijn MT, Schackmann RC, Derksen PW, Medema JP, Walczak H, Borel Rinkes IHM, Kranenburg O.
Oncogenic K-Ras turns death receptors into metastasis-promoting receptors in human and mouse colorectal cancer cells.
Gastroenterology 2010; 138: 2357-2367

Nijkamp MW, van der Bilt JD, Snoeren N, Hoogwater FJ, van Houdt WJ, Molenaar IQ, Kranenburg O, van Hillegersberg R, Borel Rinkes IHM.
Prolonged portal triad clamping during liver surgery for colorectal liver metastases is associated with decreased time to hepatic tumour recurrence.
European Journal of Surgical Oncology 2010; 36: 182-188

Nijkamp MW, van der Bilt JD, de Bruijn MT, Molenaar IQ, Voest EE, van Diest PJ, Kranenburg O, Borel Rinkes IHM.
Accelerated perinecrotic outgrowth of colorectal liver metastases following radiofrequency ablation is a hypoxia-driven phenomenon.
Annals of Surgery 2009; 249: 814-823

Leenders MW*, Nijkamp MW*, Borel Rinkes IHM.
Mouse models in liver cancer research: a review of current literature.
World Journal of Gastroenterology 2008; 14: 6915-6923

van der Bilt JD, Soeters ME, Duyverman AM, Nijkamp MW, Witteveen PO, van Diest PJ, Kranenburg O, Borel Rinkes IHM.
Perinecrotic hypoxia contributes to ischemia/reperfusion-accelerated outgrowth of colorectal micrometastases.
American Journal of Pathology 2007; 170: 1379-1388

van der Bilt JD, Kranenburg O, Nijkamp MW, Smakman N, Veenendaal LM, Te Velde EA, Voest EE, van Diest PJ, Borel Rinkes IHM.
Ischemia/reperfusion accelerates the outgrowth of hepatic micrometastases in a highly standardized murine model.
Hepatology 2005; 42: 165-175

*these authors contributed equally

Curriculum vitae auctoris

Maarten Nijkamp was born on 24th of December 1979 in Eelde, The Netherlands. After graduating at the Praedinius Gymnasium in Groningen in 1998 he studied Pharmaceutical Science at Utrecht University from 1998 to 2000, during which he finished the first year of the programme. In 1999 he started his medical training at Utrecht University. He expressed his interest in research in 2001 by starting his first research project at the Department of Gastroenterology (Prof. dr. G.P. van Berge Henegouwen). Due to his increasing interest in surgery, he joined the research group of Prof. dr. I.H.M Borel Rinkes at the Department of Surgical Oncology in 2004. After obtaining his medical degree in 2006 he was able to start a PhD programme thanks to a grant from the Dutch Cancer Society. In 2008 he received a grant from The Netherlands Organisation for Scientific Research (ZonMw) to continue the research projects. During his time as a PhD-student he organised several activities, including the Symposium on Experimental Research for Surgical Specialties (SEOHS) in Utrecht in 2008. In January 2011 he will start the residency program in general surgery in the Diakonessenhuis in Utrecht (Dr. G.J. Clevers). The last two years are scheduled in the University Medical Center Utrecht under supervision of Prof. dr. I.H.M. Borel Rinkes.